

Universität Potsdam
Arbeitsgruppe Prof. Dr. Laschewsky

**The Synthesis of Well-Defined Functional Homo- and Block Copolymers
in Aqueous Media
via Reversible Addition-Fragmentation Chain Transfer (RAFT)
Polymerization**

**Dissertation
zur Erlangung des akademischen Grades
"doctor rerum naturalium"
(Dr. rer. nat.)
in der Wissenschaftsdisziplin "Kolloid und Polymer Chemie"**

**eingereicht an der
Mathematisch-Naturwissenschaftlichen Fakultät
der Universität Potsdam**

**von
Murat Mertoğlu
geboren am 18.07.1978 in İstanbul**

Potsdam, im November 2004

ACKNOWLEDGEMENTS

I am indebted to many people who helped me during the preparation of this thesis. I wish to express my gratitude to Prof. Dr. André Laschewsky for giving me the opportunity to conduct research under his supervision. He was all the time available and open to discuss about anything to support me. He encouraged and motivated me a lot, particularly, when the things go wrong in research. Lastly I want to thank him for his intimate and friendly manners both as an advisor and a person.

I am especially grateful to Dr. Joachim Storsberg and Dr. Jean-François Baussard for their contribution to my thesis and particularly for their guidance in the laboratory to develop my bench skills and learn better the modern synthetic methods.

I gratefully acknowledge the help of J.-L. Habib-Jiwan (Université catholique de Louvain) for taking FAB mass spectra, to F. Malwitz (University of Potsdam) for helping with IR measurements, to M. Kumke (University of Potsdam) for helping with fluorescence measurements, to S. Bruzzano and C. Wieland (both Fraunhofer IAP) for advices and measurements in ASEC of polycations, to H. Schlaad, G. Rother and M. Gräwert (Max-Planck-Institut für Kolloid- und Grenzflächenforschung, Potsdam) for helping with ASEC for polyanions and SEC in NMP.

Special thanks to Christoph Wieland, Kamel Silmy, Katja Skrabania, Laurent Wattebled, Nathalie Sieverling, Samira Nozari, Sébastien Garnier, Dr. Stefano Bruzzano, Dr. Habil Veronika Strehmel and all members of the Fraunhofer Institute for Applied Polymer Research in the science park of Golm for the friendly environment and their kind support.

Finally I am extremely grateful to my parents and brothers who provide me constant support and confidence however far they are.

ABSTRACT

New chain transfer agents based on dithiobenzoate and trithiocarbonate for free radical polymerization via Reversible Addition-Fragmentation chain Transfer (RAFT) were synthesized. The new compounds bear permanently hydrophilic sulfonate moieties which provide solubility in water independent of the pH. One of them bears a fluorophore, enabling unsymmetrical double end group labelling as well as the preparation of fluorescent labeled polymers. Their stability against hydrolysis in water was studied, and compared with the most frequently employed water-soluble RAFT agent 4-cyano-4-thiobenzoylsulfanylpentanoic acid dithiobenzoate, using UV-Vis and $^1\text{H-NMR}$ spectroscopy. An improved resistance to hydrolysis was found for the new RAFT agents, providing good stabilities in the pH range between 1 and 8, and up to temperatures of 70°C . Subsequently, a series of non-ionic, anionic and cationic water-soluble monomers were polymerized via RAFT in water. In these experiments, polymerizations were conducted either at 48°C or 55°C , that are lower than the conventionally employed temperatures ($>60^\circ\text{C}$) for RAFT in organic solvents, in order to minimize hydrolysis of the active chain ends (e.g. dithioester and trithiocarbonate), and thus to obtain good control over the polymerization. Under these conditions, controlled polymerization in aqueous solution was possible with styrenic, acrylic and methacrylic monomers: molar masses increase with conversion, polydispersities are low, and the degree of end group functionalization is high. But polymerizations of methacrylamides were slow at temperatures below 60°C , and showed only moderate control. The RAFT process in water was also proved to be a powerful method to synthesize di- and triblock copolymers including the preparation of functional polymers with complex structure, such as amphiphilic and stimuli-sensitive block copolymers. These include polymers containing one or even two stimuli-sensitive hydrophilic blocks. The hydrophilic character of a single or of several blocks was switched by changing the pH, the temperature or the salt content, to demonstrate the variability of the molecular designs suited for stimuli-sensitive polymeric amphiphiles, and to exemplify the concept of multiple-sensitive systems. Furthermore, stable colloidal block ionomer complexes were prepared by mixing anionic surfactants in aqueous media with a double hydrophilic block copolymer synthesized via RAFT in water. The block copolymer is composed of a noncharged hydrophilic block based on polyethyleneglycol and a cationic block. The complexes prepared with perfluoro decanoate were found so stable that they even withstand dialysis; notably they do not denaturate proteins. So, they are potentially useful for biomedical applications in vivo.

TABLE OF CONTENTS

ACKNOWLEDGEMENT	ii
ABSTRACT	iii
LIST OF SCHEMES	vii
LIST OF TABLES	viii
LIST OF FIGURES	ix
LIST OF ABBREVIATIONS	xiv
1. INTRODUCTION	1
1.1. Free Radical Polymerization.....	5
1.2. General Properties of Living Polymerization.....	7
.....1.3. Comparison of Living Polymerization Systems with Free-radical Polymerization	8
1.4. Controlled Radical Polymerization Methods (CRP)	9
1.4.1. Nitroxyl Mediated Polymerization (NMP)	10
1.4.2. Atom Transfer Radical Polymerization (ATRP)	11
1.4.3. Reversible Addition Fragmentation Chain Transfer Polymerization (RAFT)	11
1.5. A Closer Look to RAFT Polymerization	15
2. SYNTHESIS OF WATER-SOLUBLE RAFT AGENTS	24
2.1. The most used reaction routes to dithioesters	25
2.1.1. Synthesis of dithiobenzoic acids	25
2.1.2. Alkylation of dithiocarboxylates	25
2.1.3. Addition of dithiocarboxylic acids to olefins	27
2.1.4. Synthesis of dithioesters using Pinner salts	27
2.1.5. Conversion of thioesters to dithioester by using Lawesson's reagent	27
2.1.6. Free radical coupling reaction between azo initiators and bis(thiocarbonyl) disulfides	27

2.1.7. <i>Ester exchange reaction between dithiocarboxylates and thiols</i>	28
2.2 Synthetic routes to water-soluble RAFT agents	28
2.2.1. <i>Water-soluble RAFT agents via acidic addition of dithiocarboxylic acids to olefins</i>	30
2.2.2. <i>Water-soluble RAFT agents via free radical coupling reaction between azoinitiators and bis(thiocarbonyl) disulfides</i>	32
2.2.3. <i>Water-soluble RAFT agents via alkylation of dithiocarboxylates</i>	33
3. STABILITY OF RAFT AGENTS IN WATER	36
4. SYNTHESIS OF WATER-SOLUBLE HOMO- AND COPOLYMERS VIA RAFT	48
4.1. Usefulness of End Groups of Polymers Synthesized via RAFT	49
4.2. Presentation of Monomers Used	54
4.3. Homopolymerization Studies via RAFT	56
4.3.1. <i>Polymerization of vinylbenzylchloride (M16) via RAFT</i>	56
4.3.2. <i>Aqueous RAFT polymerization of methacrylic monomers</i>	57
4.3.3. <i>Aqueous RAFT polymerization of acrylic monomers</i>	64
4.3.3. <i>Aqueous RAFT polymerization of styrenic monomers</i>	72
4.3.5. <i>Attempted aqueous RAFT polymerization of other monomer classes</i>	75
4.3.6. <i>The effect of thioesters on CRP</i>	76
4.3.7. <i>Discussion about homopolymerizations</i>	77
4.4. Synthesis of the Block Copolymers via RAFT	80
5. STIMULI-SENSITIVE POLYMERS	93
6. NANO-PARTICLES IN WATER VIA COMPLEXATION OF IONIC POLYMERS	108
7. EXPERIMENTAL	116
7.1. Analytical Methods	116
7.2. Polymerization	118
7.3. Particle Preparation via Complexation of Cationic and Anionic Functional Groups	122

7.4. Synthesis	122
7.4.1. Synthesis of dithiobenzoic acid	122
7.4.2. Synthesis of di(thiobenzoyl)disulfide	123
7.4.3. Synthesis of sodium 2-(2-thiobenzoylsulfanyl propionylimino)ethanesulfonate (CTA2)	123
7.4.4. Synthesis of potassium 2-(2-thiobenzoylsulfanylpropionylimino)-naphthalene-6,8-disulfonate (CTA3)	125
7.4.5. Synthesis of sodium 2-(2-methyl-2-thiobenzoylsulfanylpropionylimino)ethanesulfonate (CTA4)	126
7.4.6. Synthesis of sodium S-benzyl-S'-2-sulfonatoethyl trithiocarbonate (CTA6)	127
7.4.7. Synthesis of Cumyldithiobenzoate (CTA7)	128
7.4.8. Synthesis of Sodium 2-(2-benzoylsulfanylpropionylimino)ethanesulfonate (thioester analogue of CTA2)	129
7.4.9. Synthesis of N-(tris(hydroxymethyl)methyl-N'-(α,α -dimethyl-3'-isopropenylbenzyl) urea (1MM1)	130
7.4.10. Synthesis of N,N-bis(2-hydroxyethyl)-N'-(α,α -dimethyl-3'-isopropenylbenzyl) urea (1MM3)	131
7.4.11. Synthesis of N-(2-sodiumsulfonatoethyl)-N'-(α,α -dimethyl-3'-isopropenylbenzyl) urea (1MM15)	132
7.4.12. Synthesis of 1MM63	133
7.4.13. Synthesis of sodium β - styrene sulfonate	134
7.4.14. Synthesis of 2-phenyl-prop-2-en sulfonate sodium salt	135
7.4.15. 4-(2-sulfoethyl)-1-(4-vinyl-benzyl) pyridinium betain (M17)	135
8. CONCLUSIONS	138

APPENDIX 1. Structures of monomers, RAFT agents and initiators used in this study

APPENDIX 2. $^1\text{H-NMR}$ spectra

APPENDIX 3. IR spectra

LIST OF SCHEMES

Scheme 1.1.	Schematic representation of phases of free radical polymerization	5
Scheme 1.2.	General mechanism for the propagation step of NMP	10
Scheme 1.3.	General mechanism of the propagation step of ATRP	11
Scheme 1.4.	The proposed RAFT mechanism using dithiocarbonyl derivatives	12
Scheme 1.5.	Effect of the R group in reversible addition chain transfer, exemplified for the polymerization of methylmethacrylate	16
Scheme 1.6.	The illustrated chain transfer step of RAFT polymerization for block copolymer synthesis when a macro RAFT agent is employed	19
Scheme 5.1.	Schematic representation of the synthesized stimuli-sensitive block polymers	95
Scheme 5.2.	Idealized model for the behavior the salt- and pH-sensitive triblock copolymers, when exposed to different sequences of stimuli	102
Scheme 6.1.	Preparation of particles by complexation of cationic block of copolymer polyM1-block-M3 with ionic surfactants	110

LIST OF TABLES

Table 1.1.	Apparent transfer constants C_{tr} for benzyl thiocarbonylthio compounds for styrene polymerization at 110 °C	17
Table 1.2.	Apparent transfer constants C_{tr} for the initial chain transfer step of methyl methacrylate polymerization at 60 °C by employing dithiobenzoate derivatives PhC(=S)SR	17
Table 3.1.	Stability of RAFT agents at 40°C in water, in dependence on pH	37
Table 4.1.	Characteristic absorbance bands of RAFT agents and polymers in aqueous solution	51
Table 4.2.	Molar mass and compositional data of the synthesized block copolymers and their precursors	82
Table 7.1.	dn/dc values of polymers	118
Table 7.2.	Reagents and conditions used for homopolymerization experiments	120
Table 7.3.	Polymerization conditions used for the preparation of block copolymers ...	121

LIST OF FIGURES

Figure 1.1.	Molar mass vs. conversion and conversion vs. time graphs for living, and radical polymerizations (idealized)	9
Figure 1.2.	Examples of RAFT agents with different R and Z groups	16
Figure 2.1.	The most used reaction routes to dithioesters	26
Figure 2.2.	R and Z fragments proving good control in RAFT polymerization	29
Figure 2.3.	The attempted acidic addition of dithiocarboxylic acids to α -methylstyrene analogues.....	30
Figure 2.4.	The acidic addition trial of dithiobenzoic acid to 2-phenyl-prop-2-en sulfonic acid	31
Figure 2.5.	The chemical structures of azo initiators 1MM63 and VA-80	32
Figure 2.6.	The structures of new water soluble RAFT agents	33
Figure 3.1.	Stability of CTA1 , and CTA6 at 40°C followed by UV-Vis spectroscopy at 493 nm and 425 nm, respectively	38
Figure 3.2.	¹ H-NMR of the phenyl groups of CTA1 and CTA2 before and after hydrolysis in D ₂ O at pH =6	39
Figure 3.3.	Stability of RAFT agents in D ₂ O at pH 6 at different temperatures, followed by ¹ H-NMR	40
Figure 3.4.	Evolution of the ¹ H NMR spectra of CTA1 in D ₂ O at pH=6 with decomposition at 70°C	41
Figure 3.5.	Evolution of the ¹ H NMR spectra of CTA2 in D ₂ O at pH=6 with decomposition at 80°C	42
Figure 3.6.	Evolution of the ¹ H-NMR spectra of CTA3 in D ₂ O at pH=6 with decomposition at 70°C	43
Figure 3.7.	Evolution of the ¹ H NMR spectra of CTA4 in D ₂ O at pH=6 with decomposition at 70°C	44
Figure 3.8.	Evolution of the ¹ H NMR spectra of CTA6 in D ₂ O at pH=6 with decomposition at 70°C	45
Figure 4.1.	Optical spectra of CTA3 , CTA1 and CTA6	51
Figure 4.2.	Fluorescence emission spectra of CTA3 , and polyM14 polymerized using CTA 3	54

Figure 4.3.	The structures of the monomers used in this study	56
Figure 4.4.	Figures related with the controlled radical polymerization of M16 in toluene using initiator V-60 and the RAFT agents CTA7	57
Figure 4.5.	Figures related with the controlled radical polymerization of M6 in water using initiator V-50 and the RAFT agent CTA1	58
Figure 4.6.	Figures related with the controlled radical polymerization of M7 in water using initiator V-50 and the RAFT agents CTA1	60
Figure 4.7.	Figures related with the controlled radical polymerization of M5 in water using initiator V-50 and the RAFT agents CTA4	61
Figure 4.8.	Figures related with the controlled radical polymerization of M11 in water using initiator V-50 and the RAFT agents CTA4	63
Figure 4.9.	Figures related with the controlled radical polymerization of M12 in water using initiator V-50 and the RAFT agents CTA 3	65
Figure 4.10.	Figures related with the controlled radical polymerization of M2 in water using RAFT agents CTA1 and CTA3	66
Figure 4.11.	Figures related with the controlled radical polymerization of M3 in water using initiator V-545 and the RAFT agent CTA3	68
Figure 4.12.	Figures related with the controlled radical polymerization of M1 in water using initiator V-545 and the RAFT agents CTA3	69
Figure 4.13.	Figures related with the controlled radical polymerization of M9 in water using initiator V-545 and the RAFT agents CTA3	71
Figure 14.4.	Figures related with the controlled radical polymerization of M13 in water using initiator V-545 and the RAFT agents CTA3	73
Figure 4.15.	Figures related with the controlled radical polymerization of M13 in water using initiator V-50 and the RAFT agents CTA6	75
Figure 4.16.	Plots of the evolution of the aqueous size exclusion chromatograms with conversion in the aqueous solution polymerization of M13 in the presence of thioester analogue of CTA2	77
Figure 4.17.	ASEC traces of the macro RAFT agent polyM1 and polyM1-block-M3	84
Figure 4.18.	SEC traces of polyM7 and polyM7-block-M4 in THF and ¹ H-NMR spectra of block copolymer polyM7-block-M4 in CDCl ₃	87
Figure 4.19.	ASEC traces of macro RAFT agent polyM13 and polyM13-block-M10	89

Figure 5.1.	DLS analysis of particles prepared from polyM7-block-M4 in H ₂ O and temperature dependant turbidity of polyM7 and polyM7-block-M4 in water	96
Figure 5.2	¹ H-NMR of polyM3 in D ₂ O, of polyM17 in 0.5 M NaBr D ₂ O, and of polyM15 in D ₂ O	97
Figure 5.3.	¹ H-NMR of polyM3-block-M17 in D ₂ O, and in 0.5 M NaBr D ₂ O	99
Figure 5.4.	¹ H-NMR spectra of polyM14 in D ₂ O and polyM14-block-polyM17 in 0.1 M NaBr D ₂ O, with growing size of the polyM17 block	99
Figure 5.5.	DLS analysis of the diblock copolymers polyM3-block-M17 , polyM10-block-M17 , polyM14-block-M17 in 0.5 M (aq) NaBr and after dialysis of these salt solutions against DI water	100
Figure 5.6.	DLS analysis of the triblock copolymers polyM3-block-M17-block-M15 , and poly M14-block-M17-block-M15	102
Figure 5.7.	DLS analysis of the triblock copolymers polyM3-block-M17-block-M15 , polyM10-block-M17-block-M15 , polyM14-block-M17-block-M15	103
Figure 5.8.	¹ H-NMR of polyM3-block-M17-block-M15 in 0.5 M NaBr D ₂ O, in D ₂ O (ambient pH), and in D ₂ O (pH=1)	105
Figure 6.1.	DLS analysis of polyM1-block-M3 , and the particles prepared with its complexation with perfluorodecanoate and decanoate	111
Figure 6.2.	DLS analysis of particles prepared with sodium decanoate and perfluorodecanoate with ongoing dilution	111
Figure 6.3.	¹ H-NMR spectra of copolymer polyM1-block-M3 , the particles of sodium decanoate, and the particles of sodium perfluoro decanoate in D ₂ O	113
Figure 6.4.	Circular dichroism of Human Serum Albumin (HSA) and the mixture of HSA with particles prepared with sodium perfluoro decanoate	114
Figure A2.1.	¹ H-NMR of CTA1 in CDCl ₃	I
Figure A2.2.	¹ H-NMR of di(thiobenzoyl) disulfide in CDCl ₃	I
Figure A2.3.	¹ H-NMR of CTA3 in D ₂ O	II
Figure A2.4.	¹ H-NMR of sodium 2-(2-bromo propionylamino) ethanesulfonate in D ₂ O	II
Figure A2.5.	¹ H-NMR of CTA3 in D ₂ O	III
Figure A2.6.	¹ H-NMR of 2-(2-bromo-propionylamino)-naphthalene-6,8-disulfonic acid dipotassium salt in D ₂ O	III

Figure A2.7.	$^1\text{H-NMR}$ of CTA4 in D_2O	IV
Figure A2.8.	$^1\text{H-NMR}$ of sodium 2-(2-bromo 2-methyl propionylamino) ethanesulfonate in D_2O	IV
Figure A2.9.	$^1\text{H-NMR}$ of CTA6 in DMSO	V
Figure A2.10.	$^1\text{H-NMR}$ of CTA7 in CDCl_3	V
Figure A2.11.	$^1\text{H-NMR}$ of dithiobenzoic acid in CDCl_3	VI
Figure A2.12.	$^1\text{H-NMR}$ of 1MM1 in DMSO	VI
Figure A2.13.	$^1\text{H-NMR}$ of 1MM3 in DMSO	VII
Figure A2.14.	$^1\text{H-NMR}$ of 1MM15 in D_2O	VII
Figure A2.15.	$^1\text{H-NMR}$ of 1MM58 in D_2O	VIII
Figure A2.16.	$^1\text{H-NMR}$ of 1MM68 in D_2O	VIII
Figure A2.17.	$^1\text{H-NMR}$ of polyM1 in D_2O	IX
Figure A2.18.	$^1\text{H-NMR}$ of polyM2 in D_2O	IX
Figure A2.19.	$^1\text{H-NMR}$ of polyM3 in D_2O	X
Figure A2.20.	$^1\text{H-NMR}$ of polyM4 in CDCl_3	X
Figure A2.21.	$^1\text{H-NMR}$ of polyM5 in D_2O	XI
Figure A2.22.	$^1\text{H-NMR}$ of polyM6 in D_2O	XI
Figure A2.23.	$^1\text{H-NMR}$ of polyM7 in D_2O	XII
Figure A2.24.	$^1\text{H-NMR}$ of polyM8 in D_2O	XII
Figure A2.25.	$^1\text{H-NMR}$ of polyM9 in D_2O	XIII
Figure A2.26.	$^1\text{H-NMR}$ of polyM10 in D_2O	XIII
Figure A2.27.	$^1\text{H-NMR}$ of polyM13 in D_2O	XIV
Figure A2.28.	$^1\text{H-NMR}$ of polyM14 in D_2O	XIV
Figure A2.29.	$^1\text{H-NMR}$ of polyM15 in D_2O	XV
Figure A2.30.	$^1\text{H-NMR}$ of polyM17 ($M_n \sim 10\text{ K}$) in 0.5 M NaBr D_2O	XV
Figure A2.31.	$^1\text{H-NMR}$ of polyM18 in D_2O	XVI
Figure A3.1.	FT-IR spectra of CTA2 (KBr, pellet)	I
Figure A3.2.	FT-IR spectra of CTA3 (KBr, pellet)	I

Figure A3.3.	FT-IR spectra of CTA4 (KBr, pellet)	II
Figure A3.4.	FT-IR spectra of CTA6 (KBr, pellet)	II
Figure A3.5.	FT-IR spectra of 1MM1 (KBr, pellet)	III
Figure A3.6.	FT-IR spectra of 1MM3 (KBr, pellet)	III
Figure A3.7.	FT-IR spectra of 1MM15 (KBr, pellet)	IV
Figure A3.8.	FT-IR spectra of M17 (KBr, pellet)	IV

LIST OF ABBREVIATIONS

1MM1	N-(tris(hydroxymethyl)methyl)-N'-(α,α -dimethyl-3'-isopropenylbenzyl) urea
1MM3	N,N-(bis(2-hydroxyethyl))-N'-(α,α -dimethyl-3'-isopropenylbenzyl) urea
1MM15	N-(2-sodiumsulfonatoethyl)-N'-(α,α -dimethyl-3'-isopropenylbenzyl) urea
ASEC	Aqueous size exclusion chromatography
ATRP	Atom transfer radical polymerization
CD	Circular dichroism
CRP	Controlled radical polymerization
CTA	Chain transfer agent
CTA1	4-cyano-4-thiobenzoylsulfanyl pentanoic acid
CTA2	Sodium 2-(2-thiobenzoylsulfanylpropionylimino)ethane sulfonate
CTA3	Potassium 2-(2-thiobenzoylsulfanylpropionylimino) naphthalene-6,8-disulfonate
CTA4	Sodium 2-(2-methyl-2-thiobenzoylsulfanylpropionylimino) ethanesulfonate
CTA5	N-methyl-N-(thiobenzoylsulfanylmethylenephnylmethyl) morpholinium chloride
CTA6	Sodium S-(benzyl)-S'-(2-sulfonatoethyl) trithiocarbonate
CTA7	Cumyldithiobenzoate
DLS	Dynamic light scattering
DMF	Dimethyl formamide
DMSO	Dimethyl sulfoxide
FRP	Free radical polymerization
h	Hour
LCST	Lower critical solution temperature

M1	((2-acryloyloxy)ethyl)trimethyl ammoniumchloride
M2	Potassium (3-acryloyloxy)propane sulfonate
M3	Poly(ethyleneglycol) methyl ether acrylate
M4	n-butyl acrylate
M5	(2-methacryloyloxyethyl) trimethyl amonium chloride
M6	Potassium (3-methacryloyloxy) propan sulfonate
M7	Poly(ethyleneglycol) methyl ether methacrylate
M8	2-methylene succinic acid bis (3-sulfo-propyl) ester dipotassium salt
M9	(3-(dimethyl)aminopropyl) acryl amide
M10	dimethylacryl amide
M11	(3-(dimethyl)aminopropyl) methacryl amide
M12	Methacrylamide
M13	(Vinylbenzyl) trimethyl ammonium chloride
M14	Sodium 4-styrene sulfonate
M15	4-vinylbenzoic acid
M16	4-vinylbenzylchloride
M17	4-(2-sulfo-ethyl)-1-(4-vinylbenzyl)pyridinium betain
M18	1-(3-sulfo-propyl)-2-vinyl pyridinium betain
MADIX	Macromolecular Design via the Interchange of Xanthates
MALLS	Multi angle light scattering
min.	minute
M_n	Number average molar mass
M_w	Weight average molar mass
PDI	Polydispersity index
NMP	Nitroxyl Mediated Polymerization
RAFT	Reversible Addition-Fragmentation Chain Transfer
RI	Refractive index

SEC	Size exclusion chromatography
THF	Tetrahydrofurane
V-50	2,2'-azobis (2-methylpropionamidine) dihydrochloride
V-545	2,2'-azobis (2-methyl-N-phenylpropionamidine) dihydrochloride
V-60	2,2'-azobis (2-methyl-propionitrile)
VA-80	2,2'-azobis(2-methyl-N-[1,1-bis(hydroxymethyl)-2-hydroxyethyl] propionamide)

1. INTRODUCTION

Polymers are an indispensable part of modern life. They have a wide usage from agriculture to space research, and are present in every field of our daily life. Polyethylene and polystyrene are used in enormous amounts for packing chemicals, foods and many other materials, as they are cheap and easily processable, and do not threaten human health. Glass fiber reinforced cross linked polyester laminates have application in boats hulls, lorry cabs, and roofing panels and in chemical plants to store chemicals because of their resistance to chemicals, water, shock and being much lighter than steel. Polyester and polyamide fibers are widely used in textile industry. Rubbers are used in almost every equipment from cars to refrigerators for different purposes. All these examples illustrate that polymers are used in enormous quantities for various purposes.

The need for sophisticated materials has increased in parallel to the development of science. Therefore, the properties of polymers as being widely used material must continuously be improved, too. In the last decades, it has been figured out that mankind can benefit from polymers also for more complicated tasks. They can be employed in the production of high-tech electronic devices like chip production, or in medicine such as for the replacement of some body parts like bones, for intelligent drug, or gene delivery. But all these last mentioned applications need specially designed polymers. Polymers with desired electrical, optical, interfacial and other properties have to be produced according to the particular needs. This can be achieved via the synthesis of new polymers by making new building blocks, e.g. new monomers with new backbones, or arranging established building blocks in new ways, e.g. varying the topology of polymers (linear, branched, hyper branched, stars etc.) or the internal composition of polymeric chains (statistical/gradient copolymers, block). The latter approach is particularly economical. It implies the need for well-defined polymers, which can be synthesized by powerful, well controlled polymerization methods.

A classification of polymers is useful to understand how and to which extend the control could be exerted on which kind of polymers. Polymers were originally classified by Carothers (1929) into condensation and addition polymers on the basis of the compositional difference between the polymer and the monomer, from which it was synthesized [1]. This classification is applicable to the composition, or the structure of

1. Introduction

polymers. In condensation polymerization, polyfunctional monomers are used. These monomers are reacted with each other by using various organic condensation reactions with elimination of small molecules like water. Addition polymerization is the repetitive addition of monomer units, mostly containing vinyl segments, successively to active centers. The structure of the monomer does not change in the polymer chain, and there is no elimination of small molecules. The other classification was done by Flory (1953) [1] on the basis of the polymerization mechanism as step growth and chain growth polymerization. Step growth polymerization proceeds by the stepwise reaction between any molecule having reactive sites. Chain growth polymerization require initiator species, which can produce reactive centers, and then polymerization only take place over these created reactive centers. The classification of Flory depending on mechanism is more appropriate to discuss about the possible ways of exerting control over polymer chain.

The synthesis of well-defined polymers via step growth polymerization does not look trivial if we consider that every reactive side has the equal probability to react. All these reactive sides should be controlled. This has been extremely difficult up to now, and therefore the synthesis of block copolymers, stars, or dendrimers is only possible applying very demanding methods such as group transfer chemistry or solid phase synthesis. In chain growth polymerization, polymerization is carried out via active chain centers, and the limited number of these and their reactivity could be controlled. Synthetic methods for different chain growth polymerization methods, which can fully or partially exert control over active chains centers, are available.

There are several chain growth polymerization methods: free radical (FR), ionic, group transfer and coordination polymerization. Free radical polymerization is the most used of them. Ionic and group-transfer polymerization do not have wide industrial application, though they can provide better-defined polymers compared to free radical polymerization. First of all, they are only applicable to a limited number of monomers as these polymerizations are very sensitive to the most functional groups such as halogens, nucleophilic functional groups, acidic protons etc., existing on most monomers. Additionally, they require highly pure solvents and monomers, highly reactive initiators, in general anhydrous conditions and mostly low polymerization temperatures. These demanding conditions prevent them from finding large industrial application. The group transfer polymerization is mostly limited to methacrylates and related monomers. Today,

1. Introduction

the biggest quantities of polymers are produced via coordination polymerization. Recent progress in the catalysts used enables increasingly the synthesis of polymers with well-defined structures. Even the stereochemistry of polymers can be controlled, but the method is so far applicable to a limited number of non-functional monomers, such as ethylene, propylene, or butadiene.

Free-radical polymerization (FRP) is industrially the most widespread method used to produce polymeric materials, including plastics rubber and fibers [2]. It has numerous advantages over ionic and coordination polymerization methods. It is relatively tolerant to functional groups on the monomers like ionic moieties, ligands, nucleophilic and electrophilic sites, acids and bases, and can be carried out in wide variety of solvents. Many impurities including water are not a real problem. Complicated procedures and sophisticated equipments are not necessary in order to work under strictly humidity free conditions as in the case of ionic polymerization methods. On the contrary, polymerizations can even be done directly in water (as a solution, suspension or emulsion) provided that oxygen is excluded. Depending on the monomer-initiator couple, polymerization can be done in a wide temperature window.

A limitation of free radical polymerization is the lack of the control over the polymer structure, because of slow initiation, fast propagation and inherent chain-termination reactions. Actually, a newborn radical propagates and terminates within seconds. Such short life times prevent any manipulation, or control over the structure of produced polymer chains. The advent of the so-called controlled radical polymerization (CRP) methods gave a fresh impetus to the synthesis of well-defined macromolecules via free radical polymerization. These methods combine the inherent advantages of conventional free-radical polymerization with that of living polymerization methods in their own way. Compared to the classical free radical process, these methods enable the synthesis of the functional homopolymers and block copolymers with predetermined molecular weights, low polydispersities, and well-defined end groups, which are more difficult to obtain, or even not accessible by other synthetic methods. These new CRP methods are much more tolerant to functional groups on the monomers than classical "living polymerization" methods, and can be run in many conventional solvents and over a wide range of temperatures. They also provide an easy access to complex polymer architectures like star, graft and hyper-branched polymers. The mostly used methods are

1. Introduction

the so-called "Nitroxide Mediated Polymerization" (NMP) [3-5], "Atom Transfer Radical Polymerization" (ATRP) [6-8], and more recently "Reversible Addition-Fragmentation chain Transfer polymerization" (RAFT) [9-11] and, as special case, "Macromolecular Design via the Interchange of Xanthates" (MADIX) [12]. Each of the methods presents inherent advantages and inconveniences.

The CRP methods have been mostly developed in bulk and in organic solvents for the synthesis of well-defined (co)polymers with different architectures by using different functional monomers. However, the number of examples related with their application in water was small at the beginning of this thesis, although their usage in aqueous environment is a promising research field. To benefit from water, as solvent for any purpose instead of organic solvents is attractive by itself, as it is non-flammable and non-toxic, there are plenty of resources, it is cheap, and waste-water treatment is very well developed. Therefore, CRP in water is highly attractive due to the new macromolecular structures which can be synthesized and the properties of them.

Water is a very particular solvent. It favors self-organization, and enables the formation of aggregates and supramolecular structures. For example, amphiphilic polymers which bear both hydrophilic and hydrophobic parts, and polymers which reacts to external stimuli -like temperature, electrical field, or the salinity of medium-, have a great potential to be used as smart material which can be useful in aqueous environment. These kinds of polymers can be used to prepare micro or nano-assemblies in water, and they have a great potential to find applications in fields of pharmaceuticals, medical diagnostic, personal care, and biotechnology and, they may be the answer of some other technical, or medical problems waiting for a solution. But, the synthesis of such polymers with controlled structure is chemically challenging with traditional polymerization methods. If CRP methods can be applied in water, they could simplify the synthesis of this kind of water-soluble macromolecules.

CRP in homogeneous aqueous media was an underdeveloped, but attractive field for the development of water soluble-macromolecules. Therefore, this thesis focused on the applicability and the development of CRP methods for aqueous environment. The Reversible Addition Fragmentation Chain Transfer (RAFT) polymerization was chosen among the CRP methods, as it is arguably the most promising one to synthesize polymers

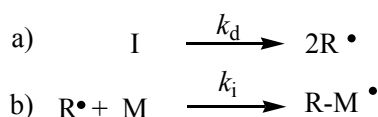
1. Introduction

in water (see Chapter 1.4). In this chapter, first, conventional radical polymerization, and the general properties of ionic polymerizations are discussed and compared. Then, CRP and its similarities to both radical and living polymerization are explained. The established CRP methods are briefly described and compared with each other to explain the reasons behind why RAFT among them was chosen for the work in aqueous media.

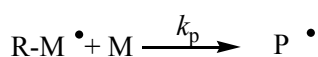
1.1. Free Radical Polymerization

A free radical is an atomic or molecular species whose normal bonding system is modified such that an unpaired electron remains associated with the structure. A radical is capable of reacting with an olefinic monomer to generate a chain carrier which can retain its activity long enough to propagate a macromolecular chain under the appropriate conditions [13].

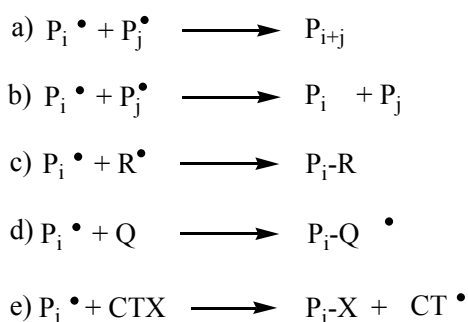
Initiation:



Propagation:



Termination



Scheme 1.1. Schematic representation of phases of free radical polymerization (FRP).

A conventional radical polymerization is composed of three major steps; initiation, propagation and termination (Scheme 1.1). Basically, two reactions occur in the initiation step. First one is the production of reactive radicals from an initiator source. The most usual method is the homolytic dissociation of an initiator to yield a pair of primary radicals. Alternative radical sources are also available, but these are beyond the discussion

1. Introduction

herein. Second one is the reaction of the primary radical with a monomer to yield a growing radical center. Since the first step is generally much slower than the second step, the rate-determining step is the dissociation of initiator as given in equation 1 (eq. 1; f = factor for initiator efficiency, k_d is the dissociation rate constant of the initiator, $[I]$ is the initiator concentration). The propagation step is the successive addition of a large number monomer units to the active radical center to produce a long polymer chain. The rate of polymerization (R_p) is directly proportional to radical and monomer concentrations as given in equation 2 (eq. 2; k_p is the polymerization rate constant, $[P\cdot]$ is molar concentration active growing chains, $[M]$ is the molar concentration of monomer).

$$R_i = f \cdot k_d \cdot [I] \quad (\text{eq. 1})$$

$$R_p = k_p [P\cdot][M] \quad (\text{eq. 2})$$

The final step of FRP is the termination (chain breaking reactions). The radicals can terminate in several ways as shown Scheme 1.1. a: coupling of two growing chains (recombination), b: a radical transfer from one chain to other one (disproportionation) c: coupling of a growing chain with a primary initiator derived radical, d: reaction of a growing chain with radical stabilizing compounds like O_2 , or e: transfer of a radical to another species in the system, like solvent or impurities. The main portion of termination generally happens through bimolecular reactions between the active radical centers. Therefore the rate of termination (R_t) is normally of second order with respect to the radical concentration as given in equation 3 (eq. 3; k_t is the rate constant of termination, $[P\cdot]$ is molar concentration active growing chains). Thus, a change in radical concentration affects more the rate of termination reactions rather than the rates of polymerization. In successful radical polymerizations, momentary radical concentration is therefore kept low to obtain high molecular weight polymers, since the high radical concentration extremely increases the termination reactions, and so reduces the average chain length. From equation 4 which defines the kinetic chain length (ν), it can be seen that the chain length is inversely proportional with R_t , namely it inversely proportional with active radical concentration for polymerizations initiated by thermal homolysis of an initiator (eq 4; the meanings of symbols are same as in the previous equations).

$$R_t = k_t[R\cdot]^2 \quad (\text{eq. 3})$$

$$v = \frac{R_p}{R_t} = \frac{k_p \cdot [M]}{2 \cdot (f \cdot k_d \cdot k_t \cdot [I])^{1/2}} \quad (\text{eq. 4})$$

Initiation, propagation and termination reactions continuously occur throughout FRP. Although in FRP, the time required for high conversion can be hours, the average lifetime of a radical is not longer than a few seconds at most. Radicals are born, propagate and terminate in seconds. The FRP process can therefore be described as a serial growth polymer chains.

Although the conventional FRP is the most versatile method for synthesizing polymers, it cannot provide the well-defined polymers that are desired for specific purposes. The molar mass is difficult to predefine, as is determined by the complicated combination of many parameters such as polymerization temperature, monomer, solvent, viscosity, radical source etc. The resulting polymers have a broad molecular mass distribution because of the continuous initiation and termination reactions in the course of the polymerization. In the optimal case, a Schulz-Zimm distribution is obtained with the ratio of $M_w/M_n = 1.5-2.0$, depending on the relative importance of termination by recombination or disproportionation, respectively (M_n = the number average molecular mass; M_w = weight average molar mass; M_w/M_n = polydispersity), because pairs of propagating chains are born and die one after another. There is no direct access to complex architectures like star, block copolymers etc. Since several termination reactions coexist, chain end-groups are poorly defined.

1.2. General Properties of Living Polymerization

The living polymerization systems can be placed into the category of chain growth polymerizations. The living polymerization systems are capable of producing polymers with pre-determined molar mass and very narrow molar mass distribution (M_w/M_n), and can be used to prepare block polymers by successively adding of different monomers. The process can also be used to produce other polymers having complex

1. Introduction

architectures, including various homo- and copolymers (like stars, statistical copolymer with statistical gradients).

Quirk and Lee defined [14] the criteria to be presented by a polymerization reaction, to be qualified as living polymerization as such:

- a) Polymerization proceeds till all monomer is consumed. Further addition of monomer results in continued polymerization.
- b) The number average molar mass M_n is a linear function of the conversion.
- c) The number of growing polymer chains (active chains) is constant and independent of the conversion.
- d) The molar mass can be controlled by the stoichiometry of the monomer and initiator.
- e) Polymers having narrow molecular weight distribution are produced.
- f) Block polymers can be synthesized by sequential monomer addition.
- g) Chain end-functionalized polymers can be prepared in quantitative yield.

These properties of living polymerizations could be closely fulfilled only with ionic and coordination polymerization methods for a limited number of monomers under demanding conditions in the past.

1.3. Comparison of Living Polymerization Systems with Free-radical Polymerization

The differences between living and free radical polymerizations are illustrated in molar mass vs. conversion and conversion vs. reaction time graphs in Figure 1.1. In living polymerizations, all growing chains are simultaneously initiated, and grow parallel to each other. So, there is a continuous increase of molar mass with conversion as illustrated in Figure 1.1.a. In the course of free-radical polymerization, the growing chains are activated only slowly after beginning of polymerization. There is continuous initiation and termination, as discussed before. Since the chains are not initiated simultaneously, there is no linear evolution molar mass with conversion (cf. Figure 1.1). Polymers with high molar mass appear already at very low conversions. Under similar conditions, the rates of free-radical polymerizations are low compared to living polymerizations (cf. figure 1.1.b), as the polymer chains are activated in a serial manner in free-radical polymerization and the momentary concentration of active centers is low.

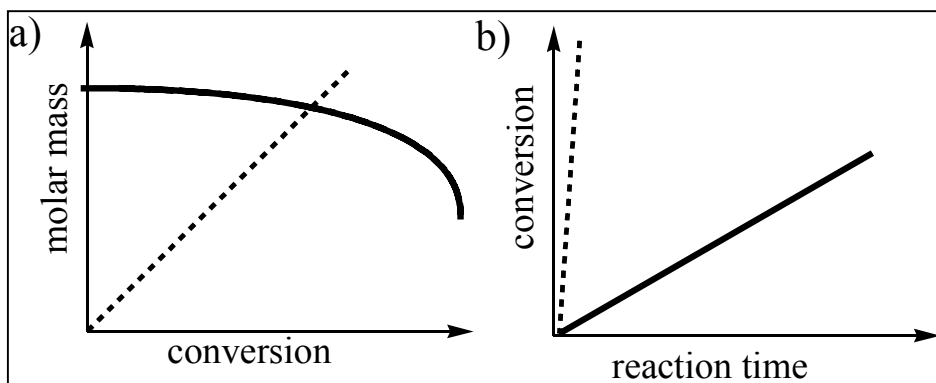


Figure 1.1. a) Molar mass vs. conversion and b) conversion vs. time graphs for living (dashed line), and radical (solid-line) polymerizations (idealized).

1.4. Controlled Radical Polymerization Methods (CRP)

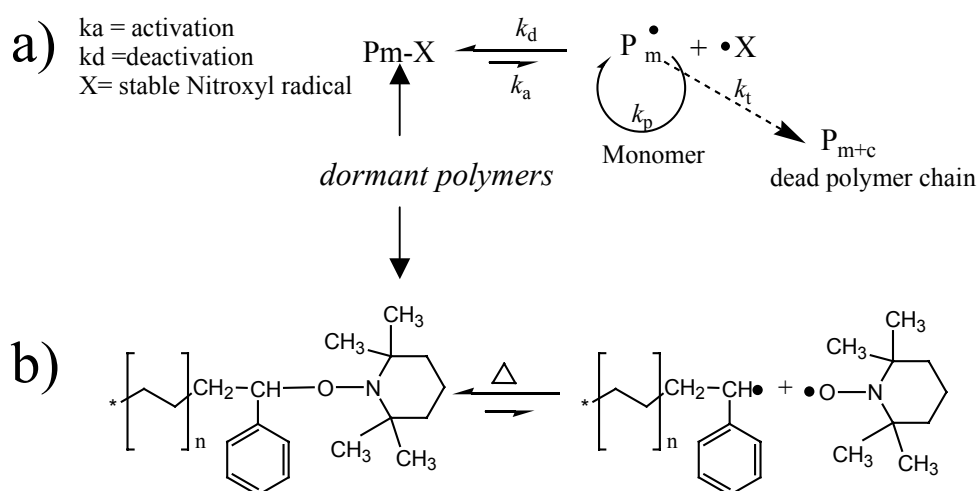
The success of living polymerization systems stems from the parallel growing chains without the termination reactions. In analogy, CRP methods also provide parallel growth of the polymer chains, while keeping the radical concentration as low as in the conventional free-radical polymerization. The key idea of CRP is the addition of a dominant termination reaction, which is reversible in one or the other way, to the kinetic scheme (see Scheme 1.1) Accordingly, two types of growing chains exist in the polymerization, namely active polymer radicals and temporarily inactive (“dormant”) polymer species which can be reversibly transformed into active chains. The number of dormant chains is much higher than the number of active chains. The CRP methods benefit from different fast dynamic equilibriums between active and dormant chains to obtain parallel propagation chains. The rates of these equilibrium reactions should be reasonably faster than the rate polymerization. By this strategy, momentary radical concentration is kept low. But the continuous activation-deactivation of the reversibly terminated polymer chains enables continuous chain growth for every macromolecule over the full span of monomer conversion. Thus, average lifetime of a polymer chain capable of growing is long enough to satisfy mostly criteria of Quirk and Lee for living polymerizations. But, differing from living polymerization systems, the inherent termination reactions of radicals are not eliminated.

The CRP methods are a good imitation of living polymerization systems. They present properties between living and free radical polymerizations. There is a linear

1. Introduction

evolution of molar mass like in living systems. But the rates of polymerization are similar to that of free radical polymerization or even lower, since only small percentage of the parallel growing chains can be active simultaneously, in contrary to living systems. Similar to living polymerization systems, CRP provides polymers with low polydispersities, defined end groups and complex architectures (e.g. star, branched or block copolymers) but with lesser degree of perfection. However compared to ionic polymerizations, CRP can be run under much milder conditions, and be used for a much wider ranged monomers, temperatures and solvents.

1.4.1. Nitroxyl Mediated Polymerization (NMP)



Scheme 1.2. a) General mechanism for the propagation step of NMP b) polymerization of styrene under the control of TEMPO.

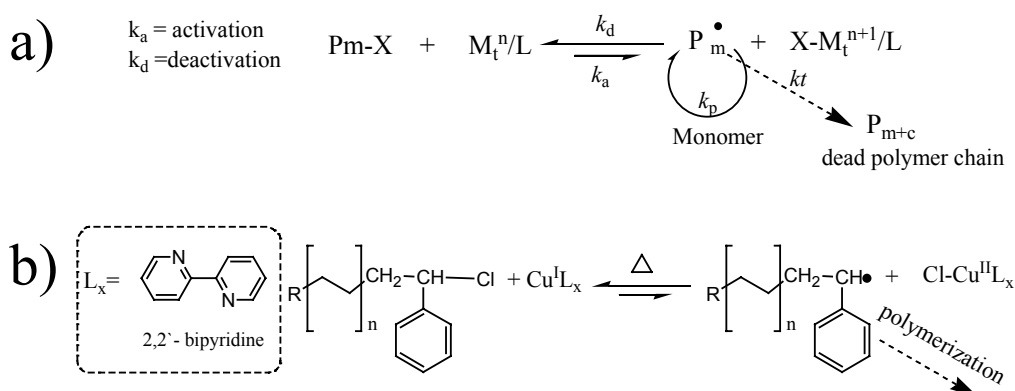
FRP involving stable nitroxyl radical radicals in the polymerization medium is called Nitroxyl Mediated Polymerization (NMP). Usage of NMP was first demonstrated by Solomon et al [3], and the method is one of the most successful CPR methods.. Nitroxyl radicals are stable radicals which cannot initiate the polymerization of olefins, but they can reversibly react with carbon-centered radicals ' $P_i\cdot$ ' to form N-alkyloxyamines. The formed covalent ' P_i -O-' bond of N-alkyloxyamines (P_i -O-N<) are weak and can be broken by thermal homolysis to regenerate the radicals. A general mechanism for propagation step of NMP, and the polymerization of styrene in the presence of 2,2,6,6-tetra methylpiperidin-1-yloxy (TEMPO) as a special example are presented in Scheme 1.2. The equilibrium between dormant and active chains is shifted in the direction of the dormant side. The

1. Introduction

equilibrium can be shifted in the direction of active side by increasing the polymerization temperature. Polymers prepared by this method have oxyamine groups at one end of the chains and an initiator residue at the other end.

1.4.2. Atom Transfer Radical Polymerization (ATRP)

ATRP is a radical process to fulfill the conditions required for CRP by using a redox-active transition metal compound in combination with a suitable alkyl halide. The transition metal compound reversibly activates an alkyl halide to form an active radical and a metal halide complex by oxidative addition of the halide. The radical concentration is kept low compared to the alkyl halide concentration by arranging the concentration of the transition metal ligand complex. A general mechanism for the propagation step of ATRP, and the polymerization of styrene via ATRP in the presence of metal ligand complex of CuCl and 2,2'-bipyridine as an example are depicted in Scheme 1.3.



1.4.3. Reversible Addition Fragmentation Chain Transfer Polymerization (RAFT)

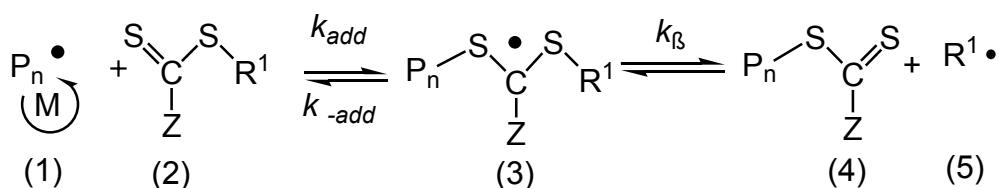
RAFT polymerization is the most successful one among degenerative chain transfer polymerizations (see Figure 1.2). The method typically employs dithiocarbonyl derivatives as chain transfer agents. In RAFT polymerizations, there is no reversible deactivation of growing polymer chains, but there is a transfer of activity between polymer chains bearing dithioester moieties instead. The widely accepted mechanism of RAFT polymerization is shown Scheme 1.4 [9]. It comprises 5 steps. The first step is the

1. Introduction

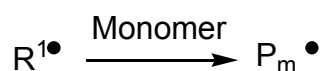
initiation:



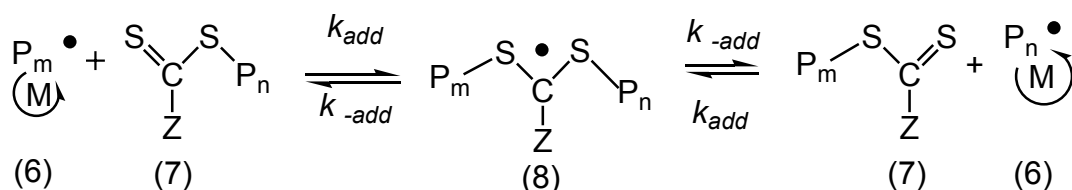
chain transfer:



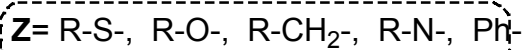
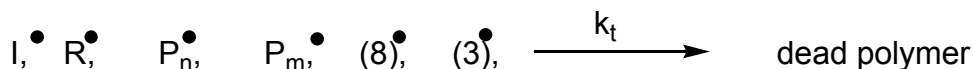
reinitiation:



chain equilibration:



termination



Scheme 1.4. The proposed RAFT mechanism using dithiocarbonyl derivatives [9].

conventional production of radicals, which can add to monomer to produce propagating oligomeric-radicals, from any radical source. The chain transfer step includes the reaction of the propagating oligomeric-radicals (1) with specially designed RAFT agents (2) to form transient radicals (3). These transient radicals can fragment back to the original oligomeric radicals, or to the direction of a leaving group ‘R¹·’(5) of the RAFT agent and the newly formed Macro chain transfer agent (CTA) (4). The driving forces for the direction are the thermodynamic stability of emitted radical and the strength of the S-C bonds in both CTAs (2) and (4). If the homolytic cleavage is favored in the direction of oligomeric-radicals (1) derived from the monomer being polymerized, the RAFT agent only plays the role of a retarder. Thus, ‘R¹·’(5) should be carefully chosen to prevent any complication. It should be a good free radical leaving group by itself and also in

1. Introduction

comparison to the original propagating oligomeric radicals (1). The next step is the re-initiation. The radicals ' R^1 ' (5) produced from the RAFT agent must be able to react with the monomer to produce new propagating polymer chains. If the intermediate radical ' R^1 ' (5) is too stable relative to the propagating radicals ' P_n ' (1), the RAFT agent will act as an inhibitor. For instance, the triphenylmethyl radical is a perfect leaving group for the chain transfer step, but it cannot react with monomers to produce new growing chains, since it is a too stable radical. When the previous steps are successful, the controlled polymerization takes place in the chain equilibration step. As both fragmentation pathways of the formed Macro transient radicals (8) are equivalent, active and dormant chains are interconverted efficiently. The only important parameter is the affinity of the propagating radicals (6) towards the macro-RAFT agents (7), which is regulated by the Z group. Different monomers may need different Z groups. The last reaction occurring in reaction sequence is the classical termination. Terminations exist throughout the whole polymerization, but it is a minor process compared to propagation unless long polymerization times employed. In addition to the termination reactions seen for conventional free-radical polymerization, it has also been claimed that transient- macro RAFT radicals (3), and (8) may undergo some irreversible termination reactions [16,17, 18], e.g. by recombination with species $I\cdot$, $R_1\cdot$, or $P_n\cdot$. But this is a matter of ongoing controversy [19, 20].

Before describing some important details about RAFT polymerizations, its differences from ATRP and NMP and the reasons for choosing RAFT for the application of CRP in water are discussed. NMP often needs high polymerization temperatures above 100 °C. If the boiling point of water is considered, the usage of pressurized reactors may be necessary. In addition, water is an aggressive solvent, and the hydrolytic stability various reactants will be reduced at high temperatures. Further, NMP is applicable to a relatively small number of monomers. It works very well with styrenic monomers, but it is difficult to apply to methacrylates and methacrylamides. Controlled polymerization of acrylates and acrylamides is possible, but needs specially designed nitroxyl compounds. To use them in a water-based system, hydrophilic moieties have to be chemically attached to these compounds [21-23]. If the need of different nitroxyl compounds for different functional monomers is taken into consideration, NMP synthetically looks challenging to be applied in water, as well.

1. Introduction

ATRP can be used for many monomers (styrenic, (meth)acrylates, and (meth)acrylamides) in a large range of temperatures similar to RAFT. But the solvent selection is important for proper catalyst activity. Many ATRP catalysts are sensitive to the presence of water. Many of the ligands used in ATRP are based on nitrogen, and their protonation prevent their coordination to the transition metal center. Moreover, many hydrophilic functional groups, which may act as ligands for the metal center (such as –CONR₂, -CN, -OH, -COOH, -S(=O)-, etc.) can interfere with the formation of the active catalyst. Therefore the polymerization of monomeric carboxylic acids, or monomers like vinylpyridine may be problematic. Vinylpyridine containing polymers are water-soluble, and find application as coordination reagents for transition metals. However, their coordinating ability for transition metals makes their polymerization via ATRP challenging. As the monomer exists in excess compared to the ligands, it replaces the ligands in the catalyst complexes of the transition metals, render them inefficient catalyst for ATRP [24]. Apart from these difficulties, most of the used transition metals are toxic. Therefore they have to be removed from the polymer after synthesis. This is not trivial, in particular when the polymer bears many complexing moieties, and this is typically the case for water-soluble polymers.

Another difference of NMP and ATRP to RAFT is the continuous reduction in active radicals as polymerization proceeds [25]. Termination reactions are only delayed but not prevented, and the polymerization system is not fed continuously from a radical source like RAFT polymerization to compensate for terminated radicals. After a while, because of the reduction in both radical concentration and monomer concentration, the rates of polymerization decrease to a level where the conversion is virtually stopped. RAFT does not suffer from this problem. The steady state approximation done for conventional free-radical polymerization is also valid for RAFT polymerization, as the terminated radicals are compensated by newly initiated chains from the radical source.

RAFT appears to be extremely versatile in term of tolerance to monomer functionality and solvent, and is applicable to nearly all types of radically polymerizable monomers. It works under mild conditions, similar to conventional free-radical polymerization. Conventional radical initiators are used. Many RAFT agents behave as ideal chain-transfer agents so that the rates of the polymerizations are similar (within ±20 %) to those in the absence of the RAFT agents [26]. RAFT gives slightly colored

1. Introduction

compounds due to the weak dithioester absorption in the visible band (the forbidden $n \rightarrow \pi^*$ transition of the C=S group). A possible disadvantage is the production of sulfur containing compounds due to the dithiocarbonyl end groups. But the color and the sulfur in the final products can be easily avoided by hydrolyzing end groups after polymerization with bases or by oxidants. In conclusion, RAFT is arguably the most promising among the CRP methods to employ in aqueous systems. It was therefore the method of choice for the synthesis of well-defined water-soluble macromolecules.

1.5. A Closer Look to RAFT Polymerization

There are numerous available RAFT agents, which vary in the nature of the R and Z groups (see in Figure 1.2. the general structure of a RAFT agent). The structure of the R and Z groups plays a crucial role in controlling the molar mass distribution and the rates of polymerization. The Z group either activates or deactivates radical reactions towards the C=S bond. This is one of the determining factors for the average lifetime of the transient-macro-RAFT radicals (3) and (8) (cf. Scheme 1.4), and this controls the rates of polymerization. Figure 1.2 presents various examples of Z and R groups for RAFT agents. Two or more polymer chains can be simultaneously initiated from a RAFT agents (Figure 1.2 a1, d1). RAFT agents can have different functional groups like double bonds, or some halogens, which may be used for further functionalization of the polymers after the polymerization. (respectively Figure 1.2 “b1”, “c1”). Fluorescent labels can be attached to both R and Z groups (see Figure 1.2 e1).

For conventional chain transfer reactions, the chain transfer constant C_{tr} is defined as the ratio of the rate constant for chain transfer to that of propagation (k_{tr}/k_p). In chain transfer step of RAFT polymerization, k_{tr} is defined as in equation 5 [26], as a term composed of the rate constant of the addition to the thiocarbonyl group k_{add} (Scheme 1.4), and the rate constants of the homolytical cleavage of the transient persistent radical (3) to the side of the propagating oligomers (1) k_{-add} and to the side of the leaving R group of RAFT agent (5) k_{β} . When the polymerization gets into the chain equilibration step (cf. Scheme 1.4.), k_{tr} is defined as in equation 6 [27].

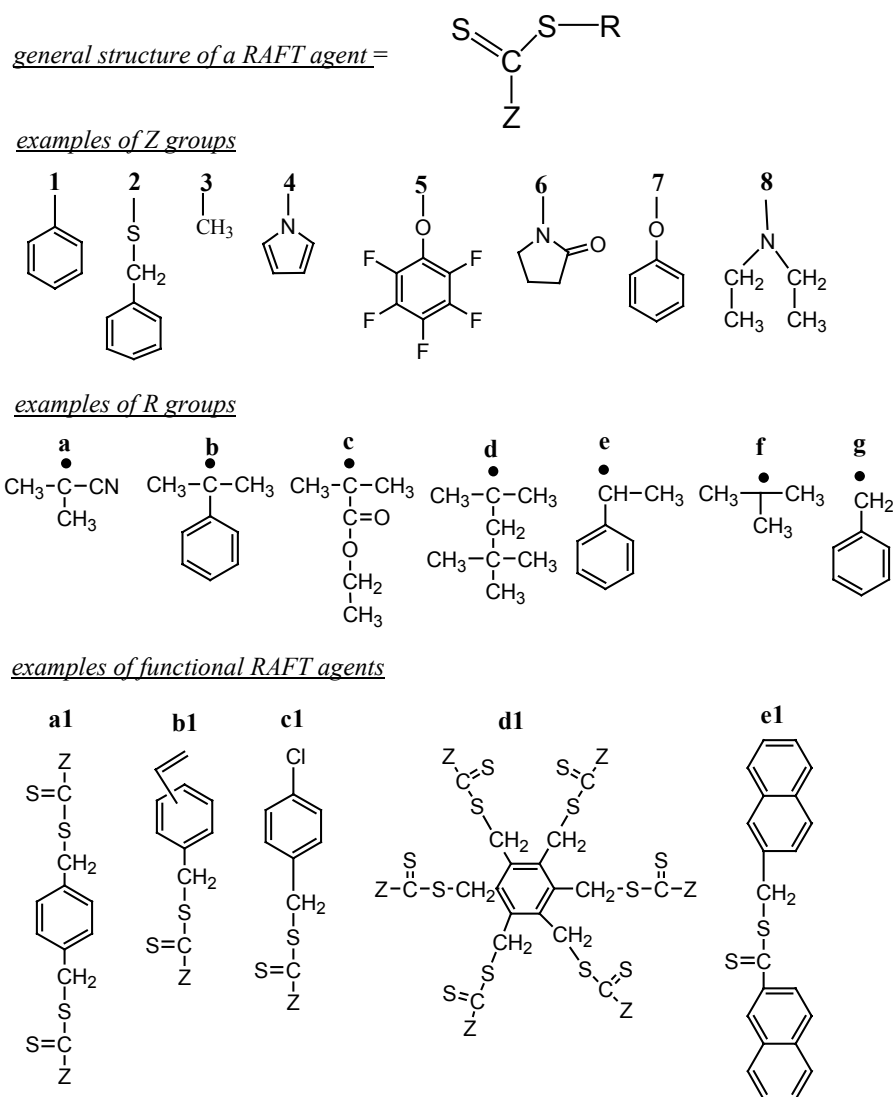


Figure 1.2. Examples of RAFT agents with different R and Z groups.

$$k_{tr} = k_{add} \cdot \frac{k_{\beta}}{k_{-add} + k_{\beta}} \quad (\text{eq. 5})$$

$$k_{tr} = \frac{k_{add}}{k_{-add}} \quad (\text{eq. 6})$$

Depending on both R and Z groups, various thiocarbonylthio compounds may show a difference of order of several magnitudes in chain transfer constants C_{tr} (< 0.01 to >1000) [28]. In order to obtain decent control over the polymerization ($PDI < 1.5$), C_{tr} should be greater than 2 according to the theory [29,30].

1. Introduction

Depending on the Z group, the chain transfer constants C_{tr} decrease in the following order aryl > alkylthio ~ alkyl ~ pyrrole > perfluoro aryloxy > amido > aryloxy > dialkylamino (cf Figure 1.2). C_{tr} values obtained from the study of Moad et al [26] for the polymerization of styrene under the control of different benzylthiocarbonylthio compounds [ZC(S)SCH₂Ph] are given for comparison in Table 1.1.

Table 1.1. Apparent transfer constants C_{tr} for benzyl thiocarbonylthio compounds for styrene polymerization at 110 °C. (The Z groups represented with numbers are shown in Figure 1.2)

Z	1	2	3	4	5	6	7	8
C_{tr}	26	18	10	9	2.3	1.6	0.72	0.01

For a polymerization of monomer, the R groups are only effective for C_{tr} in the initial chain transfer step (see Scheme 1.4). The C_{tr} values obtained from the study of Moad et al [26] for chain transfer step are given in Table 1.2. for controlled polymerization of methyl methacrylate by employing different dithiobenzoate derivatives PhC(=S)SR. After the initial chain transfer step, it should be taken into account that, the R group changes, since it is converted into a monomer derived polymer.

Table 1.2. Apparent transfer constants C_{tr} for the initial chain transfer step of methyl methacrylate polymerization at 60 °C by employing dithiobenzoate derivatives PhC(=S)SR (The R groups represented with letters are shown in Figure 1.2)

R	a	b	c	d	e	f	g
C_{tr}	13	10	2	0.4	0.16	0.03	0.03

In RAFT, molar masses increase with conversion, and can be predetermined by the stoichiometric ratio of RAFT agent to monomer. In case of monofunctional RAFT agents, theoretical molar mass ($M_{w,theoretical}$) is calculated by using equation 7. Since the number of initiator-derived chains are generally small compared to the number of RAFT agent derived chains, the term $2f[I]X$ can be neglected in most cases.

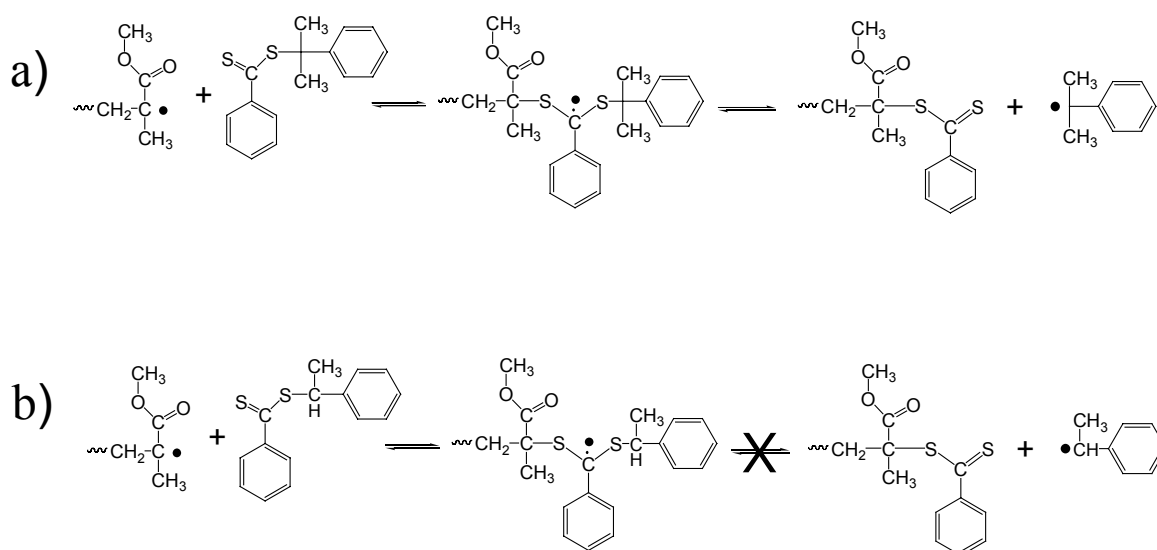
$$M_{w,theoretical} = \frac{[M] \cdot [Mwt_{monomer}]}{[CTA] + 2 \cdot f \cdot [I] \cdot \chi} \cdot \%conv + Mwt_{CTA} \quad (\text{eq. 7})$$

-“%conv.” is percent monomer conversion,

1. Introduction

- “[M_{wtCTA}]” is molecular weight of RAFT agent,
- “[M]” is the moles of the monomer used,
- “[CTA]” is mole of chain transfer agent,
- “2” is a factor used for thermal initiators, since their decomposition produces 2 radicals,
- “ f ” is the initiator efficiency (it generally lies between 0.5 and 1),
- “ X ” is the percent of radical decomposition at a given temperature after a certain time,
- “ $2f[I]X$ ” all together corresponds to the number of initiator-derived chains.

The choice of the RAFT agent plays the key role in CRP of a monomer. As a specific example, vinyl acetate (VA), which is a commercially important monomer, can only be polymerized in a controlled manner via RAFT if xanthates are used as CTA. Xanthates are poor controlling agents for many monomers, but in the case of VA polymerization, they are necessary to reduce the stability of transient macro RAFT radicals (Scheme 1.4. (8)) [31].



Scheme 1.5. Effect of the R group in reversible addition chain transfer, exemplified for the polymerization of methylmethacrylate [32].

Another specific example can be given for the polymerization of methyl methacrylate with CTAs 1-phenylethyl dithiobenzoate and cumyldithiobenzoate in the study of Quinn et al [32]. The UV initiated polymerization of methyl methacrylate yielded no evidence of living behavior when 1-phenylethyl dithiobenzoate is used as a CTA. However, there is control if cumyl dithiobenzoate is used. The reason why polymerization does not proceed in a controlled manner with 1-phenylethyl dithiobenzoate is that the

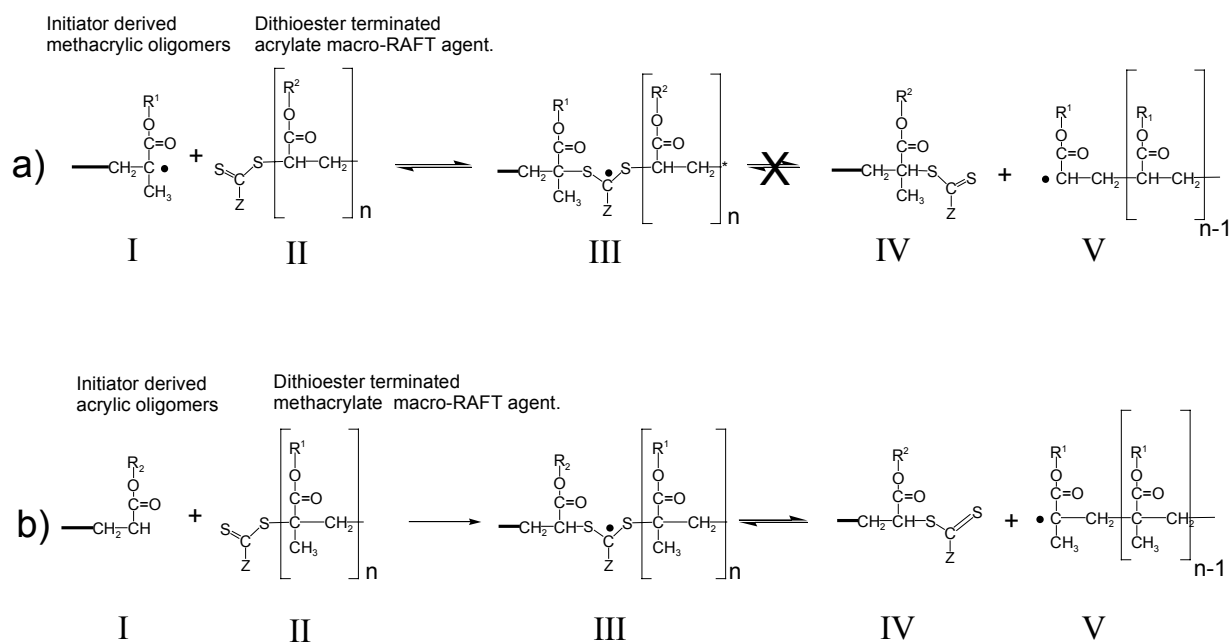
1. Introduction

leaving group 1-phenylethyl “R” is not a good leaving group relative to the methylmethacrylate oligomers. As depicted in Scheme 1.5, in both cases propagating methyl methacrylate radicals add to the thiocarbonyl group of dithioester. However, when the leaving group is 1-phenylethyl (scheme 1.5. b), the macro radical will preferentially dissociate back to produce propagating methacryloyl radicals. This will prevent the degenerative exchange of growing polymer chains with the RAFT agent, and the polymerization will proceed in an uncontrolled way. On the other hand, when the leaving group is cumyl, it can leave the transient macro RAFT radical, and initiate a new propagating chain in the polymerization of methylmethacrylate.

By RAFT polymerization, the preparation of block copolymers is also possible by sequential monomer addition. For this purpose, the polymer chains bearing dithioester end groups made from one monomer are employed as macro RAFT agents in the polymerization of second monomer. The R¹ leaving group (see “5” in Scheme 1.4.) becomes the previously polymerized chain. So the requirements described for R¹ must be fulfilled by the first polymerized polymer block. If the polymer blocks of a copolymer are based on the same polymerizable group e.g. styrenic - styrenic, the blocking often works smoothly. But, if the synthesis of a block copolymer from monomers having different reactivity (like methacrylic and acrylic) are aspired, the order in which the monomers are polymerized, is important. The reason for that is again the preferential fragmentation of transient macro-RAFT radicals (Scheme 1.4. “3”) in the direction of most stable radical in chain transfer step. That can be exemplified for the synthesis of diblock copolymer of a methacrylic and an acrylic monomer. The tertiary radicals derived from methacrylates are more stable than the secondary radicals derived from acrylates. If the controlled polymerization of the acrylic monomer is carried first, the blocking of methacrylic monomer can be problematic. Because the transient macro RAFT radicals (see Scheme 1.6. a “III”) which form after the addition of the methacrylic oligomers (Scheme 1.6.a “I”) to the acrylic macro RAFT agent (Scheme 1.6.a “I”). The macro-RAFT agent Scheme 1.6.a “II”) cannot be activated to give an acrylic radical (Scheme 1.6.a “V”). However, if the methacrylic macro-RAFT agent Scheme 1.6.a “II”), decay preferentially back to the direction of the methacrylic oligomers (as in scheme 1.6.b “II” is used, the transient macro-RAFT radicals obtained after the addition of acrylic oligomers (Scheme 1.6.b “III”) decay to produce polymethacrylate radicals (Scheme 1.6.b “V” which can react with acrylic monomer in the reinitiation step. Later the polymerization can get into the chain

1. Introduction

equilibration step (see Scheme 1.4) without problem, and CRP proceeds to give a block copolymer.



Scheme 1.6. The illustrated chain transfer step of RAFT polymerization (cf. Scheme 1.4) for block copolymer synthesis when a macro RAFT agent is employed.

Polymerization conditions like temperature, molar ratio of RAFT agent to initiator, or solvent, should be chosen carefully. The increase in temperature will fasten both the rate of fragmentation and polymerization; a decrease in temperature slows down the polymerization rate but hardly the rates of termination reactions. RAFT agent and initiator should be well soluble in the monomer, or in the solvent (if used). The employed initiator, solvent and eventual other additives should have very low transfer constants towards the propagating radicals. Otherwise, unwanted chain transfer reactions will reduce the control over the polymerization.

It should always be kept in mind that RAFT polymerizations yield inactive chains at least equal to the number of initiator derived chains at the end of the polymerization. Therefore, the molar ratio between RAFT agent and the initiator should be precisely arranged to minimize initiator-derived chains. It is suggested by Le et al. [9] that the total moles of initiator derived chains during polymerization should be less than half the moles RAFT agent (more preferably $[\text{initiating radicals}]/[\text{CTA}] < 0.2$). Moreover, the

1. Introduction

decomposition half-life of the initiators should be taken into consideration at a given polymerization temperature. It is not important how much initiator is engaged compared to the RAFT agent, but how many radicals are produced during the polymerization at the given temperature.

The rate of radical production is a key parameter for the success of RAFT polymerizations. On the one hand, the system has to provide enough new radicals to compensate for terminated chains, and to keep the polymerization at a decent rate. On the other hand, the rate of new radical production should not be so high to reduce termination reactions. Therefore a good compromise must be found. In contrary to ATRP and NMP methods as mentioned before, RAFT polymerization have a constant radical concentration in a defined system.

Another crucial parameter that should be kept in mind is conversions. The RAFT polymerization should not be pushed to very high conversions if the synthesized polymers shall serve as macro-RAFT agents for the addition of another block. At high conversion, the rate of polymerization decreases with the reduction of the monomer concentration, and so, chain propagation slows down. But there is no reduction in the rates of termination reactions, as the radical concentration is kept constant by new initiated chains. It is therefore highly probable that dithioester end groups are partially transferred to new initiated chains, and so the number of dead long chains without dithioester end groups increases. The latter cannot be used as macro-RAFT agent anymore. Moreover, the new created chains cannot reach high molar masses, as the rate of propagation is slow at high conversions. It is highly probable that these oligomeric chains, which take over the dithioester end groups, will be lost during the purification steps (e.g. dialysis or precipitation of the polymer) which are often employed to remove unreacted monomer. Note that this effect cannot be quantified by physical analysis done on polymers like size exclusion chromatography, but can only be determined by end group analysis, for instance via optical spectroscopy, because the dithioester derivatives absorb the at UV-vis bands.

To summarize, the RAFT agent should be carefully chosen for a given monomer. The blocking sequence must be taken into the consideration for the synthesis of block copolymers. If thermal initiators are employed, the polymerization temperatures should be selected according to the half-life of the initiator employed to keep a decent constant

1. Introduction

radical concentration which provides a fast rate of the polymerization with minimum termination reactions. If the above stated details are respected, RAFT method is effective tool for the synthesis of well-defined polymers with complex architectures.

References

- [1] Odian G. Principles of Polymerisation, 3rd ed. John Wiley& Sons, Inc, 1991 ISBN 0-471-61020-8.
- [2] Moad G, Solomon DH. *The Chemistry of Free Radical Polymerization*. Oxford: Pergamon 1995.
- [3] Solomon DH, Rizzardo E, Cacioli P. **1986**; *US patent* 4,581429.
- [4] Georges MK, Veregin RPN, Kazmaier PM, Hamer GK. *Macromolecules* **1993**, *26*: 2987.
- [5] Hawker CG, Bosman AW, Harth E. *Chem. Rev.* **2001**, *101*, 3661.
- [6] Matyjaszewski K. *Macromol. Symp.* **2000**, *152*, 29.
- [7] Coessens V, Pintauer T, Matyjaszewski K. *Prog. Polym. Sci. Symp.* **2001**, *26*, 337.
- [8] Kamigaito M, Ando T, Sawamoto M. *Chem. Rev.* **2001**, *101*, 3689.
- [9] Le TPT, Moad G, Rizzardo E, Thang S. *Intern. Pat. Appl.* 1998; PCT WO9801478 [CA 1998: 115390].
- [10] Moad G, Mayadunne RTA, Rizzardo E, Skidmore M, Thang SH. *Macromol. Symp.* **2003**, *192*, 1.
- [11] Barner-Kowollik C, Davis TP, Heuts JPA, Stenzel MH, Vana P, Whittaker M. *J. Polym. Sci. Polym. Chem.* **2003**, *A41*, 365.
- [12] Charmot D, Corpart P, Michelet D, Zard SZ, Biadatti T. *Intern. Pat. Appl.* **1998**; PCT WO9858974.
- [13] Cowie JMG, *Polymers: Chemistry and Physics of Modern Materials, Second edition Blackie Academic & Professional* 1991, ISBN 075140134X.
- [14] Quirk RP, Lee B. *Poly. Int.* **1992**, *27*, 359.
- [15] Wang J-S, Matyjaszewski K. *J. Am. Chem. Soc.* **1995**, *117*, 5614.
- [16] Monteiro MJ, Brouwer H. *Macromolecules* **2001**, *34*, 349.
- [17] Kwak Y, Goto A, Komatsu K, Sugiura Y, Fukuda T. *Macromolecules* **2004**, *37*, 4434.
- [18] Kwak Y, Goto A, Fukuda T. *Macromolecules* **2004**, *37*, 1219.
- [19] Coote ML. *Macromolecules* **2004**, *37*, 5023.

1. Introduction

- [20] Toy AA, Vana P, Davis TP, Barner-Kowollik C. *Macromolecules* **2004**, *37*, 744.
- [21] Nicolas J, Charleux B, Guerret O, Magnet S. *Macromolecules* **2004**, *37*, 4453.
- [22] Olive G, Rozanska X, Smulders W, Jacques A, German A. *Macromol. Chem. Phys.* **2002**, *203*, 1790.
- [23] Huang W, Charleux B, Chiarelli R, Marx L, Rassat A, Vairon JP. *Macromol. Chem. Phys.* **2002**, *203*, 1715.
- [24] Matyjaszewski K, Patten TE, Xia J. *J. Am. Chem. Soc.* **1997**, *119*, 674.
- [25] Fischer H. *J. Polym. Sci. Part A: Polym. Chem.* **1999**, *37*, 1885.
- [26] Moad G, Moad CL, Rizzardo E, Thang SH. *Macromolecules* **1996**, *29*, 7717.
- [27] Barner-Kowollik C, Quinn JF, Nguyen TLU, Heuts JPA, Davis T. *Macromolecules* **2001**, *34*, 7849.
- [28] Moad G, Chiefari J, Chong YK, Krstina J, Mayadunne RT, Postma A, Rizzardo E, Thang SH. *Poly. Int.* **2000**, *49*, 993.
- [29] Müller AHE, Zhuang R, Yan D, Litvenko G. *Macromolecules* **1995**, *28*, 4326.
- [30] Müller AHE, Litvenko G. *Macromolecules* **1997**, *30*, 1253.
- [31] Stenzel, MH, Cummins L, Roberts GE, Davis TP, Vana P, Barner-Kowollik C. *Macromol Chem. Phys.* **2003**, *204*, 1160.
- [32] Quinn JF, Barner L, Barner-Kowollik C, Rizzardo E, Davis TP. *Macromolecules* **2002**, *35*, 7620.

2. SYNTHESIS OF WATER-SOLUBLE RAFT AGENTS

RAFT polymerization has been in the focus of many research groups. Numerous publications have been reported on the mechanism, parameters effecting performance, or the application of method to synthesis well defined macro molecular structures. But, its application to aqueous systems has been neglected. There are several reasons behind this. One of them is that the number of water-soluble-RAFT agents was limited, as their synthesise is not as trivial as organic soluble ones. Some common routes used to synthesis RAFT agents cannot be applied to obtain water-soluble RAFT agents. Because most hydrophilic groups, which should be attached to RAFT agents to provide water solubility, are not compatible with the used solvents, reagents or the dithioester functionality of the RAFT agents themselves. In addition, their purification is often challenging, too. When the hydrophilic groups are attached to the RAFT agents, they become amphiphilic. To benefit from column chromatography, which is often used for purification, is not trivial for the purification of such amphiphilic compounds. If silica gel is used, the hydrophilic fragment tends to stick to the column; if reverse phase columns are employed, the hydrophobic fragments trouble the separation. Beside, in many synthetic routes to RAFT agents, inorganic salts are side product of the reactions. Their removal from water-soluble RAFT agents cannot be achieved by simple selective precipitation of inorganic salts as in the case of organic soluble RAFT agents, since the solvents are the same for both the RAFT agents and the salts, such as DMF, DMSO, methanol or water. Therefore, they have to be purified by fractionate precipitation, which is not trivial.

Water-soluble RAFT agents are needed to perform RAFT polymerizations in water. However, contrary to the wide diversity of organic soluble-RAFT agents reported, 4-cyano 4-thiobenzoylsulfanylpentanoic acid (**CTA1**) was the only established water-soluble RAFT agent at the beginning of this thesis. But, **CTA1** is soluble only if the pH is arranged to a certain value (>5), and suffers from a low stability in water at elevated temperatures, as it will be described later. The synthesis of new RAFT agents, which are more stable compared to **CTA1** and soluble in water independent of pH, was crucial for the studies on the feasibility of RAFT polymerization in water and for further developing the technique

2. Synthesis of water-soluble RAFT agents

for the synthesis of new homo- and block polymers in aqueous media. Therefore, first efforts focused on the synthesis of new CTAs for RAFT polymerization.

In this chapter, the most used synthetic methods to obtain RAFT agents are described, and later the usefulness of them for the synthesis of water-soluble RAFT agents is discussed. Finally both successful and failing synthetic routes, which were tried, are presented.

2.1. The most used reaction routes to dithioesters

2.1.1. *Synthesis of dithiobenzoic acid*

Dithiocarboxylic acids and their salts are the main precursors for the synthesis of RAFT agents (dithioesters, see Figure 2.1). There are several ways for their synthesis, but the usage of Grignard reagents is the most convenient method, as CS₂, many alkylating agents, and many Grignard compounds are commercial products, or are readily made. However as dithiobenzoates are susceptible to light and oxygen, the fresh production and fast consumption of them is the best. The general scheme for the formation of dithiocarboxylic acids by the Grignard method is described in Figure 2.1 **I-a**. In this study, the method of Becke and Hagen [1] was explored alternatively to synthesize dithiobenzoates. The reaction is shown in Figure 2.1 **I-b**. However, when the sodium salt of dithiobenzoate, synthesized by this method, is used to prepare dithioesters via the alkylation of anions, the resulting dithioesters are contaminated with the thioester analogs, which are difficult to separate with conventional purification methods. In fact, thiobenzoate is a byproduct of the method of Becke and Hagen because of an uncompleted reaction. Another disadvantage of this method is that, the procedure is time consuming, and that made it necessary to synthesize large amounts of dithiobenzoate and to store them. But the storage may result e.g. in hydrolysis and reduce the quality of the compound. Therefore, this method was given up in the course of thesis.

2.1.2. *Alkylation of dithiocarboxylates*

One of the most popular methods for the synthesis of RAFT agents is the alkylation of salts of dithiocarboxylic acids. Many RAFT agents can be synthesized via this route.

2. Synthesis of water-soluble RAFT agents

The reaction works smoothly and fast with primary and secondary alkyl halides without sterically hindering, bulky groups (see Figure 2.1 **II-a**). But for tertiary alkyl halides, the yields are reduced, and higher temperatures are needed depending on the bulkiness of the alkyl group. As a specific example of this approach, benzyl dithioacetate is prepared by the alkylation of dithioacetate with benzyl bromide (Figure 2.1 **II-b**)[2].

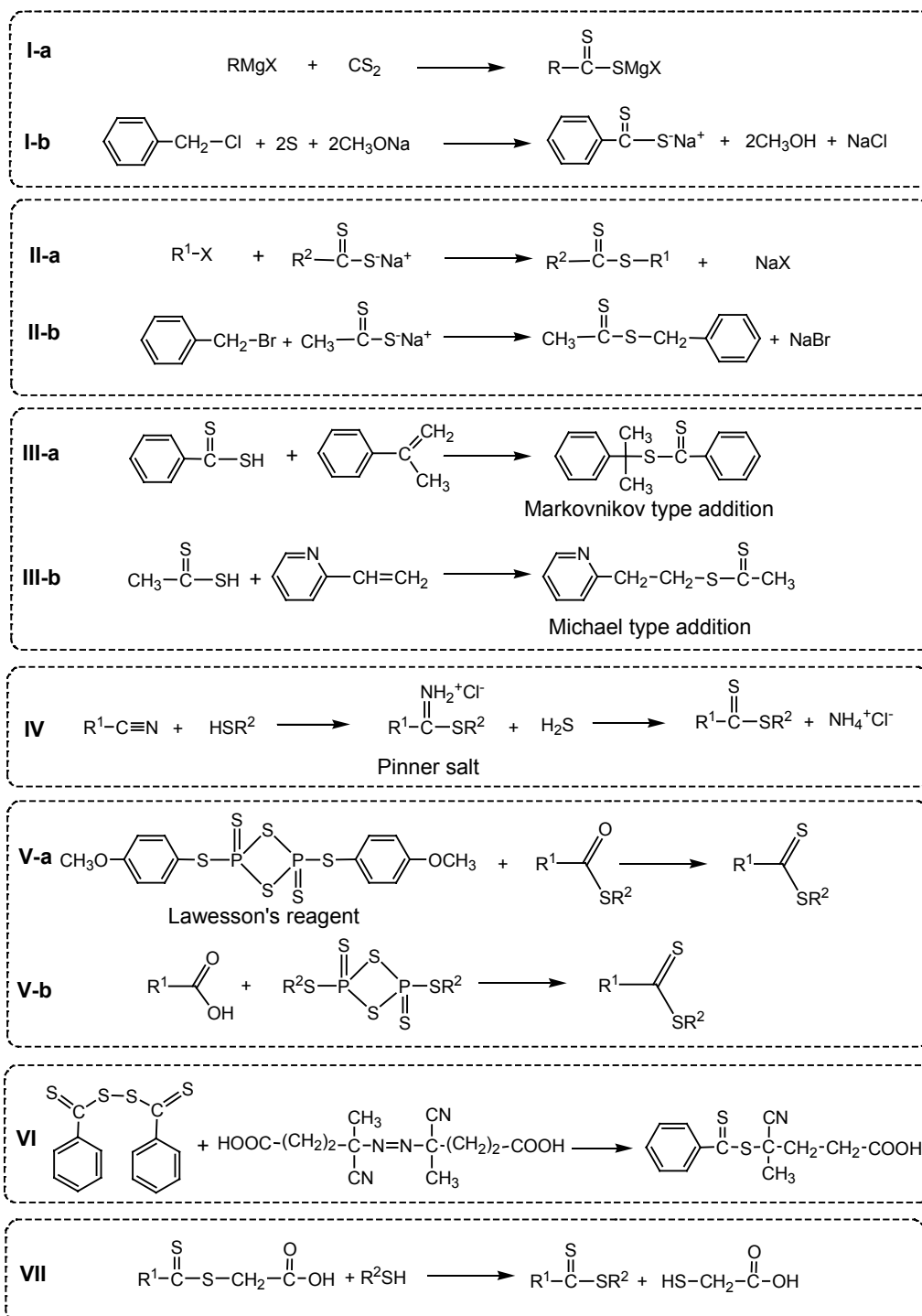


Figure 2.1. The most used reaction routes to dithioesters.

2. Synthesis of water-soluble RAFT agents

2.1.3. Addition of dithiocarboxylic acids to olefins

Dithiocarboxylic acids can add to electrophilic olefins such as acrylonitrile and vinyl pyridine, as well as to nucleophilic olefins such as α -methylstyrene. The reaction follows Markovnikov type addition when the olefin is nucleophilic and Michael type addition when the olefin is electrophilic [3]. The general procedure is to mix dithioic acid and the corresponding olefin in a solvent like CCl_4 and heating. As an example of the Markovnikov type addition, the addition of dithiobenzoic acid to α -methylstyrene is shown in Figure 2.1. **III-a** [3]. The Markovnikov addition is influenced by the ability of the substituents to stabilize the carbenium ion formed by the initial protonation. As an example of the Michael addition, the addition of dithioacetic acid to 2-vinyl pyridine is shown in Figure 2.1. **III-b** [3].

2.1.4. Synthesis of dithioesters using Pinner salts

Thiols react with nitriles in the presence of hydrogen chloride to give imidothioesters (Pinner salts). They are the key intermediates in the synthesis of dithioesters. The Pinner salts are reacted with H_2S to obtain the corresponding dithioester (cf. Figure 2.1. **IV**) [4, 5].

2.1.5. Conversion of thioesters to dithioesters by using Lawesson's reagent

Thioesters, which are more stable and easier to synthesize compared to dithioesters, can be converted to dithioesters by thionation reagents like Lawesson's reagent (Figure 2.2. **V-a**). Another possibility is the reaction of carboxylic acids with S-alkyl dithioxodithiadiphosphetanes to synthesize the corresponding dithioesters (Figure 2.1. **V-b**) [6]. It is also possible to synthesize different S-alkyl dithioxodithiadiphosphetanes depending on the desired R group on dithioesters [7].

2.1.6. Free radical coupling reaction between azo initiators and bis(thiocarbonyl) disulfides

The process involves the heating of a solution of the appropriate bis(thiocarbonyl) disulfides with an aliphatic azo compound in the absence of oxygen. Radicals are the

2. Synthesis of water-soluble RAFT agents

reaction intermediates. The water-soluble RAFT agent, 4-cyano-4-thiobenzoyl-sulfanylpentanoic acid (CTA1), is synthesized by this method (Figure 2.1. VI) [8].

2.1.7. Ester exchange reaction between dithiocarboxylates and thiols.

Alternatively, an ester exchange reaction between carboxymethyl dithiocarboxylate and thiols is used [9]. A general example is shown in Figure 2.1. VII. The method is limited by the small number of commercial dithioesters. The specific example is attractive for the synthesis of hydrophobic RAFT agents, as in a two phase system (aqueous/oil), the equilibrium can be shifted by extracting the thioglycolic acid, while formed, to the aqueous phase.

2.2 Synthetic routes to water-soluble RAFT agents

As it is discussed before, the choice of the right RAFT agent having the proper R and Z groups is one of the most important parameters for CRP of a given monomer. In Figure 2.2, commonly used R and Z groups which give good control in RAFT polymerizations are presented. On the one hand, hydrophilic functional groups have to be imparted to the RAFT agents to provide water solubility, on the other hand, the chain transfer ability of them must be preserved. The best way to achieve both goals at the same time is the addition of hydrophilic groups to R and Z groups, which have been proven to be successful (see Figure 2.2).

Among the Z groups, the usage of xanthates and carbamates (see Figure 2.2. Z= I and II) for water-soluble RAFT agents is critical, as these groups could be readily hydrolyzed. Unfortunately, the addition of hydrophilic groups to dithiobenzoate and phenyl dithioacetate (see Figure 2.2. Z= IV and V), which are widely used Z groups to obtain good control, is synthetically challenging, as their synthesis necessitates powerful nucleophiles like Grignard reagents or sodium methoxide [1]. These compounds do not tolerate functional groups like carbonyl, epoxy, nitro, alcohol, or sulfonate. However, such functional groups are needed either to attach hydrophilic groups, or to impart directly solubility in water. Therefore, the addition of hydrophilic segments to the dithiobenzoate and phenyl dithioacetate is not practical. The addition of permanently ionic groups to Z fragment seems reasonable only for trithiocarbonates (see Figure 2.2. Z= III).

2. Synthesis of water-soluble RAFT agents

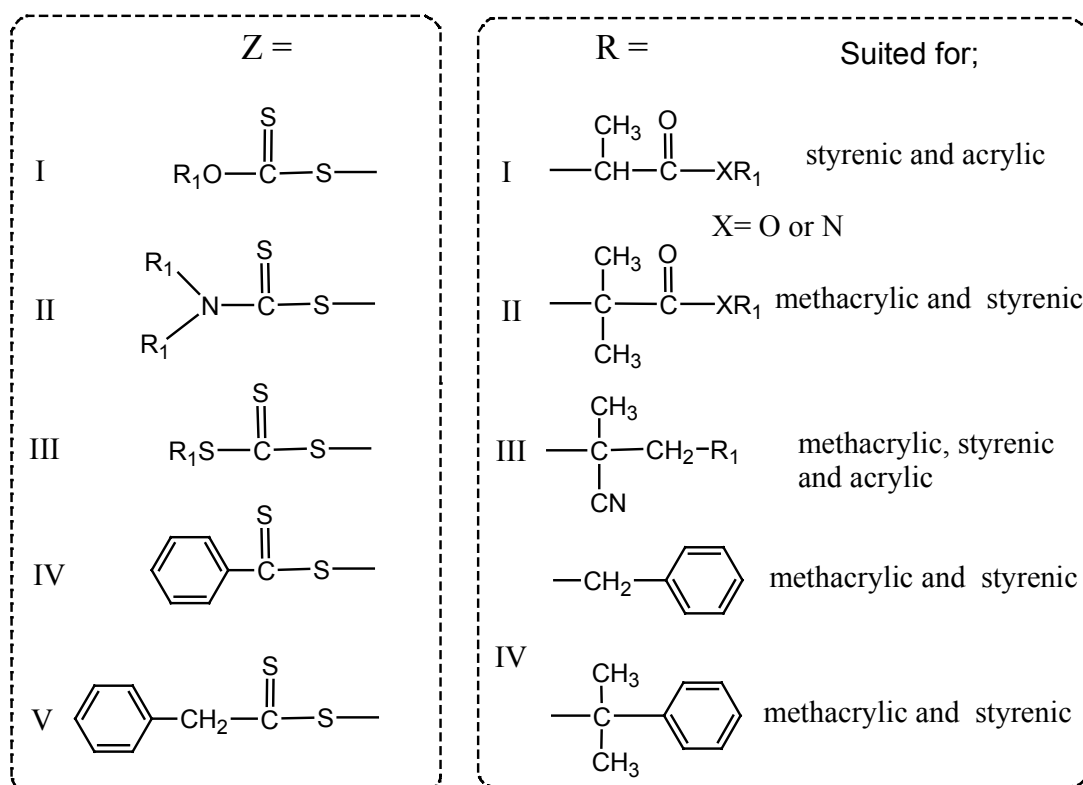


Figure 2.2. R and Z fragments proving good control in RAFT polymerization.

The other possibility is the attachment of permanently ionic groups to the R fragment of dithioesters. Like the Z fragment, the structure of the R groups next to dithioester has to be preserved. The functional groups I and IV, which are presented in Figure 2.2. are suited for polymerization of acrylic and styrenic monomers. II and V (see Figure 2.2) are suited for polymerization of methacrylic and styrenic monomers. The structure III is suited for the polymerization of almost all kind of monomers but it may lower the stability of the RAFT agents in water as in case **CTA1** (see Chapter3). The existence of readily hydrolysable fragments like ester on R, should be avoided, too.

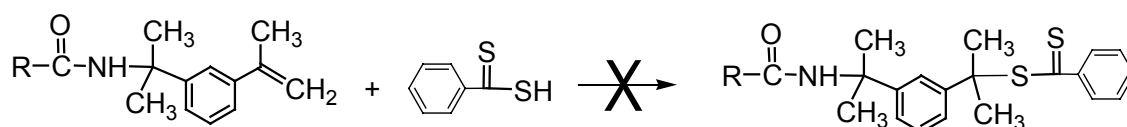
If the synthetic routes used for conventional RAFT agents are examined, it is obvious that some of them are less suited for the synthesis of water-soluble ones. Because the key reagents used for the synthesis are neither soluble nor tolerant to polar protic solvents needed for the synthesis water-soluble RAFT agents. Three synthetic routes were

2. Synthesis of water-soluble RAFT agents

explored; a) the acidic addition of dithiocarboxylic acids to olefins, b) the free radical coupling reaction between azoinitiators and bis (thiocarbonyl) disulfides which is the method used for the synthesis of **CTA1**, c) the alkylation of dithiocarboxylates and trithiocarbonates.

2.2.1. Water-soluble RAFT agents via acidic addition of dithiocarboxylic acids to olefins

First attempts to synthesize water-soluble RAFT agents were inspired by the acidic addition of the dithiocarboxylic acids to olefins as in the synthesis of cumyldithiobenzoate (**CTA7**) (see Figure 2.2. **IIa**), which is rather easy and gives high yields. Three new olefins based on α -methylstyrene and bearing hydrophilic moieties were synthesized; N-(tris(hydroxymethyl)methyl-N'-(α,α -dimethyl-3'-isopropenylbenzyl) urea (**1MM1**), N,N-bis(2-hydroxyethyl)-N'-(α,α -dimethyl-3'-isopropenylbenzyl) urea (**1MM3**), and N-(2-sodiumsulfonatoethyl)-N'-(α,α -dimethyl-3'-isopropenylbenzyl) urea (**MM15**). The detailed synthetic procedures and analytic data for these new compounds are provided in Chapter 7.



R; 1MM1 = $(HOCH_2)_3C-NH-$ **1MM3** = $(HOCH_2CH_2)_2-N-$ **1MM15** = $NaO_3S-(CH_2)_2-NH-$

Figure 2.3. The attempted acidic addition of dithiocarboxylic acids to α -methylstyrene analogues

A control experiment was carried out to examine the method and experimental conditions: dithiobenzoic acid was reacted with α -methyl styrene in $CHCl_3$, to give cumyl dithiobenzoate (**CTA7**) in high yields (see Chapter 7 synthesis of **CTA7**). The addition of dithiobenzoic acid to **1MM1** in dry THF at 65 °C, to **1MM3** in dry $CHCl_3$ at 65 °C, and to **1MM15** in dry dioxane at 70 °C were thus tried, but none of the attempts was successful (see Figure 2.3.). Putatively, the reason for the failure of the reactions is that the double bonds of the new monomers cannot be protonated to form the transient cations. The existing urea linkages in the backbones of the olefins are more basic compared to their

2. Synthesis of water-soluble RAFT agents

double bonds. The acidic protons of dithiobenzoic acid add to the urea moiety instead of the α -methylstyrene, and so prevent the targeted reaction.

To overcome the problem, strong acids were added to the reaction medium, to catalyze the addition. Phosphorous acid was used with monomers **1MM1** and **1MM15** in dioxan. In an another experiment, phosphorous pentoxide was employed as an acid catalyst for the reaction of **1MM1** with dithiobenzoic acid in dioxane at 70 °C. But again, dithioesters were not obtained in these experiments. However, the urea linkage of **1MM1** and **1MM15** was partially hydrolyzed according to ¹H-NMR measurements. The urea linkage is not strong enough to resist to the harsh acidic conditions, and is hydrolyzed before the dithiobenzoate group adds to the α -methylstyrene moiety.

The water soluble olefins sodium β -styrenesulfonate and sodium 2-phenyl-prop-2-en sulfonate were synthesized as described in Chapter 7. The functional groups of these compounds are very weakly basic. So, the protonation of the functional groups should not pose a problem as in the case of the olefins containing the urea linkage. However, no good solvent for both dithiobenzoic acid and these olefins could be found to carry out the reaction. So, the sodium 2-phenyl-prop-2-en sulfonate was used in the acidic form to be able to find a proper solvent for the reaction. Moreover, the acidic proton of 2-phenyl-prop-2-en sulfonic acid could theoretically help to catalyze the addition reaction (see Figure 2.4.). But this trial failed, too. An explanation could be that the sulfonic acid group is too bulky, and so it may sterically hinder the addition of the dithiobenzoate group to the double bond.

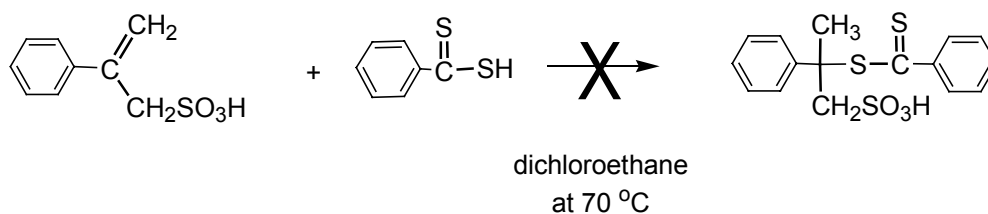


Figure 2.4. The acidic addition trial of dithiobenzoic acid to 2-phenyl-prop-2-en sulfonic acid.

After all these trials, it was concluded that the acidic addition of dithiocarboxylic acids to olefins is not a fertile method for the synthesis of water soluble RAFT agents

2. Synthesis of water-soluble RAFT agents

bearing hydrophilic segments although it is efficient for the synthesis of organic soluble ones.

2.2.2. Water-soluble RAFT agents via the free radical coupling reaction between azoinitiators and bis(thiocarbonyl) disulfides

The next strategy was an adaptation of the synthetic strategy used for the oldest water-soluble RAFT agent **CTA1**. For this purpose, a new water-soluble azo-compound **1MM63** was prepared. (See Chapter 7 for the synthesis of **1MM63**), and the commercial initiator 2,2'-azobis(2-methyl-N-[1,1-bis(hydroxymethyl)-2-hydroxyethyl] propionamide) **VA-80** (see Figure 2.5. for structures) were used. However, a proper solvent which dissolves both **1MM63** and di(thiobenzoyl)disulfide could not be found. In the case of the reaction of **VA-80** with di(thiobenzoyl)disulfide, both compounds are soluble in hot DMF and hot dioxane. But when the reactions were carried out in these solvents by heating for 10 hours at 80 °C under N₂ atmosphere, the target dithioesters were not obtained. One of the probable reasons could be the possible trans-esterification reactions between the formed dithioesters and the hydroxyl groups of **VA-80** at elevated temperatures. Namely, the just prepared dithioester may be consumed by itself.

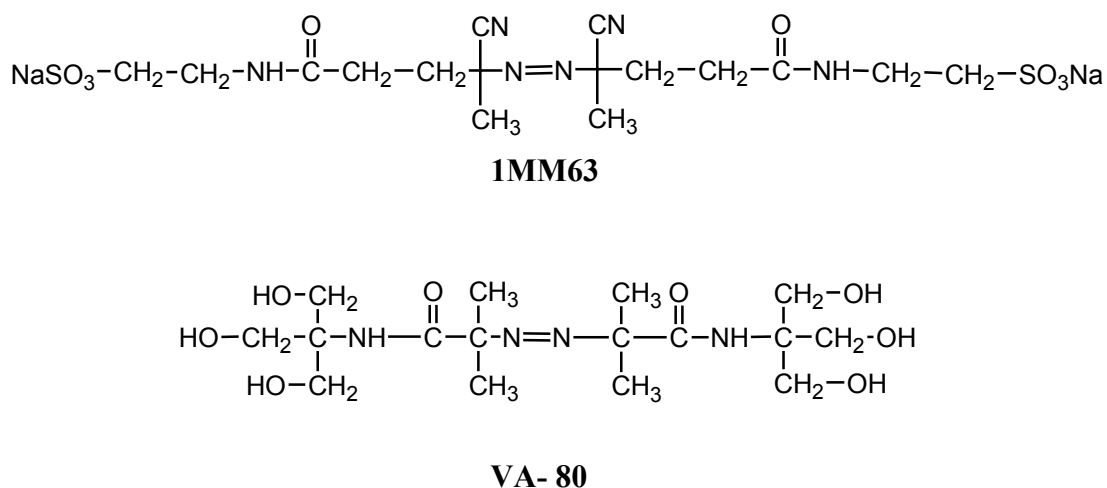


Figure 2.5. The chemical structures of azo initiators **1MM63** and **VA-80**.

As a conclusion, this synthetic route was found not convenient for the development of new water-soluble RAFT agents, neither.

2. Synthesis of water-soluble RAFT agents

2.2.3. Water-soluble RAFT agents via alkylation of dithiocarboxylates

The new water soluble dithiobenzoates (see Figure 2.6.) **CTA2**, **CTA3**, and **CTA4** are synthesized by reacting a functional alkyl halide with the sodium salt of dithiobenzoate. This approach is known to work very well for primary and secondary alkyl halides in organic solvents [2]. But in the case of **CTA2**, **CTA3** and **CTA4**, the solubility of the respective intermediate halides requires their coupling to dithiobenzoate in water. Nevertheless, **CTA2**, **CTA3** were accessible via this approach at ambient temperature. The synthesis of **CTA4** was more difficult, as tertiary alkyl halides require thermal activation for the coupling reaction in order to compensate for the increased steric restrictions. However, higher temperatures favor the decomposition of the just prepared dithioesters by hydrolysis. In fact, coupling in aqueous reaction media at about 60°C proved the best compromise, as no coupling was observed at ambient temperature, while hydrolysis is too fast at 70°C.

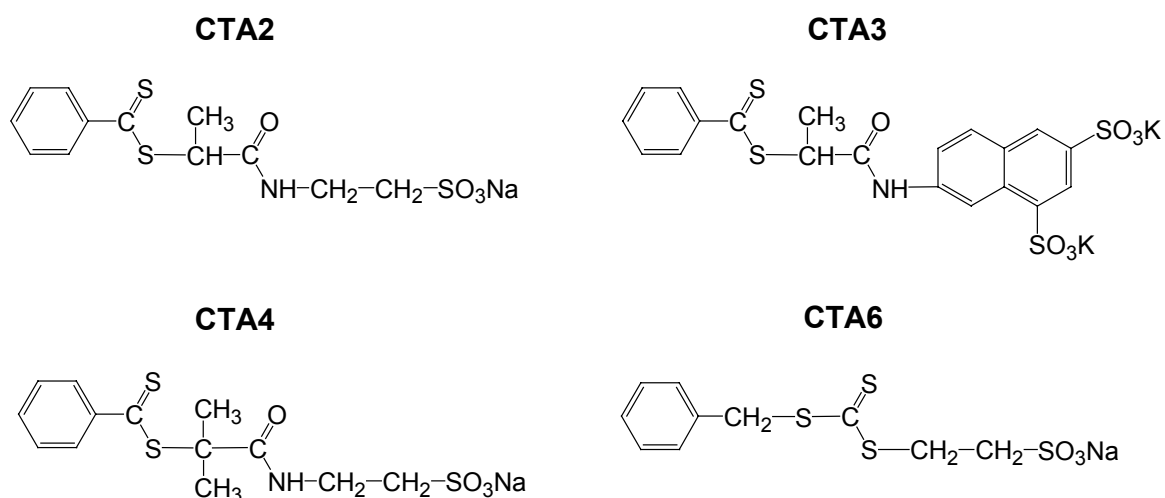


Figure 2.6. The structures of new water soluble RAFT agents.

The anionic trithiocarbonate (Figure 2.6.) **CTA6** was also synthesized with the same strategy. It is prepared by adding carbon disulfide on the double salt of 2-mercapto ethane sulfonic acid, and then alkylating the adduct with benzyl chloride. Anionic **CTA6** has the additional advantage to be purified by crystallization from water, thus the inorganic salts and other water-soluble side products can be easily and efficiently removed. Different from most trithiocarbonates described in the literature [10-13], **CTA6** is not bifunctional, but acts as a monofunctional chain transfer agent like dithioesters. Namely, only the benzyl

2. Synthesis of water-soluble RAFT agents

substituent is a potential leaving group for the addition fragmentation process, whereas the n-alkyl group is not expected to participate. Note that this compound is one of the rare cases in which hydrophilic segment providing water solubility is added to the Z group of the CTA.

The detailed synthesis of **CTA2**, **CTA3**, **CTA4**, and **CTA6** is described in the Chapter 7. The $^1\text{H-NMR}$, and IR of these compounds are presented in related in Appendixes II and III. These new RAFT agents have the advantage of bearing permanent anionic groups which make them soluble in water in the full pH-range. In contrast, the classical water-soluble RAFT agent 4-cyano-4-thiobenzoylsulfanylpentanoic acid (**CTA1**) is only soluble at neutral or basic pH. Different from others, compound **CTA2** proved difficult to purify, notably from the inorganic by-products. If no analytical pure samples are needed, the RAFT agent can be isolated as mixture with 2 mole equivalents of sodium halogenide. The pure **CTA2** free from salt can be obtained by fractionate precipitation of saturated solution in methanol by adding successive aliquots of acetone, rejecting first and last fractions. Actually, during the course of the thesis, an alternative synthesis of **CTA2** was reported [14]. But differing from the analytical data here, the reported analytical data for **CTA2** [14] do not match fully the proposed structure, and indicate the presence of impurities.

Note that in **CTA3**, the 2-naphthylamino-6,8-disulfonate fragment imparts not only water-solubility to the RAFT agent, but may also serve as analytical tool. The naphthyl fragment of **CTA3** fluoresces, and therefore the polymers synthesized by using it, as well. In addition, both end groups of the polymers synthesized by using **CTA3** can be tracked via optical spectroscopy, to enable a good estimation of the number average molecular weights. This will be discussed later in Chapter 4 in more detail.

CTA2 and **CTA3** have the same vicinity next to the dithioester moiety, a secondary leaving group. This R group makes these RAFT agents suitable for the polymerization of acrylics and styrenics. **CTA4** has a tertiary leaving group, and it is suited for the polymerization of methacrylics, and styrenics. The potential leaving group of **CTA6** is the benzyl group, and so it is also suited for the polymerization acrylic and styrenics. But, different from others, the dithiocarbonyl fragment is part of a trithiocarbonate. The chain transfer constants of trithiocarbonates differ from dithioesters.

2. Synthesis of water-soluble RAFT agents

Trithiocarbonates can provide better control or worse over polymerization in comparison to dithioesters, in dependence on the polymerization conditions and the monomer engaged [15].

In conclusion, alkylation of dithiocarboxylates was the best synthetic method for the synthesis of water-soluble RAFT agents. New RAFT agents soluble in water independent of pH were synthesized. These new compounds enabled comparative studies to show the usefulness of the RAFT technique to synthesize macromolecules in aqueous media.

References

- [1] Becke F, Hagen H. 1968, German patent DE 1274121(CA 1969; 70: 322, 3573v)
- [2] Le TPT, Moad G, Rizzardo E, Thang S. Intern Pat Appl. 1998, PCT WO9801478 [CA 1998: 115390.
- [3] Oae S, Yagihara T, Okabe T. *Tetrahedron* **1972**, 28, 3203.
- [4] Poupaert J, Bruylants A, Crooy P. *Synthesis* **1972**, 622.
- [5] Neugebauer W, Pinet E, Kim M, Carey PR. *Can. J. Chem.* **1996**, 74, 341.
- [6] Davy H, Metzner P. *J. Chem. Research (S)*, **1985**, 272.
- [7] Davy H. *Sulfur Letters* **1985**, 3(2), 39.
- [8] Thang SH, Chong YK, Mayadune RTA, Moad G, Rizzardo E. *Tetrahedron Lett.* **1999**, 40, 2435.
- [9] Leon NH, Asquith RS. *Tetrahedron* **1970**, 26, 1719.
- [10] Moad G, Mayadunne RTA, Rizzardo E, Skidmore M, Thang SH. *Macromol Symp* **2003**, 192, 1.
- [11] Lai JT, Filla D, Shea R. *Macromolecules* **2002**, 35, 6754.
- [12] Ferguson CJ, Hughes RJ, Pham BTT, Hawkett BS, Gilbert RG, Serelis AK, Such CH. *Macromolecules* **2002**, 35, 9243.
- [13] Mayadune RTA, Rizzardo E, Chiefari J, Moad G, Postma A, Thang SH, *Macromolecules* **2000**, 33, 243.
- [14] McCormick CL, Lowe AB, Sumerlin BS, Thomas DB. **2003**, PCT WO 03/066685 A2 Chain Transfer Agents for RAFT Polymerization in Aqueous Media
- [15] Szablan Z, Toy AA, Davis TP, Hao X, Stenzel MH, Barner-Kowollik C. *J. Polym. Sci. Part A: Polym. Chem.* **2004**, 42, 2432.

3. STABILITY OF RAFT AGENTS IN WATER

RAFT polymerization is based on dithiocarbony derivatives. If the chemical structure of these compounds cannot be preserved throughout the reaction, polymerization is either inhibited or carried out without control. The commonly used classes of RAFT agents, dithioesters and trithiocarbonate compounds, are known to be sensitive to aminolysis [1] and hydrolysis [2]. These side reactions pose a potential handicap for the application of the RAFT method in aqueous media, and make it more complicated than the ones carried out in aprotic solvents such as THF or benzene. The hydrolytic stability of dithioesters is known to depend strongly on the temperature according to Levesque et al. [1], but no information was available related to the hydrolytic stability of RAFT agents at the beginning of this thesis. It was therefore important to examine the pH and heat dependent hydrolytic stability of RAFT agents, to find out the optimum polymerization window with minimum hydrolysis of the dithioesters.

The reaction of dithioesters with primary and secondary amines is well known, and for instance it is used to modify proteins via thioacylation [1, 3, 4]. However useful aminolysis reactions are, they cause problems for RAFT polymerization. But, they can be avoided by working in slight acidic conditions in which almost all of the amines are protonated [5-7], and so the nucleophilic attack on the dithioesters is prevented.

Since little information was available to which extent dithioesters and trithiocarbonates are sensitive to hydrolysis, the stabilities of the new compounds **CTA1** – **CTA6** in water were investigated, and compared with the behavior of the in water most frequently used RAFT agent **CTA1** that is well water-soluble as sodium salt.

First, the useful pH window at 40°C for RAFT agents **CTA1** - **CTA6** was elaborated (see Table 3.1). The degradation of the RAFT active dithioester in water seems to be easily tracked by the characteristic absorption peak of the forbidden $n \rightarrow \pi^*$ transition of the C=S group in the visible band (**CTA1**: $\lambda_{\max} = 497$ nm; **CTA2**: 483; $\lambda_{\max} =$ nm; **CTA5**: $\lambda_{\max} = 480$ nm; **CTA6**: $\lambda_{\max} = 425$ nm). The onset of the degradation is sensitively indicated by following the evolution of the absorbance via Vis-spectrometry, but the measurements could not be exploited for quantitative kinetic studies because

3. Stability of RAFT agents in water

degradation results in at least two opposing effects. On the one hand, the absorbance is decreased due to the loss of the chromophore. On the other hand, the solutions become turbid, as some of the degradation products are insoluble in water (for **CTA5** and **CTA6**). That is well illustrated in the decomposition test of **CTA6** (see Figure 3.1), where ongoing degradation dramatically increases the absorbance. Moreover, dithiobenzoate which absorbs in the same visible range, may also be produced as one of the hydrolysis products, pretending the stability of the dithioesters. In fact, the dithiobenzoic acid was isolated from the hydrolytic stability test of **CTA2** and, its structure was confirmed by ¹H-NMR. In the case of **CTA1**, the solution stays clear with a slight reduction in absorbance with time between pH=7 and pH10 and 70°C (see Figure 1). The observed decomposition seems to be quite slow. But, the true stability of the compound is lower than the apparent one. By comparing the UV/vis spectra with ¹H-NMR spectra, it was found that the extent of hydrolysis is underestimated by UV/vis spectra. For instance, **CTA1** is fully hydrolyzed according to ¹H-NMR after 3 h at 70°C at pH 10, but the residual absorbance at $\lambda_{\text{max}} = 497$ nm is still about 36 % of the original value, pretending partial stability. Therefore, though UV/vis studies are convenient for preliminary tests and may provide an upper estimation limit, a proper evaluation of the stability (or instability) must be done by other methods, such as ¹H-NMR spectroscopy.

Table 3.1. Stability of RAFT agents at 40°C in water, in dependence on pH.

pH	RAFT Agents				
	buffer	CTA1	CTA2	CTA5	CTA6
1	no	insoluble	stable	stable	stable
2	no	insoluble	stable	stable	stable
4	A	insoluble	n.d. ^a	n.d. ^a	n.d. ^a
5	B	insoluble	stable	stable	stable
6	C	stable	stable	stable	stable
7	D	n.d. ^a	n.d. ^a	stable	n.d. ^a
8	E	O	O	O	O
9	F	-	-	-	-
10	G	=	=	=	=

Tracked at 497 nm (**CTA1**), 483 nm (**CTA2**), 480nm (**CTA5**), 425 nm (**CTA6**). Symbols “O”, “-” and “=” indicate increasing rates of decomposition as followed by the decrease of absorbance in the vis-spectrum, or by separation of decomposition products. Used buffer solutions given in the experimental part (Chapter 7)

n.d.^a : cloudy solution with partial precipitation of the RAFT agent due to interaction with buffer components.

3. Stability of RAFT agents in water

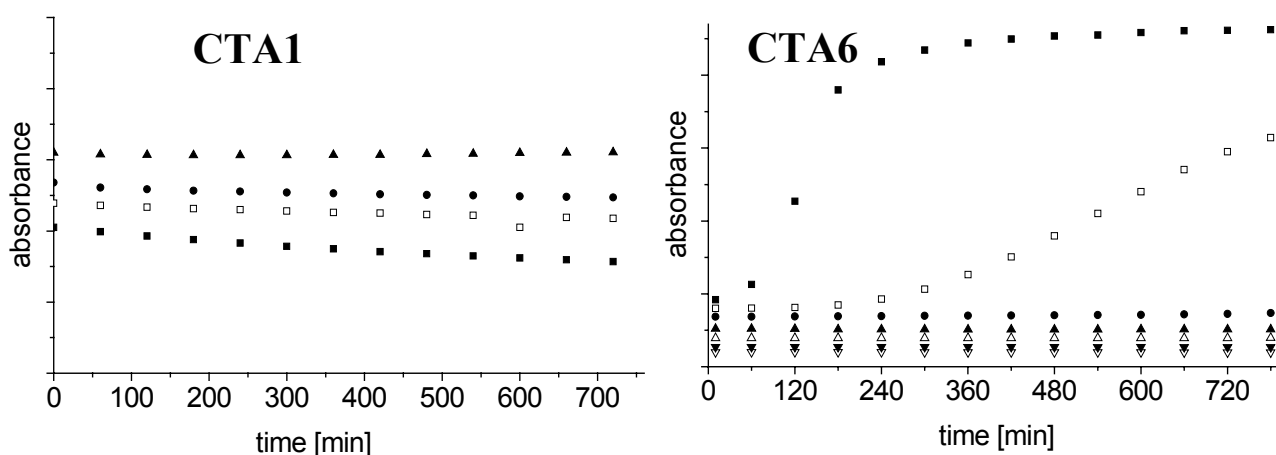


Figure 3.1. Stability of **CTA1** and **CTA6** at 40°C followed by UV-Vis spectroscopy at 493 nm, 425 nm respectively. (■) buffer of pH=10.0, (□) buffer of pH=9.0, (●) buffer of pH=8.0, (○) buffer of pH=7.0, (▲) buffer of pH=6.0, (△) buffer of pH=5.0, (▼) buffer of pH=2.0, (▽) buffer of pH=1.0. Note: the concentrations of solutions used for the stability tests at different pH values were the same for each series of RAFT agents, but absorbance values were moved up or down in the absorbance scale for better visualization of data.

Combining Vis-spectroscopic studies with $^1\text{H-NMR}$, hydrolysis was not observed at 40°C over a period of 24 h in the range between pH 5.8 to pH 7. Concerning more acidic conditions, the established RAFT agent **CTA1** is not soluble in water at lower pH values, but the new agents are. When potassium hydrogen phthalate / HCl solution was used as a buffer solution of pH = 4, solutions of **CTA2** and **CTA6** became cloudy nearly instantaneously, or form a precipitate in the case of **CTA5**. The same problem occurred for **CTA1**, **CTA2** and **CTA6**, in the buffer solution of pH = 7, containing potassium dihydrogen phosphate / di-sodium hydrogen phosphate. However these precipitates are due to a specific interaction of the RAFT agents with the buffer ingredients rather than the hydrolysis. Agents **CTA2**, **CTA5** and **CTA6** did not decompose at pH=1 and pH=2 within 12 h at 40°C according to UV-vis data, if the pH is adjusted by concentrated HCl (Table 3.1). These results are also confirmed by $^1\text{H-NMR}$ analysis.

Whereas the RAFT agents seem to be rather stable to acidic conditions, they are sensitive to base. While at pH=8, Vis-spectroscopy indicated a slow onset of degradation after 10 h, more basic conditions led to accelerated degradation (cf. Table 3.1). Depending on the detailed structure of the compounds, the solution stayed transparent (for **CTA1** and **CTA2**) or produced precipitate (for **CTA5** and **CTA6**). Therefore, when employing typical

3. Stability of RAFT agents in water

RAFT agents in water, the pH is best maintained below a value of 8 to assure hydrolytical stability.

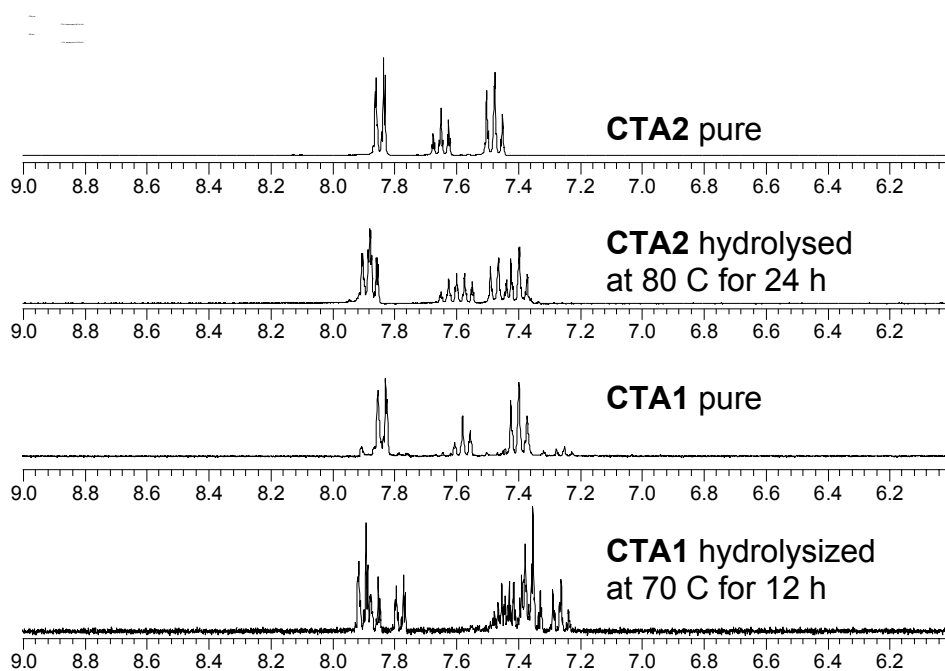


Figure 3.2. $^1\text{H-NMR}$ of the phenyl groups of **CTA1** and **CTA2** before and after hydrolysis in D_2O pH =6.

Having thus defined the most useful pH window, we investigated the hydrolytic stability of **CTA1-CTA6** at ambient pH, i.e. at pH=6, for elevated temperatures, as most free radical polymerizations are performed with thermal initiators. In order to get some chemical information about eventual degradation products, $^1\text{H-NMR}$ spectroscopy in D_2O was used for these studies. The stability of RAFT agents was followed by the reduction in the integrated $\beta\text{-CH}_3$ signal of **CTA1 – CTA4**, or of the $\alpha\text{-CH}_2$ signals of **CTA5** and **CTA6** relative to the internal standard dioxane, as decomposition products do not interfere with these peaks, and any chemical modification of the dithioester moiety is reflected as a shift of these signals. Alternatively one might have thought to follow the integration changes of protons on the dithiobenzoate fragment. But, like the examples given in Figure 3.2. for **CTA1** and **CTA2**, the protons signals resulting from decomposition products of the dithioesters appear in the same region, so it is not trivial to get any quantitative information from this region of $^1\text{H-NMR}$ spectra.

3. Stability of RAFT agents in water

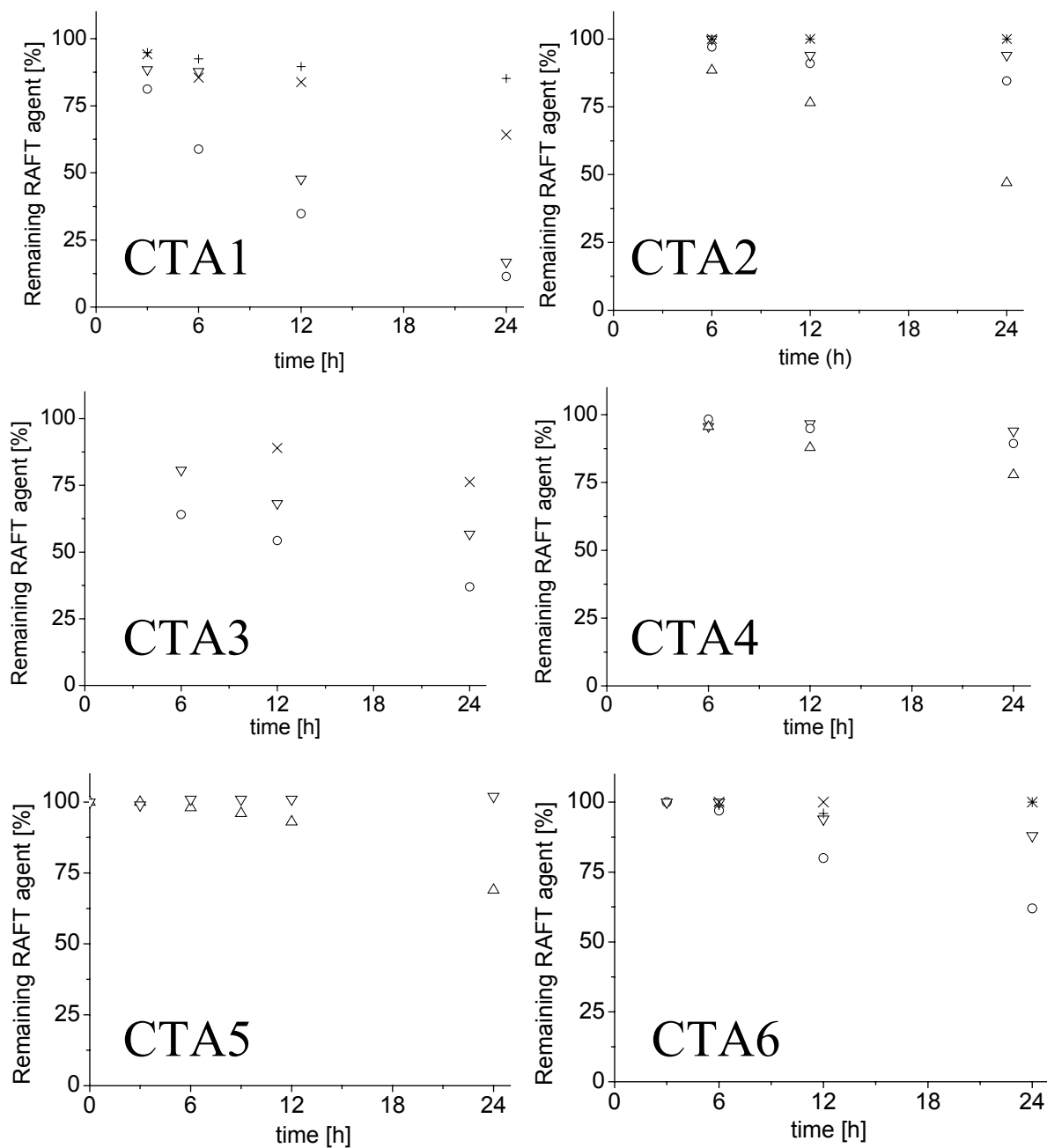


Figure 3.3. Stability of RAFT agents in D₂O at pH 6 at different temperatures, followed by ¹H-NMR: 40°C = (+), 50°C = (X), 60°C = (▽), 70°C = (O).

The decomposition tests of the reference compound 4-cyano-4-thiobenzoyl-sulfanyl-pentanoic acid **CTA1** are presented in Figure 3.3. at different temperatures. After 24 h, nearly 36% of the reagent already decomposed at 50°C, 84% degraded at 60°C, and even 90% are lost at 70°C. In the series of the decomposition spectra at 70°C (Figure 3.4.), two different types of decomposition patterns could be observed. The new singlet at 1.857 ppm, showing up next to the singlet at 1.863 ppm that is attributed to the methyl group

3. Stability of RAFT agents in water

($\text{CH}_3\text{-C}(\text{CN})\text{-SC}(\text{=S})\text{-}$), was only observed at reaction temperatures of 60°C or more. In analogy to the findings for the degradation of **CTA2** (see below), this singlet is attributed to the conversion of the $\text{C}=\text{S}$ into the $\text{C}=\text{O}$ group, without cleavage of the C-S-C linkage. The hydrolysis reaction is assumed to produce the newly rising singlet at 1.66 ppm, putatively attributed to the signal of the $\text{CH}_3\text{-C}(\text{CN})\text{-S-}$ moiety after hydrolysis.

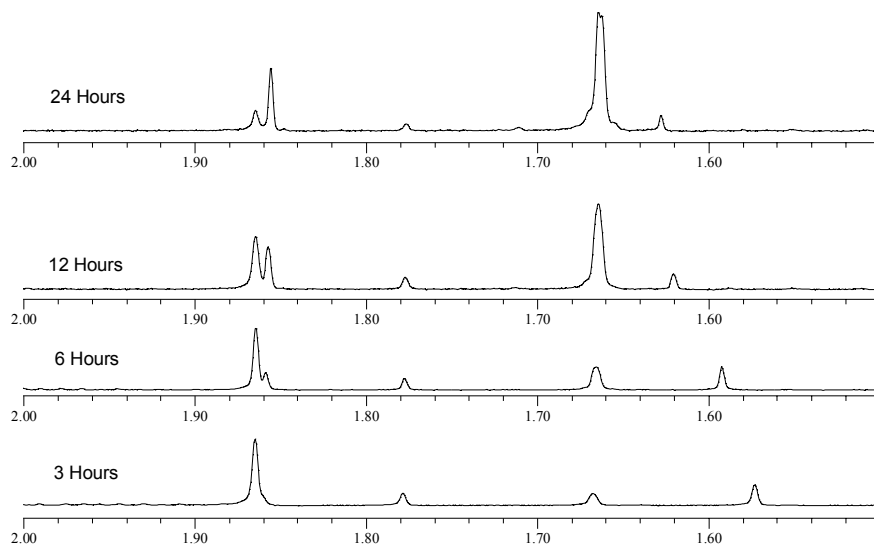


Figure 3.4. Evolution of the ^1H NMR spectra of **CTA1** in D_2O at $\text{pH}=6$ with decomposition at 70°C

The results of the stability test of the RAFT agent **CTA2** are exhibited in Figure 3.3. Anion **CTA2** is relatively stable at 60°C and lower temperatures. But at higher temperatures, notable degradation is observed after 24 h: 15% of the starting compound were decomposed at 70°C , and 53% at 80°C . According to the ^1H -NMR spectra taken at regular intervals (Figure 3.5), three major degradation products are found. By comparing the newly developing signals with the prepared thioester derivative of **CTA2**, it was found that the first one results from the conversion of the dithioester moiety- $\text{C}(\text{=S})\text{S-}$ to the thioester moiety- $\text{C}(\text{=O})\text{S-}$. I.e., dithioester is converted into thioester as indicated by the increase of the minor duplet at 1.51 ppm ($-\text{CH}_3$) with time, while the duplet at 1.60 ppm ($-\text{CH}_3$) of **CTA2** decreases simultaneously. Parallel to the ^{13}C -NMR spectra, the signal at 228 ppm attributed to the $-\text{C}(\text{=S})\text{S-}$ moiety is gradually replaced by a signal at 194 ppm attributed to the $-\text{C}(\text{=O})\text{S-}$ moiety (data related to the synthesis and analysis of the thioester analogue of **CTA2** is given in the Chapter 7). This reaction is particularly notable at temperatures above 60°C . The two other degradation products result from the hydrolysis of the dithioester moiety, too (Figure 3.5.). The new two doublets rising at 1.36 ppm and 1.41

3. Stability of RAFT agents in water

ppm can be attributed to degradation products bearing the 2-(2-propionylimino) ethanesulfonate fragment (presumably the alcohol and the thiol). In contrast to the dithioester moiety, the amide bond is not affected by the storage in water under these conditions according to the NMR spectra, nor is the aromatic core.

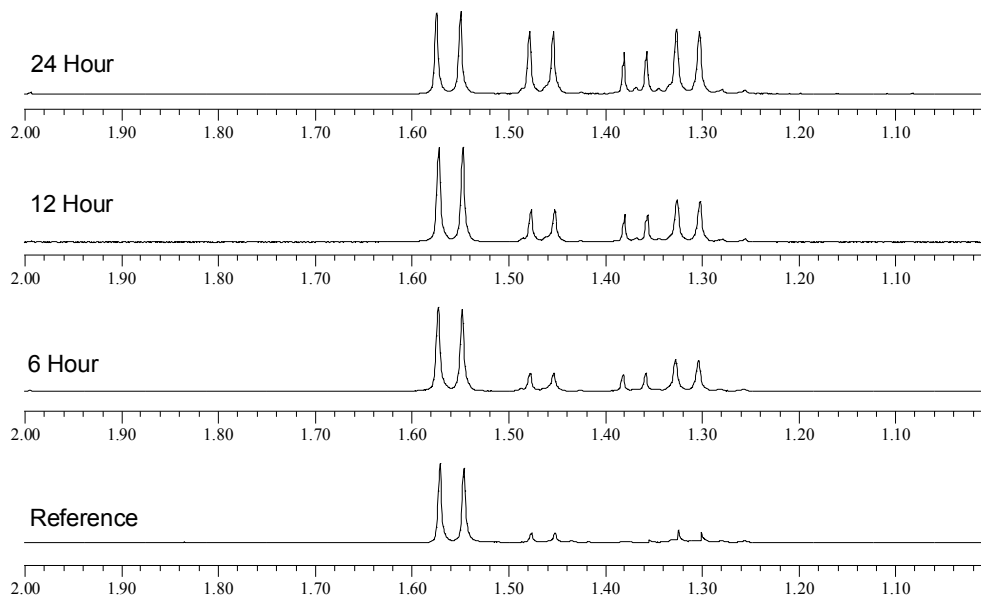


Figure 3.5. Evolution of the ^1H NMR spectra of **CTA2** in D_2O at $\text{pH}=6$ with decomposition at 80°C .

Analogously, the decomposition of compound **CTA3** is followed by the decay of the proton peak at 1.71 ppm (see Figure 3.6), and the results are given in Figure 3.3. Since the vicinity of **CTA3** next to the dithioester moiety is same as that of **CTA2**, they were expected to present similar stability under the same conditions. However, **CTA3** is much less stable compared to **CTA2** (see Figure 3.3). Whereas **CTA2** hardly decomposed at 60°C after 24 h, almost half of **CTA3** is decomposed under the same conditions. This means not only that the close vicinity of the dithioester group is of importance for the hydrolytic stability (which e.g. is identical for **CTA2** and **CTA3**). Putatively, the reduced stability of **CTA3** may be attributed to an increased hydrophilic environment around the molecule caused by the naphthalene disulfonate fragment. Whilst the doublet of **CTA3** at 1.71 ppm is subdued with ongoing decomposition, a doublet at 1.61 ppm is arising together with a singlet at 1.60 ppm (See Figure 3.6). The doublet is attributed to the thioester derivative of **CTA3**. Note that like **CTA2**, a part of the degradation of **CTA3** is due to the conversion of the dithioester group to the thioester, and not only due to full hydrolysis of

3. Stability of RAFT agents in water

the $-C(=S)-S$ moiety. The new peaks which appear between 1.51 and 1.40 ppm, are attributed to the products resulting from complete hydrolysis.

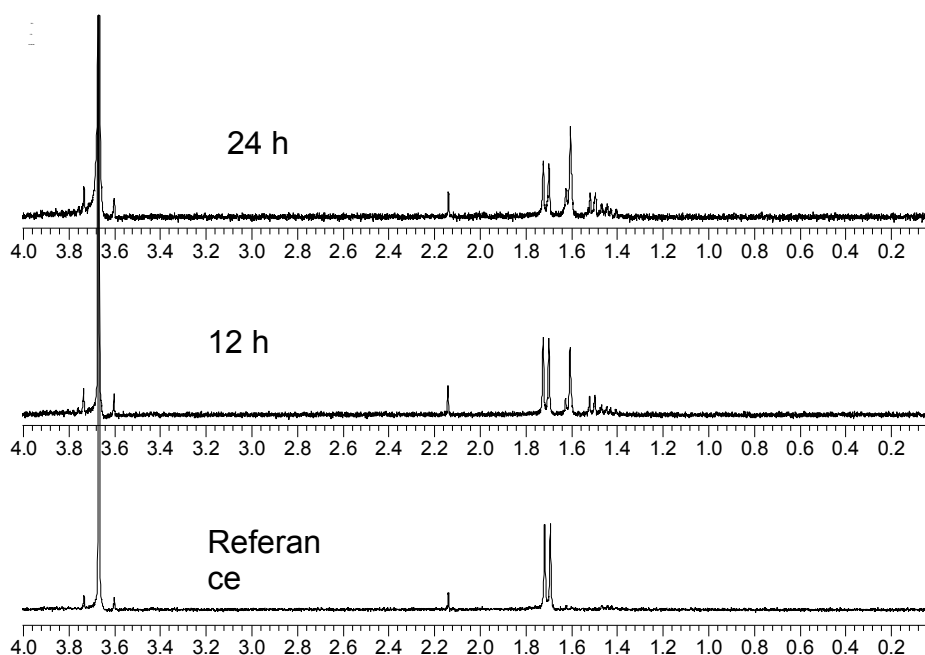


Figure 3.6. Evolution of the ^1H -NMR spectra of **CTA3** in D_2O at $\text{pH}=6$ with decomposition at 70°C .

The stability of **CTA4** was measured by following the decay of the integrated proton signal of the $-C(=S)-S-C-\text{CH}_3$ fragment at 1.67 ppm (cf. Figure 3.7) that is sensitive to the loss of the dithioester group. If the stability of **CTA4** is compared with others (cf. Figure 3.3), **CTA4** is the most stable RAFT agent tested up to now, even excelling the very stable cationic **CTA5** [8], only 25 % of the compound were decomposed after 24 h at 80°C . Putatively, the hydrophobic shielding around the dithioester moiety is increased by two β -methyl groups, and this is particularly efficient to increase hydrolytical stability. The tiny singlet at 1.59 ppm which also exists in the reference sample (cf. Figure 3.7) stems from the thioester derivative of **CTA4**, and the intensity of the peak is slightly increasing relative to the internal reference dioxane. Although the percent deactivation of the dithioester via conversion to the thioester is minor, it exists for **CTA4**, too.

The results of the stability tests for cationic **CTA5** in D_2O are summarized in Figure 3.3. This compound was synthesized and tested by Jean-Francois Baussard [8,9], but for complete comparison of RAFT agents, the data are included here. This RAFT agent

3. Stability of RAFT agents in water

shows no detectable decomposition by $^1\text{H-NMR}$ within 24 h up to 60°C . Though at 80°C , slow decomposition is observed. After 24 h, about 70% of the starting compound are still preserved. Similar to **CTA4**, the increased stability may be attributed to more hydrophobic environment around the dithioester moiety.

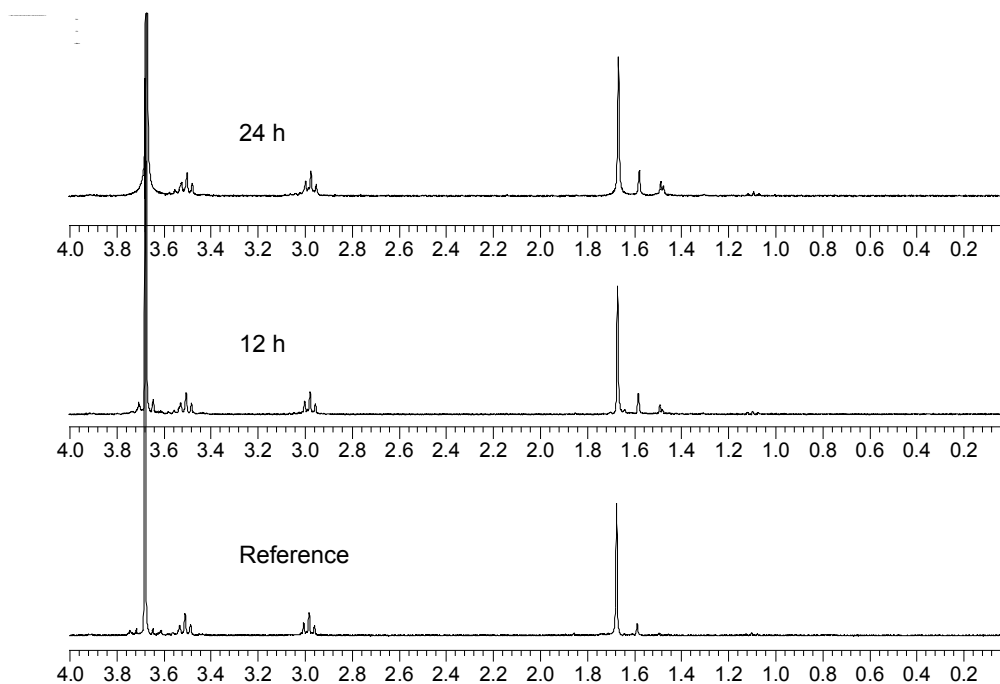


Figure 3.7. Evolution of the ^1H NMR spectra of **CTA4** in D_2O at $\text{pH}=6$ with decomposition at 70°C .

Different from dithioesters, the water-soluble anion **CTA6** is a trithiocarbonate. The stability of **CTA6** is summarized in Figure 3.3. The compound is fully stable during 24 h storage in water up to 50°C , but not at higher temperatures. Storage at 70°C produces some turbidity. Following the decrease in the intensity of the singlet at 4.64 ppm ($-\text{S}-\text{C}(=\text{S})-\text{S}-\text{CH}_2\text{Aryl}$) (Figure 3.8), 12% of **CTA6** were degraded at 60°C , while 38% were decomposed at 70°C . The newly rising singlet at 4.05 ppm and the new multiplet at 6.70 ppm are difficult to attribute. Interestingly, the new $^1\text{H-NMR}$ signals give no indication for the formation of benzyl mercaptane or 2-mercaptoethanesulfonate resulting from the complete hydrolysis of the trithiocarbonate moiety.

In summary, the stability of the RAFT agents increases in the series **CTA1** < **CTA3** < **CTA6** < **CTA2** < **CTA5** < **CTA4**, i.e. the hitherto widely employed

3. Stability of RAFT agents in water

dithiobenzoate **CTA1** is the least stable compound, while the anionic **CTA4** proved to be the most stable one. Whereas the former exhibits already marked degradation at 50°C, the latter shows virtually no decomposition at 60°C. Even after 24h of storage in water at 80°C, 75% of the starting compound are still preserved. Compared to the different dithiobenzoates, trithiocarbonate **CTA6** exhibits an intermediate resistance to hydrolysis. These findings might be explained by a hydrophobic shielding of the dithioester moiety against the attack by water. Namely, the more is the hydrophobic shielding next to the dithioester, the more stable the RAFT agent. Possibly, the electron withdrawing CN group in α -position to the dithioester bond is responsible for the faster hydrolysis of **CTA1**.

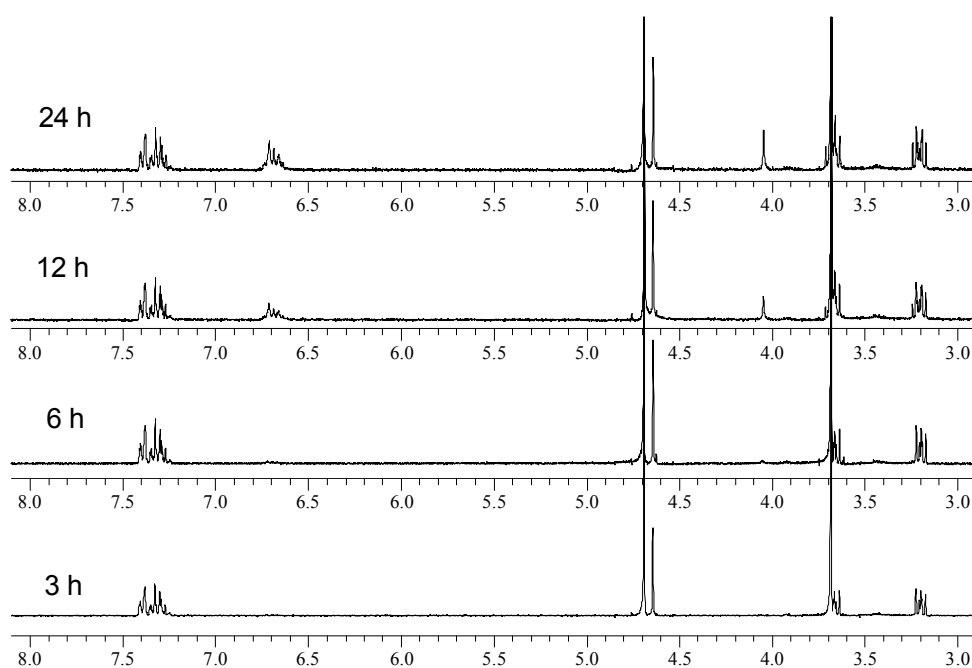


Figure 3.8. Evolution of the ^1H NMR spectra of **CTA6** in D_2O at $\text{pH}=6$ with decomposition at 70°C .

According to the generally accepted mechanism of the RAFT process (scheme 1.4.) [10, 11], the hydrolytic stability of a RAFT polymerization system in aqueous media is only in parts given by the stability of the initial RAFT agent Z-C(=S)-S-R . When the chain transfer step is over, the hydrolytic stability of the "dormant" polymer chains, i.e. of the adducts of the growing radical chains and the Z-C(=S)-S- fragment of the RAFT agent employed, will play a crucial role, but not the original RAFT agent. If the structure of the leaving group in the RAFT agent is not a mimic of the growing polymer chain, a direct correlation cannot be expected. So the stability of the active end groups in the growing polymers is very important. But, no reliable analytical method for studies on polymers was

3. Stability of RAFT agents in water

available. The concentration of active end groups becomes extremely diluted with ongoing polymer growth, so that a sensitive quantitative method is needed. Unfortunately, the "obvious" UV/Vis determination of the dithioester moiety (or of the trithiocarbonate moiety) seems not reliable according to the degradation studies on the low molar mass RAFT agents, because some degradation products exhibit similar optical properties as the end groups. Note that a part of the degradation of dithioester is due to the conversion of the dithioester group to the thioester according to the NMR spectra of partially decomposed mixtures (see above), and not only due to full hydrolysis of the $-C(=S)-S$ moiety. Therefore, any hydrolytical stability test based on UV-vis should be taken into account with great care. For example, in the study of McCormick et al [5], the hydrolyzed macro chain transfer agent aliquots were separated by high-pressure liquid chromatography (HPLC), and the percent hydrolysis was determined from the reduced absorbance of dithioester moieties in the UV band 300 nm. But if a part of hydrolysis happens via the conversion of the dithioester to the thioester moiety, as found in our tests with **CTA2**, **CTA3** and **CTA4**, it cannot be detected by this method to which extent the absorbance stems from thioester end groups. Thioester end groups pretend stability. Therefore, the hydrolytic stability tests for growing polymer chains in aqueous solution, based on UV-detection like in the study of McCormick et al [5], may overestimate the stability of such dithioester end groups on polymer chains.

In RAFT polymerization, retardation times are frequently observed [12] which can be as long as hours depending on polymerization ingredients and conditions. Thiols are known to be good inhibitors for radicals, and they are produced as a result of hydrolysis of dithioester compounds. The more thioester produced via hydrolysis in the early steps of the polymerization, the longer would be the retardation period. So, it is obvious that for obtaining best results in controlling a polymerization, attention should be paid to use a RAFT agent that provides good stability under the reaction conditions chosen. Since the stability of the low molar mass RAFT agents can be problematic at temperatures above 60°C depending on structure, similar problems may exist for growing macro RAFT agents. Therefore, it seems wise to work at lower temperatures in aqueous medium for RAFT polymerizations - when possible -, in order not to reduce end group functionality.

To summarize, CRP via RAFT should be carried out at polymerization temperatures below 60°C, and at pH<8, to prevent a loss of end group functionality in

3. Stability of RAFT agents in water

water. This is crucial to maintain good control over the polymerization and to obtain highly functionalized macro RAFT agents that can be used for block polymer synthesis.

References

- [1] Levesque G, Arsène P, Fanneau-Bellenger V, Pham TN. *Biomacromolecules* **2001**, *1*, 400.
- [2] Janssen MJ. Chapter 15 in: *The Chemistry of Carboxylic Acids and Esters*, Patai S ed, New York: Interscience; 1969, p 706-764.
- [3] Kjaer A. *Acta Chem. Scand.* **1950**, *4*, 1347.
- [4] Kjaer A. *Acta Chem. Scand.* **1952**, *6*, 327.
- [5] Thomas DB, Convertine AJ, Hester RD, Lowe AB, McCormick CL. *Macromolecules* **2004**, *37*, 1735.
- [6] Vasilieva YA, Thomas DB, Scales CW, McCormick CL. *Macromolecules* **2004**, *37*, 2728.
- [7] Thomas DB, Sumerlin BS, Lowe AB, McCormick CL. *Macromolecules* **2003**, *36*, 1436.
- [8] Baussard JF, PhD Thesis, University of Catholique de Louvain (Belgium), **2004**
- [9] Baussard JF, Habib-Jiwan JL, Laschewsky A, Mertoglu M, Storsberg J. *Polymer* **2004**, *45*, 3615.
- [10] Moad G, Mayadunne RTA, Rizzardo E, Skidmore M, Thang SH. *Macromol. Symp.* **2003**, *192*, 1.
- [11] Barner-Kowollik C, Davis TP, Heuts JPA, Stenzel MH, Vana P, Whittaker M. *J. Polym. Sci. Polym. Chem.* **2003**, *A41*, 365.
- [12] Coote ML. *Macromolecules* **2004**, *37*, 5023.

4. SYNTHESIS OF WATER-SOLUBLE POLYMERS VIA RAFT

Water-soluble polymers have a great potential for applications in the fields of nanoscience, biotechnology, personalcare, pharmaceuticals, and related fields. Advantageously, polymers or polymer building blocks should have defined structures to be employed in these fields. Therefore they should be synthesized in a controlled manner. As discussed in the introduction, CRP methods are the most promising because of their tolerance to functional groups on monomers, solvent, small amount of impurities etc. The synthesis of such polymers should be carried out preferentially in water, particularly if they are planned to be used in medicine. Other possible solvents like DMF, formamide or dioxane which a priori are suited for the polymerization of hydrophilic monomers, are noxious to living organisms. If small traces remain in the polymer, they can cause severe health problems. If a polymer is synthesized in these solvents, it must be purified by time and money consuming procedures to remove the solvents completely. However, water is non-toxic, cheap, and easy to handle, and is of great interest as solvent for these reasons. Consequently, the implementation of CRP methods in aqueous environment has become a focus of interest.

CRP is still a challenge in aqueous solution, due to a number of practical problems (e.g. solubility and stability in water of the reagents needed), as well as inherent difficulties to characterize properly the water-soluble polymers obtained (as needed to evaluate the CRP process). Within the various CRP methods, RAFT seems the most promising one for aqueous systems [1]. "Nitroxide Mediated Polymerization" often needs relatively high temperatures and high monomer concentrations, while many ATRP catalysts are sensitive to the presence of water and tend to bind strongly to typical hydrophilic groups in the monomers and polymers. The limited number of RAFT agents and their stability in water are the most obvious barriers for applying RAFT polymerization in water. With the synthesis of new RAFT agents in this study, the diversity of RAFT agents has increased. Moreover, the stability tests carried out on the different RAFT agents showed that hydrolysis reactions which may interfere with the aqueous RAFT polymerization process, can be minimized by adjusting the pH and the temperature of the reaction medium to appropriate values.

4. Synthesis of water-soluble polymers via RAFT

In parallel to this thesis, some examples of aqueous controlled radical polymerization of water soluble styrene [2,3], acrylate [4], and (meth)acrylamide [5-7] based monomers via RAFT in water were reported, to yield homopolymers with increasing molar masses, ongoing conversion, and low polydispersities [1-7]. But different from our studies, these polymerizations were carried out at higher temperatures ($>60^{\circ}\text{C}$) which increase the risk of hydrolysis. Also, when polymers made by RAFT in water were employed as macro-RAFT agents and their blocking ability was tested, they failed in some cases [3]. The failure was attributed to preferential fragmentation of the intermediate radical formed during chain equilibration step (see similar problem in Scheme 1.6. as an example), apparently particular to the use of an aqueous reaction medium [3].

Having successfully synthesized different water-soluble RAFT agents, and having explored the best stability window in water, first the homopolymerization of hydrophilic monomers bearing non-charged as well as charged functional groups via RAFT was investigated in water. Then, functional block copolymers which are hardly accessible in any other solvent, were synthesized in water. In this chapter, these results will be presented, and discussed by comparing them with the other published data on polymers synthesized in water via RAFT.

4.1. Usefulness of the End Groups of Polymers Synthesized via RAFT

In RAFT polymerization, most of the polymer chains bear one R and one Z fragment of the employed RAFT agent, if the polymerization is carried out carefully. These defined end groups can be useful for various purposes depending on their properties. This includes analytical uses like estimating the number average molecular weight (M_n), the incorporation of fluorescent tags to the chain ends, or grafting the polymer chains to surfaces. In this study, the absorption of the RAFT agents in the visible band which stems from the $n \rightarrow \pi^*$ forbidden transition of the C=S group, i.e. which is indicative of intact dithioester end groups, was explored. The UV-vis spectrum of **CTA3** illustrates well the typical visible band (Figure 4.1). Other RAFT agents and polymers bearing active end groups, like dithioesters and trithiocarbonates show a similar absorbance in the visible band, but their molar extinction coefficient and the position of the absorbance maximum may differ somewhat. The absorbance of the C=S group in visible band is a valuable tool to determine the amount of active dithioester end groups when the polymers are employed

4. Synthesis of water-soluble polymers via RAFT

as macro-RAFT agents, in order to be able to arrange a correct macro-RAFT agent-to-initiator ratio. Moreover, the absorbance of these end groups is used to make a good estimation of M_n by assuming that all polymer chains bear exactly one dithioester end group (disregarding the chains initiated by the initiator). This is a valuable analytical option as the molar mass analysis of water-soluble polymers, in particular of polyelectrolytes, requires mostly the use of expensive equipment, and even so is notoriously troubled with difficulties, including artifacts due to association and adsorption phenomena. The equation 4.1 was used to calculate M_n from end group analysis. Abs is the maximum absorption measured in visible band when ' χ ' g of polymer are dissolved in ' y ' ml of solvent, and ' ϵ_{CTA} ' is the molar extinction coefficient of the RAFT agent used for the synthesis of the polymer.

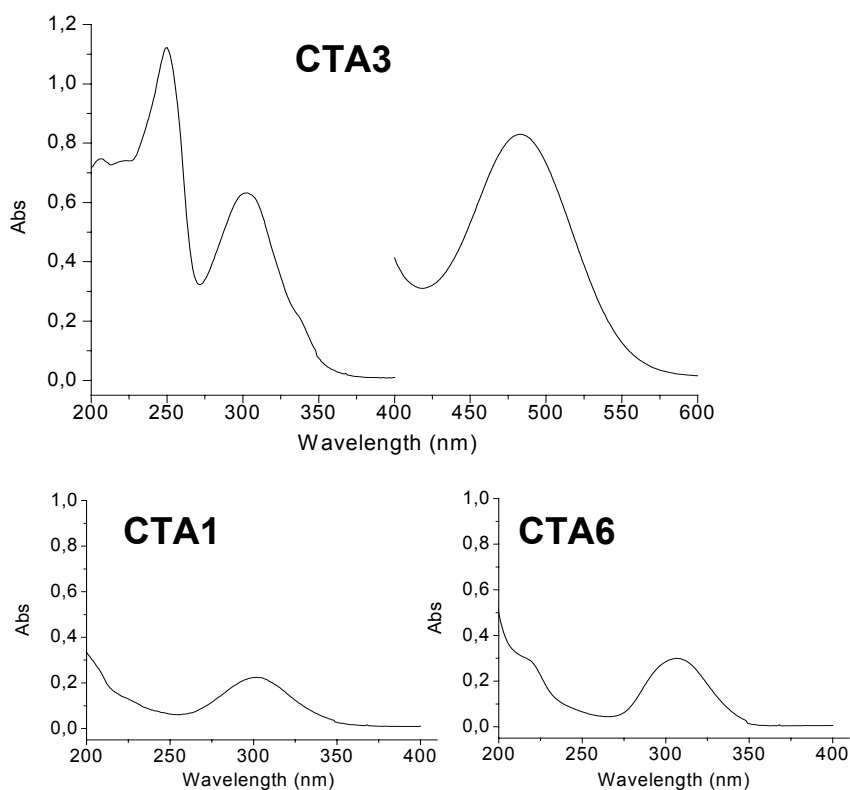


Figure 4.1. The optical spectra of **CTA3** in water (UV-vis absorption spectra; concentration = 2.39×10^{-6} M for the measurement done between 200 nm to 400 nm and = 7.5×10^{-3} M for the measurement done between 400 nm to 600 nm). The optical spectra of **CTA1** in water (concentration = 1.46×10^{-5} M). The optical spectra of **CTA6** in water (concentration = 2.06×10^{-5} M).

$$M_n = \frac{x \cdot \epsilon_{CTA}}{y \cdot 10^{-3} \cdot Abs} \quad (\text{eq. 4.1})$$

4. Synthesis of water-soluble polymers via RAFT

Since the initiator driven chains are not taken into account, the calculated M_n values are expected to be bigger than the true values. This method is generally applicable to polymers produced via RAFT using dithioesters [2]. But the extinction coefficient of the forbidden $n \rightarrow \pi^*$ band is small (typically around $10^2 \text{ l}\cdot\text{mol}^{-1}\text{cm}^{-1}$, cf. Table 4.1), implying that high polymer concentrations are necessary to obtain sufficient absorbance signals (between 0.1 and 0.8) when the molar mass increases. Not all polymers are sufficiently soluble in water, or they give cloudy solutions, thus limiting this method.

Table 4.1. Characteristic absorbance bands of RAFT agents and polymers in aqueous solution.

compound	ϵ at 251 nm		ϵ at 301 nm		visible band	
	$[\text{l}\cdot\text{mol}^{-1}\cdot\text{cm}^{-1}]$	$[\text{l}\cdot\text{g}^{-1}\cdot\text{cm}^{-1}]$	$[\text{l}\cdot\text{mol}^{-1}\cdot\text{cm}^{-1}]$	$[\text{l}\cdot\text{g}^{-1}\cdot\text{cm}^{-1}]$	λ_{max} [nm]	ϵ $[\text{l}\cdot\text{mol}^{-1}\cdot\text{cm}^{-1}]$
CTA1	2.29×10^3	7.60	11.7×10^3	38.87	497	115
CTA2					483	
CTA3	47.1×10^3	80.13	25.0×10^3	42.43	483	110
CTA4	2.98×10^3	8.06	13.0×10^3	35.17	489	130
CTA5*					480	97
CTA6					425	55
polyM1		0.084		0.025	485	
polyM2		0.182		0.022	483	
polyM3					489	
polyM5					497	
polyM6					490	
polyM7					509	
polyM9		0.044		0.023	485	
polyM11					493	
polyM12					494	
polyM13		1.22		0.023	490	
polyM14		1.30		0.020	488	

* data taken from ref. 2

The comparison of dithiobenzoates demonstrates that the absorbance maxima as well as the molar extinction coefficient of the C=S group in dithiobenzoates depend somewhat on the chemical structure of the thiol fragment of the dithioester. Increasing substitution on the α -C seems to induce a bathochromic shift of the band, i.e. the C=S bond becomes easier to activate. The molar extinction coefficient may vary somewhat in the course of the polymerization with the changing neighboring groups, thus reducing the precision. Often, this effect is accompanied by a slight shift of the absorbance maximum relative to the used RAFT agents for polymerization. That effect is visible in Table 4.1. CTAs bearing same Z but different R groups have different maximum molar extinction

4. Synthesis of water-soluble polymers via RAFT

coefficient at different wavelengths, and the absorbance maximum is also changing for different polymers bearing dithiobenzoate as end group. The end group analysis can be applied also for polymers synthesized with trithiocarbonate **CTA6**.

The high extinction of the UV band at ca. 300 nm of all dithiobenzoates (aromatic $\pi \rightarrow \pi^*$ transition) may also be useful for the end group analysis with small amounts of polymer for many acrylic and methacrylic polymers, and even for some styrenic polymers (such as **poly-M13** and **poly-M14**), if the inherent absorbance of these polymers at this wavelength is still very low (see Table 4.1). The use of this band is generally less applicable than the use of the visible band of the C=S moiety, as the UV absorbance of numerous functional groups may interfere. Moreover, this band is inherently confined to aromatic dithiocarboxylates, which are only one subclass of useful RAFT agents. However, as discussed for the extinction coefficient of the visible band, the molar extinction coefficient of the UV band may change somewhat with ongoing polymerization, as well. All dithiobenzoates used in this study except **CTA3**, have similar absorbance between 200 and 400 nm as it is presented for **CTA1** in Figure 4.1, but their extinction coefficients differ slightly (cf. Table 4.1). In case of **CTA3**, there is also a contribution of the naphthyl fragment at 301 nm, so its extinction coefficient is almost the double of the other dithioesters.

Note that in **CTA3**, the 2-naphthylamino-6, 8-disulfonate fragment imparts not only water-solubility to the RAFT agent, but may serve also as analytical tool. The UV-vis absorption spectrum exhibits three characteristic absorption maxima, at 251 nm, 301 nm, and 483 nm, respectively (cf. Figure 4.1). The absorption band of **CTA3** at 301 nm has, according to the comparison with the extinction coefficients of other dithiobenzoates at this wavelength, contributions from both the dithiobenzoate moiety and the naphthalene chromophore, with the naphthalene fragment accounting for almost half of the molar extinction (cf. Table 4.1.). Note that for the other dithiobenzoates used in this study, the contributions of the thiol fragments to the absorbance at 301 nm and 251 nm are negligibly low. That was determined by measuring the UV absorption of the precursors used for the synthesis of RAFT agents; *[4,4'-azobis(4-cyanopentanoic acid)]* for **CTA1**, *[2-(2-bromopropionylamino)-ethanesulfonic acid sodium salt]* for **CTA2**, and *[2-(2-bromo-2-methylpropionylamino)-ethanesulfonic acid sodium salt]* for **CTA4**. The absorption band at 251 nm is characteristic for the naphthalene chromophore of **CTA3** (cf. Table 4.1. and Figure

4. Synthesis of water-soluble polymers via RAFT

4.1), and therefore may serve for its specific detection. The extinction coefficients of **CTA1** and **CTA4** at this wavelength are much lower (no specific band). Furthermore, **CTA3** is a fluorescent compound, like its precursor 2-naphthylamino-6, 8-disulfonate. Consequently, polymers prepared in the presence of **CTA3** become inherently labeled with a fluorescent end group. The fluorescence emission spectra of the RAFT agent and of such polymers are exemplified in Figure 4.2, demonstrating that the spectra of **CTA3** and of the polymers derived from are virtually identical.

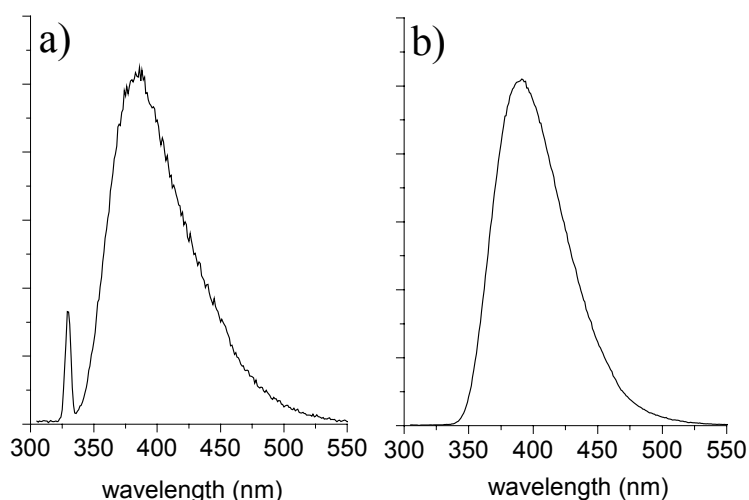


Figure 4.2. a) The fluorescence emission spectra of **CTA3**, excitation at 300 nm; b) fluorescence emission spectra of **poly-M14** polymerized using **CTA 3**, excitation at 300 nm ($M_n = 22$ K according to end group analysis via the visible band of the dithioester unit at 488 nm and the naphthalene band at 251 nm).

The different absorbance maxima in the visible and in the UV range can be used to determine number average molar masses M_n of the polymers prepared by **CTA3** via end-group analysis at different wavelengths. Specific to **CTA3**, the additional naphthalene chromophore gives rise to a third, specific intense maximum at 251 nm. The inherent absorbance of some styrenic polymers at this wavelength interferes with this band of the RAFT agent, but the 251 nm band of the naphthalene chromophore is very useful for end group analysis of acrylic and methacrylic polymers (cf. Table 4.1). When used together, the three different absorbance bands allow not only a simple cross-check on the reliability of the end-group analysis of the M_n values, but enable also a facile estimation of the amount of active polymer chain ends. Whereas the band at 251 nm is a measure for the amount of initiating fragments "R" of the RAFT agent in the polymers, the band at 483 nm is a measure for the amount of dithioester groups present, i.e. of "living" chain ends. The band at 301 nm with mixed contributions from the dithiobenzoate group and the "R" group

4. Synthesis of water-soluble polymers via RAFT

can serve to verify the reliability of this comparison. If the dithioester groups are consumed by whatever side reaction (such as recombination of growing chains, hydrolysis etc.), this will result in a mismatch of the M_n values calculated from the different absorbance bands. This information is hard or impossible to deduce from other techniques employed to determine molar mass. But it is precious e.g. when employing polymers made by RAFT as macro RAFT agents in a second polymerization reaction, in order to synthesize block copolymers.

In this thesis, the end group analysis was used as an efficient tool to verify the results obtained from GPC measurement. Furthermore, if polymers were used as macro RAFT agent, the content of active chain ends was determined from optical measurements of the visible band, rather than making the calculations with the M_n values obtained by GPC measurements. M_n values obtained from GPC measurements may better reflect the true values compared to the UV-vis estimated M_n values. But they are in any case inferior to end group analysis via UV-vis spectroscopy to quantify the active end groups.

4.2. Presentation of Monomers Used

The structure of the monomers used in this thesis is depicted in Figure 4.3. The monomers (2-acryloyloxy)ethyl)trimethyl ammoniumchloride **M1**, (2-methacryloyloxy-ethyl)trimethylammonium chloride **M5**, and vinylbenzyltrimethylammonium chloride **M13** give permanently water-soluble cationic polymers. Similarly, the polymers of monomers 3-(acryloyloxy)propansulfonate potassium salt **M2**, 3-(methacryloyloxy)-propanesulfonate potassium salt **M6**, 2-methylene-succinic acid bis-(3-sulfo-propyl)ester-dipotassium salt **M8** and 4-vinylstyrenesulfonate **M14** give permanently water soluble anionic polymers. The monomers poly(ethyleneglycol) acrylate **M3**, and N,N-dimethylacrylamide **M10** gives non-ionic hydrophilic polymers. These polymers are non-toxic and biocompatible, with a high potential for biomedical applications. The polymers of **M7** which is methacrylate analogue of **M3**, additionally exhibit a LCST in water at about 83 °C i.e. it is water-soluble at low, but insoluble at high temperatures. The carboxylic acid **M15** produces pH-sensitive polymers which are only water-soluble at high pH [8, 9]. The monomers N-(3-(dimethylaminopropyl) acrylamide **M9**, and N-(3-dimethylaminopropyl)methacrylamide **M11** provide polymers soluble in water in the full

4. Synthesis of water-soluble polymers via RAFT

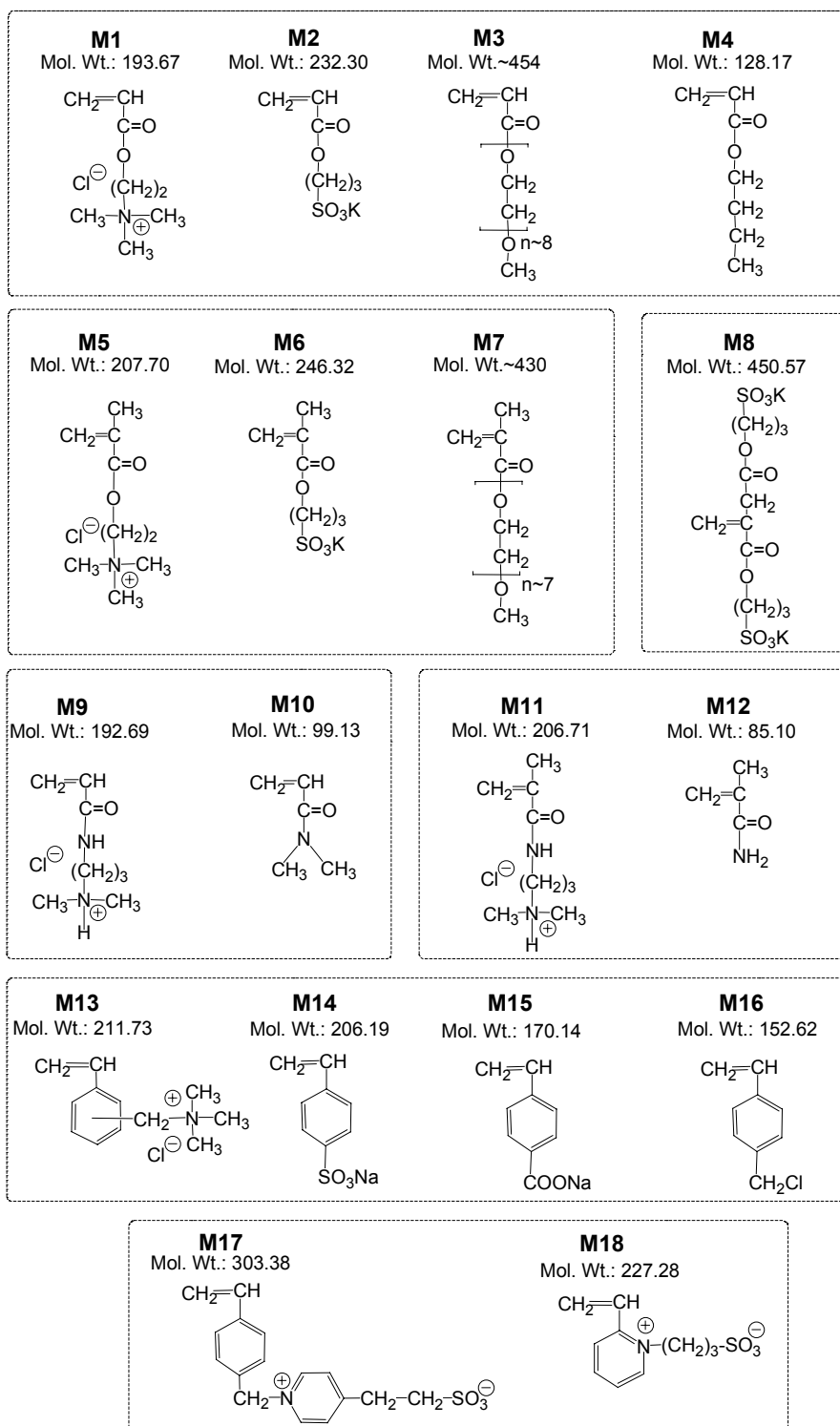


Figure 4.3. The structures of the monomers used in this study.

pH range. Their polymers can be converted into crosslinked structures by reacting their diethyl amine moieties with other reactive molecules such as α - ω - dibromoalkanes at high pH [3]. The monomers n-butyl acrylate **M4** and 4-vinylbenzylchloride **M16** give permanently hydrophobic monomers. **M16** has a reactive benzyl chloride moiety which is

4. Synthesis of water-soluble polymers via RAFT

susceptible to nucleophilic attack, and it may therefore be further functionalized. The monomers 4-(2-sulfoethyl)-1-(4-vinyl-benzyl) pyridinium betain **M17** and 3-(2-vinylpyridinio)propanesulfonate **M18** are zwitterionic, and their polymers should be biocompatible, too. Moreover, alike many polyzwitterions [10-12], **poly(M17)** is insoluble in aprotic solvents, including dimethylformamide, NMP and dimethylsulfoxide, but even so in formamide, chloroform and methanol, or their mixtures, though it dissolves in trifluoroethanol. In particular, the solubility of **poly(M17)** in aqueous solvents is sensitive to the type and the concentration of inorganic salts added: Whereas the polymer does not dissolve in pure water or in 1 M HCl, it is readily soluble in 0.5 M aqueous NaBr, NaCl or NaClO₄.

4.3. Homopolymerization Studies via RAFT

4.3.1 Polymerization of vinylbenzylchloride (M16) via RAFT

The goal of this thesis was to synthesize well-defined water-soluble polymers via RAFT in water. But at the beginning, it was not obvious whether RAFT polymerization in water is going to work or not. Therefore, the polymerization of functional monomers which can be converted to a hydrophilic derivative by simple reactions, was initiated in parallel. Styrenic monomer 4-vinylbenzylchloride (**M16**) is one of them. Its polymer can be quaternized with amines to obtain water-soluble polymers. This method is one of the conventional methods for obtaining water-soluble polymers [13]. CRP of **M16** was carried out using initiator **V-60** and **CTA7** at 80°C in toluene. **CTA7** is a standard RAFT agent which is known to be good for CRP of styrenic monomers [14]. The homopolymers of **M16** can be used as a macro-CTA to synthesize block copolymers. By subsequent quaternization of **poly-M16** block, water-soluble amphiphilic block polymers can be synthesized. Figure 4.4.a shows that polymerization of **M16** follows pseudo-first-order kinetics, and there is no observable retardation period. But polymerization proceeds very slowly. The bulk polymerization of **M16** in the study of Baussard et al.[14] was reported at 60°C, and it yields 23 % conversion after 3 h. One reason for sluggishness could be that THF is not a good solvent for **poly-M16**, but for **M16** it is. So the monomers could have some difficulty to reach the growing polymer chains. Although the polymerization is slow, M_n evolves linearly according to **PS** calibration, and fits well to the theoretical expected values. Low polydispersities of about 1.1 are accessible.

4. Synthesis of water-soluble polymers via RAFT

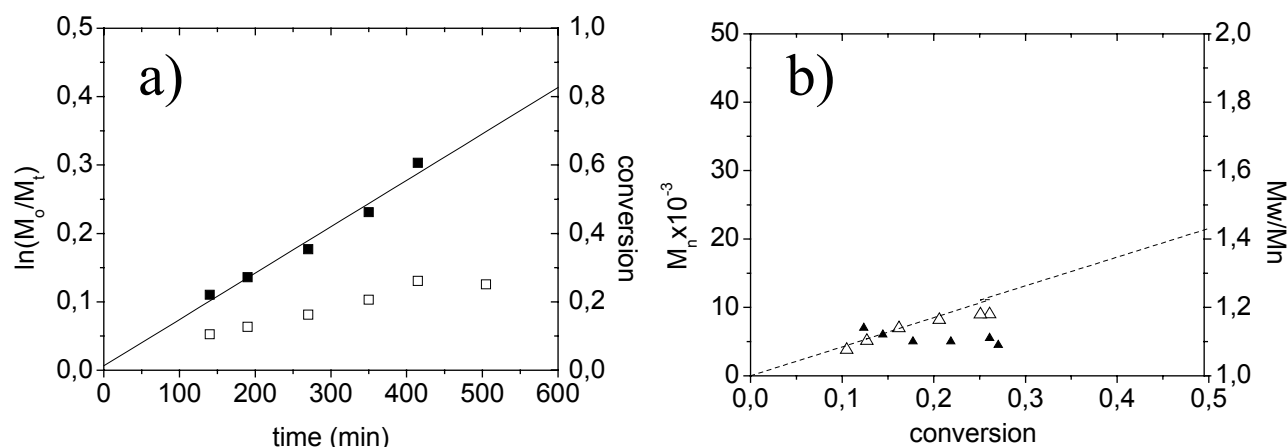


Figure 4.4. Polymerization of **M16** in toluene using initiator **V-60** and the RAFT agent **CTA7** at 80°C ($[CTA]/[I]=6.1$). a) (\square) conversion vs. time (conversion values determined by using IR signal ratios of monomer and polymer obtained from SEC), (\blacksquare) $\ln(M_0/M_t)$ vs. time, the solid line is the linear fit of $\ln(M_0/M_t)$ vs. time data; b) evolution of M_n and PDI (M_w/M_n) with conversion according to SEC in THF, (\triangle) M_n according to calibration with PS standards, (\blacktriangle) polydispersity according to calibration with PS standards.

4.3.2. Aqueous RAFT polymerization of methacrylic monomers

Whereas dithioesters with leaving groups R such as benzyl (as in **CTA5** and **CTA6**) or propion-2-yl (as in **CTA2** or in **CTA3**) are known as efficient RAFT agents for styrenic and acrylic monomers, they are much less efficient in the case of methacrylic monomers [15, 16]. Therefore, we investigated the usefulness of classical **CTA1** as well as of the new, permanently anionic dithiobenzoate **CTA4** for aqueous polymerizations at relatively low temperatures. All details related to the polymerizations are given in Table 7.1 in Chapter 7.

One of the first polymerization trials was carried out with anionic methacrylic monomer **M6**, as its polymer is known to be well soluble in water at neutral pHs. The classical anionic RAFT agent **CTA1** and the cationic azo initiator **V-50** were employed for the CRP of **M6** in water at 55°C. Note that 55°C is a rather low polymerization temperature compared to the conventionally employed ones (>60 °C) for RAFT polymerization. After a short retardation period of about 15 min, the polymerization of **M6** is relatively fast at 55°C and follows pseudo-first-order kinetics until ca. 70% conversion but then deviates from this behavior (Figure 4.5.a). ASEC traces of the polymers obtained from ongoing

4. Synthesis of water soluble polymers via RAFT

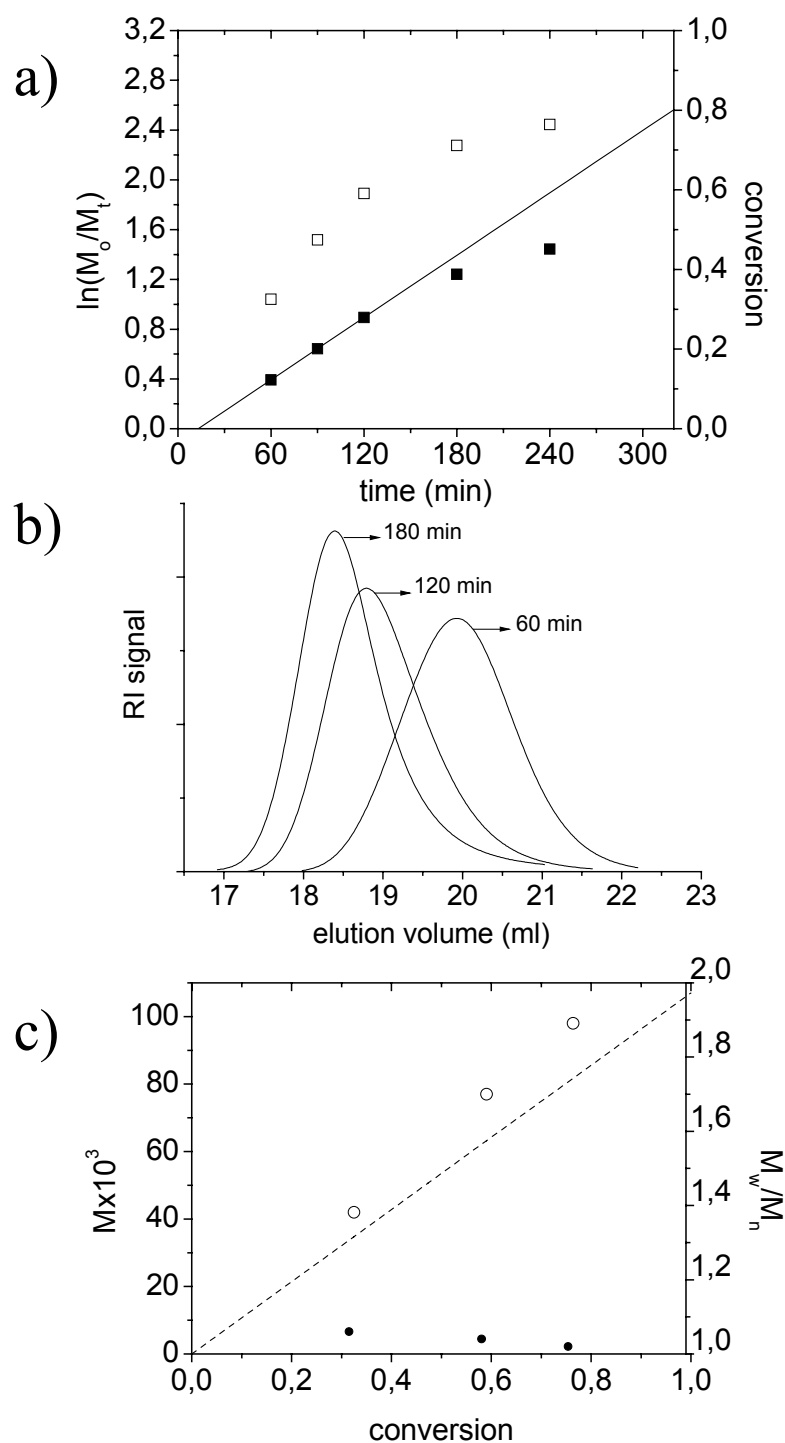


Figure 4.5. Polymerization of M6 in water using initiator V-50 and the RAFT agent CTA1 at 55°C ([CTA]/[I])=3.7). a) (□) conversion determined by gravimetry vs. time, (■) $\ln(M_0/M_t)$ vs. time, the solid line is the linear fit of $\ln(M_0/M_t)$ vs. time data; b) the evolution of ASEC elugram with polymerization time (eluent: 0.1 M aq NaNO₃); c) evolution of M_n and PDI (M_w/M_n) with conversion, (○) M_n according to MALLS, (●) polydispersity of sample determined with MALLS. The dashed line (---) is the theoretically calculated evolution of M_n .

4. Synthesis of water soluble polymers via RAFT

polymerization shift to lower elution volumes with increasing conversion as expected for CRP (Figure 4.5.b). The evaluation by MALLS in Figure 4.5.c shows linear growth of the molar mass close to the theoretically calculated values and low polydispersities (down to 1.05). In parallel to this study, polymerization of **M6** in water was mentioned briefly in successful RAFT polymerizations using **CTA 1** at 70°C recently [4].

Having verified the basic usefulness of **CTA1** for the CRP of methacrylates with **M6** in water even at 55°C, the non-ionic macro monomer **M7** was polymerized in aqueous solution using **CTA1** and **V-50** at 55 C°, as illustrated in Figure 4.6. In fact, **M7** (and equally **M3**, *vide infra*) is a versatile monomer with interesting properties, such as being soluble in many organic solvents and in water, or being non-toxic and biocompatible, with a high potential for biomedical applications. After a somewhat extended retardation time of about 25 min in comparison to the classical monomer **M6**, a rapid polymerization is observed following pseudo-first-order-kinetics (Figure 4.6.a). The SEC traces of the polymer samples in THF exhibit the continuous shift towards lower elution volumes with the reaction time (Figure 4.6.b). Evaluating the SEC data by calibration with polystyrene standards, polydispersities are about 1.1. (see Figure 4.6.c). The apparent M_n values increase linearly with increasing conversion, but are by a factor of 3 smaller than the theoretically calculated ones. Polystyrene is not a good standard for polymethacrylate **poly-M7**. The molar mass M_n was therefore additionally determined by analysis of the dithioester end group visible band using the visible band with $\lambda_{\max}=509$ nm, providing values ($M_n = 56$ K at 73% conversion) that are close to the theoretically calculated ones.

The usefulness of the new, pH-independently water-soluble RAFT agent **CTA4** was investigated in the polymerization of the cationic methacrylate **M5** using initiator **V-50** at 55°C. The polymerization is rapid after a very short retardation period, reaching 80% conversion within less than 4 h. The plot of reaction time vs. $\ln(M_0/M_t)$ and conversion as shown in Figure 4.7.a illustrates that the reaction follows pseudo-first-order kinetics. Although ASEC analysis of **poly-M5** samples which are produced by conventional free radical polymerization works correctly, the ASEC analysis of the polymers obtained by CRP with **CTA4** failed surprisingly. Under the conditions needed to make the polymers pass through the columns, very high apparent molar masses and relatively high apparent polydispersities were found, which changed only slightly with monomer conversion

4. Synthesis of water soluble polymers via RAFT

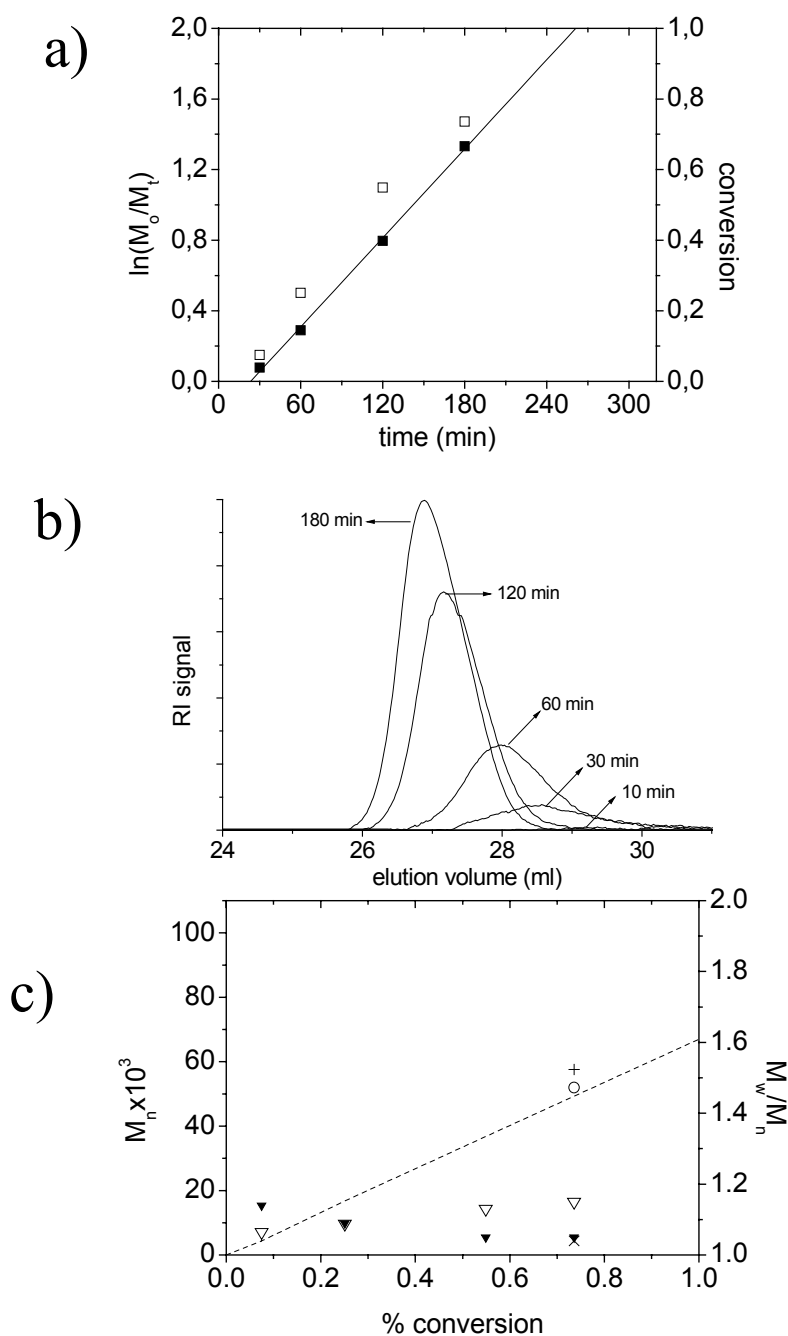


Figure 4.6. Polymerization of **M7** in water using initiator **V-50** and the RAFT agent **CTA1** at 55°C ([CTA]/[I])=3.8). a) (□) conversion vs. time (conversion values determined by using IR signal ratios of monomer and polymer obtained from SEC), (■) $\ln(M_0/M_t)$ vs. time, the solid line is the linear fit of $\ln(M_0/M_t)$ vs. time data; b) evolution of SEC elugram with polymerization time (eluent: THF), c)) plot of evolution of M_n and PDI (M_w/M_n) with conversion, (○) M_n according to MALLS eluent: aqueous 0.2 M Na_2SO_4 containing 1 wt% of acetic acid, (▽) M_n according to calibration with **PS** standards (eluent:THF), (+) M_n estimated by using the visible band at $\lambda_{max} = 509$ nm of the dithioester end group, (X) polydispersity of sample determined with MALLS (▼) polydispersity according to calibration with **PS** standards. The dashed line (---) indicates the theoretically calculated evolution of M_n .

4. Synthesis of water soluble polymers via RAFT

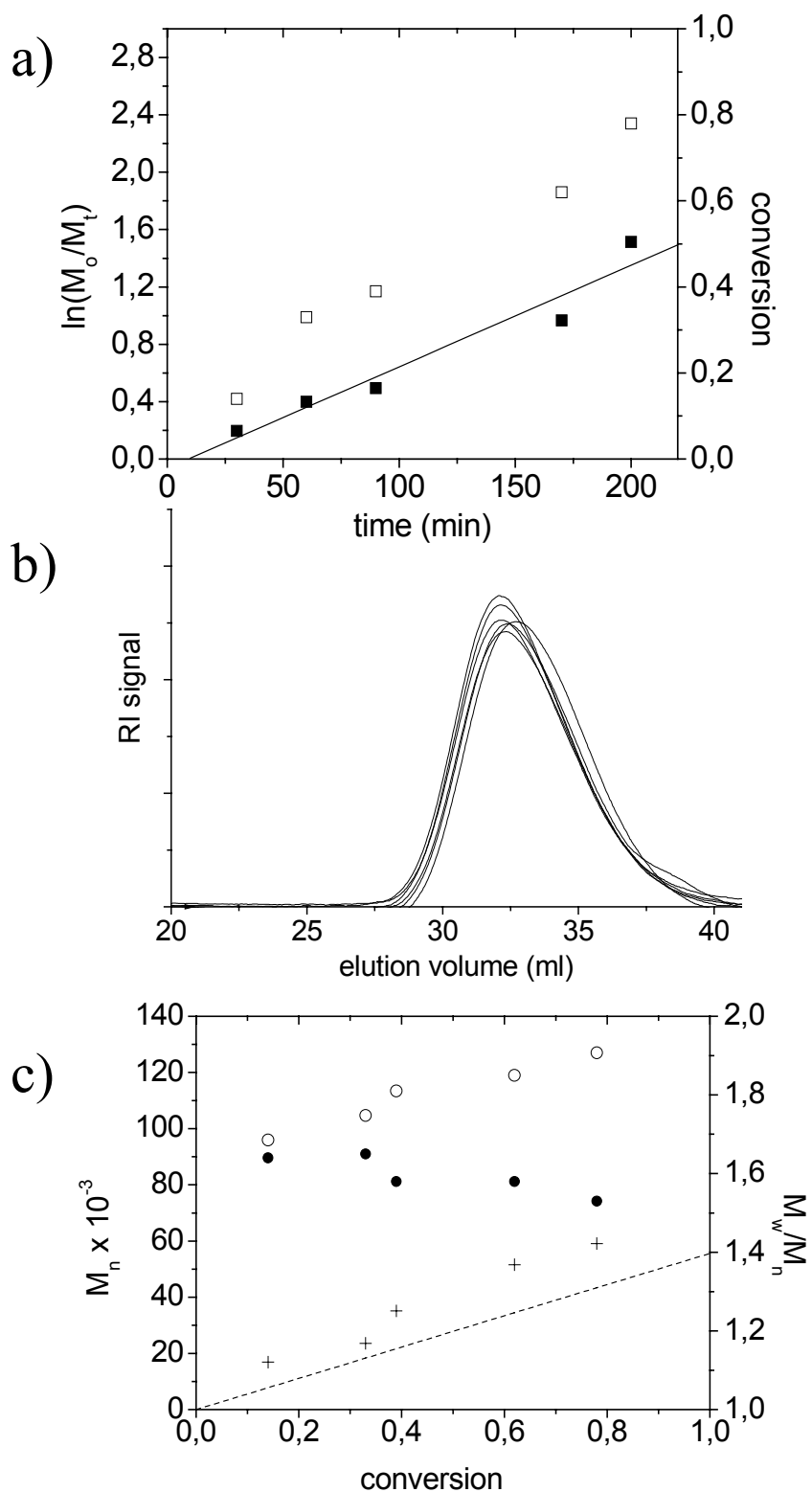


Figure 4.7. Polymerization of **M5** in water using initiator **V-50** and the RAFT agent **CTA4** at 55°C ([CTA]/[I])=5/1). a) (□) conversion vs. time, (■) $\ln(M_0/M_t)$ vs. time and the solid line is the linear fit of $\ln(M_0/M_t)$ vs. time data. b) evolution of ASEC elugram with polymerization time (eluent: 0.2 M Na_2SO_4 in 1 wt% aqueous acetic acid); c) evolution of M_n and PDI (M_w/M_n) with conversion, (○) M_n according to MALLS, (+) M_n estimated by the visible band of the dithioester end group, (●) polydispersity of sample determined with MALLS. The dashed line (---) is the theoretically calculated evolution of M_n .

4. Synthesis of water soluble polymers via RAFT

(Figure. 4.7.b and c). These findings are attributed to polymer aggregates, presumably formed due to the electrostatic interaction of the anionic end groups with the cationic polymer in the high ionic strength eluent. At this point, end group analysis was employed to see whether it can be used as a useful tool to cross-check the apparent molar masses obtained by MALLS. As it is seen in Figure 4.7.c, the M_n values derived from the absorbance of the dithioester band at 493 nm evolve linearly with conversion, and are close to the theoretically calculated ones. In this situation, molar mass determination by end group analysis was proved to be very helpful.

The attempted CRP of pH sensitive methacrylamide **M11** at 55°C with **CTA1** and **CTA4** failed in water at about pH 6 when **V-50** was employed as an initiator. Putatively, the hydrolysis of **M11** or of **V-50** may produce some amines, and these amines could lead to the aminolysis of employed RAFT agents, and thus, the failure of CRP of **M11**. According to the results of the stability tests, the RAFT agents were found rather stable at acidic pHs. Thus, it was thought that CRP of **M11** might work at low pHs if the aminolysis of RAFT agents was the reason for the failure of CRP. **CTA1** is not soluble at low pHs, but **CTA4** is. The usefulness of the new RAFT agent **CTA4** was verified, and polymer was obtained when polymerizing at pH=4 (see Table 7.1 in chapter 7 for the details of polymerization). The reaction of **M11** shows a retardation time of ca 30 min and is slow in comparison with the cationic methacrylate **M5**, reaching only 50% conversion after 4h, while following pseudo first order kinetics (Figure 4.8.a). The ASEC traces in Figure 4.8.b present a continuous shift to lower elution volumes. Evaluating the data by MALLS, a linear increase of molar mass is found. The calculated M_n values are in good agreement with those determined by end group analysis using the dithioester band at 497 nm (Figure 4.8.c). Polydispersities are between 1.3 and 1.4. However, the determined M_n values are systematically about 20% higher than the theoretically calculated values. Calibration of the ASEC with poly-(2-vinylpyridine) standards corroborated the linear increase of the molar mass, and gave good agreement of the apparent M_n values with the theoretically calculated ones while the derived polydispersities are between 1.4 and 1.5.

CTA4 was also engaged in attempts to polymerize the unsubstituted methacrylamide **M12** using initiator **V-50** at 55°C, at pH values of 6.2, 5.4, and 3. Alike acrylamide, **M12** is inherently critical for RAFT polymerization due to the risk of slow

4. Synthesis of water soluble polymers via RAFT

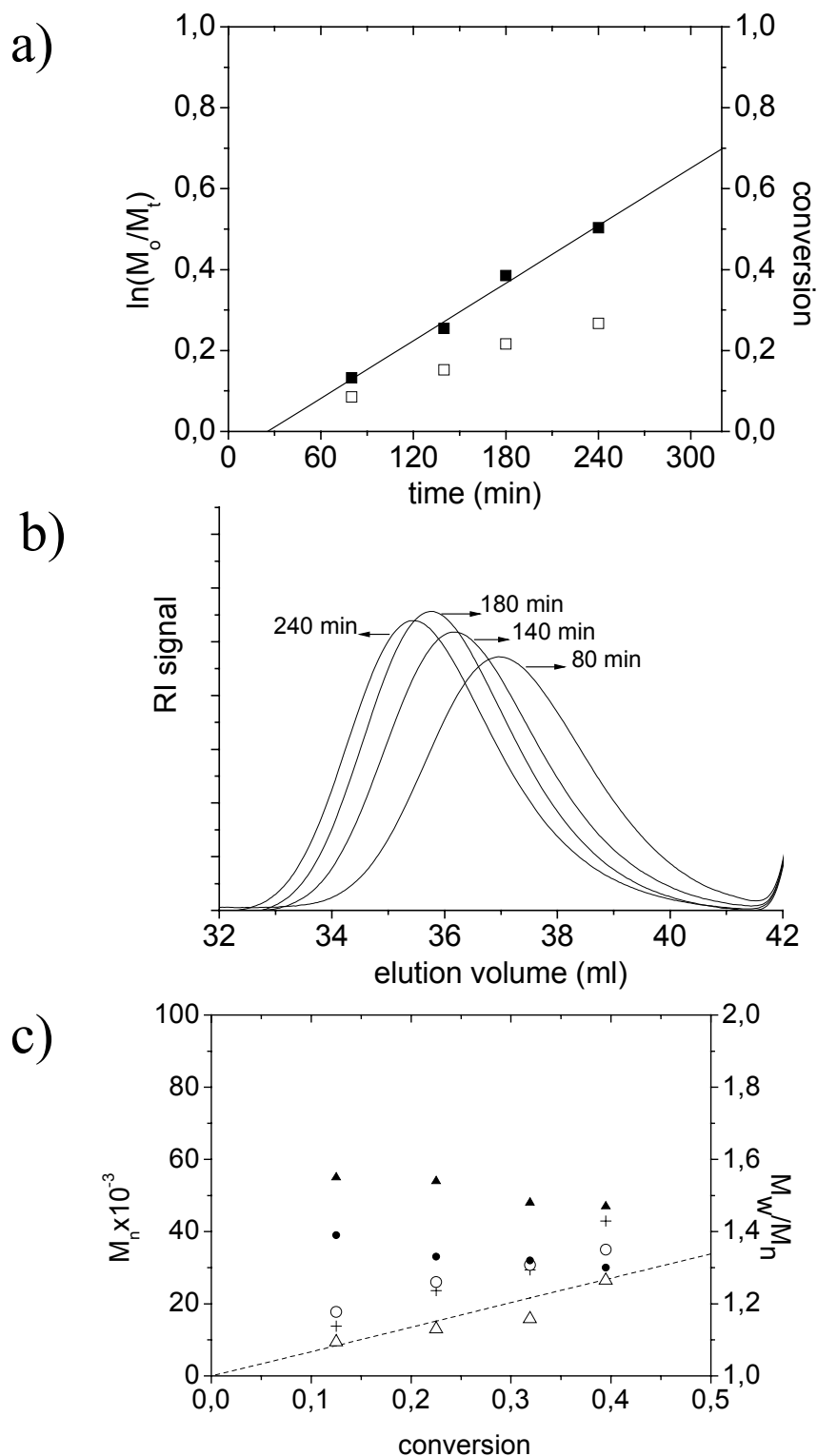


Figure 4.8. polymerization of **M11** in water using initiator **V-50** and the RAFT agent **CTA4** at 55°C ($[CTA]/[I]=5/1$). a) (\square) conversion vs. time, (\blacksquare) $\ln(M_0/M_t)$ vs. time and the solid line is the linear fit of $\ln(M_0/M_t)$ vs. time data b) evolution of ASEC elugram with polymerization time (eluent: 0.2 M Na_2SO_4 in 1 wt% aqueous acetic acid); c) evolution of M_n and PDI (M_w/M_n) with conversion, (\circ) M_n according to MALLS, (+) M_n estimated by the visible band of the dithioester end group, (\bullet) polydispersity of sample determined with MALLS. The dashed line (---) is the theoretically calculated evolution of M_n

4. Synthesis of water soluble polymers via RAFT

hydrolysis of the primary amide and subsequent aminolysis of the dithioester group [5,6]. Indeed, even after 8 h of reaction, only traces of colorless polymers (conversion less than 2%) were obtained at pH of 6.2 and 5.4. But polymerization worked out at pH=3, where **CTA4** is easily water-soluble (different from **CTA1**), though the rate of the reaction is slow compared to the other polymerizations conducted at 55°C in the studies undertaken. The reaction seems to follow pseudo-first order-kinetics for up to 6 h after a retardation period of ca. 50 min (Figure 4.9.a). But the ASEC traces are very close to each other and there is only a small shift towards low elution volumes with conversion (Figure 4.9.b). The M_n values determined from MALLS and from end group analysis with the band at 494 nm show a continuous increase (Figure 4.9.c), but deviate by a factor of 2 from the theoretical values, while the calculated polydispersities are about 1.4.

4.3.3. Aqueous RAFT polymerization of acrylic monomers

The R living group of labeled **CTA3** is propion-2-yl group, and this makes **CTA3** suited for the RAFT polymerization of acrylic and styrenic monomers. To verify the usefulness of **CTA3** for double end group labelling and CRP via RAFT, it was first used for the polymerization of anionic acrylic ester **M2**. For comparison, the CRP of **M2** was carried out using the established RAFT agent **CTA1** at low temperature as well. As shown in Figure 4.10.a, the polymerization of **M2** in the presence of **CTA1** at 55°C reached 90% conversion after 5h, and follows pseudo-first-order kinetics after an initial retardation period of about 60 min. The ASEC traces of samples taken at increasing reaction times (Figure 4.10.b) present basically unimodal peaks with decreasing elution volumes and reducing width, as expected for controlled polymerization. At short elution volumes, a small band indicative of additional high molar mass polymer (>1,000,000) is detected, too, whose relative importance decreases with conversion. This peak was always present in the samples of **poly-M2** (with or without RAFT agents present), and is attributed to uncontrolled polymerization of the destabilized monomer when it is dissolved in water before the addition of RAFT agent. Neglecting this high molar mass impurity, the number average molar mass M_n increases steadily with conversion, according to analysis by MALLS as well as by end group determination using the visible dithioester band at 483 nm (Fig. 4.10.c). Both M_n values match well and are close to the M_n value expected theoretically for the given ratio of monomer to RAFT agent. The polydispersities according to MALLS are very narrow ($M_w/M_n < 1.1$.) Replacing RAFT agent **CTA1** by the

4. Synthesis of water soluble polymers via RAFT

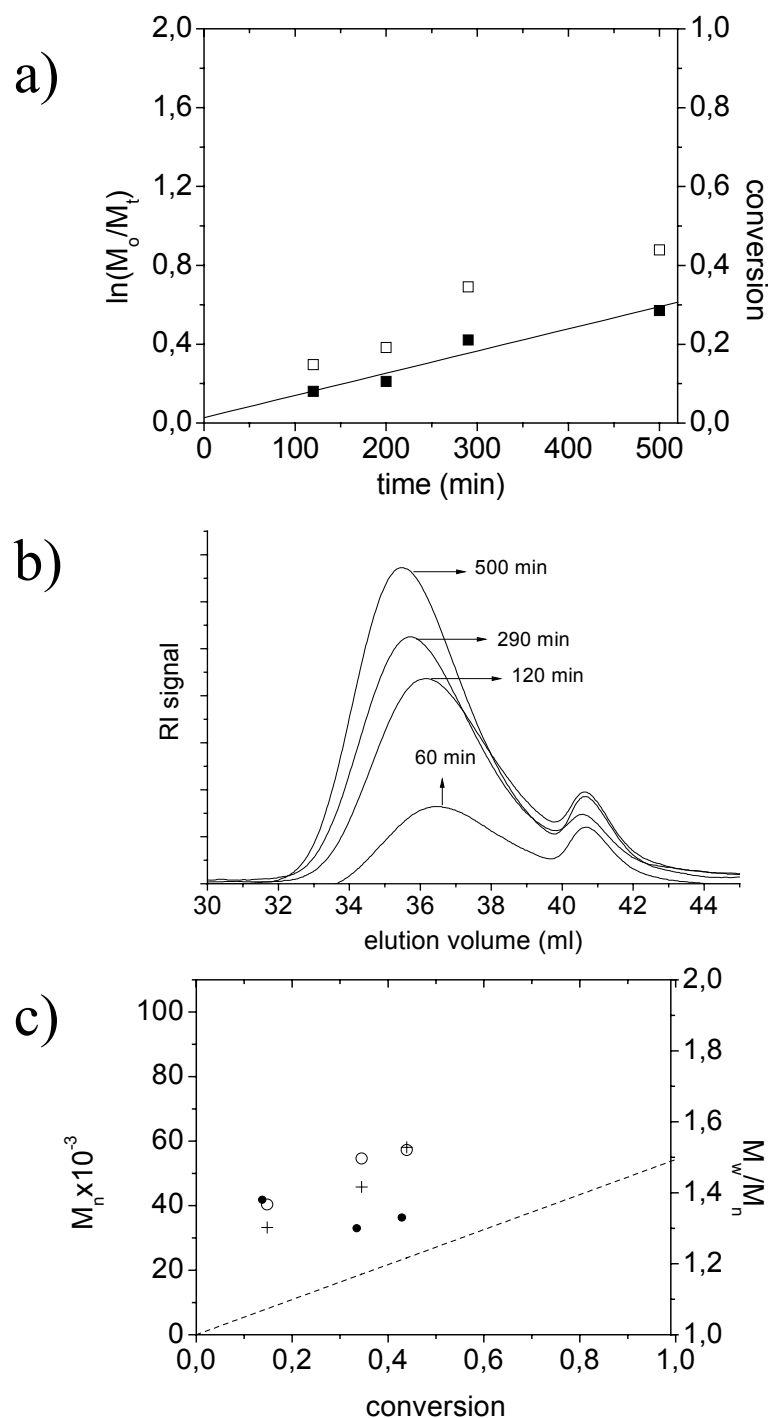


Figure 4.9. Polymerization of **M12** in water using initiator **V-50** and the RAFT agent **CTA3** at 55°C ($[CTA]/[I]=5/1$). a) (\square) conversion vs. time, (\blacksquare) $\ln(M_0/M_t)$ vs. time and the solid line is the linear fit of $\ln(M_0/M_t)$ vs. time data; b) evolution of ASEC elugram with polymerization time (eluent: 0.2 M Na_2SO_4 in 1 wt% aqueous acetic acid); c) evolution of M_n and PDI (M_w/M_n) with conversion, (\circ) M_n according to MALLS, (+) M_n estimated by the visible band of the dithioester end group, (\bullet) polydispersity of sample determined with MALLS. The dashed line (---) is the theoretically calculated evolution of M_n .

4. Synthesis of water soluble polymers via RAFT

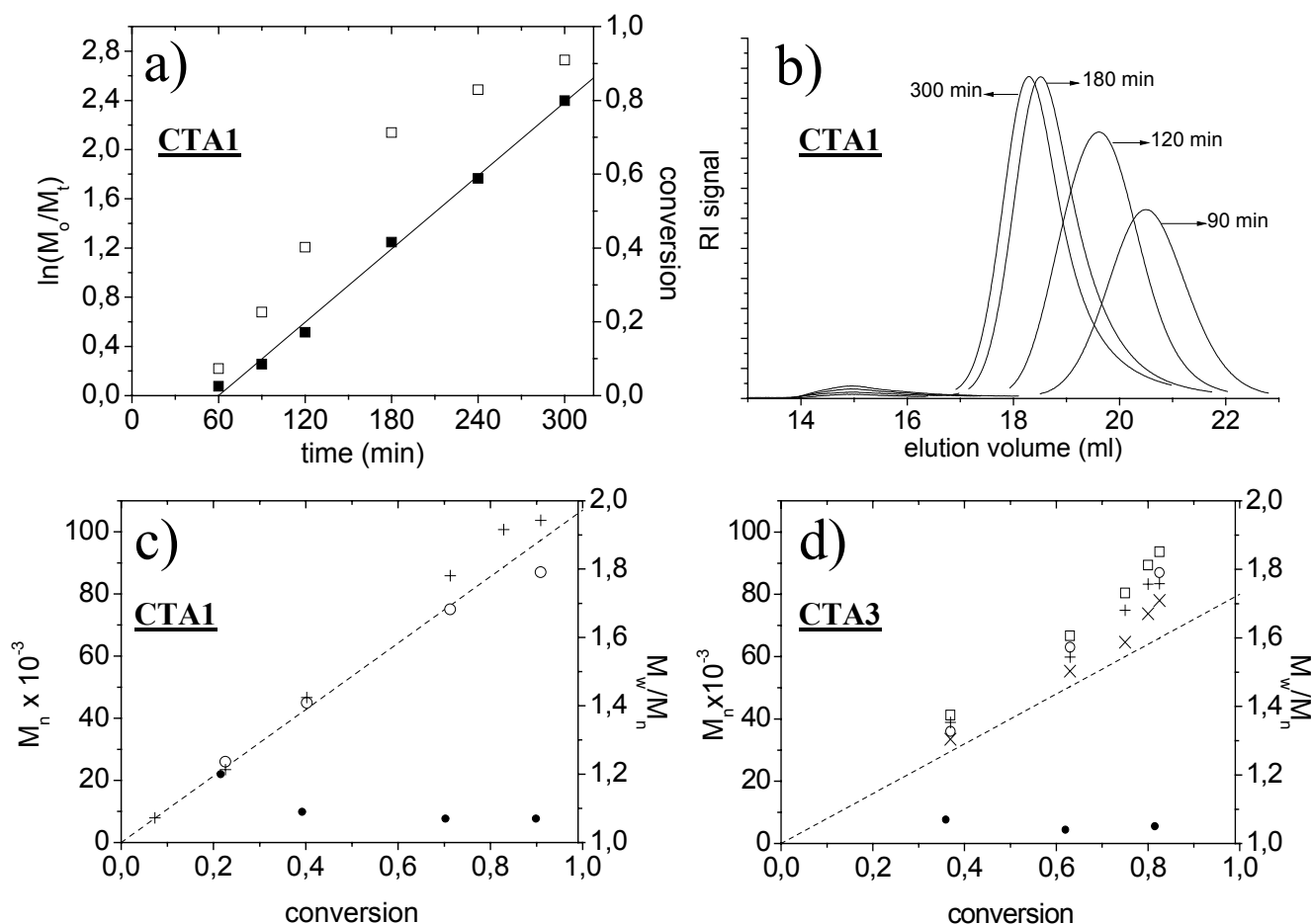


Figure 4.10. Polymerization of **M2** in water using initiator **V-50** and the RAFT agent **CTA1** at 55°C ($[CTA]/[I]=3.8$). a) (□) conversion determined by gravimetry vs. time, (■) $\ln(M_0/M_t)$ vs. time and the solid line is the linear fit of $\ln(M_0/M_t)$ vs. time data; b) evolution of ASEC elugrams with polymerization time (eluent: 0.1 M aq $NaNO_3$); c) evolution of M_n and PDI (M_w/M_n) with conversion, d) polymerization of **M2** in water using initiator **V-545** and the RAFT agents **CTA3** at 48°C ($[CTA]/[I]=5/1$). Symbols: (○) M_n according to MALLS, (●) polydispersity of the sample determined with MALLS, (+) M_n estimated by the visible band of the dithioester end group (□) M_n estimated by using the UV band at $\lambda_{max} = 301$ nm, (X) M_n estimated by using the UV band at $\lambda_{max} = 251$ nm. The dashed line (---) is the theoretically calculated evolution of M_n .

new labeled **CTA3**, polymerization of **M2** behaves very similarly. The initial retardation period is about 60 min, kinetics are equally fast, number average molar mass M_n increases steadily with conversion, and polydispersities are very narrow (Figure 4.10.d). Exploiting the multiple absorption bands introduced into the system by **CTA3**, M_n values calculated by end group determination via the dithioester band at 483 nm, and via the UV naphthalene band at 251 nm match well. Estimating M_n values by analyzing the combined band at 301 nm also shows a good agreement of the data, although the values seem to overestimate the true values somewhat. Clearly, the use of the labeled RAFT agent is an attractive method

4. Synthesis of water soluble polymers via RAFT

to complement molar mass data by a simple and low cost analytical method such as UV/vis spectroscopy.

Having established the usefulness of **CTA3** in aqueous solution polymerization for ionic monomers **M2**, its use was studied for the non-ionic macro monomer **M3** (Figure 4.11). **M3** is the acrylate analogue of the methacrylate macro monomer **M7** studied above, and has a similar potential as functional monomer. Figure 4.11.a shows that polymerization of **M3** proceeds about as fast as for **M2**, and follows pseudo-first order kinetics up to 85% conversion after an initial retardation period of about 60 min. But with longer reaction times, kinetics slows down (sample taken after 300 min). This suggests that the radical concentration in the reaction medium is reduced. The ASEC elugrams show a continuous shift to lower elution volumes, indicating a steady increase in molar mass (Fig. 4.11.b). Evaluation by online MALLS shows a linear increase in the molar mass, close to the theoretically expected one, and low polydispersities of about 1.3 (Figure 4.11.c). In Figure 4.11.d, the ASEC data for **poly-M3** were cross-checked by SEC using NMP as eluent and calibrating with polystyrene standards. Polydispersities are low (about 1.15) and molar masses increase linearly with increasing conversions, too. As found for SEC of the analogous polymethacrylate **poly-M7** in THF (*vide supra*), the apparent M_n values are lower by a factor of 3, indicating that calibration with polystyrene is not appropriate for the polymerized macro-monomer, as well, due to the strong structural differences. When calculating M_n values from the dithioester band at 489 nm and the naphthalene band at 251 nm, as well as from the mixed band at 301 nm, the numbers for all bands are close to each other as well as to the theoretically expected value (Figure 4.11.d), corroborating the usefulness of the labeled RAFT agent. Noteworthy, for the last sample taken after 300 minute of polymerization (which does not fit to first order kinetics any more), the M_n value calculated from the 489 nm band is somewhat higher than the one derived from the 251 nm band, as well as than the theoretical value. This discrepancy may reflect a partial loss of dithioester end groups at extended reaction times, e.g. due to hydrolysis.

The new-labeled RAFT agent **CTA3** controlled the polymerizations of anionic **M2** and noncharged macro monomer **M3**, smoothly. To clarify whether the anionic **CTA3** can be employed for a cationic monomers as well, the cationic acrylate **M1** was also polymerized at 48°C in water by employing **CTA3** and **V-545** (Figure 4.12). Similar to the other acrylate monomers **M2** and **M3**, polymerization proceeds to 90% conversion within

4. Synthesis of water soluble polymers via RAFT

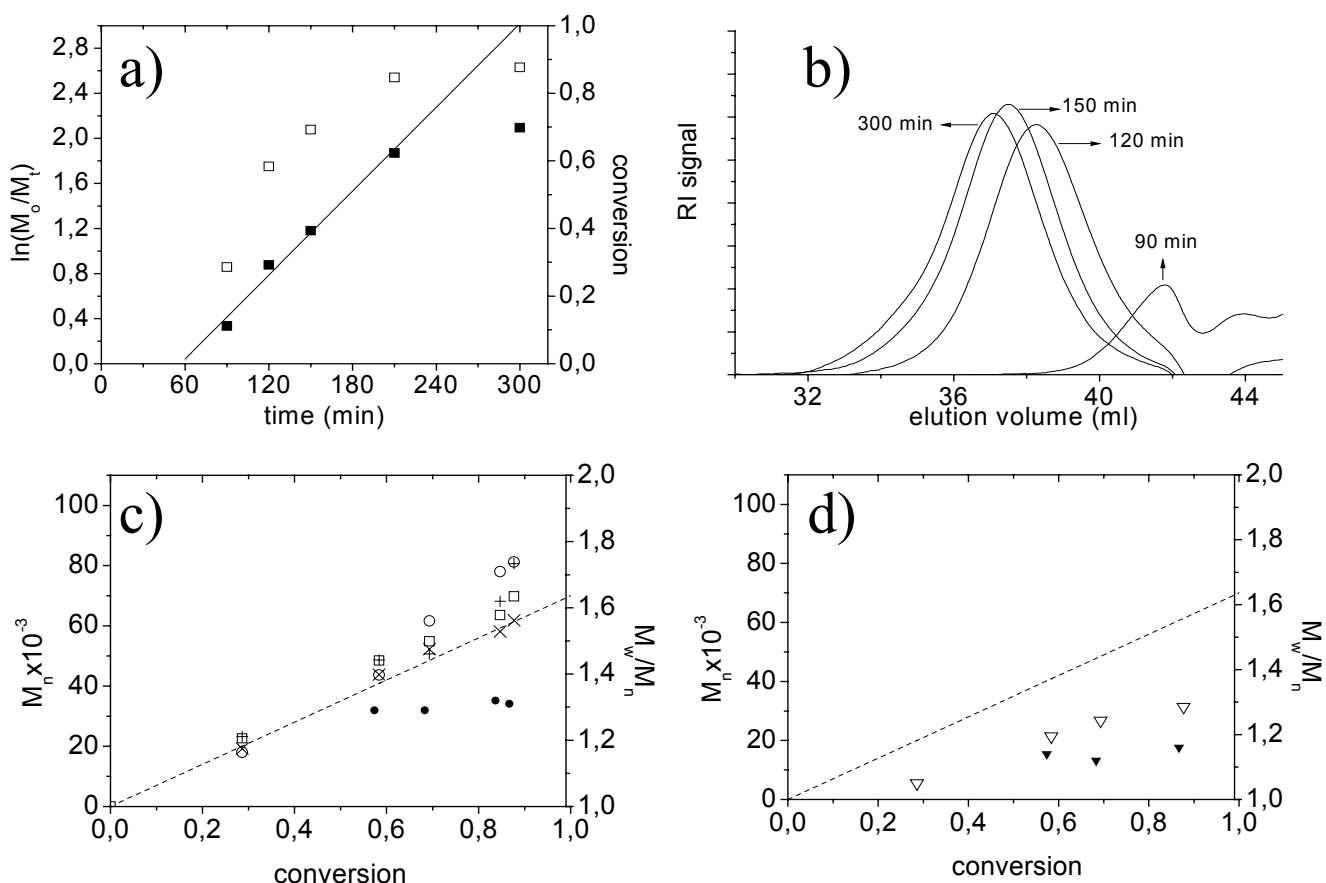


Figure 4.11. Polymerization of **M3** in water using initiator **V-545** and the RAFT agent **CTA 3** at 48°C ($[CTA]/[I]=5/1$). a) (\square) conversion determined by gravimetry vs. time, (\blacksquare) $\ln(M_0/M_t)$ vs. time and the solid line is the linear fit of $\ln(M_0/M_t)$ vs. time data (point at 300 min was excluded) b) evolution of ASEC elugrams with polymerization time (eluent: 0.2 M Na_2SO_4 in 1 wt% aqueous acetic acid) c) evolution of M_n and PDI (M_w/M_n) with conversion, (\circ) M_n according to MALLS, (+) M_n estimated by the visible band of the dithioester end group, (\square) M_n estimated by using the UV band at $\lambda_{max} = 301$ nm, (X) M_n estimated by using the UV band at $\lambda_{max} = 251$ nm, (\bullet) polydispersity of sample determined with MALLS. The dashed line (---) is the theoretically calculated evolution of M_n . d) SEC in N-methyl pyrrolidone (eluent: 0.05 M LiBr NMP) (∇) M_n according to calibration with **PS** standards, (\blacktriangledown) polydispersity according to calibration with **PS** standards.

a few hours, and follows pseudo-first order kinetics up to high conversion after an initial retardation period of about 60 min (Fig. 4.12.a). Again, the ASEC elugrams shift steadily to lower elution volumes with increasing conversion (Fig. 4.12.b). Evaluation of the MALLS data in Figure 4.12.c shows a linear increase in the molar mass, close to the theoretically expected behavior, and low polydispersities of about 1.15. An attempted calibration of the ASEC with poly-(2-vinylpyridine) standards indicated rather low polydispersities (about 1.35) and molar masses increasing linearly with the conversion, too.

4. Synthesis of water soluble polymers via RAFT

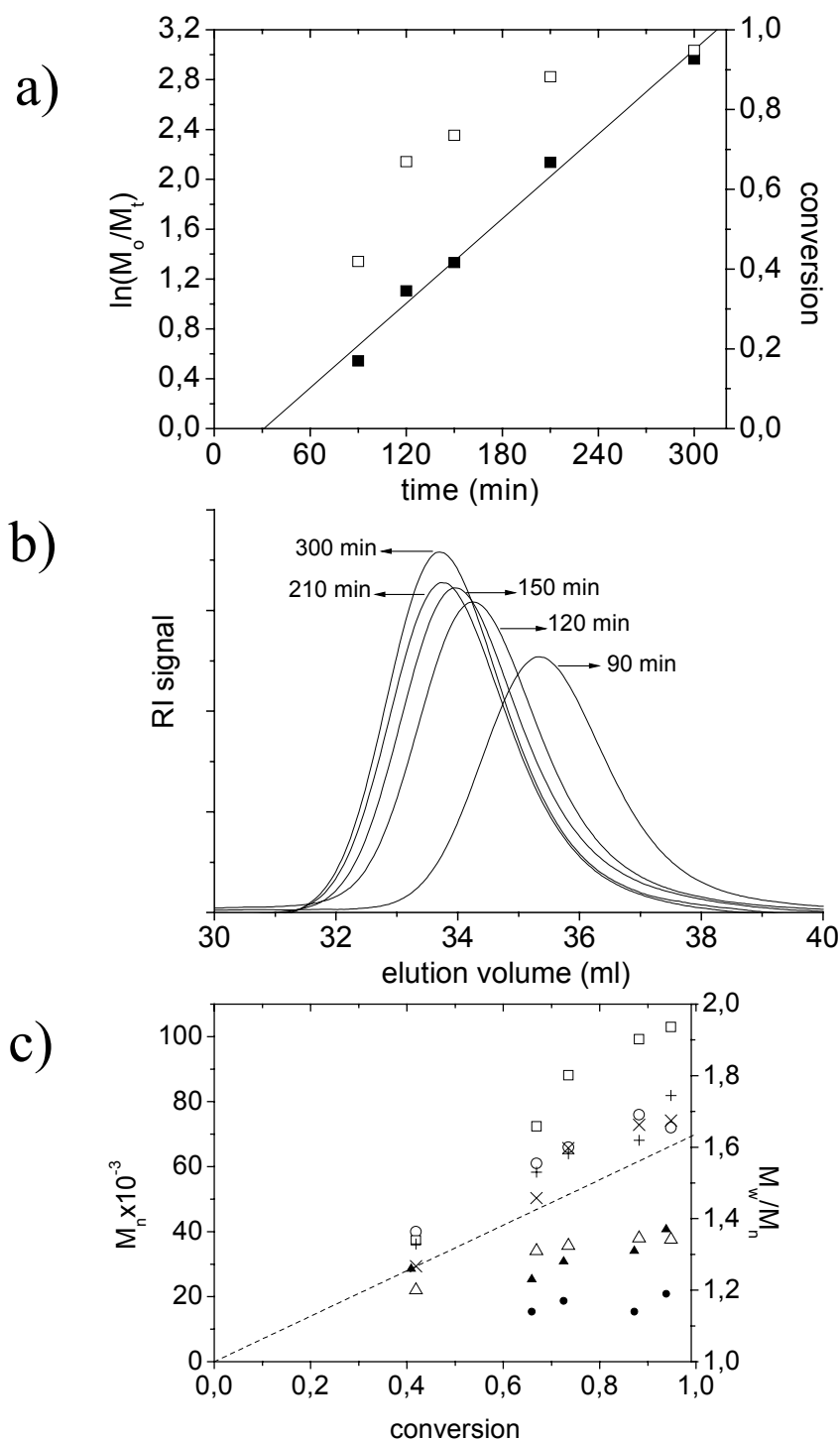


Figure 4.12. Polymerization of **M1** in water using initiator **V-545** and the RAFT agent **CTA3** at 48°C ([CTA]/[I])=5/1). a) (□) conversion determined by gravimetry vs. time, (■) $\ln(M_0/M_t)$ vs. time and the solid line is the linear fit of $\ln(M_0/M_t)$ vs. time data; b) evolution of ASEC elugrams with polymerization time (eluent: 0.2 M Na₂SO₄ in 1 wt% aqueous acetic acid); c) evolution of M_n and PDI (M_w/M_n) with conversion, (○) M_n according to MALLS, (Δ) M_n according to calibration with **P2VP** standards, (+) M_n estimated by the visible band of the dithioester end group, (□) M_n estimated by using the UV band at $\lambda_{max} = 301$ nm, (X) M_n estimated by using the UV band at $\lambda_{max} = 251$ nm, (●) polydispersity of sample determined with MALLS (▲) polydispersity according to calibration with **P2VP** standards. The dashed line (---) is the theoretically calculated evolution of M_n .

4. Synthesis of water soluble polymers via RAFT

But the apparent M_n values are considerably lower than the values derived from MALLS (by a factor of 2), indicating that the polymer standard is not appropriate. In contrast, M_n values calculated by end group analysis both from the dithioester band at 485 nm and the naphthalene band at 251 nm, agree well with the ASEC and theoretical numbers (Figure 4.12.c), indicating the good preservation of the dithioester end group during the polymerization process. In the case of **poly-M1** however, the UV data for the mixed band at 301 nm give only approximate M_n values which exceed systematically the ones derived from the other analytical data. This suggests that the extinction coefficient of the 301 nm band, presumably due to a changing contribution from the dithiobenzoate chromophore, differs in the RAFT agent and in the polymer.

Having established the usefulness of **CTA3** for acrylates (**M1**, **M2** and **M3**), its usefulness for the aqueous RAFT polymerization of the pH sensitive acrylamide N-(3-(dimethylaminopropyl) acrylamide (97%) **M9** was tested. By employing **V-545** as initiator at 48°C, the polymerization was attempted at pH=6 and pH=3.2, adjusting the pH of the solutions by addition of small quantities of NaOH and HCl, respectively. As in the case of methacrylamides **M11** and **M12**, no polymer could be obtained at pH 6, even after 300 min of reaction, but the polymerization carried out at pH 3.2 was successful. After a retardation period of around 70 min, polymerization goes up to about 70% conversion within 5 h (Figure 4.13.a). The kinetics deviate from pseudo-first-order beyond 60% conversion. The ASEC traces in Figure 4.13.b show a shift of the peak to lower elution volumes, i.e. a steady evolution of the molar mass with conversion until 240 min. But after since, the molar masses rather stagnate. Nevertheless, the evaluation of the data in Figure 4.13.c shows a linear increase in the molar mass, close to the theoretically expected one, according to MALLS and to end group analysis using the dithioester band at 485 nm and the naphthalene band at 251 nm. Polydispersities according to MALLS are as low as 1.2. As for the cationic polyacrylate **polyM1**, an attempted calibration of the ASEC with poly-(2-vinylpyridine) standards exhibited a linear increase of the molar masses of **polyM9** with conversion. But the apparent M_n values are by a factor of 2 lower than the values derived from MALLS, indicating once more that the polymer standard is not appropriate. The apparent polydispersity is relatively high with about 1.5. In analogy to **polyM1**, the UV data for the mixed band at 301 nm exceeds systematically the ones derived from the other analytical data. Once more, the extinction coefficient of the 301 nm band seems to differ in

4. Synthesis of water soluble polymers via RAFT

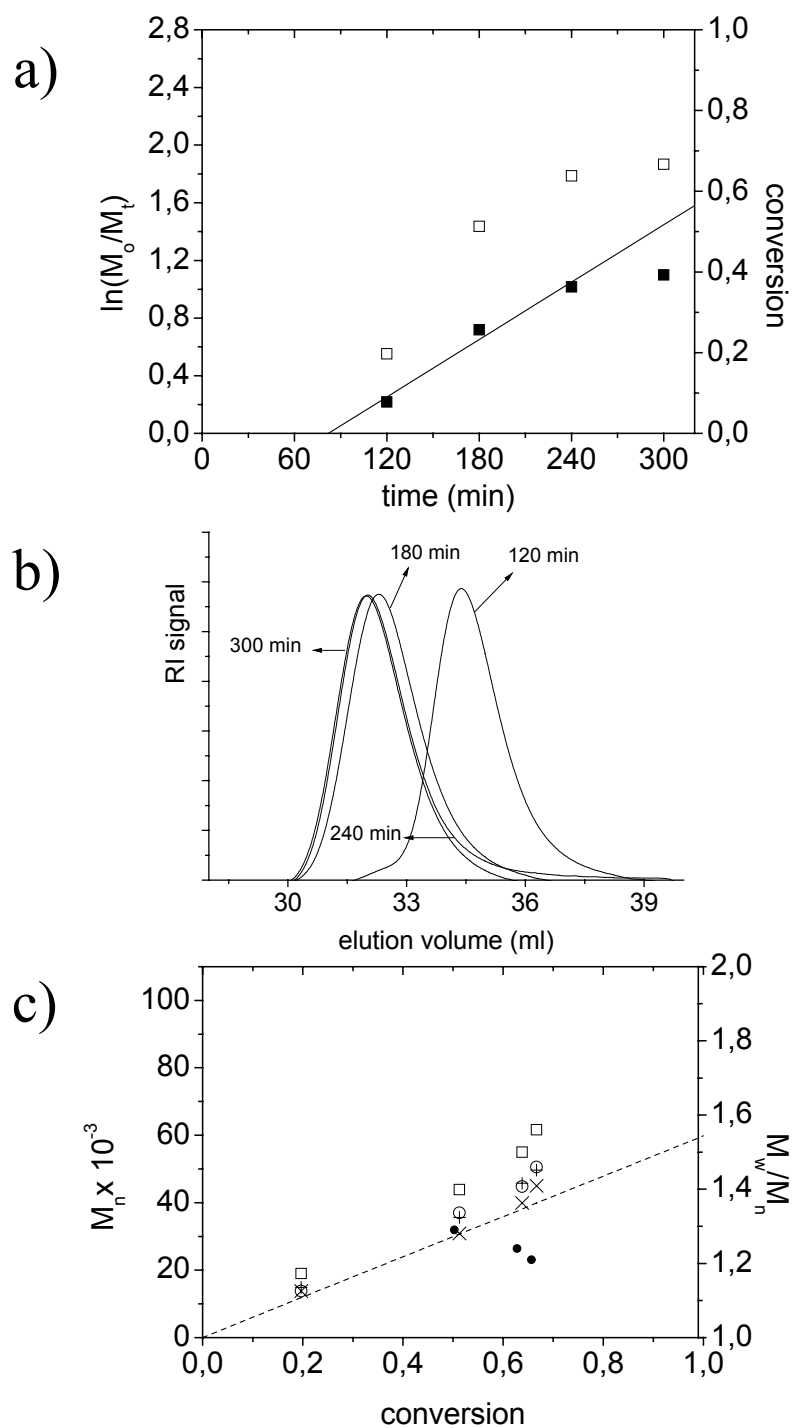


Figure 4.13. Polymerization of **M9** in water using initiator **V-545** and the RAFT agents **CTA3** at 48°C ([CTA]/[I])=5/1). a) (□) conversion determined by gravimetry vs. time, (■) $\ln(M_0/M_t)$ vs. time and the solid line is the linear fit of $\ln(M_0/M_t)$ vs. time data (data point at 300 min was excluded); b) evolution of ASEC elugrams with polymerization time (eluent: 0.2 M Na_2SO_4 in 1 wt% aqueous acetic acid); evolution of M_n and PDI (M_w/M_n) with conversion, (○) M_n according to MALLS, (⊕) M_n estimated by the visible band of the dithioester end group, (□) M_n estimated by using the UV band at $\lambda_{\text{max}} = 301$ nm, (X) M_n estimated by using the UV band at $\lambda_{\text{max}} = 251$ nm, (●) polydispersity of sample determined with MALLS. The dashed line (---) is the theoretically calculated evolution of M_n .

4. Synthesis of water soluble polymers via RAFT

the RAFT agent and in the polymer, presumably due to a changing contribution from the dithiobenzoate chromophore.

4.3.4. Polymerization of styrenic monomers via RAFT

The CRP of acrylates (**M1**, **M2**, and **M3**) and acrylamide (**M9**) with **CTA3** yielded both end groups labeled polymers with low polydispersities. To examine the ability of **CTA3** to control the polymerization of styrenic monomers in water, as well, the anionic styrenic monomer **M14** was polymerized at 55°C with initiator **V-545** (see Chapter 7 Table 7.1). CRP of **M14** was attempted first among the styrenic monomers used in this study, because the first reported aqueous RAFT polymerization using **CTA1** at 70°C was about this monomer [15], and its CRP is therefore known to work smoothly. After 7h, 90 % conversion was achieved at 55°C. But it is highly probable that the high conversions were accessed in much shorter polymerization times if the CRP kinetic of **M13** is considered (*vide infra*). The analysis of **poly-M14** by MALLS in eluent: 0.1 M (aq) NaNO₃ presented a low polydispersity ($M_n/M_w=1.10$) and M_n of 28 K. The molar mass determination by end group analysis gave similar M_n values (22 K), when using both the band at 251 nm of the naphthyl chromophore and the visible band of the dithioester unit at 488 nm, but it is somewhat higher than theoretically expected M_n of 18 K. MALLS method neglects the small chains due to their low scattering intensity [2], and that could be an explanation for the high M_n value obtained with MALLS compared to the end group analysis. The consistency of end group analysis at different bands demonstrates that the dithioester end group were preserved in the polymerization. Since the polymerization of **M14** works at 55°C smoothly, there is no need to run the polymerization at higher temperatures, risking the dithioester stability. Figure 4.2b exemplifies the usefulness of the naphthalene end group as fluorescence label that is incorporated onto **polyM14** via the initiating group "R".

In order to check the ability of **CTA3** to control the polymerization of a cationic styrenic monomers, too, in water, **CTA3** was employed for the polymerization **M13** at 48°C with initiator **V-545**. As shown in Figure 4.14.a, the polymerization of **M13** reached ca. 90% conversion after 5h, and follows pseudo-first-order kinetics after an initial retardation period of about 90 min. The ASEC traces of samples taken at increasing reaction times (Figure 4.14b) present basically unimodal peaks with decreasing elution volumes and reducing width, as expected for controlled polymerization. The number

4. Synthesis of water soluble polymers via RAFT

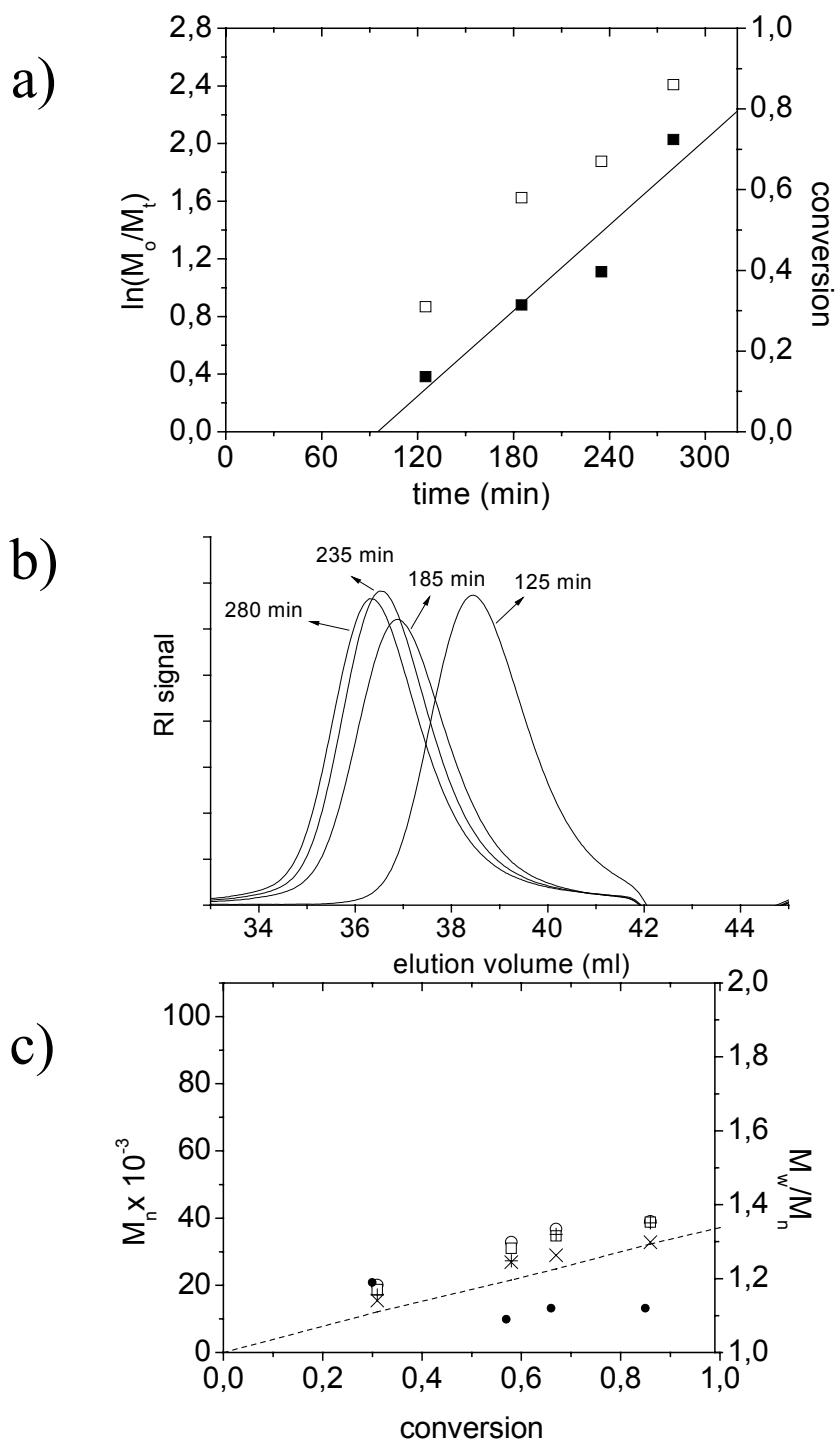


Figure 14.4. Polymerization of **M13** in water using initiator **V-545** and the RAFT agents **CTA3** at 48°C ([CTA]/[I])=5/1). a) (□) conversion determined by gravimetry vs. time, (■) $\ln(M_0/M_t)$ vs. time, the solid line is the linear fit of $\ln(M_0/M_t)$ vs. time data; b) evolution of ASEC elugrams with polymerization time (eluent: 0.2 M Na₂SO₄ in 1 wt% aqueous acetic acid); c) evolution of M_n and PDI (M_w/M_n) with conversion, (○) M_n according to MALLS, (+) M_n estimated by the visible band of the dithioester end group, (□) M_n estimated by using the UV band at $\lambda_{\max} = 301$ nm, (X) M_n estimated by using the UV band at $\lambda_{\max} = 251$ nm, (●) polydispersity of sample determined with MALLS. The dashed line (---) is the theoretically calculated evolution of M_n .

4. Synthesis of water soluble polymers via RAFT

average molar mass M_n increases steadily with conversion, according to analysis by MALLS as well as by end group determination using UV/vis bands at 490 nm, 251 nm and 301 nm (Figure 4.14.c). Polydispersities are about 1.1 even at high conversions according to MALLS.

CRP of the new styrenic betain **M17** was carried out in 0.5 M (aq) NaBr solution using **CTA3** and **V-545** at 55°C, too. Polymerization proceeded fast as in the case of **M13**, and 80% conversion was obtained after 5 hours. The theoretical M_n according to conversion is the same as the one calculated from end group analysis at the visible band ($\lambda_{\max} = 491$ nm), and it is 24 K. Unfortunately, a SEC system which is proper for the analysis of this zwitterionic polymer, could not be found. In addition, although **CTA3** was used as a CTA, the UV absorption bands of naphthyl chromophore at 251 nm and 301 nm do not allow to cross-check M_n , as **polyM17** has also a strong chromophore absorbing in the UV band. Note that **polyM17** is not soluble in water without salt.

The new chain transfer **CTA6** is a monofunctional RAFT agent differing from many other cited trithiocarbonates which are bifunctional [18-20]. The potential leaving group in the addition fragmentation process is the benzyl radical, which is known to be proper for the polymerization of styrenic monomers [14]. So it is employed for the polymerization of **M13** to verify its ability to control the polymerization of styrenic monomers at relatively low temperatures (<60°C) in water. **V-50** was used as initiator at 55°C for the polymerization. Figure 4.15 presents the results from the evaluation of the ASEC elugrams with MALLS and standard calibration with poly-2-pyrrolidone (**P2VP**). The continuous increase of M_n with conversion is visible for both evaluation methods. Also, independently whether the GPC data were evaluated by MALLS or by help of the polymer standard, M_n/M_w are low (between 1.1 and 1.5). As it is seen in Figure 4.15, **P2VP** is not a good standard to determine M_n for **polyM13**. The M_n values are much smaller than the ones obtained from MALLS. M_n values calculated for the highest conversion by end group analysis at $\lambda_{\max} = 425$ nm, agree well with the theoretical values (Figure 4.15), but the M_n values obtained by MALLS are somewhat higher than theoretical ones, as in the case of **CTA3**. These results show that **CTA6** is a good RAFT agent for styrenic monomers. It yields polymers with low polydispersities and provides linear increase of M_n .

4. Synthesis of water soluble polymers via RAFT

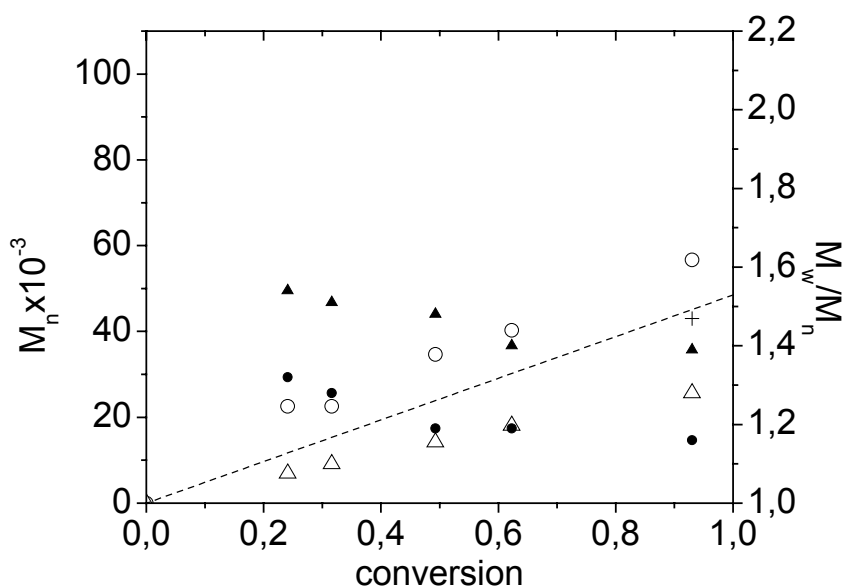


Figure 4.15. Plots of the evolution of number-average molar mass M_n and of polydispersity index M_w/M_n with conversion for the polymerization of **M13** in aqueous solution, using RAFT **CTA6** at 55 °C: (○) M_n according to MALLS, (Δ) M_n according to calibration with **P2VP** standards, (+) M_n estimated by using the visible band at $\lambda_{max} = 425$ nm of the trithiocarbonate end group, (▲) polydispersity according to calibration with **P2VP** standards, (●) polydispersity of sample determined with MALLS. The dashed line (---) indicates the theoretically calculated evolution of M_n .

4.3.5. Attempted aqueous RAFT polymerization of other monomer classes

The parent compound 2-vinyl pyridine was reported to undergo successful CRP by RAFT, at least in bulk [21]. Therefore, CRP using RAFT agent **CTA3** and initiator **V-545** in aqueous solution was attempted for monomer **M18**, the sterically demanding betaine derivative of 2-vinyl pyridine whose polymer is not soluble in standard organic solvents, at 55°C. However, no polymer was obtained, although **M18** polymerizes in the absence of the RAFT agent under similar conditions. Additional attempts to polymerize the monomer in the presence of the RAFT agents **CTA4** and **CTA5** using the initiator **V-50** failed, too. Adjusting the pH to 4, as found helpful in the case of acrylamide **M9**, did not improve the situation, either. It was noted that in all cases the reaction mixture became discolored after prolonged times, indicating the degradation of the dithiobenzoate group. Possibly, hydrolysis of the RAFT agents produces large amounts of thiols that lead to low molar mass oligomers. However, no satisfactory explanation can be given yet for this finding, as the RAFT agents were stable in the case of the other monomers studied under comparable conditions.

4. Synthesis of water soluble polymers via RAFT

The itaconate **M8** bears two sulfonate groups and thus is an interesting speciality to confer high anionic charge density and hydrophilicity to polymers, but reports on **polyM8** are scarce [21-24]. Therefore, the polymerization of **polyM8** in water via RAFT was attempted, using **CTA 1**, **CTA4** and **CTA 5** at 55°C (cf. Table 1), but none of these trials produced polymer that could be isolated. Different from the attempts of RAFT polymerization of **M18**, the red color of the solutions was not been lost throughout the polymerization reactions, suggesting that hydrolysis etc. of the RAFT agents cannot be blamed for the failure. In a control experiment, the classical free radical polymerization of **M8** under comparable conditions (2.2 mmol of **M8**, 7.36×10^{-5} mol of **V-50**, in 15 ml water at 55°C without any RAFT agent) gave 17 % conversion after 22 h. Therefore, it is assumed that controlled radical polymerization of **M8** by employing dithiobenzoate derived RAFT agents at reduced temperatures is not possible in solution because of strongly reduced rates of polymerization. Therefore, the claims made in patents [25] on the utility of itaconates for aqueous RAFT polymerization must be taken with care. In fact, a most recent study [26] on RAFT polymerization of itaconate diesters at 65°C using various RAFT agents revealed the sluggishness of such polymerizations even in bulk, and the need to carefully fine-tune the stabilizing group ("Z-group") as well as the leaving group ("R-group") simultaneously when CRP of such monomers is intended.

4.3.6. The effect of thioester on CRP

The stability tests done on water-soluble RAFT agents in water proved the conversion of dithioester moiety to thioester as one of the main degradation products (see Chapter 3). It is highly possible that thioesters will be produced in the course of the polymerizations in water. Therefore it is important to know whether thioesters have an adverse effect on radical polymerization. To discover whether thioesters have any inhibition or chain transfer effect over free radical polymerization, the polymerization of **M13** was carried out in presence of the thioester analogue of **CTA2** in aqueous solution at 50°C with azo-initiator **V-50**. **M13** was chosen for this control experiment, as its CRP works well in water. Any effect on polymerization should therefore stem from the thioester analogue of **CTA2**. The molar concentration of the thioester analogue of **CTA2** was 5 times higher than that of the initiator as the usual ratio used for CRP. Figure 4.16. presents the aqueous size exclusion chromatograms (ASEC) traces obtained from the ongoing polymerization. Elution volumes are small from the very beginning of the reaction, and

4. Synthesis of water soluble polymers via RAFT

slightly move to higher ones with ongoing polymerization. This means that the average molar masses are high already in the early polymerization (after 30 min, $M_n=6.2 \times 10^5$ according to **P2VP** standards, $PDI=1.8$) and slowly decrease as the polymerization proceeds (after 3h, $M_n=3.5 \times 10^5$ vs. **P2VP** standards, $M_w/M_n=2.4$). These data indicate an uncontrolled, "normal" free polymerization. This implies, that any thioester which may be present as impurity in RAFT agents, or may be formed by partial hydrolysis in-situ, does neither contribute to the control of the polymerization, nor inhibit the polymerization process. This result suggests that the eventual formation of small amounts of thioesters at elevated temperatures from dithioesters during the controlled radical polymerization in aqueous media should not be problematic (NB this may be different for thiols formed eventually).

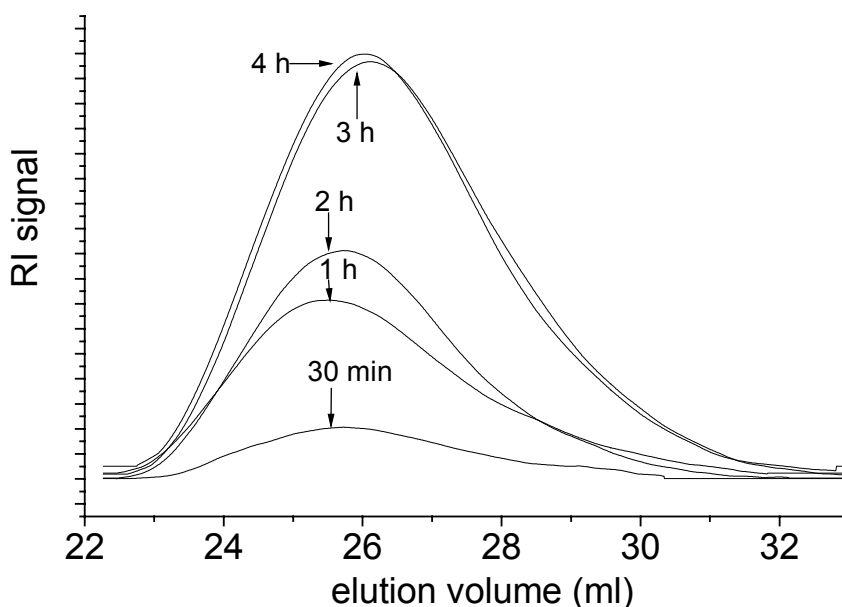


Figure 4.16. Plots of the evolution of the aqueous size exclusion chromatograms with conversion in the aqueous solution polymerization of **M13** in the presence of thioester derivative of **CTA2** (see Chapter 7 Table 7.2 for the polymerization conditions).

4.3.7. Discussion about homopolymerizations

The results presented for the various representative water-soluble monomers and the new RAFT agents clearly demonstrate, that CRP via RAFT is possible in aqueous solution for most systems, with respect to polymerizable groups as well as hydrophilic moieties, and including macro monomers. Typically, molar masses follow pseudo first-order kinetics up to reasonably high conversions, number molar masses increase linearly

4. Synthesis of water soluble polymers via RAFT

with conversion, calculated M_n values are close to the theoretically expected ones, and polydispersities are low. This implies that the known sensitivity of the $-C(=S)-S-$ moiety to hydrolysis is not an inherent obstacle to a versatile use of the RAFT method in aqueous solution. Concerning the choice of suited RAFT agents, all tested dithiobenzoates provided *a priori* reasonably well-controlled polymerization reactions, though retardation periods were observed in all cases. Still, for the controlled radical polymerization of a given monomer, the incorporation of an appropriate functionality on the initiating fragment ("R") or the active end group ("Z") in the RAFT agent may be important, in addition to the appropriate choice of the active end group ("Z") that must match the polymerizable group to be effective. The use of RAFT agents bearing sulfonate groups has for instance the advantage to enable reactions even at low pH-values, as required for the polymerization of certain monomers, such as polymerizable tertiary amines.

Different from the analysis of standard polymers such as polystyrene, poly(methylmethacrylate), poly(butylacrylate) and the like, it is difficult to quantify precisely the perfection of the control on the aqueous polymerizations, because the analysis of water-soluble polymers is troubled with problems and assumptions to be made. Therefore the analytical data must be evaluated with care for detailed conclusions, and the analysis of each polymer system ought to be optimized individually. Noteworthy, ASEC data evaluated by on-line MALLS analysis are not as reliable as often assumed, because the various polymers of different structure may interact differently with the column material, thus modifying the elution behavior in an undesired way. Moreover in model runs, MALLS seems to underestimate systematically the amount of low molar mass material in the ASEC set ups, giving apparently correct M_w values, but too high M_n values [2]. Consequently, the apparent polydispersities in our studies are presumably somewhat too low (the true values are still very low compared to samples prepared without RAFT agent). Thus, subjecting the polymer samples to dialysis with a low molar mass cut-off membrane prior to ASEC, in order to remove efficiently residual monomer which can interfere with the analysis, does virtually not change the polydispersities determined. But some polymer material may be lost by the work up of the polymerization mixtures, so that the assumed conversions may be somewhat too low. Therefore, the small deviation of the obtained M_n values from the theoretically calculated molar mass frequently observed at high conversions, may be at least partially apparent. In any case, as shown, the use of "general purpose" polymer standards for ASEC calibration, or the switching to non-

4. Synthesis of water soluble polymers via RAFT

aqueous columns (if possible at all) does not improve the situation, but in the contrary, provides much less reliable figures.

Keeping these analytical difficulties in mind, conclusions should be therefore based on the combination of several analytical methods. In this respect, end group analysis of the polymers in addition to the ASEC data proved to be valuable, in particular when employing the chromophore labeled **CTA3**. But even the inherently present dithioester group is a useful label. Its visible band is in the range of 483 nm - 489 nm for acrylic polymers, of about 490 nm for styrenic polymers, and of 493 nm - 509 nm for methacrylic polymers (Table 4.1), and thus is facile to follow. Despite some uncertainties concerning a strict constancy of the extinction coefficient of the C=S band in the visible spectra, due to a changing environment with ongoing polymerization, this specific end group analysis of RAFT-made polymers works reasonably well for most systems up to 70% of conversion and beyond. The usefulness of end group analysis is strikingly exemplified in the case of polycation **poly-M5**, obtained in the presence of the anionic **CTA4**, that forms big aggregates under the ASEC conditions used here. Indeed, aggregation is a widespread problem of polymers in aqueous solution, but not always obvious. End group analysis does not require molecular dissolution for the determination of the molar mass, different from most other methods, and therefore is still operative. When employing the chromophore labeled **CTA3**, the combined end group analysis of the initiating end group ("R") and the terminating dithioester end group becomes possible, and is instructive. On the one hand, good agreement of both results, and also with the theoretically expected molar mass, indicates reliable meaningful data. On the other hand, systematically higher values of M_n derived from analysis of the dithioester end group compared to the M_n values derived from analysis of the initiating end group ("R"), - and to the theoretical M_n values -, are a strong hint to an increasing loss of active dithioester chain ends. The utility of this test was exemplified by aminolyzing the dithioester end groups in the various samples obtained in the kinetic study of **M13** with **CTA3**, by the addition of diethylamine. Whereas the M_n values calculated from the UV band at 251 nm (indicative of the naphthyl chromophore of the "R" group) stay constant, the apparent M_n values calculated from the mixed UV band at 301 nm and even more the ones calculated from the visible dithioester band increase steadily with increasing exposure to diethylamine.

4. Synthesis of water soluble polymers via RAFT

Information on the extent of active end group preservation is most precious if the polymers made are intended to be used as macro RAFT agents for the preparation of block copolymers. In fact, a closer look to the data exhibited in Figs. 4.11.c (**M3**), 4.12.c (**M1**), and 4.13.c (**M9**) suggests that at prolonged reaction times, some dithioester end groups got lost indeed. This underlines the advantageous use of low polymerization temperatures, in order to minimize side reactions, and the need of relatively fast polymerization rates. Within this reasoning, it is not surprising that (under the low temperature conditions chosen) the slowly reacting methacrylamides **M11** and **M12** seem to perform the least well in aqueous RAFT. In any case, the CRP of **M12** needs still optimization work concerning the best pH conditions, as additional problems deriving from some hydrolysis of the primary amide moiety and subsequent partial aminolysis of the dithioesters under the conditions chosen might interfere (cf. work on poly(acrylamide) in ref. 5).

4.4. Synthesis of Block Copolymers via RAFT

As discussed in the introduction, since the hydrophilic functional groups are generally not compatible with ionic polymerization methods and coordination polymerization, the majority of the water-soluble monomers can be polymerized only via free radical polymerization. The synthesis of block copolymers via conventional free radical polymerization is not possible, as the life time of a growing chain is shorter than seconds. It is therefore not possible to react a growing chain with a second monomer. The CRP methods convert the serially growing polymer chains of free radical polymerization to parallel growing chains, and increase average life time of the active chain centers to times needed for the full conversion. In addition, after polymerization is completed, the active polymer chains can even be isolated in the different dormant forms depending on the CRP method employed, and can be re-activated to synthesize block copolymers. The RAFT polymerization is one of the most successful CRP methods, and as proven in homopolymerization experiments Chapter 4.3, it works well in aqueous media for the polymerization of anionic, cationic and noncharged hydrophilic monomers with different polymerizable groups i.e. (meth)acrylics and styrenics. What makes aqueous RAFT polymerization, particularly attractive is not the ability of synthesizing low molecular weight monodisperse water-soluble homopolymers, but rather the usefulness of the method to synthesize complex water-soluble polymer architectures with defined structures such as multiblock, hyperbranched, star etc.

4. Synthesis of water-soluble polymers via RAFT

In the RAFT polymerization, the active chain end groups (e.g. dithioester, or trithiocarbonate) have to be preserved, to enable the synthesis of block copolymers. Since the RAFT agents engaged for CRP polymerization are prone to hydrolysis above 60°C in aqueous environment (see chapter 3), the same risk exists for the active end groups of the propagating polymers chains. Therefore, the homopolymerizations were carried out at 55°C and 48°C in this study. To protect the end groups, similar polymerization temperatures should be used for block copolymer synthesis, too, for an efficient blocking.

Although the RAFT polymerization is powerful method to synthesize block copolymers, and provides enormous versatility for the polymer blocks which can be bound together, some details should be respected to obtain best control and blocking efficiency. In the homopolymerization studies which were carried out in semi dilute conditions at 55°C and 48°C, high conversions (>70%) were accessed in 2-4 hours except for methacrylamides. Higher conversions necessitate prolonged polymerization times to compensate the reduction in rates of polymerization which is naturally caused by the dwindling monomer concentration. Employing longer polymerization times to increase the conversions, is not suggested if the polymers should be used as macro RAFT agents to add another block. Because while pushing the reaction to increase the conversion, the radical production continues at the same rate. This leads to more and more termination reactions. Moreover, some of the active chain ends will be transferred to the the newly initiated chains as a result of ongoing chain transfer reaction. Since the polymerization rate is slow at high conversions, the newly initiated chains will never reach a high degree of polymerization. But the number of long polymer chains without active end groups and of small chains with dithioester end groups will be increased. This effect may be recognized by end groups analysis if the polymer sample is dialysed before the analysis, as the small molar mass polymers are lost during the dialysis. This cannot be recognized by MALLS, as the small molar mass molecules are anyhow neglected. Putatively, this explains also the increased discrepancy between M_n values obtained by MALLS and end groups analysis, at high conversions for dialyzed samples.(see homopolymerization experiments Fig. 4.11.c for **M3**, Fig. 4.12.c for **M1**, and Fig. 4.13.c for **M9**). Therefore, the polymerization times should not be prolonged to obtain higher conversions, but should be stopped around 70-80% conversion if the polymer is going to be used as a macro RAFT agent.

4. Synthesis of water-soluble polymers via RAFT

Table 4.2. Molar mass and compositional data of the synthesized block copolymers and their precursors

sample	conv (%)	wt. % of newly added block by ¹ H-NMR	wt. % of newly added block by elem. analysis	M _n (x 10 ³ g·mol ⁻¹)	DP _n of blocks
polyM1	80			9 ⁽²⁾ 10 ⁽⁷⁾ 12 ⁽¹⁾ 14 ⁽³⁾	47
polyM1-block-M3	91	75	76	37 ⁽²⁾ 39 ⁽⁷⁾ 8.0 ⁽¹⁾ 57 ⁽³⁾	47-64
polyM3	76			14 ⁽¹⁾ 10 ⁽⁷⁾	31
polyM3-block-M17	70	65	66	39 ⁽⁴⁾	31-82
polyM3-block-M17-block-M15		⁽⁵⁾	13	45 ⁽⁴⁾	31-82-29
polyM7	96			69 ⁽¹⁾	160
polyM7-block-M4		10	7	77 ⁽⁴⁾	160-62
polyM10	37			31 ⁽¹⁾	318
polyM10-block-M17	38	49	49	61 ⁽⁴⁾	318-99
polyM10-block-M17-block-M15		⁽⁵⁾	8	66 ⁽⁴⁾	318-99-29
polyM13				33 ⁽⁷⁾ 27 ⁽¹⁾	155
polyM13-block-M10		79	75	124 ⁽⁷⁾ 93 ⁽²⁾ 107 ⁽⁴⁾	155-918
polyM14	87			22 ⁽¹⁾ 25 ⁽³⁾ 28 ⁽⁸⁾	107
polyM14-block-M17	70	⁽⁵⁾	60	50 ⁽⁴⁾ 45 ⁽¹⁾	107-92
polyM14-block-M17-block-M15	80	⁽⁵⁾	24	66 ⁽⁴⁾	107-92-94

(1) M_n calculated via end-group analysis in visible band **(2)** M_n calculated via end-group analysis in UV band at 251 nm **(3)** M_n calculated via end-group analysis in UV band at 301 nm **(4)** Note: elemental analysis and ¹H-NMR results were used to calculate monomer composition in block polymer samples. When no other method available in order to estimate Mn values, it was assumed that there is no loss of dithioester end groups through polymerization, and all the polymerization goes on dithioester end groups, and depending on the Mn of used Macro RAFT agent Mn of final block polymer calculated (when there is a mismatch between the values obtained for wt.% of blocks from elemental analysis and ¹H-NMR, the average of them used to for Mn estimations). **(5)** ¹H-NMR data not useful because of low solubility of polymer not a good signal obtainable. **(6)** Mn determined by RI-SEC in THF, PS Standard. **(7)** Mn determined by MALLS in 0.2 M Na₂SO₄ 1% wt acetic acid solution. **(8)** Mn determined by MALLS in 0.1 M NaNO₃ solution.

Another important parameter for the block copolymers synthesis is the blocking sequence. The reactivity of the different polymer blocks in the chain transfer step of the RAFT polymerization must be considered. For example, acrylic based macro RAFT agents

4. Synthesis of water-soluble polymers via RAFT

cannot be used efficiently to block a methacrylic monomer as detailedly described in the introduction.

Keeping in mind these important points, the RAFT studies were extended to the synthesis of block copolymers in water. For the initiated block copolymer synthesis experiments, the type and the amounts of RAFT agent (or Macro RAFT agent), initiator and monomer engaged, the polymerization media and the temperatures, are given in Chapter 7 Table 7.3. The data related with the analysis of the block copolymers synthesized are provided in Table 4.2.

The preparation of block copolymers via RAFT is known to work smoothly if both block are based on monomers with the identical polymerizable moiety, or with polymerizable moieties of comparable reactivity [16]. Therefore, the first attempt was made to synthesize the block copolymer **polyM1-block-M3**, in which both block are acrylates. **PolyM1** which was synthesized by using **CTA4** at 55°C (see table 1 for details), was used as macro-RAFT agent. The M_n values of **polyM1** calculated by MALLS (10 K with polydispersity of 1.22) and by end group analysis using the visible band at 485 nm (12 K) are consistent, thus indicating a high dithioester end group functionality (M_n (MALLS)). **V-50** was used as initiator for the blocking of **M3** at 55°C in water. The ASEC traces of the macro RAFT agent **polyM1** and of the final polymer show that the non-ionic monomer **M3** was successfully blocked on the cationic acrylate **polyM1** (Figure 4.17). The ASEC peak of **polyM1** shifts to lower elution volumes after blocking, while still being monomodal. According to evaluation by MALLS, M_n increases from 10 K to 39 K after the blocking experiment. The polydispersity of **polyM1-block-M3** is low with $M_w/M_n=1.45$. The weight percentages of polymer blocks are analyzed by different methods. Consistently, the copolymer is composed of 24 wt% of **polyM1** block according to elemental analysis, and of 25 wt% of **polyM1** block according the integration of the ¹H-NMR spectra. These values agree well with the increase of M_n deduced by MALLS from the ASEC data (26 wt% of **polyM1**). Since **CTA3** was used, end group analysis was performed at different wavelengths, too. But the M_n values for **polyM1-block-M3** determined by end group analysis at different UV-vis bands are inconsistent ($M_n=80$ K at $\lambda_{max} = 489$ nm; $M_n=37$ K at $\lambda_{max} = 251$ nm; $M_n=57$ K at $\lambda_{max} = 301$ nm). This mismatch strongly suggests that the dithioester end groups are partially lost during polymerization and purification (prolonged dialysis in water). Since the UV-vis bands at 301 nm and 485

4. Synthesis of water-soluble polymers via RAFT

nm depend on the conservation of the dithioester end groups, they pretend apparently higher M_n values with ongoing hydrolysis. In contrast, the UV band at 251 nm is calculated via the initiating naphthyl chromophore. Therefore, the M_n value estimated by this end group should be close to the true value, as obtained by MALLS analysis. Consequently, the **polyM1-block-M3** was efficiently produced. But the copolymer is not suited for the use as macro-CTA agent for further blocking experiments, as many of the active chains ends were hydrolyzed. This is very good example for the usefulness of end group analysis in addition to ASEC/MALLS, since it is hard to get this information otherwise.

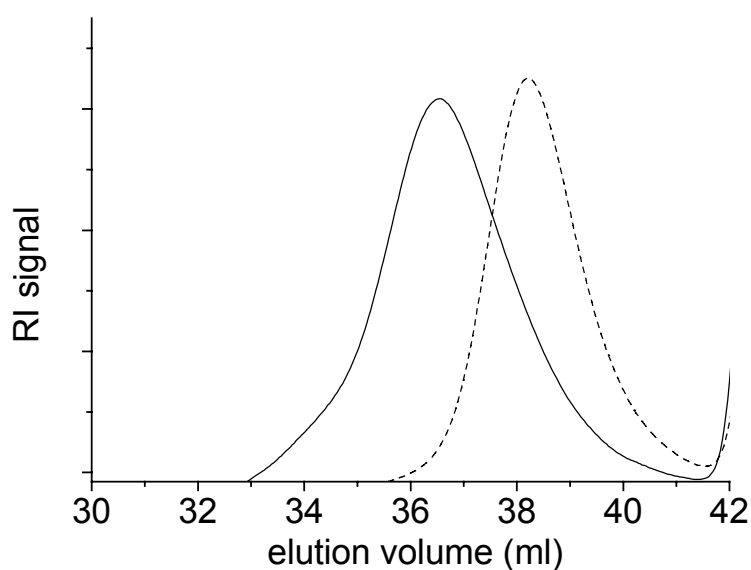


Figure 4.17. ASEC traces of the macro RAFT agent **polyM1** (----) and **polyM1-block-M3** (—). The eluent was 0.2 M Na_2SO_4 in 1 wt% aqueous acetic acid.

The successful synthesis of **polyM1-block-M3** verified the usefulness of RAFT polymerization in aqueous environment to synthesize well defined block copolymers in addition to homopolymers. The main interest of the attempts for RAFT polymerization in water is to synthesize macromolecules which can hardly be synthesized in any other solvent. So, the next trials focused on the synthesis of block copolymers containing a block of the zwitterionic monomer **M17**. The homopolymer of **M17** is only soluble in a limited number of solvents e.g. trifluoroethanol, but it is insoluble in the polar aprotic solvents DMSO, DMF and NMP, but even so in formamide, chloroform, and methanol, or their mixtures. In particular, **polyM17** is soluble in certain aqueous salt, but strongly depending on the presence and the concentration of the inorganic salts chosen. Aqueous salt solutions

4. Synthesis of water-soluble polymers via RAFT

are therefore the best choice, or even the only choice to synthesize block copolymers of **M17** to overcome the solubility problem of its polymer. So, the block copolymers **polyM3-block-M17**, **polyM10-block-M17**, and **polyM14-block-M17**, were synthesized to show the ability of aqueous RAFT polymerization to build complex systems. In addition, the blocking ability of styrenic monomers on a polystyrene based macro-RAFT agent in aqueous media was investigated with the synthesis of **polyM14-block-M17**. Subsequently, the blocking ability of styrenic monomers on polyacrylate and polyacrylamide macro-RAFT agents was tested with the synthesis of **polyM3-block-M17**, **polyM3-block-M10**, respectively.

The macro RAFT agents **polyM3**, **polyM10** and **polyM14** were engaged for the copolymerization. They have M_n values of 14 K, 31 K, and 22 K, respectively, according to the end group analysis via the visible band. **CTA3** was employed for the synthesis **polyM3** and **polyM14**, while **CTA1** was used for the synthesis of **polyM10**. In the synthesis of **polyM3-block-M17**, **polyM10-block-M17**, and **polyM14-block-M17**, **V-50** was used as initiator. The polymerizations were carried out at 55°C in 0.5 M aqueous NaBr to overcome the solubility problem of **polyM17** block (see for details Table 7.3 in Chapter 7). The analysis of the diblock copolymers was complicated, as no SEC systems could be found where the copolymer did not interact with the column material. Qualitatively this points to the formation of a block copolymer, but it precludes from analyzing its size. But, when polymer solutions were dialyzed to remove salt, no precipitation of **polyM17**, which is not soluble in water, was observed. Note that when homopolymers of **M17** mixed with **polyM3**, **polyM10** in 0.5 M aqueous NaBr, and then dialysed, **polyM17** precipitates. In addition, the stimuli-sensitive aggregation behavior as discussed in Chapter 5, is only possible if indeed a diblock copolymer was synthesized. Determination of M_n by dithioester end group analysis in the visible was only possible for **polyM14-block-M17**, as sufficiently concentrated, transparent solutions of **polyM3-block-M17** and **polyM10-block-M17** could not be prepared. Unfortunately, for **polyM3-block-M17**, and **polyM14-block-M17**, which were synthesized with labeled **CTA3**, the more sensitive UV bands at 301 nm and 251 nm suffer from the interference of the inherent absorption of **poly-M17** in the UV. Moreover, elemental analysis of the products indicates that the copolymers contain **polyM17**. The **polyM17** contents are 66 wt% for **polyM3-block-M17**, 49 wt% for **polyM10-block-M17**, and 60 wt% for **polyM14-block-M17**. By assuming that all the polymerization took place through dithioester end groups, the M_n values of the diblock

4. Synthesis of water-soluble polymers via RAFT

copolymers are calculated as 39 K for **polyM3-block-M17**, 60 K for **polyM10-block-M17**, and 50 K for **polyM14-block-M17** according to the copolymer composition. As stated above, only the determination of M_n for **polyM14-block-M17** was possible; it was found as 45 K. This is consistent with the value of 50 K obtained from the elemental analysis, and suggest that the assumptions done are justified.

While the efficient synthesis of diblock copolymers is already not trivial, the synthesis of ABC triblock copolymers is even more challenging. Therefore examples of ABC triblock copolymers by RAFT have been very limited. Since the polymerization of the block copolymers **polyM3-block-M17**, **polyM10-block-M17**, and **polyM14-block-M17** were done at 55°C (which is low enough to preserve the dithioester moieties), they can be used as macro RAFT agents to synthesize triblock copolymers. **M15** was chosen as a third block because its solubility in water depends on the pH of the medium. Therefore, the aqueous solution state of the triblock copolymers **polyM3-block-M17-block-M15**, **polyM10-block-M17-block-M15**, and **polyM14-block-M17-block-M15** should be orthogonally triggered by pH and/or the salinity of aqueous solution to present multi-stimuli sensitivity (see Chapter 5). The polymerization was carried out in aqueous solution at 55°C using **V-50** as initiator (see for details Table 7.3 in Chapter 7). The analysis of the triblock copolymers were troubled by the same problems as described above for the diblock copolymers which were used as macro RAFT agents. Determining the weight fraction of the **polyM15** blocks in the final polymers by elemental analysis gives 13 wt% for **polyM3-block-M17-block-M15**, 8 wt% for **polyM10-block-M17-block-M15**, and 24 wt% for **polyM14-block-M17-block-M15**. By assuming that all the polymerizations happened by the dithioester end groups of the precursor diblock copolymers, the M_n values were calculated as 45 K for **polyM3-block-M17-block-M15**, 66 K for **polyM10-block-M17-block-M15**, and 66 K for **polyM14-block-M17-block-M15**. Again, the proof for the formation of the ABC triblock polymer is indirect: when its aggregation behavior is examined, it differs markedly from the one of precursor diblock copolymers (see chapter 5). Moreover, no precipitation of eventual homopolymer **polyM6** formed occurred at low pH in aqueous solution, where the homopolymer is insoluble. These findings demonstrate that the attempted synthesis of the triblock copolymers was successful.

4. Synthesis of water-soluble polymers via RAFT

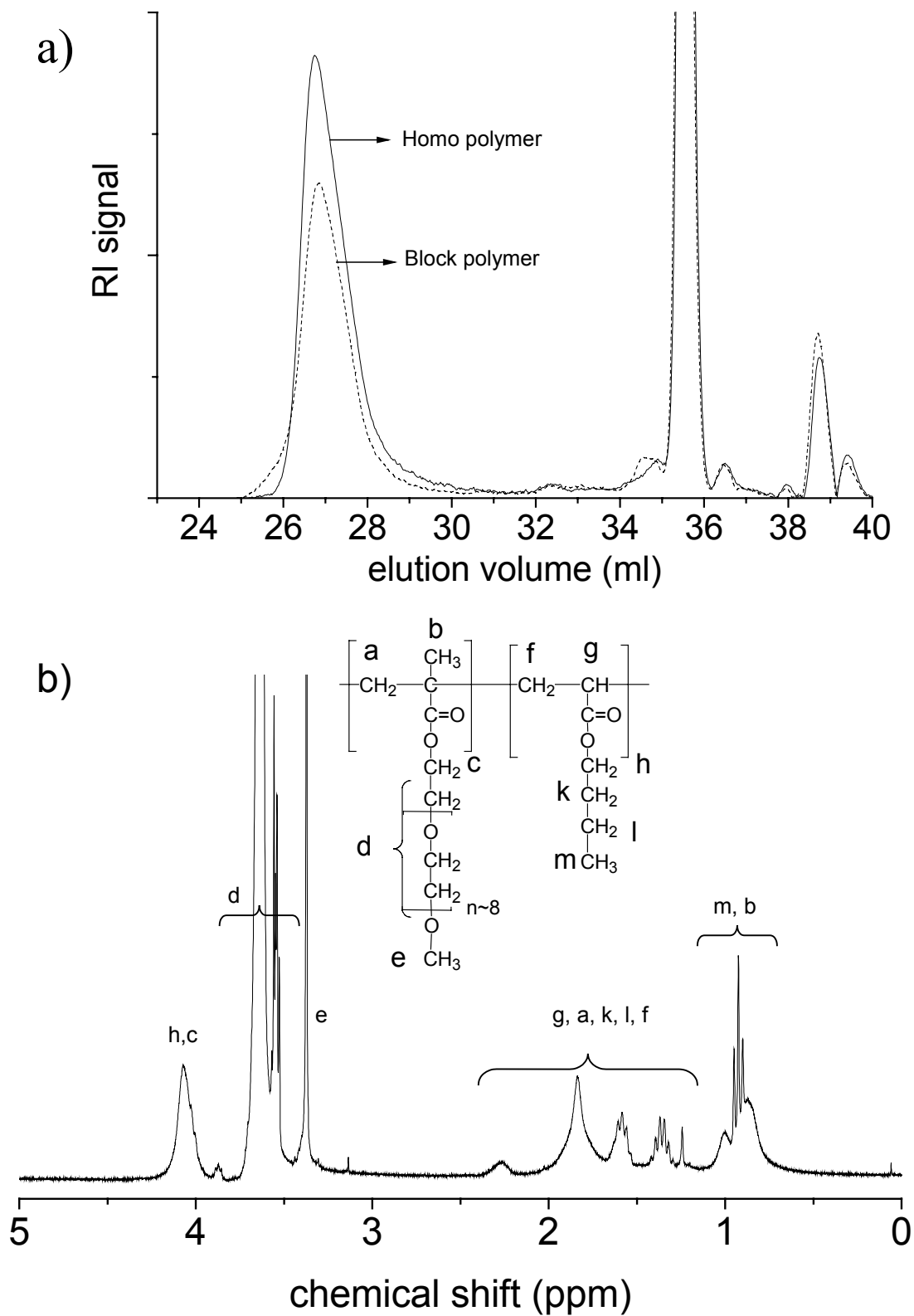


Figure 4.18. a) SEC traces of **polyM7** and **polyM7-block-M4** in THF b) $^1\text{H-NMR}$ spectra of block copolymer **polyM7-block-M4** in CDCl_3

4. Synthesis of water-soluble polymers via RAFT

The attempts to synthesize the amphiphilic block copolymer **polyM7-block-M4** in THF using initiator **V-60** and macro CTA **polyM7** at 60°C surprisingly, failed to yield a copolymer (see Chapter 7 in Table 7.3 for details of trial). The successful blocking of acrylic monomers on methacrylic macro RAFT agents is known to work, so the choice of the blocking sequence could not be the reason. The reason for that failure is not clear, but putatively, THF may not be the proper solvent. Subsequently, the synthesis of **polyM7-block-M4** was attempted in water as a heterogeneous system. **PolyM7** with a M_n of 69 K according to end group analysis was used as macro RAFT agent, and **V-50** was employed as initiator. The polymerization of suspended **M4** in aqueous solution was carried out at 55°C. In fact **polyM7** seems to act not only as a macro RAFT agent, but also as an efficient compatibilizer for the sparingly water-soluble butyl acrylate **M4**. After polymerization, the solution became homogeneous but cloudy, pointing to the formation of large micellar aggregates. This solution was extracted with diethylether thrice to remove unreacted monomer, then the aqueous solution was lyophilized. The analysis of the polymer obtained by SEC in THF was not conclusive: the elugrams for both the macro RAFT agent **polyM7** and the block copolymer **polyM7-block-M4** were found to be identical, although THF is a good solvent for both blocks. As it is seen in Figure 4.18a, precursor **polyM7** and **polyM7-block-M4** present almost identical elugrams, pretending that at the first sight the blocking to **polyM7** failed in water, too. But, $^1\text{H-NMR}$ of the copolymer in CDCl_3 proved the presence of **polyM7-block-M4** (Figure 4.18.b). The association behavior of **polyM7-block-M4** in water again indirectly proves the formation of a block copolymer (see chapter 5). The M_n values derived from calibration with polystyrene standards are only apparent, since the standard is not appropriate. But, the measured polydispersity index is rather low ($M_w/M_n = 1.10$). Therefore, the molar masses were estimated as well for **polyM7-block-M4** from the average copolymer composition determined by elemental analysis and $^1\text{H-NMR}$ as 77 K. The resulting analytical data of the block copolymers are listed in Table 4.2.

As a last system, the synthesis of another double hydrophilic block copolymer **polyM13-block-M10** was attempted in water by using a macro chain transfer agent based on **poly-M13** onto which dimethylacrylamide (**M10**) was polymerized. The system was chosen due to apparently conflicting results in the literature. Whereas **M10** was successfully blocked on polystyrene macro chain transfer agents by RAFT in organic solvents [27-29], a recent report claimed that this very blocking sequence is troubled by inherent problems in aqueous systems. The difficulties were attributed to unfavorable

4. Synthesis of water-soluble polymers via RAFT

fragmentation equilibrium of the intermediate radicals formed by the addition of the growing polymer chain onto the RAFT agent [3]. It was concluded that only the reverse blocking sequence, namely **polyM10-b-M13** using a macro RAFT agent **polyM10 CTA** could be efficiently realized in water. Therefore, a sample obtained from the kinetic study of **M13** (**polyM13**, $M_n = 27K$ by end group analysis) was used as a macro RAFT agent for the polymerization of **M10**. The second polymerization step was conducted for 6 h to achieve high conversion, in order to increase the molar mass by the blocking experiment substantially and thus to simplify polymer analysis. According to elemental analysis, the polymer product is composed of 25 wt% of **polyM13**, and 75 of **polyM10** spectrum indicates that the polymer product is made of 21 wt% of **polyM13** and of 79 wt% of **polyM10**.

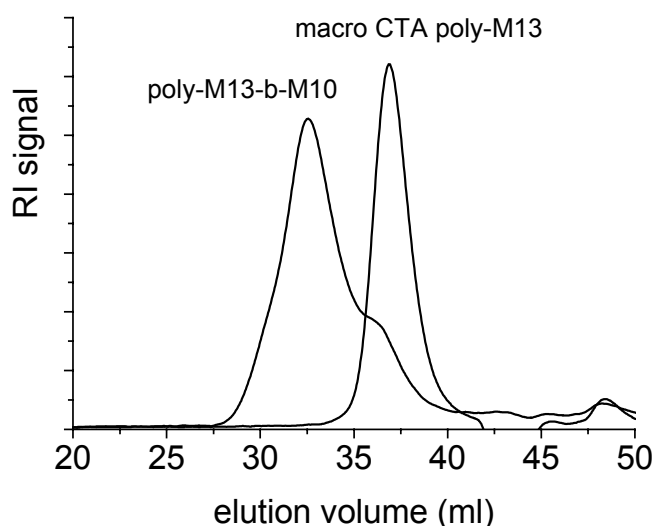


Figure 4.19. ASEC traces of macro RAFT agent **polyM13** (sample from kinetic study of **M13** after 185 min and its M_n estimated as 27.3 K by endgroup analysis at visible band), and **polyM13-block-M10** with $M_n = 125$ K (by MALLS) and polydispersity of PDI 1.39 (MALLS). The eluent was 0.2 M Na_2SO_4 in 1 wt% aqueous acetic acid.

Figure 4.19 exhibits the ASEC traces of the macro RAFT agent and the block copolymer. The signal of the polymer recovered after the blocking experiment is shifted to lower elution volumes ($V_e = 32.6$ ml) compared to the signal of the macro RAFT agent **poly-M13-CTA** ($V_e = 37.1$ ml), but exhibits a shoulder at intermediate elution volume [$V_e = 36.4$ ml]. The fact that the signal of the original Macro RAFT agent has nearly completely disappeared, together with the high UV signal of the new elution peak that is characteristic for the **polyM13** block (but not for **polyM10**), indicates a high blocking

4. Synthesis of water-soluble polymers via RAFT

efficiency. The shoulder in the elugram is putatively attributed to a small amount of inactive **polyM13** homopolymer due to termination reactions by combination. Evaluation of the GPC elugrams by MALLS gave a nominal M_n of 124 K for the synthesized diblock, with a polydispersity of 1.39, keeping in mind that molar mass determination of block copolymers by light scattering is a critical issue. Assuming that the molar mass of the **polyM13** block has not changed during reaction and work up, the block copolymer should have a molar mass of $M_n = 107$ K on the basis of elemental analysis (25 wt% of **polyM13** block, 75 wt% of **polyM10**). In good agreement, the evaluation of the block copolymer by end group determination via the UV band at 251 nm (naphthyl chromophore), as possible by using the labeled **CTA3** in the synthesis of the macro RAFT agent, gives a value of 93 K for M_n . In contrast, end group analysis of the dithiobenzoate end group was not possible, because the prolonged polymerization conditions had led to marked discoloration of the polymers, i.e. to a marked loss of the dithiobenzoate end groups. In the light of the inherent difficulties to evaluate GPC/MALLS data for copolymers, the agreement of the M_n values derived from the various analytical methods is good.

Clearly, our results show that block copolymers **polyM13-block-M10** can be easily and efficiently prepared in aqueous solution using the macro RAFT agent **polyM13**. This apparent contradiction of results is probably explained by a misinterpretation of the experiments in [3]. In the study, the two macro RAFT agents employed were prepared differently: **polyM10** used as a macro RAFT agent, was obtained by polymerization at 80°C for 3h, whereas **polyM13** was made by polymerization at 80°C for 24 h. Considering our findings concerning the sensitivity of the dithioester moiety towards hydrolysis, we believe that in the latter sample, many dithioester end group were hydrolyzed due to the prolonged polymerization time at high temperature. Evidently, this must result in poor blocking efficiency. In our study, **polyM13** was made at 48°C during about 3.5 h only, i. e. under conditions where hydrolysis is still negligible. This is evident from the double end group analysis (via both the "R" and dithioester groups) indicating the virtually complete functionalization of the macro RAFT agent by the dithioester moiety. Consequently, successful blocking of **M10** could be performed. Therefore, the hypothesis of a preferential fragmentation of intermediate RAFT radicals bearing an acrylic and a styrenic potential leaving group, in favor of the styrenic group, in aqueous solution [3], should be dismissed. The analysis of the block copolymer formed illustrates also, that the use of simple and convenient polymerization conditions (high monomer yields, use of relatively small

4. Synthesis of water-soluble polymers via RAFT

amounts of the precious macro RAFT agent) convenes to obtain diblock copolymers. However, samples made in this way lost majority of the RAFT end groups, and therefore are no more suited for preparing triblock copolymers in a subsequent step.

The preliminary attempts to synthesize di- and triblock copolymers proved that RAFT method is an effective method for the synthesis of block copolymers in aqueous media as well, if the loss of active chain ends is prevented. If it is possible, it is recommended to determine the number of active chain ends for a polymer planned to be used as macro RAFT agent before employing it. This is not only important to determine whether the sample can be used as macro RAFT agent or not, but also to arrange the ratio of initiator to chain transfer agent correctly. Low polymerization temperatures (<60°C) should also be preferred for the synthesis of block copolymers. The synthesis of stimuli sensitive block copolymers using the monomers **M17** and **M15** are good examples what kind of novel polymers can be accessed via RAFT in aqueous media. Particularly, the preparation of block copolymers of **M17** may not be possible in any other solvent.

References:

- [1] McCormick CL, Lowe AB. *Acc. Chem. Res.* **2004**, *37*, 312.
- [2] Baussard JF, Habib-Jiwan JL, Laschewsky A, Mertoglu M, Storsberg J. *Polymer* **2004**, *45*, 3615.
- [3] Sumerlin BS, Lowe AB, Thomas DB, Convertine AJ, Donovan MS, McCormick CL. *J. Polym. Sci. Part A: Poly Chem.* **2004**, *42*, 1724.
- [4] Lowe AB, Sumerlin BS, McCormick CL. *Polymer* **2003**, *44*, 6761.
- [5] Thomas DB, Sumerlin BS, Lowe AB, McCormick CL. *Macromolecules* **2003**, *36*, 1436.
- [6] Vasilieva YA, Thomas DB, Scales CW, McCormick CL. *Macromolecules* **2004**, *37*, 2728.
- [7] Donovan MS, Stanford AB, Lowe AB, Sumerlin BS, Mitsukami Y, McCormick CL. *Macromolecules* **2002**, *35*, 4570.
- [8] Gabaston LI, Furlong SA, Jackson RA, Armes SP. *Polymer* **1999**, *40*, 4505.
- [9] Mitsukami Y, Donovan MS, Lowe AB, McCormick CL. *Macromolecules* **2001**, *34*, 2248.

4. Synthesis of water-soluble polymers via RAFT

- [10] Huglin MB, Radwan MA. *Polym. Int.* **1991**, *26*, 97.
- [11] Köberle P, Laschewsky A, Lomax TD. *Macromol. Chem. Rapid. Commun.* **1991**, *12*, 427.
- [12] Arotçarèna M, Heise B, Ishaya S, Laschewsky A. *J. Am. Chem. Soc.* **2002**, *124*, 3787.
- [13] Baussard JF, Habib-Jiwan JL, Laschewsky A. *Langmuir* **2003**, *19*, 7963.
- [14] Chong YK, Krystina J, Le TPT, Moad G, Postma A, Rizzardo E, Thang SH. *Macromolecules* **2003**, *36*, 2256.
- [15] Le TPT, Moad G, Rizzardo E, Thang S. *Intern Pat Appl* **1998**, PCT WO9801478 [CA 1998: 115390].
- [16] Moad G, Mayadunne RTA, Rizzardo E, Skidmore M, Thang SH. *Macromol Symp* **2003**, *192*, 1.
- [17] Thomas DB, Convertine AJ, Hester RD, Lowe AB, McCormick CL. *Macromolecules* **2004**, *37*, 1735.
- [18] Lai JT, Filla D, Shea R. *Macromolecules* **2002**, *35*, 6754.
- [19] Ferguson CJ, Hughes RJ, Pham BTT, Hawkett BS, Gilbert RG, Serelis AK, Such CH. *Macromolecules* **2002**, *35*, 9243.
- [20] Mayadunne RTA, Rizzardo E, Chiefari J, Moad G, Postma A, Thang SH. *Macromolecules* **2000**, *33*, 243.
- [21] Convertine AJ, Sumerlin BS, Thomas DB, Lowe AB, McCormick CL. *Macromolecules* **2003**, *36*, 4679.
- [22] Hayashi N, Kawamura Y, Kimura T. (Toa Gosei Chemical Industry Co., Ltd., Japan) Jpn. Kokai Tokkyo Koho 1990, CODEN: JKXXAF JP 02184332 A2 19900718.
- [23] Laschewsky A, Wischerhoff E, Kauranen M, Persoons A. *Macromolecules* **1997**, *30*, 8304.
- [24] Arys X, Laschewsky A, Jonas AM. *Macromolecules* **2001**, *34*, 3318.
- [25] McCormick CL, Donovan MS, Lowe AB, Sumerlin BS, Thomas DB. US Patent; US 2003/0195310 A1.
- [26] Szablan Z, Toy AA, Davis TP, Hao X, Stenzel MH, Barner-Kowollik C. *J. Polym. Sci. Part A: Polym. Chem.* **2004**, *A42*, 2432.
- [27] Chong YK, Le TPT, Moad G, Rizzardo E, Thang SH. *Macromolecules* **1999**, *32*, 2071.
- [28] Baum M, Brittain WJ. *Macromolecules* **2002**, *35*, 610.
- [29] Baum M, Brittain, WJ. *Polym. Prepr. Am. Chem. Soc.* **2001**, *42(1)*, 586.

5. STIMULI-SENSITIVE POLYMERS

Stimuli-responsive polymers have been investigated for the development of "smart" materials in various fields. The term "stimuli-responsive" implies that marked changes of key properties can be induced by an external stimulus. In the strict sense, the induced property changes should be reversible if the stimulus is suppressed or if a second "reverse" stimulus is applied. Many types of stimuli are theoretically useful, but usually, the choice is limited for practical reasons. In water, stimuli-sensitive systems are generally aimed at changing the hydrophilic character of functional groups into a hydrophobic one, or vice versa [1]. Both chemical and physical stimuli (which may be coupled) can be employed for that purpose. Chemical stimuli include for instance acid-base reactions, complexation, bond breaking or making, redox and electrochemical reactions, or photochemical reactions. Physical stimuli comprise e.g. changes of the pH-value, ionic strength, temperature, pressure, light, or electrical and magnetic fields [2].

Much interest in aqueous solutions of stimuli-sensitive polymers derives from their potential application to biotechnology, medicine, (phyto)pharmacy, or cosmetics [3] for the controlled transport and delivery of active substances, such as drugs. One main strategy aims at a permeability control of polymeric matrixes or barrier coatings. The other main strategy concentrates on the controlled formation and destruction of hydrophobic micro domains in aqueous media. The latter approach implies typically the interconversion of amphiphilic and non-amphiphilic compounds. Although amphiphilic homopolymers and statistical copolymers of the polysoap type [4, 5] were the main stimuli-sensitive micellar polymer systems investigated for long, studies concentrate nowadays on amphiphilic block copolymers.

Amphiphilic block copolymers are typically diblock copolymers consisting of a hydrophobic block aggregating in aqueous solution, and of a hydrophilic block that prevents the aggregates from precipitation [5-9]. They have gained much impetus in recent years due to the uprise of the controlled free radical polymerization methods (CRP). [9-14]. In this study, the synthesis of stimuli-responsive diblock copolymers **polyM7-block-M4**, **polyM3-block-M17**, **polyM10-block-M17**, and **polyM14-block-M17** and triblock copolymers **polyM3-block-M17-block-M15**, **polyM10-block-M17-block-M15**, and

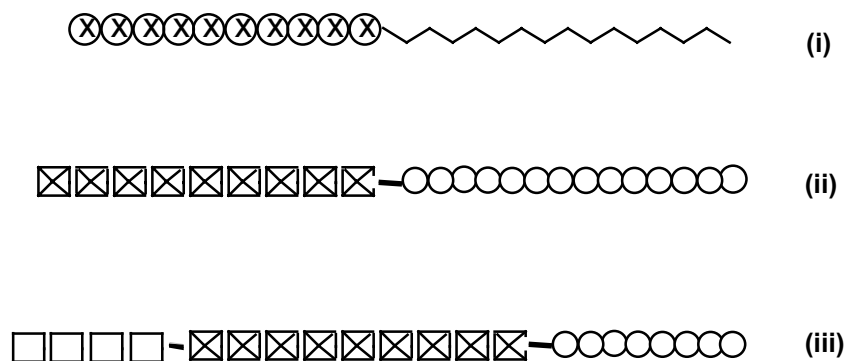
5. Stimuli-sensitive polymers

polyM14-block-M17-block-M15, proved that RAFT polymerization in aqueous media is a powerful tool to synthesize stimuli-sensitive polymers as well (see the Chapter 4 for the synthesis of block copolymers).

Poly(butyl acrylate) **polyM4** was employed as a permanently hydrophobic unit. The polymers of poly(ethyleneglycol) methyl ether acrylate **M3**, and N,N-dimethylacrylamide **M10** served as non-ionic permanently hydrophilic blocks, whilst poly(styrene sulfonate) **polyM14** was used as an ionic permanently hydrophilic block. Monomers poly(ethyleneglycol) methyl ether methacrylate **M7**, vinylbenzoic acid **M15** and 4-(2-sulfoethyl)-1-(4-vinyl-benzyl) pyridinium betain **M17** were used to construct the stimuli-sensitive blocks. The non-ionic polymers of **M7** exhibit a LCST, i.e. it is water-soluble at low, but insoluble at high temperatures. The carboxylic acid **M15**, however, produces pH-sensitive polymers which are only water-soluble at high pH [15, 16]. The new zwitterionic monomer **M17** gives polymers with a particular switching behavior. Although **polyM17** dissolves in trifluoroethanol, alike many polyzwitterions [17-20], it is insoluble in aprotic solvents, including dimethylformamide, NMP and dimethylsulfoxide, and even so in formamide, chloroform and methanol, or in their mixtures. In particular, the solubility of **polyM17** in aqueous solvents is sensitive to the type and the concentration of inorganic salts added. Whereas the polymer does not dissolve in pure water or in 0.01 M HCl, it is readily soluble in 0.5 M aqueous NaBr, NaCl or NaClO₄. The structures of the monomers used are drawn in Appendix I.

Copolymer **polyM7-block-M4** is an example of thermally sensitive macro-surfactants with a switchable hydrophilic block as illustrated in Scheme 5.1.(i), and it is only functional at low temperatures. **PolyM3-block-M17**, **polyM10-block-M17**, and **polyM14-block-M17** are also macro-surfactants with a switchable hydrophobic block. However, the stimulus is a change of salt content instead of temperature as illustrated in Scheme 5.1.(ii). The triblock polymers **polyM3-block-M17-block-M15**, **polyM10-block-M17-block-M15**, and **polyM14-block-M17-block-M15** contain the same sequence of two orthogonally stimuli-sensitive blocks as depicted in Scheme 5.1 (iii), namely the pH-sensitive block **polyM15**, and the salt-sensitive block **polyM17**, but they differ in the nature of the third permanently hydrophilic block. The variation of the latter concerns the use of non-ionic bulky hydrophilic groups **polyM3**, non-ionic small ones **polyM10**, and ionic small ones **polyM14**, respectively.

5. Stimuli-sensitive polymers



Scheme 5.1. Schematic representation of the synthesized stimuli-sensitive block polymers: (i) temperature-responsive chain *-block-* hydrophobic chain, (ii) salinity-responsive hydrophilic chain *-block-* permanently hydrophilic chain; (iii) pH-responsive chain *-block-* salinity-responsive chain *-block-* permanently hydrophilic chain; (⊗⊗⊗) = temperature responsive chain; vvvv = permanently hydrophobic chain, ○○○ = permanently hydrophilic chain, ⊗⊗⊗ = salinity responsive chain; □□□ = pH responsive chain).

In preliminary investigations, the stimuli-sensitive amphiphilic behavior of the block copolymers was studied by ¹H-NMR spectroscopy, turbidimetry, and dynamic light scattering (DLS). The latter two methods are sensitive to the formation of aggregates in the nanometer range, as typically formed by amphiphilic block copolymers in aqueous solution. Therefore, changes in the amphiphilic character of the copolymers should be reflected by changes of their hydrodynamic radii, and their aggregate sizes. ¹H-NMR spectroscopy is an easy qualitative test for the aggregation of the copolymers in D₂O, as the proton signals of the aggregating blocks become strongly broadened or even disappear eventually in the spectra, while the signals of the water-soluble block(s) persist.

The stimuli-sensitive amphiphilic behavior of the **polyM7-block-M4** was studied by turbidimetry, and dynamic light scattering (DLS). Since the block copolymer **polyM7-block-M4** is amphiphilic at ambient temperature, this should be reflected by the formation of aggregates in water. Moreover, the amphiphilic character of the block copolymer should change to the double hydrophobic one at elevated temperatures. Such thermal transitions should induce precipitation of the aggregates, or their transformation into bigger, presumably, unstable particles at elevated temperatures.

As **polyM4** cannot be dissolved in water directly, the block copolymer was first dissolved in the water-miscible organic solvent THF, which is a good solvent for both blocks. Subsequently, the solution was dialyzed extensively against water. This technique

5. Stimuli-sensitive polymers

allows the continuous and slow exchange of solvents, avoiding the formation of large aggregates [7, 8]. Indeed, the procedure resulted in transparent aqueous solutions of the block copolymer, for which DLS indicated the presence of aggregates in the nanometer range. The distribution of the hydrodynamic radii of the aggregates obtained from **polyM7-block-M4** as analyzed by DLS is shown in Figure 5.1.a. The thermal behavior of these aggregates was followed by turbidimetry. Figure 5.1.b depicts the evolution of turbidity showing a cloud point at about 93°C. The process is reversible upon cooling with a small hysteresis of about 1°C between the heating and cooling cycle. Interestingly, the precursor homopolymer **polyM7** shows a cloud point of 83°C under the identical conditions (Figure 5.1.b), i.e. the aggregated block copolymer exhibits a higher transition temperature. Such a behavior matches well with the reported increase of LCST in tethered polymer brushes on surfaces [21], and may be explained by a hindered collapse of the polymer chains in confined geometry.

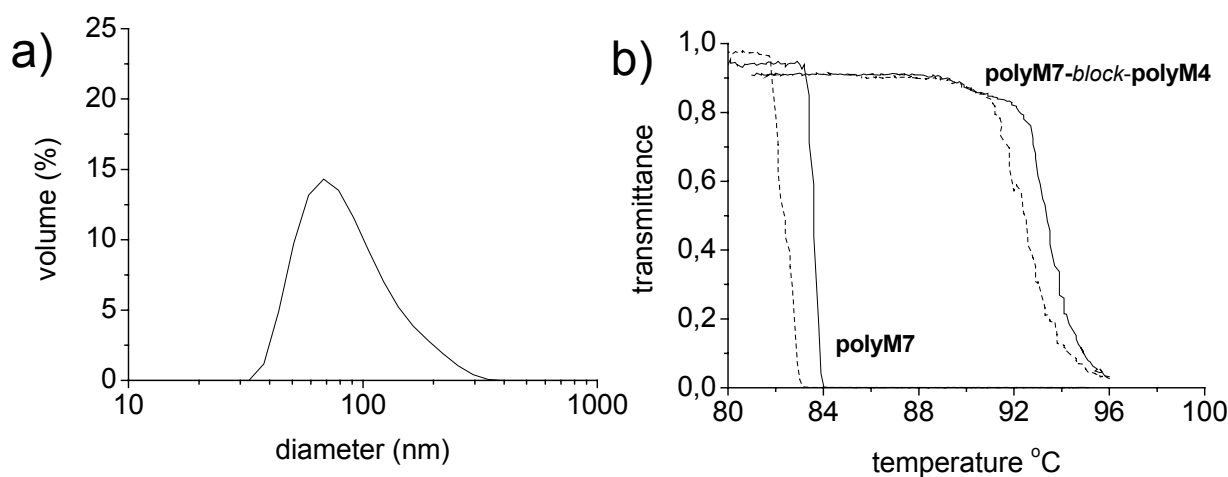


Figure 5.1. a) DLS analysis of particles prepared from **polyM7-block-M4** in H₂O (1wt%) at 25°C. b) temperature dependant turbidity of 1 wt % aqueous solutions of **polyM7** and **polyM7-block-M4** (solid line = heating, dotted line = cooling; rate = 1°C/min).

The other synthesized stimuli-sensitive block copolymers represent structures according to Schemes 5.1. (ii) and (iii), and thus are all directly water soluble under appropriate conditions. Aggregation only takes place if at least one of the hydrophilic blocks is switched to a water-insoluble state. A priori, such block copolymers seem more attractive as stimuli-sensitive amphiphilic **polyM7-block-M4**. This is not only by virtue of the ease of the preparation of their aqueous solutions, but also due to their potentially easier recovery: typically, surfactants in water are aimed at solubilizing hydrophobic

5. Stimuli-sensitive polymers

compounds. If the hydrophobic solubilize ought to be separated later on, this is achieved by breaking the solution/emulsion via a stimulus-driven switching of the amphiphilic character of the emulsifier. Then, it will be much more practical to have the emulsifier stay in its inactive form in the aqueous phase, thus separating it from the solubilize, than to have it go into the organic phase together with solubilize.

Copolymers **PolyM3-block-M17**, **polyM10-block-M17**, and **polyM14-block-M17** represent a new type of amphiphilic diblock copolymers with a stimulus-sensitive associating block according to Scheme 5.1. (ii), which is sensitive to the concentration and type of added salts. The key feature of these diblock copolymers is the insolubility of the zwitterionic block **polyM17** in pure water, as **polyM17** requires the presence of certain salts to become soluble ("salting-in" behavior). Qualitatively, their aggregation behavior was first attempted to detect by $^1\text{H-NMR}$ spectroscopy in D_2O . **PolyM3-block-M17** and **polyM10-block-M17** behave similarly. The $^1\text{H-NMR}$ spectra of the homopolymers **polyM3** and **polyM17** and block copolymer **polyM3-block-M17** in 0.5 M NaBr D_2O and in D_2O , are presented in Figures 5.2 and 5.3, respectively. The relative intensities of the peaks are provided for comparison in Figure 5.3, as well. The hydrogen atoms of **polyM3** (at α -position to ester moiety ($-\text{C}(=\text{O})\text{O}-\text{CH}_2-$)) were used as internal reference assuming that there is no change in the intensity of its signal both in the presence or absence of NaBr. As it is seen in Figure 5.3, $^1\text{H-NMR}$ spectrum of **polyM3-block-M17** in aqueous 0.5 M NaBr is superposition of the individual spectra of homopolymers. However, when its $^1\text{H-NMR}$ spectrum is measured in D_2O , the relative intensity of protons originating from **polyM17** are strongly attenuated (aromatic protons between 9 ppm and 5 ppm and the protons of ethyl sulfonate moiety at about 3.2 ppm). This qualitatively shows the aggregation of **polyM17** blocks in the absence of salt, but the complete hydrophobic aggregate formation cannot be claimed as the signals of **polyM17** did not disappear.

In the case of **polyM14-block-M17**, no signal is detectable for the $^1\text{H-NMR}$ spectrum in D_2O . Contrary to **polyM3-block-M17**, **polyM10-block-M17**, the signals of the permanently hydrophilic anionic block **polyM14** become strongly broadened and subdued with increasing length of the zwitterionic block even in 0.5 M NaBr (see Figure 5.4). Presumably, the reason for that is the presence of strong electrostatic interactions between the **polyM14** and **polyM17** blocks.

5. Stimuli-sensitive polymers

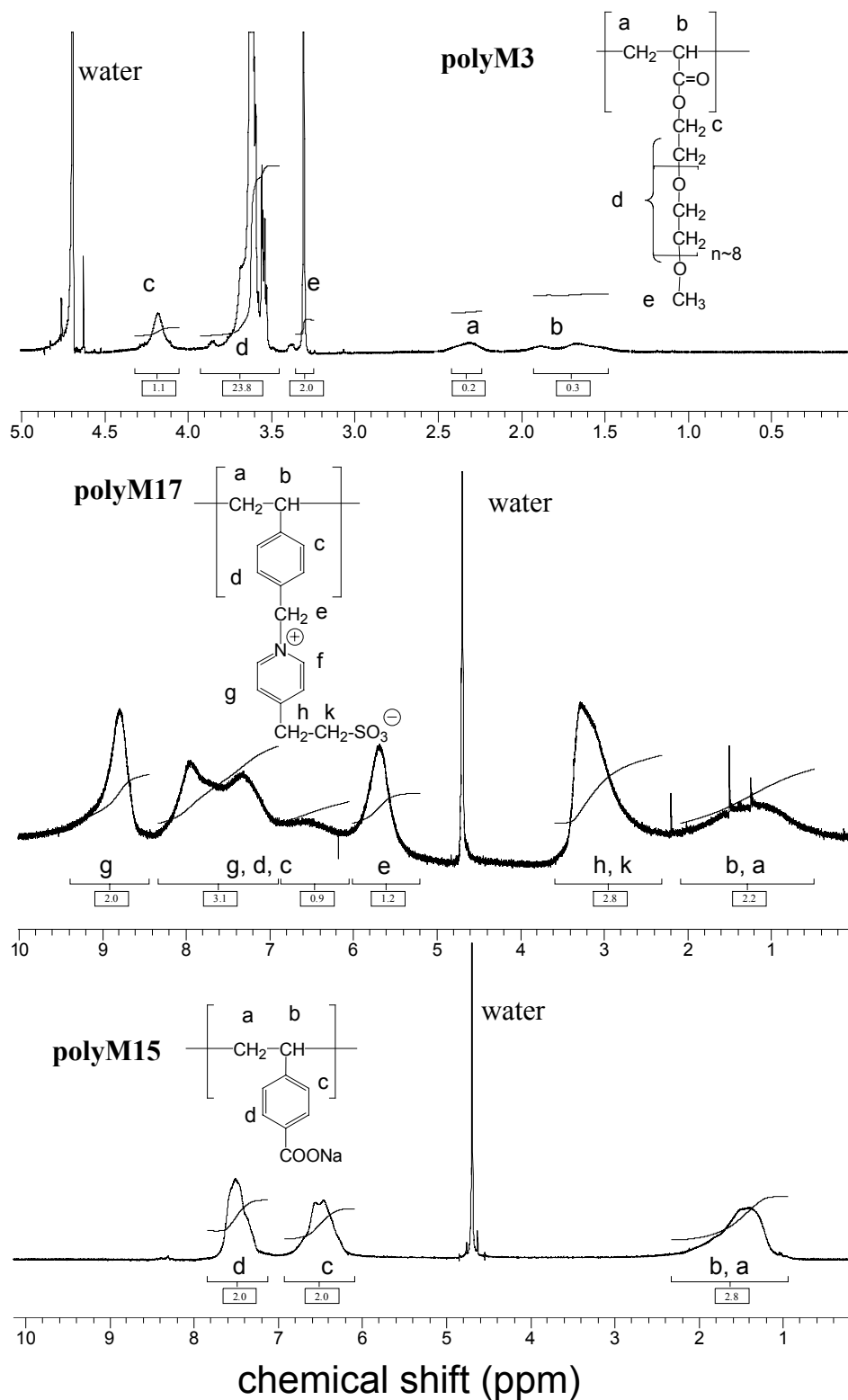


Figure 5.2 From top to bottom, $^1\text{H-NMR}$ of **polyM3** in D_2O , **polyM17** in 0.5 M NaBr D_2O , and **polyM15** in D_2O .

5. Stimuli-sensitive polymers

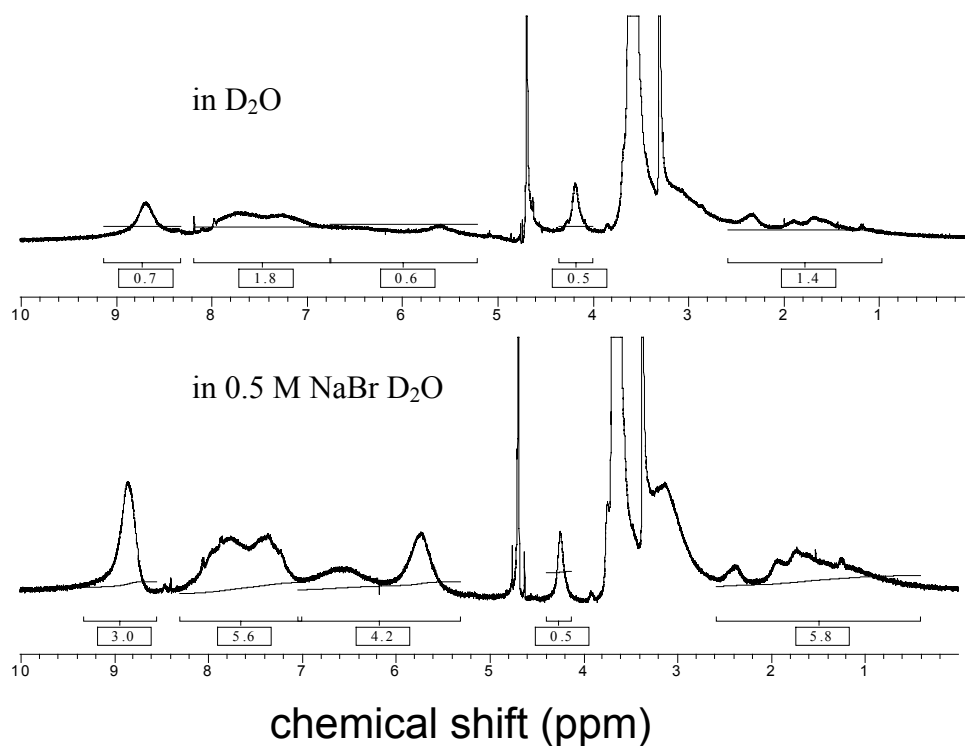


Figure 5.3. $^1\text{H-NMR}$ of polyM3-block-M17 from top to bottom, in D_2O , and in 0.5 M NaBr D_2O .

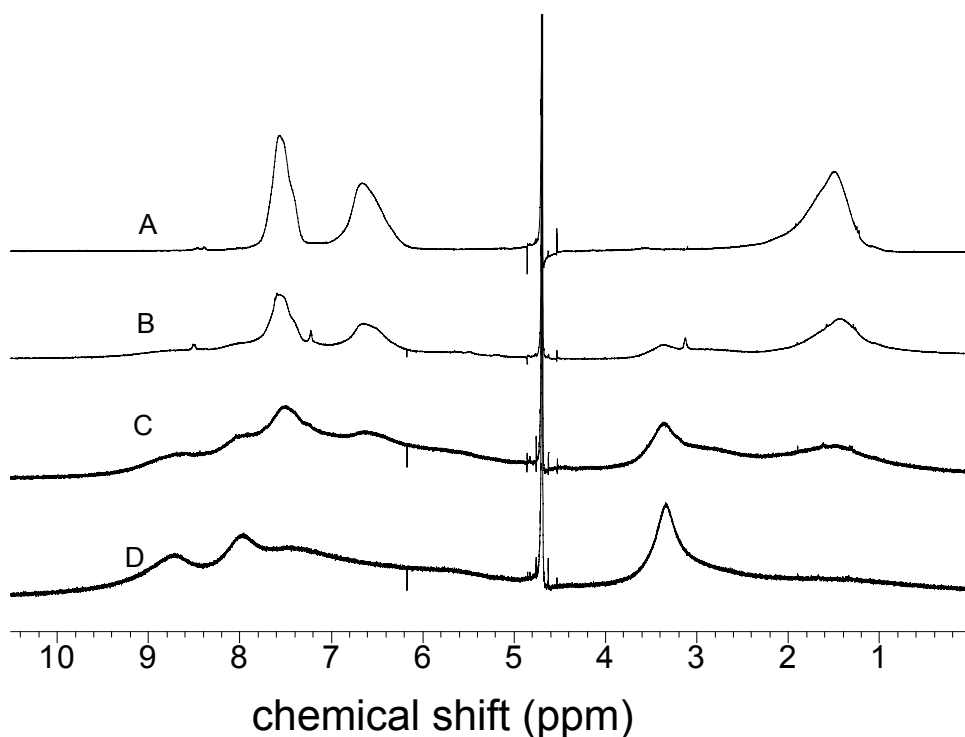


Figure 5.4. $^1\text{H-NMR}$ spectra of polyM14 in D_2O (A), and polyM14-block-polyM17 in 0.1 M NaBr in D_2O , with growing size of the polyM17 block as $M_n = 8\text{ K}$, 13 K, and 23 K for (B), (C) and (D), respectively. The size of the polyM14 block is $M_n = 22\text{ K}$ for all samples.

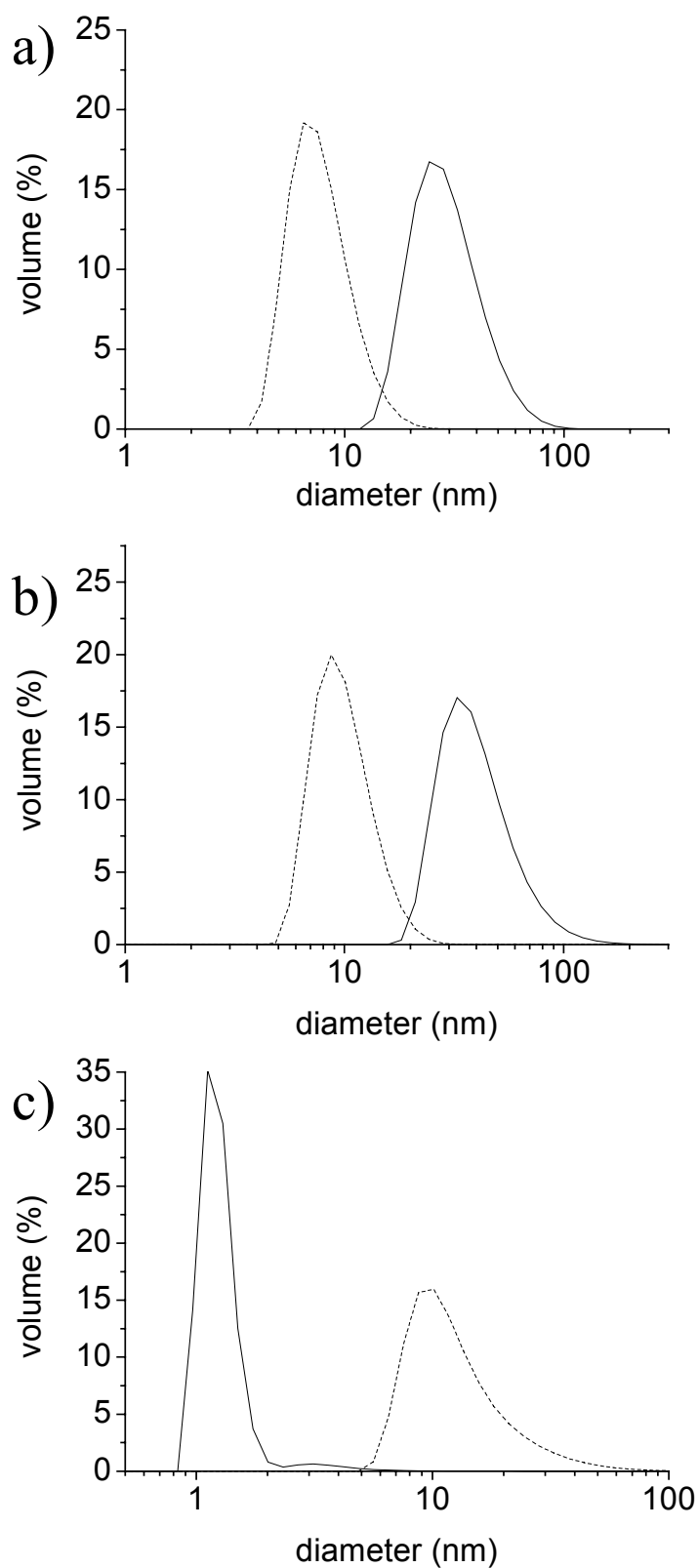


Figure 5.5. DLS analysis of the diblock copolymers a) **polyM3-block-M17**, b) **polyM10-block-M17**, c) **polyM14-block-M17** as 0.5 wt% solutions in 0.5 M (aq) NaBr (dotted lines) and after dialysis of these salt solutions against water (solid lines).

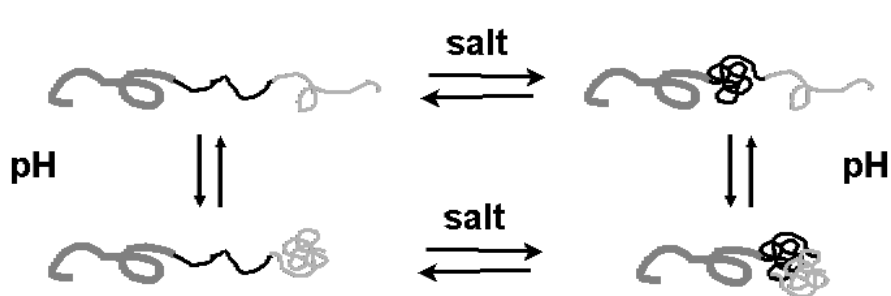
5. Stimuli-sensitive polymers

DLS studies of these copolymers in aqueous NaBr and in pure water are exemplified in Figure 5.5. To induce aggregation, the copolymers are first dissolved in brine, and then dialyzed. **PolyM3-block-M17** and **polyM10-block-M17** form small aggregates in pure water, with a diameter of about 32 nm and 41 nm, respectively. If the polymer concentration is increased, the size of the aggregates grows, too. The aggregates are stable upon heating until at least 70°C. But the aggregates redissolve in semi-concentrated solutions of certain salts such as NaBr. Typically, the salt controlled dissociation does not exhibit a sharp transition at a precise salt concentration, but the size of the aggregates decreases continuously with increasing salt content. The final particles with diameters well below 10 nm appear to be individual macromolecules. The analogous copolymer **polyM14-block-M17** of similar size (cf. Table 4.2.), disposing with **polyM14** of a permanently hydrophilic ionic block, behaves surprisingly different. Whereas the block copolymer exhibits a hydrodynamic radius of about 10 nm in 0.5 M aqueous NaBr alike the two other copolymers containing **M17**, the polymer seems to collapse onto itself in pure water, forming extremely small, compact colloids (Figure 5.5.c). Speculating on the reasons, we presume an attractive interaction between the anionic and the zwitterionic monomer units in this copolymer, which leads to dense polymer coils and aggregates when not screened by salt. This assumption is supported also by the ¹H-NMR studies of **polyM14-block-M17** as discussed above.

In the light of the salt sensitive aggregation of block copolymers **polyM3-block-M17**, **polyM10-block-M17** and **polyM14-block-M17** (Figure 5.5), and of reports on the pH-sensitive aggregation of block copolymer **polyM14-block-M17** [16, 22, 23], the synthesized triblock copolymers **polyM3-block-M17-block-M15**, **polyM10-block-M17-block-M15**, and **polyM14-block-M17-block-M15** were expected to be sensitive to two orthogonal stimuli, namely pH changes (**polyM15** block) and salinity (**polyM17** block) changes of their aqueous media. DLS measurements were used to follow their stimuli-sensitive behavior applying neutral and acidic pH, and varying the concentration of NaBr from 0 M to 0.5 M. Since the sequence of aggregation steps may be varied for two independent stimuli (Scheme 5.2), the effect of changing the order of the transitions was examined, too. Figure 5.6 illustrates the effects on the induced aggregation by applying the "salt switch" first (rendering the central block water-insoluble), whereas Figure 5.7 illustrates the effect of applying the "pH-switch" first (rendering one of the external blocks water-insoluble). These preliminary experiments exemplify that the encountered behavior

5. Stimuli-sensitive polymers

is rich and complex. In particular, it becomes evident that detailed molecular parameters are important, beyond having an ABC triblock copolymer in which the blocks B and C can change their water-solubility reversibly by an external stimulus.



Scheme 5.2: Idealized model for the behavior of the salt- and pH-sensitive triblock copolymers when exposed to different sequences of stimuli.

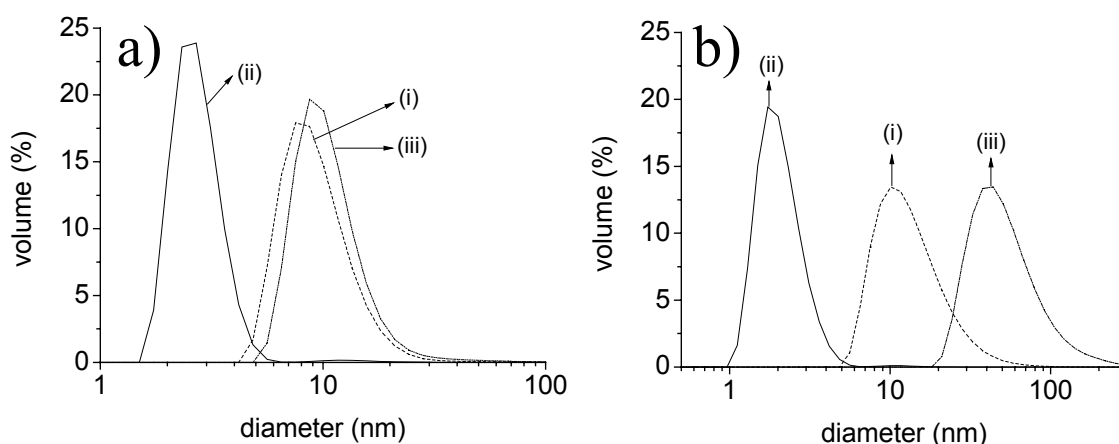


Figure 5.6. DLS analysis of the triblock copolymers a) **polyM3-block-M17-block-M15**, b) **poly M14-block-M17-block-M15**. (i) 0.5 wt% solutions of block copolymers were prepared in 0.5 M (aq) NaBr (dashed line), (ii) Polymer solutions were dialyzed against DI water (pH=5.8) (solid line), (iii) pH of solutions were adjusted to pH 1 by addition of 1 M (aq) HCl (dash dot dash).

Copolymer **polyM3-block-M17-block-M15** shows a hydrodynamic diameter of ca. 10 nm in 0.5 M aqueous NaBr at ambient pH. When the NaBr is removed by dialysis, the polyzwitterionic central block collapses, and a compact structure with a diameter of 3 nm is observed (Figure 5.6.a). Possibly, the two external hydrophilic blocks prevent the molecules from intermolecular association and thus, molecular micelles are formed. Adjusting subsequently the pH to 1, the block **polyM15** becomes hydrophobic additionally, resulting in the formation of aggregates with a diameter of about 10 nm.

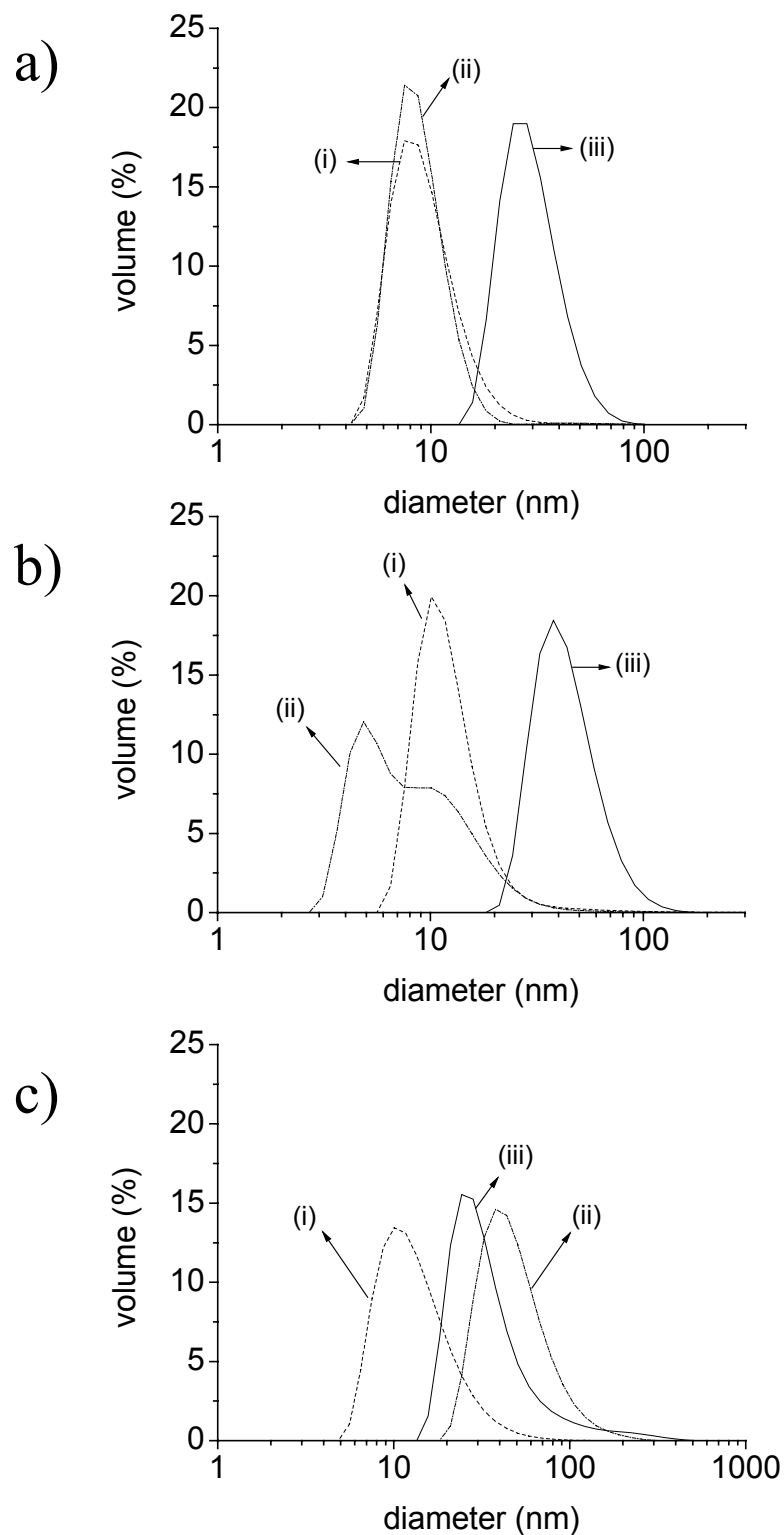


Figure 5.7. DLS analysis of the triblock copolymers a) **polyM3-block-M17-block-M15**, b) **polyM10-block-M17-block-M15**, c) **polyM14-block-M17-block-M15**. (i) 0.5 wt% solutions of block-polymers were prepared in 0.5 M (aq) NaBr, (ii) polymer solutions were dialyzed against 0.5 M (aq) NaBr having pH of 1.8, (iii) polymer solutions were dialyzed against DI water having pH of 2.5.

5. Stimuli-sensitive polymers

Noteworthy, the scattering signal is much stronger than for the original polymer, indicating the presence of small, but compact aggregates (Figure 5.6.a). When the switching sequence is reversed (Figure 5.7.a), the collapse of the small external **polyM15** block does not change the size of the structure notably, although increasing the scattering intensity. The subsequent collapse of the central **polyM17** block induced by dialyzing the NaBr, however, leads to aggregate growth resulting in particle diameters of about 30 nm. Apparently, the small hydrophobic domains created by the first transition favor intermolecular aggregation during the collapse of the second, central block.

The stimulus-sensitive behavior of the triblock copolymer **polyM3-block-M17-block-M15** was additionally investigated by $^1\text{H-NMR}$. Figure 5.2 presents the $^1\text{H-NMR}$ spectra of the individual homopolymers **polyM3**, **polyM17**, and **polyM15**. The $^1\text{H-NMR}$ spectrum of the triblock copolymer in aqueous NaBr at ambient pH is with a first approximation described as superposition of the individual spectra of the homopolymers. But the relative intensity of the aromatic protons originating from the blocks **polyM15** and **polyM17** is somewhat reduced, suggesting specific interactions between these two blocks. When the triblock **polyM3-block-M17-block-M15** is dissolved in D_2O at ambient pH without salt, the typical signals originating from the **polyM17** block are attenuated, as evidenced by comparison with the solution prepared in 0.5 M NaBr in D_2O (Figure 5.8). But, a complete hydrophobization of **polyM17** is apparently not achieved, because the protons of the pyridinium fragment of **polyM17** are still partially visible between 9.2 ppm and 7.8 ppm. But surprisingly, the typical signals originating from the aromatic protons of the **polyM15** block are attenuated, too, as seen when comparing with the spectrum taken in 0.5 M NaBr in D_2O (Figure 5.8). This finding points once more to specific interactions between the **polyM15** and **polyM17** blocks, as proposed above. After acidification of the pure aqueous polymer solution, the signals of the aromatic protons between 9 ppm and 5 ppm stemming from both **polyM15** and **polyM17** are mostly subdued, although not completely suppressed. This suggests that the triggered aggregation of these blocks leads to domains which still possess a certain polarity and may be somewhat plasticized with water.

Though structurally synthesized according to the same design (permanently hydrophilic block-betaine block-carboxylate block), copolymer **polyM14-block-M17-block-M15** behaves even qualitatively differently. When NaBr is removed by dialysis, the

5. Stimuli-sensitive polymers

polyzwitterionic central block collapses again, and a compact structure with a diameter of 2.5 nm is seen (Figure 5.6.b). But, the adjustment of the pH subsequently to 1, thus rendering the **polyM15** block water-insoluble, also results in the formation of larger aggregates with a diameter of about 45 nm (Figure 5.6.b). If the switching sequence is inverted (Figure 5.7.c), the collapse of the external **polyM15** block induces directly particles with 56 nm diameter, whereas the subsequent collapse of the central **polyM17** block after dialyzing the NaBr, leads to a shrink of the aggregates diameter to about 45 nm. It seems that the second transition takes place only within the aggregates, thus reducing their hydrodynamic radius.

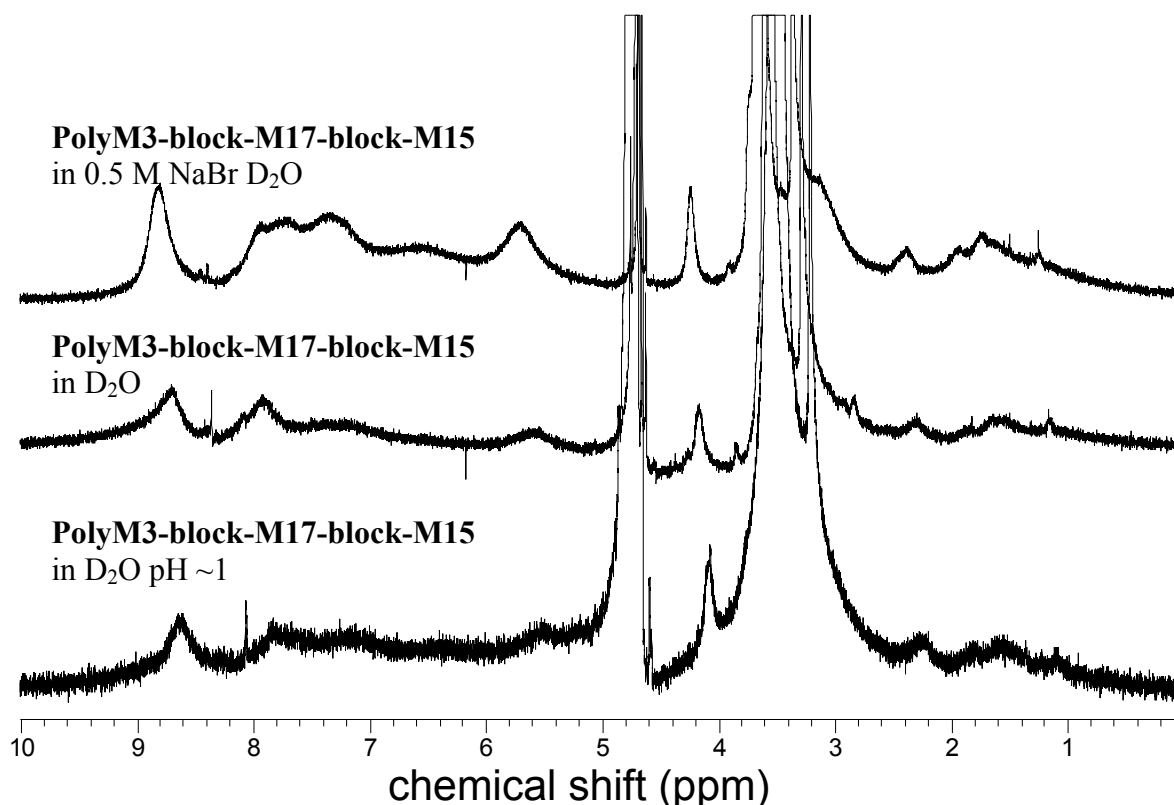


Figure 5.8. From top to bottom, ¹H-NMR of **polyM3-block-M17-block-M15** in 0.5 M NaBr D₂O, in D₂O (ambient pH), and in D₂O (pH=1).

On the basis of the few preliminary studies, it is difficult to explain the strongly contrasting behavior of **polyM3-block-M17-block-M15** and **polyM14-block-M17-block-M15**. Except for the central block of **polyM17** which has a similar size (see Table 4.2), the size and the shape of the external blocks vary strongly in the two samples. The specific interaction of the **polyM14** and **polyM17** blocks in the latter triblock copolymer (see Figure 5.4) may also play a role. In any case, it is obvious that the detailed molecular structure affects the switched aggregation markedly. This individuality is corroborated by

5. Stimuli-sensitive polymers

the behavior of the third analogously designed triblock copolymer, **polyM10-block-M17-block-M15** (Figure 5.7.b). For this polymer, acidifying of the polymer solution reduces the diameter of the structure, and broadens the size distribution, whereas the subsequent dialysis, removing the salt, induces aggregation to the particles of 45 nm in diameter.

If the appropriate polymerization conditions are chosen, aqueous RAFT polymerization is a convenient and powerful method to prepare block copolymers with complex architecture, as exemplified by the synthesis of stimuli-sensitive AB diblock- and ABC triblock copolymers. Taken together, the preliminary switching experiments on the double-sensitive triblock copolymers demonstrate that indeed orthogonal two-step switching is possible in aqueous solution, while maintaining homogeneous, clear solutions with aggregate sizes in the nano-particle range. It becomes clear that the sequence of switching is of major importance for the induced aggregation of a given polymer. Additionally, the association behavior encountered varies strongly for different polymers, even if the used blocks have the same solubility pattern in water.

References

- [1] Mc Cormick CL editor. Stimuli-responsive water soluble and amphiphilic polymers, ACS Symposium Series, vol 780. Washington DC: The American Chemical Society; 2001.
- [2] Laschewsky A, Lötsch D, Seeboth A, Storsberg J, Stumpe J. Proceedings of the European Coating Conferences, vol. "Smart Coatings III":Berlin (Germany), June 07-08.2004. p. 1-16.
- [3] Hoffman AS, Stayton PS. *Macromol. Symp.* **2004**, *207*, 139.
- [4] Hashidzume A, Morishima Y, Szczubiałka. IN, Tripathy SK, Kumar J, Nalwa HS, editors. Handbook of Polyelectrolytes and their Applications, vol 2. Stevenson Ranch: American Scientific Publishers; 2002. p. 1-63.
- [5] Laschewsky A. *Tenside. Surf. Det.* **2003**, *40*, 246.
- [6] Alexandridis P. *Curr. Opin. Coll. Interface Sci.* **1997**, *2*, 478.
- [7] Cameron NS, Corbierre MK, Eisenberg A. *Can. J. Chem.* **1999**, *77*, 1311.
- [8] Riess G. *Prog. Polym. Sci.* **2003**, *28*, 1107.
- [9] Mori H, Müller AHE. *Prog. Polym. Sci.* **2003**, *28*, 1403.
- [10] Hawker CG, Bosman AW, Harth E. *Chem. Rev.* **2001**, *101*, 3661.

5. Stimuli-sensitive polymers

- [11] Kamigaito M, Ando T, Sawamoto M. *Chem. Rev.* **2001**, *101*, 3689.
- [12] Coessens V, Pintauer T, Matyjaszewski K. *Prog. Polym. Sci.* **2001**, *26*, 337.
- [13] Moad G, Mayadunne RTA, Rizzardo E, Skidmore M, Thang SH. *Macromol. Symp.* **2003**, *192*, 1.
- [14] Barner-Kowollik C, Davis TP, Heuts JPA, Stenzel MH, Vana P, Whittaker M. *J. Polym. Sci. Polym. Chem.* **2003**, *A41*, 365.
- [15] Gabaston LI, Furlong SA, Jackson RA, Armes SP. *Polymer* **1999**, *40*, 4505.
- [16] Mitsukami Y, Donovan MS, Lowe AB, McCormick CL. *Macromolecules* **2001**, *34*, 2248.
- [17] Huglin MB, Radwan MA. *Polym. Int.* **1991**, *26*, 97.
- [18] Köberle P, Laschewsky A, Lomax TD. *Makromol. Chem. Rapid. Commun.* **1991**, *12*, 427.
- [19] Salamone JC, Volksen W, Olson AP, Israel SC. *Polymer* **1978**, *19*, 1157.
- [20] Monroy Soto VM, Galin JC. *Polymer* **1984**, *25*, 254.
- [21] Wischerhoff E, Zacher T, Laschewsky A, Rekaï ED. *Angew. Chem. Int. Ed. Eng.* **2000**, *39*, 4602.
- [22] Mitsukami Y, Donovan MS, Lowe AB, McCormick CL. *Macromolecules* **2001**, *34*, 2248.

6. NANO-PARTICLES IN WATER VIA COMPLEXATION OF IONIC POLYMERS

Supramolecular molecular assembly has been in the focus of various fields of polymer scientists. Polymeric micelles which are prepared by using the selective solubility of polymer blocks, are one of the promising topics of supramolecular assembly due to their potential applications beside the fundamental research interests, e.g. as pharmaceutical drug carriers, for catalysis, in optic-electronic devices, and for surface modification [1-8]. Particularly, the aggregates in water which have a hydrophilic shell and a hydrophobic core are promising for gene or drug delivery systems. These kinds of aggregates in water can be prepared by using amphiphilic polymers bearing both hydrophilic and hydrophobic sites, or by using hydrophilic polymers bearing ionic functional groups. The latter approach is based on the formation of complexes between oppositely charged ionic groups. In this way, the charged hydrophilic segments can be converted into insoluble hydrophobic domains.

The simplest form of ionic complexation is the well-known pairing of charged ions. If the attractive forces between oppositely charged ions are stronger than the solvation of water, they become insoluble such as silver halides. The same principle is also valid for charged macromolecules. If the aqueous solution of two homopolymers -bearing oppositely charged groups on their backbone- are mixed, they form aggregates with hydrophobic domains as a result of the mutual charge neutralization. If the mixing of charges is stoichiometric, insoluble complexes are formed, and the polymers precipitate. Similar aggregates are accessible by mixing ionic polymers with oppositely charged ions or surfactants, as well. As a result of this ability, ionic polymers are widely employed as flocculants and coagulants.

Lately, for these kinds of complexes, dihydrophilic block copolymers, having an ionic block and a noncharged block, have been used instead of ionic homopolymers. This became possible because dihydrophilic block polymers are more readily accessible due to the recent developments in polymer synthesis. If dihydrophilic block copolymers are used for such aggregates, they prevent the macroscopic phase separation even when

6. Nano-particles in water via complexation of ionic polymers

stoichiometric amounts of oppositely charged compounds are mixed (polymer, surfactants, or ions). Because their noncharged hydrophilic blocks can keep the complexed parts in solution.

The aggregates of dihydrophilic block copolymers which are prepared by using ionic surfactants, are termed block ionomer complexes (BIC) [9]. The aggregates prepared in this way have a hydrophilic corona (so far PEG based polymers are mostly used) and a hydrophobic core formed by the complexation of the charged ionic groups. In this way, water-soluble, electrically neutralized and narrowly distributed micelles can be prepared by employing BICs [10].

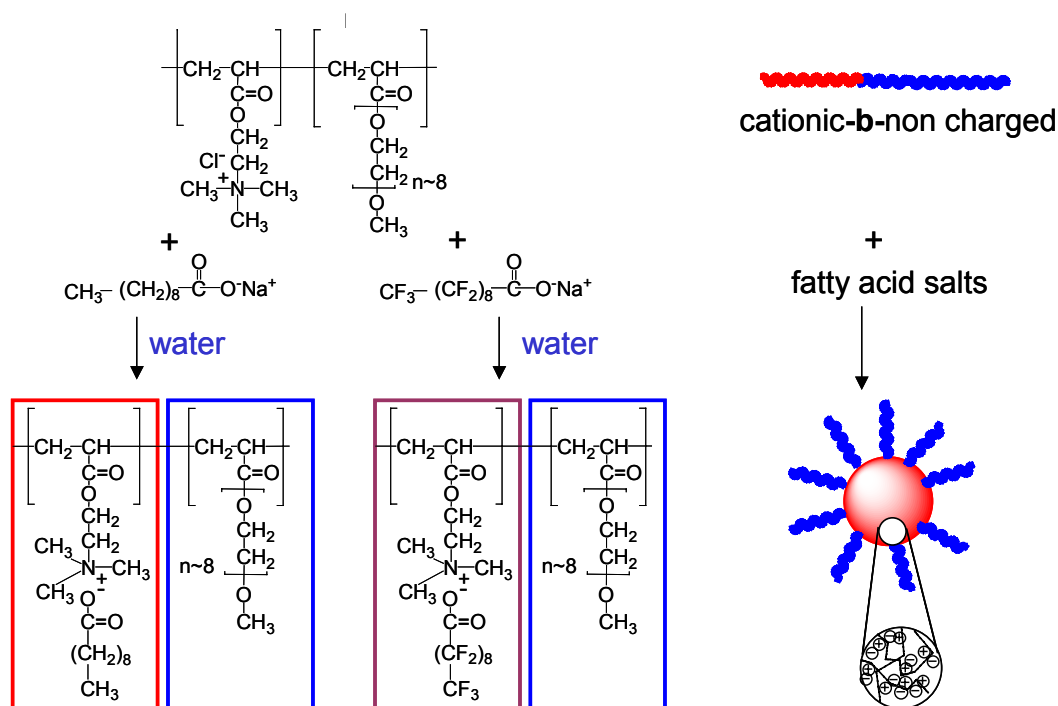
Until recently, to synthesize such ionic-nonionic dihydrophilic block copolymers was difficult and often unsatisfactory. Formerly, for instance, PEG based macro azo initiators were employed for the synthesis of such diblock copolymers. The polymers prepared via this method lack efficient control over the polymer structure. However, this is crucial to prepare reproducible micellar aggregates of narrow size distribution. Now, CRP via RAFT in water is a promising synthetic method for the synthesis of dihydrophilic block copolymers which plays a key role for these types of aggregates. The usefulness of RAFT is exemplified with the synthesis of block copolymers **polyM1-block-M3** and **polyM10-block-M13** which bear a noncharged hydrophilic block and a cationic block.

The dihydrophilic copolymer **polyM1-block-M3**, which is synthesized via RAFT in water as described before in Chapter 4 (see also chapter 7, Table 7.3), was designed to prepare BICs. The copolymer **polyM1-block-M3**, having M_n of 39 K according to MALLS, is composed of two hydrophilic blocks; a cationic block (10 K) and a polyethylene glycol based nonionic block (29 K). **PolyM1-block-M3** was mixed with the solutions of anionic surfactants (sodium decanoate and sodium perfluoro decanoate) to prepare particles as depicted in Scheme 6.1 in water. These particles are expected have a poly(ethylene glycol) based corona (which is known to be biocompatible) a hydrophobic core (which may be used as a transport domain for compounds having low water solubility).

The surfactants were mixed with the block copolymer in stoichiometric amounts (based on the charged groups) in water at 60°C. The aggregate formation was followed by

6. Nano-particles in water via complexation of ionic polymers

Dynamic Light Scattering (DLS). Whilst copolymer **polyM1-block-M3** shows a hydrodynamic diameter of ca. 8 nm only with a very low scattering signal, the copolymer mixed with sodium decanoate and sodium perfluoro decanoate presents aggregates with a hydrodynamic diameter of ca. 75 nm and 33 nm, respectively. In addition, they have much higher scattering intensity (see Figure 6.1). Noteworthy, since the Krafft-temperature of sodium perfluoro decanoate is above ambient temperature, it is not soluble in water without complexing with **polyM1-block-M3**.



Scheme 6.1. Preparation of particles by complexation of cationic block of copolymer **polyM1-block-M3** with ionic surfactants.

To determine whether the complexations were stoichiometric, ζ -potential measurements were carried out with the prepared particles. The copolymer solution presents fluctuating positive values between +15 and +40 mV, because there is no aggregate formation for **polyM1-block-M3** itself. The aggregates prepared with surfactants presents ζ -potential values close to zero (complex prepared with sodium decanoate has of -1.1 mV and complex prepared with sodium perfluoro decanoate has the ζ -potential of -1.3 mV). This means that stoichiometric complexation was achieved.

6. Nano-particles in water via complexation of ionic polymers

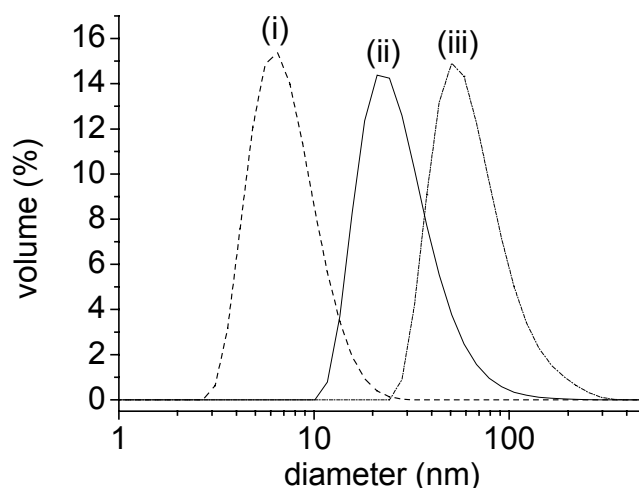


Figure 6.1. DLS analysis of (i) **polyM1-block-M3** (dashed line), (ii) the particles of sodium perfluoro decanoate (solid line) and (iii) the particles of sodium decanoate (dash-dot line).

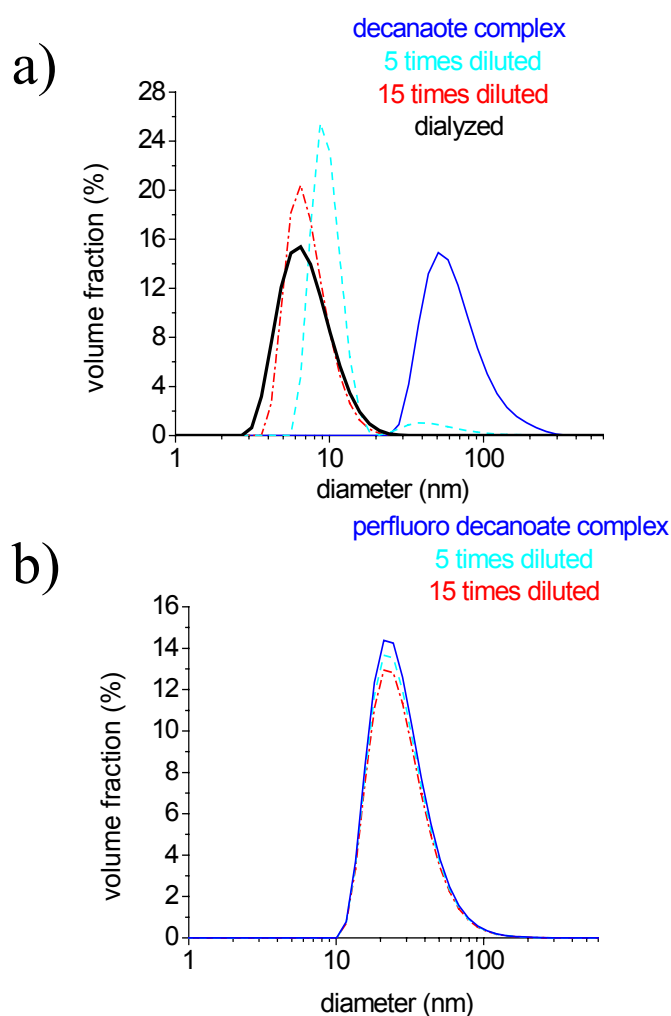


Figure 6.2. DLS analysis of a) the particles prepared with sodium decanoate and b) particles prepared with of sodium perfluoro decanoate: solution of **polyM1-block-M3** (9 mg ml^{-1} ; solid fat line); the solutions of particles contain 9 mg ml^{-1} **polyM1-block-M3**; 5 times diluted solutions (dashed line) 15 times diluted solutions (dash-dot line).

6. Nano-particles in water via complexation of ionic polymers

BIC formed by single tail surfactants are known to be unstable, and can disintegrate upon dilution [11]. So, the effect of the dilution on the aggregates was examined by DLS. Figure 6.2 depicts the evolution of the particle size upon dilution. The starting aggregate solutions contain $9 \text{ mg}\cdot\text{ml}^{-1}$ of **polyM1-block-M3**. The nanoparticles made with sodium decanoate preserved their hydrodynamic diameter when the solution was diluted by a factor of 3. But further dilution led to their disintegration, as it is seen in Figure 6.2.a. In contrast, the particles prepared with sodium perfluoro decanoate were found to be stable. Only the scattering intensity was attenuated with dilution, whereas their size did not change (see Figure 6.2.b). These particles were stable even when they were dialyzed against large volumes of water by using a cellulose membrane with a nominal molar mass cut off 3500.

Beside the dilution, the changes in the temperature and the salt concentration of medium may affect the aggregation behavior of BICs [12]. Therefore, the stability of sodium perfluorodecanoate particles were examined under physiological conditions; 0.15 M (aq) NaCl at 37°C , which is important for any potential use in pharmaceuticals. NaCl was added to the sodium perfluorodecanoate particles to convert the solution to 0.15 M (aq) NaCl. The aggregation behavior of particles were followed in this solution at 37°C by DLS (solution was equilibrated for 2 h at this temperature before measurements). No change was observed for the measured hydrodynamic diameter of the particles even under physiological NaCl concentration and temperature.

^1H -NMR spectra of particles compared to the parent copolymer **polyM1-block-M3**. The solutions of the particles were lyophilized, and then redissolved in D_2O for the ^1H -NMR measurements. In Figure 6.3, ^1H -NMR spectra of **polyM1-block-M3** and the particles prepared with decanoate and perfluoro decanoate are presented. The signal of the $\text{C}(=\text{O})\text{O}-\text{CH}_2$ groups of the **polyM3** block was used as internal reference for the integration of proton signals. As seen in ^1H -NMR spectra of decanoic acid particles, there is no strong attenuation for the protons of cationic block **polyM1**. The signals of **polyM1** and decanoate are detectable in D_2O . Still, the signals stemming from decanoate are somewhat broadened (at about 2.3 ppm, 1.2 ppm and 0.8 ppm; Figure 6.3). The aggregates of decanoate cannot completely be hydrophobized, as there is no disappearance or the strong attenuation for the protons of **polyM1** block in ^1H -NMR. So it is highly probable

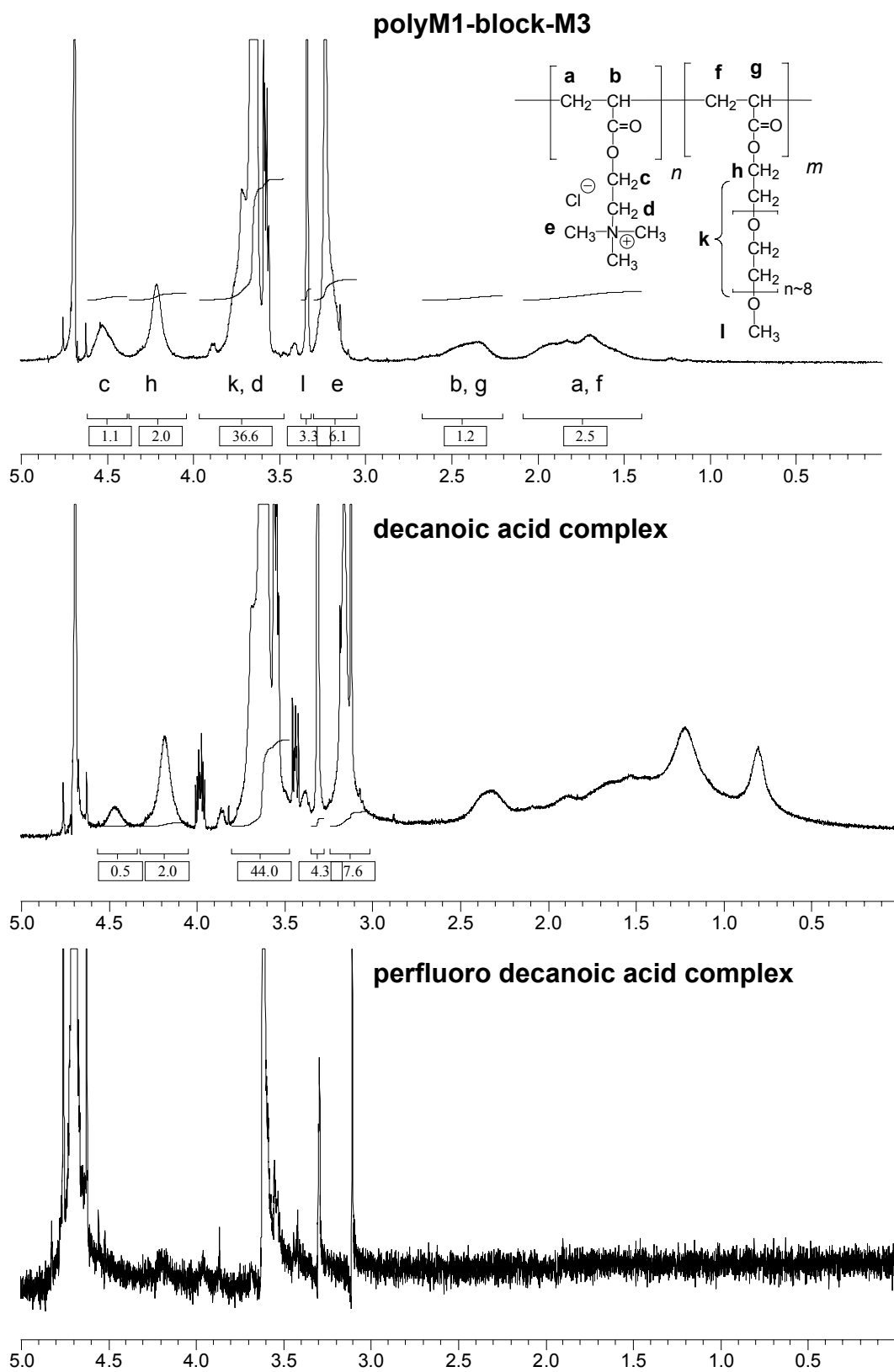


Figure 6.3. $^1\text{H-NMR}$ spectra of copolymer **polyM1-block-M3**, the particles sodium decanoate, and the particles of sodium perfluoro decanoate in D_2O .

that the aggregates of decanoate are plastified with water. This could also be an explanation for the formation of bigger aggregates ($\sim 75\text{nm}$) compared to the ones prepared with perfluoro decanoate ($\sim 33\text{ nm}$). For particles prepared with perfluorodecanoate, the proton signals of the copolymer which stems from the hydrogens atoms next to the ester moieties ($-\text{C}(=\text{O})\text{O}-\underline{\text{C}}\text{H}_2-$ between 4.1 and 4.6 ppm), and those of the copolymer backbone (between 1.4 ppm and 2.6 ppm) disappeared. Moreover, the ^1H -NMR signals of the trimethyl ammonium moiety ($-\text{N}^+(\text{CH}_3)_3$) are strongly suppressed. The disappearance or the strong attenuation of proton signals should be related with the inhibited mobility of cationic **polyM1** block without the solvation of water. So this observation is a powerful sign for the formation of the solid hydrophobic domains in the core of perfluoro decanoate particles, and therefore consistent with their stability better than the ones prepared with decanoate.

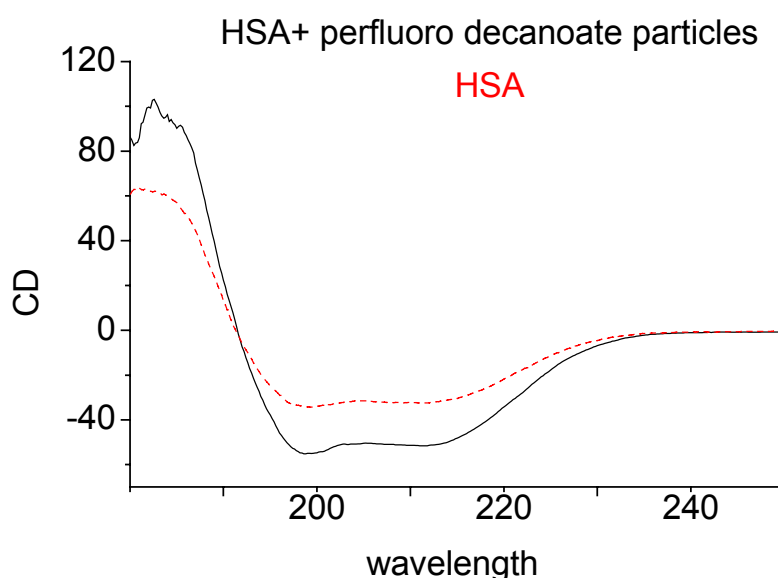


Figure 6.4. Circular dichroism of Human Serum Albumin (dashed line) and the mixture of HSA with particles prepared with sodium perfluoro decanoate (solid line).

For any vivo application, the interactions of these types of particles with natural proteins are crucial, as they may denature the natural proteins. In order to find out whether stable perfluoro decanoate particles denature proteins, a preliminary test was carried out with Human Serum Albumin (HSA). The particles were mixed with HSA in $\text{KH}_2\text{PO}_4/\text{K}_2\text{HPO}_4$ buffer solution, and the circular dichroism of this mixture was compared with that of HSA in the same solution. As it is seen in Figure 6.4, the particles did change the CD spectrum of HSA. So these particles may be tolerated in living organisms. Beside

6. Nano-particles in water via complexation of ionic polymers

that particles were found to be stable against dilution, and even stable in physiological NaCl concentration and temperature. The size of the particles are also proper for effective extravasation, namely for the selective uptake into cells (> 100 nm suitable for extravasation). Therefore these properties suggest that their hydrophobic core may be used as a delivery domain for compounds having low water solubility even in vivo.

This system exemplifies the potential of functional/complex polymers which can be synthesized via RAFT in water. For any biomedical application, the structure of such a polymer should be well defined, and this can be achieved via RAFT polymerization in water. Importantly, all the steps for the preparation particles including polymer synthesis were carried out in water. Therefore, the risk of having residual organic solvents in hydrophobic core of particles, which may cause serious problems for any vivo application, can be excluded in this strategy, as well.

References

- [1] Katoaka K, Kwon GS, Yokoyama M, Okano T, Sakurai Y. *J. Controlled Release* **1994**, 29, 119.
- [2] Zhang X, Jackson JK, Burt HM. *Int. J. Pharm.* **1996**, 132, 195.
- [3] Bronstein L, Sidorov S, Valetsky P, Hartman J, Colfen H, Antonietti M. *Langmuir* **1999** 15, 6256.
- [4] Thünemann AF, Kubowicz S, Burger C, Watson MD, Tchegotareva N, Müllen K. *J. Am. Chem. Soc.* **2003**, 125, 352.
- [5] Nagarajan R, Barry M, Ruckenstein E. *Langmuir* **1986**, 2, 210.
- [6] Hurter PN, Hatton TA. *Langmuir* **1992**, 8, 1291.
- [7] Spartz JP, Sheiko S, Möller M. *Macromolecules* **1996**, 29, 3220.
- [8] Webber SE. *J. Phys. Chem. B* **1998**, 102, 2618.
- [9] Kabanov AV, Bronich TK, Kabanov VA, Yu K, Eisenberg A. *Macromolecules* **1996**, 29, 6797.
- [10] Harada A, Katoaka K. *Langmuir* **1999**, 15, 4208.
- [11] Bronich T, Ouyang M, Kabanov VA, Eisenberg A, Szoka FC, Kabanov AV. *J. Am. Chem. Soc.* **2002**, 124, 11872.
- [12] Solomatin SV, Bronich TK, Eisenberg A, Kabanov VA, Kabanov AV *Langmuir* **2004**, 20, 2066.

7. EXPERIMENTAL

7.1. Analytical Methods

NMR spectra were recorded with a Bruker Avance 300. 1,4-dioxane was used as an internal reference at 67.19 ppm for ^{13}C -NMR measurements in D_2O [1].

IR spectra were recorded with a FT-IR spectrometer (Bruker IFS 66/s). Samples were measured in KBr pellets.

Mass spectra were recorded by a spectrometer TSQ7000 (Thermo Finnigan).

UV-Vis spectra were recorded with a UV-Vis spectrophotometer Cary-1 (Varian) equipped with a temperature controller (Julabo F-10). Turbidimetry used a temperature controlled turbidimeter model TP1 (E. Tepper, Mainz Germany).

Size exclusion chromatography: Aqueous size exclusion chromatography (ASEC) for cationic and non-ionic polymers was done by using a Spectra Physics Instruments (Columns: TSK-GEL® [polyglycidyl(meth)acrylate-Gel] from TOSOH: Guard, 6000, 5000, 3000 and 40). Aqueous 0.2 M Na_2SO_4 containing 1 wt% of acetic acid was used as eluent at a flow rate of 1.050 ml/min (unless noted otherwise). Evaluation was done by Multi-Angle Light Scattering MALLS (Wyatt DAWN DSP, Wyatt, Santa Barbara, CA/USA, laser wavelength 632 nm) and by calibration with poly(2-vinylpyridine) (P2VP) standards (PSS, Mainz/Germany).

Aqueous size exclusion chromatography (ASEC) for polyanions was done using the system Thermoquest P100 with eluent: aqueous 0.1 M NaNO_3 (Columns: Polymer Laboratories® aquagel-OH 50 μm , PL aquagel-OH 40 μm , PL aquagel-OH 30 μm , RI detection: Wyatt Optilab DSP Interferometric Refractometer) at a flow rate of 0.800 ml/min, using multi-angle light scattering MALLS (Wyatt DAWN EOS, Wyatt, Santa Barbara, USA, laser DAWN EOS 30mW GaAs laser as light source wavelength 690 nm).

7. Experimental

SEC in N-methylpyrrolidone (NMP (>99 %, Fluka) with $0.05 \text{ mol}\cdot\text{l}^{-1}$ LiBr was performed at 70°C using a TSP (Thermo Separation Products from Thermo-Finnigan GmbH, Dreieich, Germany) equipped with a Shodex RI-71 Refractive Index detector and a TSP UV detector. PSS GRAM columns (polyester columns 100\AA and 10000\AA) were used for the analysis (flow rate: $0.800 \text{ ml}\cdot\text{min}^{-1}$). All SEC systems were calibrated by poly(styrene) standards from PSS GmbH (Mainz, Germany).

Size exclusion chromatography (SEC) in tetrahydrofuran was performed at 20°C using a Waters 515 HPLC isocratic pump equipped with a Waters 2414 Refractive Index detector, a Waters 2487 UV detector and a set of Styragel columns (HR 5, HR 45, HR 3, 500-100,000 Da) from Waters. Eluent: THF (HPLC, from Roth). Flow rate: $1.0 \text{ ml}\cdot\text{min}^{-1}$. Calibration was performed with poly(styrene) standards from PSS GmbH (Mainz, Germany). If it is not stated, SEC measurements were done with this system.

Size exclusion chromatography (SEC) of **poly-M16** in tetrahydrofuran was performed at 35°C using a GPC kompaktanlage from Waters; Refractometer photodiode Array; columns (PL MIX Gel) Calibration was performed with poly(styrene) standards. Measurement were done in the Chromatography-Lab of the IDM (Teltow Kantst. 55).

Dynamic Light Scattering measurements: Dynamic Light Scattering was performed with a High Performance Particle Sizer (HPPS, from Malvern Instruments) using a light scattering apparatus equipped with an He-Ne (633 nm) laser and a thermo-electric Peltier temperature controller (temperature control range: $10\text{-}90^\circ\text{C}$). The measurements were made at the scattering angle $\theta = 173^\circ$ (“backscattering detection”), using CUMMULANTS to analyse the autocorrelation functions. Aqueous solutions of the polymers were filtered with a Sartorius Ministar-plus $0.450 \mu\text{m}$ disposable filter and were placed in a polystyrene or glass cuvette for analysis.

ζ -Potential Measurements: ζ -Potential of the particles determined by a Zeta Master S (1995) from Malvern Instruments (UK), using the software PCS (version 1.41).

Refractive index increments measurements: Refractive index increments dn/dc of the polymers were determined by the ScanRef system from PSS GmbH (Mainz, Germany), and listed in Table 7.1.

7. Experimental

Table 7.1. dn/dc values of polymers.

polymer	solvent	dn/dc
polyM1	1% wt acetic acid/ 0.2 M Na ₂ SO ₄ (aq)	0.152 ml/g
polyM2	0.1 M NaNO ₃	0.123 ml/g
polyM3	1% wt acetic acid/ 0.2 M Na ₂ SO ₄ (aq)	0.125 ml/g
polyM5	1% wt acetic acid/ 0.1 M Na ₂ SO ₄ (aq)	0.146 ml/g
polyM6	0.1 M NaNO ₃	0.125 ml/g
polyM7	1% wt acetic acid/ 0.2 M Na ₂ SO ₄ (aq)	0.132 ml/g
polyM9	1% wt acetic acid/ 0.2 M Na ₂ SO ₄ (aq)	0.182 ml/g
polyM10	1% wt acetic acid/ 0.2 M Na ₂ SO ₄ (aq)	0.162 ml/g
polyM11 ⁽¹⁾	1% wt acetic acid/ 0.1 M Na ₂ SO ₄ (aq)	0.194 ml/g
polyM13	1% wt acetic acid/ 0.2 M Na ₂ SO ₄ (aq)	0.188 ml/g
polyM14	0.1 M NaNO ₃	0.189 ml/g
polyM13-block-M10	1% wt acetic acid/ 0.2 M Na ₂ SO ₄ (aq)	0.166 ml/g

(1) : value taken from ref. [2]

7.2. Polymerization

Reagents: 4-vinylbenzoic acid (**M15**) was synthesized as described [3]. 4-(2-sulfoethyl)-1-(4-vinyl-benzyl) pyridinium betain (**M17**) was synthesized as described in the synthesis part of this chapter. Poly(ethyleneglycol) methylether acrylate ($M_r = 454$) (**M3**), (2-acryloyloxy)ethyl)trimethyl ammoniumchloride (80% aqueous soln.) (**M1**), N-(3-(dimethylaminopropyl) acrylamide (97%) (**M9**), dimethylacrylamide(99%) (**M10**) and N-(3-dimethylaminopropyl)methacrylamide (99%) (**M11**) were used as received from Aldrich. Poly(ethyleneglycol) methylether methacrylate ($M_r = 430$) (Bisomer MPEG350 MA, **M7**) was obtained from Laporte (UK). Methacrylamide (98+%) (**M12**), vinylbenzyl-trimethylammonium chloride (97%, 60:40 para:meta mixture) (**M13**), 2,2'-azobis (2-methylpropionitrile) (**V-60**) and n-butyl acrylate (+99%) (**M4**) were purchased from Acros Organics. 3-(Acryloyloxy)propansulfonate potassium salt (**M2**), 3-(methacryloyloxy)-propanesulfonate potassium salt (**M6**), 2-methylene-succinic acid bis-(3-sulfo-propyl)-ester-dipotassium salt (**M8**), 1-(3-sulfo-propyl)-2-vinyl pyridinium betain (**M18**) were gifts from Raschig AG (Ludwigshafen, Germany). 4-styrenesulfonate (90+%)(**M14**), toluene (+99.5 %) and 4-vinylbenzylchloride(+95%) (**M16**) were used as received from Fluka. (2-methacryloyloxyethyl)trimethylammonium chloride (80% aqueous soln.)(**M5**) was

7. Experimental

obtained from Degussa-Röhm (Germany). 2,2'-azobis (2-methylpropionamidine) dihydrochloride (**V-50**), and 2,2'-azobis(2-methyl-N-phenylpropionamidine)dihydrochloride (**V-545**) were gifts of Wako Pure Chemical Industries. Methanol and diethylether were analytical grade. Aluminium oxide (basic, activity 1, 0.063-0.200 mm) was from Merck. Buffer solution potassium hydrogen phthalate / HCl pH = 4.01 ± 0.02 (pH at 25°C) was purchased from Roth. Buffer solution pH = 6 was prepared from citric acid monohydrate (Fluka +99.5%) and sodium hydrogen phosphate (Riedel-deHaën, puriss). Polymers were dialyzed in water with tubes “Zellu Trans” (nominal molar mass cut off 3500) from Roth (Germany).

Procedure: Inhibitor 4-methoxyphenol was removed from monomers **M3**, **M4**, **M7**, **M10**, and **M16** by passing through basic aluminum oxide (basic, active1, 0.063-0.200 mm). **M9** was diluted by twice the volume of 0.5 M aqueous KCl, then it was brought to pH 3 by addition of concentrated HCl while cooling, thus protonating the amine moiety of the monomer. After adding the initiator and the RAFT agent, the mixture was extracted thrice with diethyl ether. Similarly, the polymerization solutions of **M1** and **M5** were extracted thrice with diethyl ether after addition of the RAFT agent and the initiator, in order to remove the inhibitor 4-methoxyphenol.

The type and the amounts of RAFT agent, initiator and monomer engaged, the polymerization media and the temperatures are listed in the Table 7.2 for the homopolymers, and in Table 7.3 for the block copolymers synthesized. Reaction mixtures were deoxygenated by bubbling N₂ for 30 min when carried out in water, and by applying three freeze-pump-thaw cycles when carried out in organic solvents. In kinetic studies done in water, samples were collected from the reaction mixture at given time intervals by a syringe through a septum. Polymerizations carried out in water were stopped by the addition of an aqueous solution of 4-methoxy phenol. All water-soluble polymer samples were dialyzed against water with tubes having a nominal molar mass cut off of 3500, and then were lyophilized. Conversions were determined on the basis of recovered polymer after lyophilization of the dialyzed samples. THF used in polymerization studies was dried refluxing over Na/K alloy. Toluene was passed through active basic aluminium oxide (active I) before using it. In the polymerization of **M16**, a stock solution was prepared, and then this solution was divided in 6 vials. Poly-**M16** was precipitated in methanol, and filtered with membrane filter. The conversions were determined gravimetrically.

7. Experimental

Table 7.2. Reagents and conditions used for homopolymerization experiments.

monomer (mmol)	RAFT agent (x 10 ⁻⁵ mol)	initiator (x 10 ⁻⁵ mol)	polym. temp.	solvent	polym. time(h)	ref.**
M1 (50.4)	CTA3 (13.9)	V-545 (2.8)	48 °C	55 0.5 M (aq) KCl	***	3MM150
M2 (55.6)	CTA1 (12.2)	V-50 (3.2)	55 °C	75 ml water	***	3MM162
M2 (52.3)	CTA3 (15.1)	V-545 (3.0)	48 °C	75 ml 0.5 M (aq) KCl	***	3MM158
M3 (29.1)	CTA3 (18.8)	V-545 (3.8)	48 °C	70 ml 0.5 M (aq) KCl	***	3MM152
M5 (38.5)	CTA4 (20.0)	V-50 (4.0)	55 °C	45 ml water	***	3MM116
M6 (64.4)	CTA1 (14.8)	V-50 (4.0)	55 °C	75 ml water	***	3MM160
M7 (30.9)	CTA1 (20.0)	V-50 (5.3)	55 °C	25 ml water	***	3MM32
M8 (6.5)	CTA1 (15.0)	V-50 (3.0)	50 °C	25 ml buffer soln pH=6	17	2MM114
M8 (2.2)	CTA4 (5.0)	V-50 (1.0)	55 °C	15 ml water	20	3MM124
M8 (2.2)	CTA5 (5.0)	V-50 (1.0)	55 °C	5 ml water	4	4MM48
M9 (69.6)	CTA3 (21.7)	V-545 (4.3)	48 °C	60 ml 0.5 M (aq) KCl	***	3MM184
M11 (44.2)	CTA4 (13.5)	V-50 (3.0)	55 °C	60 ml water pH=4	***	3MM148
M12 (125.0)	CTA4 (20.0)	V-50 (4.0)	55 °C	95 ml water	***	3MM186
M13 (7.4)	thioester analogue of CTA2 (9.0)	V-50 (1.8)	50 °C	25 ml water	***	3MM28
M13 (20.6)	CTA6 (7.4)	V-50 (1.8)	55 °C	25 ml water	***	3MM42
M13 (23.9)	CTA3 (13.6)	V-545 (2.7)	48 °C	50 ml 0.5 M (aq) NaBr	***	3MM110
M14 (21.8)	CTA3 (22.5)	V-545 (4.5)	55 °C	30 ml 0.5 M (aq) NaBr	7	2MM182-1st
M16 (321.1)	CTA7 (101.2)	V-60 (16.8)	80 °C	Toluene 50.5 g	***	1MM67
M17(8.3)	CTA 3 (8.4)	V-545 (1.7)	55	25 ml 0.5 M (aq) NaBr	5	3MM64
M18 (4.4)	CTA4 (5.0)	V-50 (1.0)	55 °C	15 ml water	22	3MM128
M18 (4.4)	CTA4 (5.0)	V-50 (1.0)	55 °C	15 ml buffer soln pH=4	22	3MM129
M18 (24.5)	CTA3 (17.0)	V-545 (3.0)	55 °C	25 ml 0.5 M (aq) NaBr	6	3MM36
M18 (4.4)	CTA5 (4.0)	V-50 (1.0)	55 °C	5 ml water	4 h	4MM50

**= 1-, 2-, 3-, or 4MM refers to related laboratory notebook, and the following numbers are the page numbers in my laboratory notebooks.

*** = polymerization kinetic was examined.

7. Experimental

sample	monomer (mmol)	RAFT agent, or macro-RAFT agent ($\times 10^{-5}$ mol)	initiator ($\times 10^{-5}$ mol)	poly. temp. ($^{\circ}\text{C}$)	solvent used for poly.	poly. time (h)	Ref. ***
polyM1 ***	M1 (17.1)	CTA3 (40.0)	V-545 (10.0)	55	20 ml 0.5 M (aq) NaBr	3.5	3MM92
polyM1-block-M3	M3 (8.4)	polyM1 1.39 g (11.6)	V-50 (3.2)	55	25 ml water	6h	4MM64
polyM3	M3 (10.1)	CTA3 (35)	V-545 (7.5)	48	12 ml 0.5 M (aq) NaBr	5	4MM68
polyM3-block-M17	M17 (11.0)	polyM3 1.34 g (9.6)	V-50 (3.35)	55	20 ml 0.5 M (aq) NaBr	5	4MM74
polyM3-block-M17-block-M15	M15 (1.2)	polyM3-block-M17 1.68 g (4.3)	V-50 (1.5)	55	13 ml 0.5 M (aq) NaBr pH = 6.5	15	4MM88
polyM7	M7 (42.9)	CTA1 (28)	V-50 (7.4)	55	19 ml water	15	3MM32
polyM7-block-M4	M4 (3.0)	polyM7 1.50 g (2.2)	V-50 (0.72)	55	20 ml water	6	3MM146
ppolyM7-block-M4	M4 (6.9)	polyM7 3.12 g (4.6)	V-60 (1.18)	60	20 ml THF	22	3MM66
polyM7-block-M4	M4 (5.3)	polyM7 3.12 g (4.6)	V-60 (1.13)	60	20 ml THF	15	3MM84
polyM10	M10 (125.0)	CTA1 (6.5)	V-545 (1.7)	48	15 ml water	5	4MM26
polyM10-block-M17	M17 (12.7)	polyM10 1.33 g (4.3)	V-50 (1.9)	53	25 ml 0.5 M (aq) NaBr	3	4MM42
polyM10-block-M17-block-M15	M15 (0.7)	polyM10-block-M17 0.60 g (1.0)	V-545 (0.75)	53	15 ml 0.5 M (aq) NaBr pH = 6.5	15	4MM54
polyM13	M1 (50.4)	CTA3 (13.9)	V-545 (2.8)	48	55 0.5 M (aq) KCl	3	3MM150
polyM13-block-M10	M10 (5.0)	polyM13 0.13 g (0.53)	V-545 (0.27)	48	4 ml water	5	4MM42
polyM14	M14 (125.0)	CTA3 (22.5)	V-545 (4.5)	55	30 ml 0.5 M (aq) NaBr	7	2MM182-1 st
polyM14-block-M17	M17 (11.0)	polyM14 1.00 g (4.6)	V-545 (1.0)	55	25 ml 0.5 M (aq) NaBr	5	3MM18
polyM14-block-M17-block-M15	M15 (2.4)	polyM14-block-M17 1.32 g (2.6)	V-545 (6.0)	55	25 ml 0.5 M (aq) NaBr pH = 6.5	17	3MM52

**= 1-, 2-, 3-, or 4MM refers to related laboratory notebook, and the following numebners are the page numbers in laboratory notebooks.

***= In this polymerization, inhibitor was not removed from monomer. For future experiments, I might use 0.5 M (aq) NaCl instead of 0.5 M (aq) NaBr, because Br ions exchange with Cl ions of the monomer

Table 7.3. Polymerization conditions used for the preparation of block copolymers.

7. Experimental

7.3. Particle Preparation via Complexation of Cationic and Anionic Functional Groups

Reagents: 1.00 g of copolymer **polyM1-block-M3** According to MALLS analysis cationic block is 10 K and polyethylene glycol based nonionic block is 29 K. Note that molar weight of repeating cationic monomer units was used as $212.7 \text{ g}\cdot\text{mol}^{-1}$ for calculations, as the counter anions of **polyM1** is the mixture of Cl^- (57%) and Br^- (43%) according to elemental analysis.], 0.70 g (1.36 mmol) of nonadecafluorodecanoic acid (97+%, Fluka), 0.23 g (1.36 mmol) of capric acid (98+%, Fluka), 0.1 M (aq) NaOH (Merck), diethylether (technical grade).

Procedure: 1.00 g of copolymer **polyM1-block-M3** was dissolved 100 ml water. 0.70 g (1.36 mmol) of nonadecafluorodecanoic acid and 0.23 g (1.36 mmol) of capric acid were dissolved separately in 15 ml of diethylether. Both solution was added 13.6 ml 0.1 M (aq) NaOH, and the two phase systems were stirred for 10 minutes. Each of the solutions was added to 50ml of the stock solution of copolymer **polyM1-block-M3** at 60 °C. These mixures were stirred vigorously for 6 h at 60 °C. The solutions were cooled to ambient temperature while stirring.

7.4. Synthesis

N-methyl-N-(thiobenzoylsulfanylmethylenephnylmethyl) morpholinium chloride (**CTA5**) was a gift from Jean-François Baussard [4,5]. 4-cyano-4-thiobenzoylsulfanylpentanoic acid (**CTA1**) was synthesized as described by Thang et al [6]. **CTA1** was converted into the sodium salt by dissolution in CH_2Cl_2 , followed by extraction into the aqueous phase via slow addition of 1M NaOH (pH always <7), and subsequent lyophilization.

7.4.1. Synthesis of dithiobenzoic acid

Reagents: phenyl magnesium chloride (2M solution in THF, Aldrich), carbon disulfide (99.9+%, Aldrich), and diethylether (technical grade).

Procedure: Inject phenyl magnesium chloride (2M THF) in a three-necked-round bottomed flask (equipped with two rubber septum and a condenser) under N_2 atmosphere. Slowly add excess CS_2 into the flask with a syringe (avoid the boiling of the reaction mixture). Mix the solution at 60 °C for 30 min. Then, stop the water cooling in the condenser, and

7. Experimental

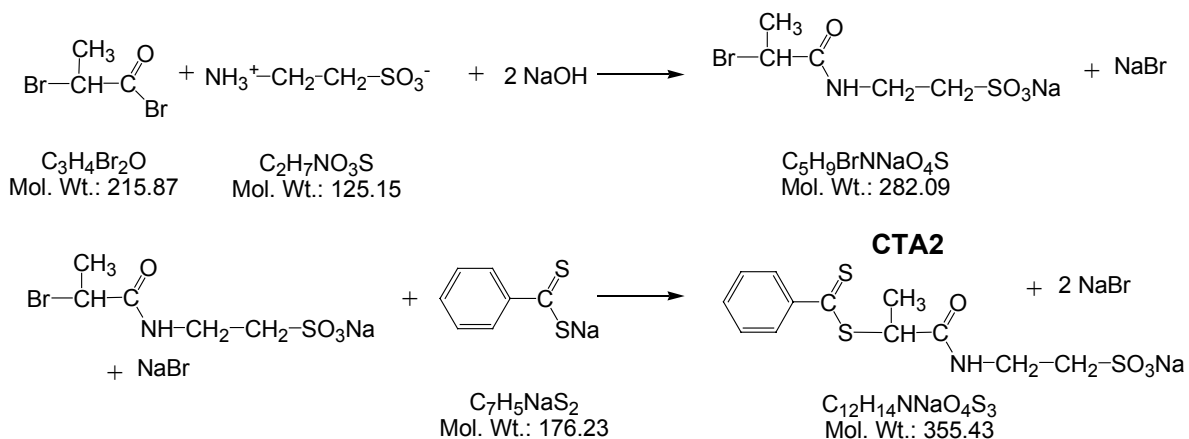
bubble N₂ through the solution for 5 min. to remove unreacted CS₂. Mix this solution in a separator funnel with water and diethylether. Then, acidify the mixture with 1M HCl to transfer the dithiobenzoic acid to the ether layer. Remove the aqueous layer, and wash the ether layer three times with small volumes of water. Dithiobenzoic acid can be transferred back to the aqueous layer by adding NaOH or KOH depending on the desired counter ion. ¹H-NMR (Bruker 300 MHz, in CDCl₃): δ in ppm= 7.26-7.44 (m, 2H, meta), 7.54-7.66 (m, 1H, para), 8.02-8.22 (m, 2H, orto). See Figure A2.11 for the ¹H-NMR spectra in CDCl₃.

7.4.2. Synthesis of di(thiobenzoyl)disulfide

Reagents: 350 ml aqueous solution of sodium dithiobenzoate (~0.28 M) alkaline solution (pH about 13), 35 g (106 mmol) of potassium ferric cyanide K₃Fe(CN)₆ (99+%, Acros), THF (ACS, Acros).

Procedure: (adapted from Mitsukami et. al.[7]) To 350 ml of sodium dithiobenzoate (~0.28 M) alkaline solution having pH about 13, 350 ml aqueous solution containing 35 g (106 mmol) of K₃Fe(CN)₆ were added slowly. Note that the sodium dithiobenzoate solution has to be basic enough for a successful reaction. The di(thiobenzoyl)disulfide forms in water brown-red colored precipitate which was recovered by filtration. The filter cake was re-dissolved in THF, and then it was re-precipitated to water. (Note that methanol may be a better alternative to water for precipitation, as reprecipitation to water was difficult). ¹H-NMR (Bruker 300 MHz, in CDCl₃): δ in ppm = 7.41-7.50 (m, 2H, meta), 7.57-7.65 (m, 1H, para), 8.10-8.12 (m, 2H, orto). See Figure A2.2 for the ¹H-NMR spectra in CDCl₃.

7.4.3. Synthesis of sodium 2-(2-thiobenzoylsulfanyl propionylimino) ethanesulfonate (CTA2)



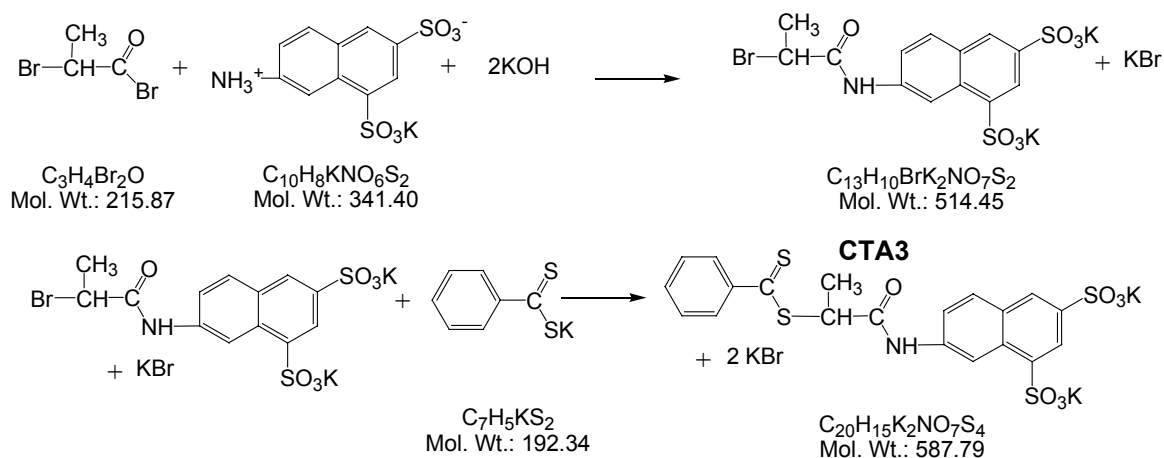
7. Experimental

Reagents: KI (99+%, Aldrich), taurine (99+%, Aldrich), 2-bromopropionyl bromide (97+%, Fluka), NaOH pellets (Merck), 1 M HBr (Merck), CH₂Cl₂ (technical), potassium dithiobenzoate (see synthesis of dithiobenzoic acid above).

Procedure: 5.62 g (44.9 mmol) of taurine and 3.57 g (89.7 mmol) of NaOH were dissolved in 70 ml of water. 10.01 g (44.9 mmol) of 2-bromopropionylbromide dissolved in 60 ml of CH₂Cl₂ were added drop-wise. The resulting two phase system was stirred vigorously for 10 h. After separation of the organic phase, the aqueous phase was extracted twice with 50 ml of diethyl ether. The aqueous phase was separated, and the pH was adjusted by 1 M NaOH to a value of 6, and the solution was freeze-dried. 8.52 g (22.1 mmol) of the solid obtained (sodium 2-(2-bromopropionylimino) ethanesulfonate + NaBr mixture; see Appendix 2 Figure 2A.. for the ¹H-NMR spectrum this intermediate compound) were added to 0.15 g (0.9 mmol) of KI and 150 ml of an about 0.4 M aqueous solution of sodium dithiobenzoate. The solution was stirred at room temperature for 5 h. Then, it was filtered, acidified with 1 M HBr and extracted thrice with 100 ml of diethyl ether. The pH was readjusted to value of 6.5 with 1 M NaOH. The solution was freeze-dried. Yield of crude **CTA2**: 14.03 g (69.7 %) (containing according to elemental analysis 61 wt% of inorganic salt: Found: C 15.92, H 1.40, N 1.95, S 10.78, Br 46.4, Cl 0.90). The crude product can be used as RAFT agent without further purification. The pure compound free from salt is obtained by fractionate precipitation of a saturated solution in methanol by adding successive aliquots of acetone, rejecting the first and the last fractions. Elemental analysis of purified **CTA2** (C₁₂H₁₄NNaO₄S₃, M_r = 355.43 g·mol⁻¹): Calc: C 40.55, H 3.97, N 3.94, S 27.07; Found: C 39.94, H 3.90, N 3.98, S 26.51. ¹H-NMR (Bruker 300 MHz in D₂O): δ in ppm = 1.58 (d, 3H, CH₃), 3.00 (t, 2H, -CH₂SO₃), 3.54 (t, 2H, -CH₂-C-SO₃) 4.51 (q, 1H, CH), 7.40 (m, 2H, (aryl =CH(meta)), 7.58 (m, 1H, (aryl =CH(para)), 7.88 (m, 2H, (aryl =CH(ortho)). ¹³C NMR (Bruker 75 MHz in D₂O) δ in ppm = 16.55 (S-C-CH₃-), 36.07 (-NH-CH₂-), 50.13 (-CH₂-SO₃Na), 50.45 (S-CH(CH₃)-), 127.27 (aryl CH(2)), 129.15 (aryl CH(3)), 133.71 (aryl C(4)), 144.53 (aryl CH(1)), 173.63 (-CONH-), 228.34 (-C=(S)S).

7. Experimental

7.4.4. Synthesis of potassium 2-(2-thiobenzoylsulfanylpropionylimino)naphthalene-6,8-disulfonate (CTA3)



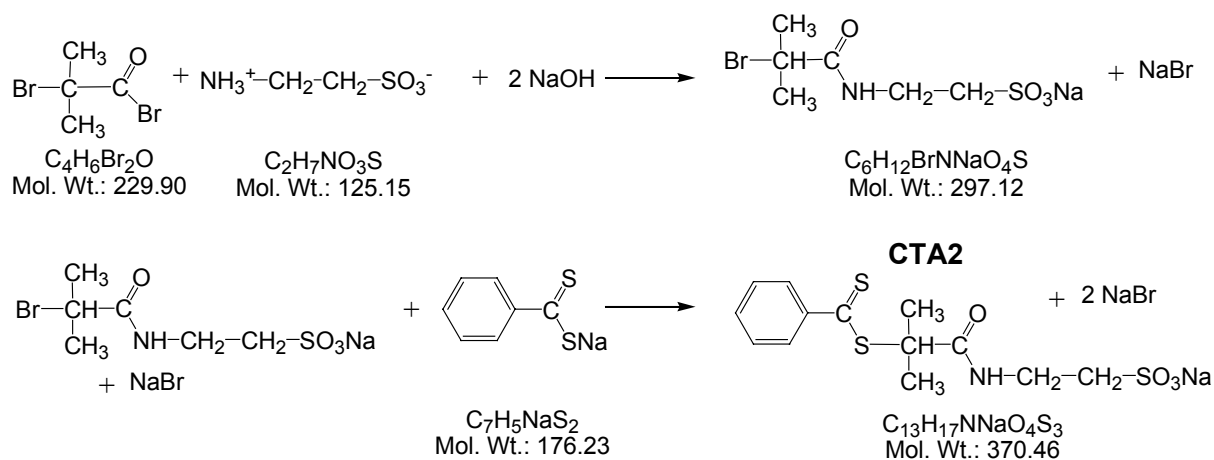
Reagents: KI (99+%, Aldrich), 2-naphthylamino-6,8-disulfonic acid monopotassium salt (85%, Aldrich), 2-bromopropionyl bromide (97+%, Fluka), KOH pellets (Aldrich), CH_2Cl_2 (technical), potassium dithiobenzoate (see synthesis of dithiobenzoic acid).

Procedure: 14.93 g (67.1 mmol) of 2-bromopropionyl bromide in 30 ml of CH_2Cl_2 were added dropwise to 15.00 g of (37.3 mmol) 2-naphthylamino-6,8-disulfonic acid monopotassium salt in 135 ml of 1 M KOH, while cooling with ice. Then, the ice-bath was removed, and the two phase system was stirred vigorously for 12 h at ambient temperature. The aqueous phase was separated and precipitated into ethanol. The precipitate was filtered off, and washed with ethanol, and dried under reduced pressure, to yield 21.13 g of crude 2-(2-bromo-propionylamino)-naphthalene-6,8-disulfonic acid dipotassium salt (containing 7% KBr determined by elemental analysis; see Appendix 2 Figure 2A.6 for the $^1\text{H-NMR}$ spectrum this intermediate compound). 6.49 g (11.7 mmol) of this intermediate and 0.126 g (7.5×10^{-4} mol) of KI were dissolved in 60 ml of 25 mmol potassium dithiobenzoate solution (pH 6). The pH of solution was rapidly adjusted to 6. This solution was mixed at ambient temperature for 13 h. The mixture was precipitated into acetone. It was redissolved in the minimum amount of water and precipitated again by addition of acetone. The first precipitated fractions (1.29 g) were contaminated by inorganic salt and removed. Yield : 3.94 g (55%) of hygroscopic solid. Elemental analysis ($\text{C}_{20}\text{H}_{15}\text{K}_2\text{NO}_7\text{S}_4$, $M_r = 587.79 \text{ g}\cdot\text{mol}^{-1}$): Calc: C 40.87, H 2.57, N 2.38, S 21.82; C/N = 17.17, C/S = 1.87. Found: C 39.07, H 2.81, N 2.24, S 20.77; C/N = 17.44, C/S = 1.88. MS (FAB, matrix glycerol,

7. Experimental

negative ions) signal at 548.0 (M-K). $^1\text{H-NMR}$ (Bruker 300 MHz in D_2O): δ in ppm = 1.62 (d, 3H, CH_3), 4.53 (q, CH), 7.22 (t, 2H, (=CH phenyl)), 7.41 (t, 1H, (CH= phenyl)), 7.61 (d, 1H, (=CH naphthyl)), 7.71 (d, 2H (=CH phenyl)), 7.91 (d, 1H (=CH naphthyl)), 8.31 (s, 2H (=CH naphthyl)), 8.72 (s, 1H (=CH naphthyl)). $^{13}\text{C NMR}$ (Bruker 75 MHz in D_2O) δ in ppm = 16.3 (CH_3), 51.4 (S-CH), 116.2 (naphthyl CH (7)), 122.9 (naphthyl CH (1)), 123.4 (naphthyl CH (3)), 127.1 (phenyl CH(2)), 129.1 (phenyl CH(3)), 130.0 and 130.2 (naphthyl C(9+10)), 131.3 and 131.6 (naphthyl $\text{O}_3\text{S-C}(6+8)$), 133.8 (phenyl CH(4)), 138.3 (naphthyl CH (5)), 138.5 (naphthyl CH (4)), 139.8 (naphthyl N-C(2)), 141.1 (phenyl C(1)), 173.0 (-CONH-), 228.7 (-C=(S)S-). FT-IR (KBr, selected bands) wavenumber in cm^{-1} = 3506, 3288, 1693, 1623, 1538, 1496, 1446, 1194, 1106, 1039, 761, 665, 615. UV-Vis (in water): band at $\lambda_{\text{max}} = 483 \text{ nm}$ ($\epsilon = 110 \text{ l}\cdot\text{mol}^{-1}\cdot\text{cm}^{-1}$), band at $\lambda_{\text{max}} = 301 \text{ nm}$ ($\epsilon = 25.0 \times 10^3 \text{ l}\cdot\text{mol}^{-1}\cdot\text{cm}^{-1}$), and band at $\lambda_{\text{max}} = 251 \text{ nm}$ ($\epsilon = 47.1 \times 10^3 \text{ l}\cdot\text{mol}^{-1}\cdot\text{cm}^{-1}$).

7.4.5. Synthesis of sodium 2-(2-methyl-2-thiobenzoylsulfanylpropionylimino)ethanesulfonate (CTA4)



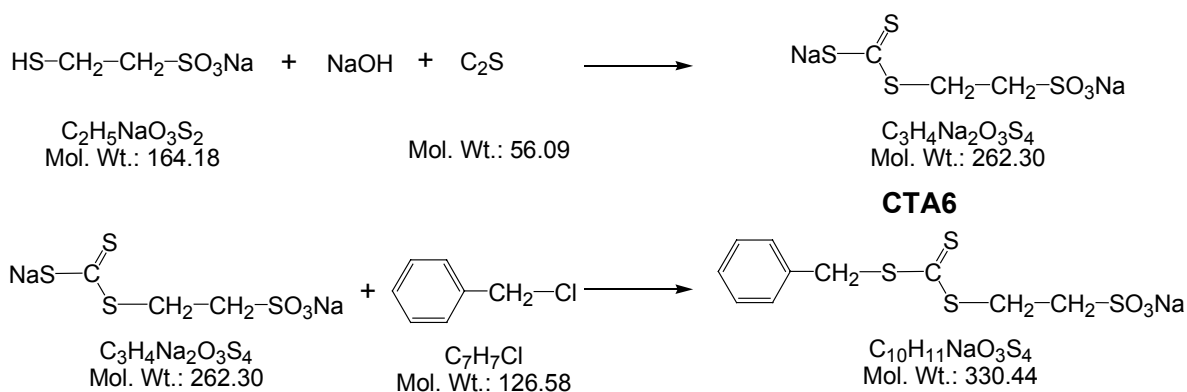
Reagents: KI (99+%, Aldrich), taurine (99+%, Aldrich), α -bromoisobutyrylbromide (97+% Fluka), NaOH pellets (Merck), CH_2Cl_2 (technical), sodium dithiobenzoate (see synthesis of dithiobenzoic acid).

Procedure: 5.42 g (42.9 mmol) of taurine were dissolved in 86.5 ml of 1M NaOH. 10.01 g (43.1 mmol) of α -bromoisobutyrylbromide dissolved in 50 ml of CH_2Cl_2 were added dropwise. The resulting two phase system was stirred vigorously for 15 h at ambient temperature. After separation of the organic phase, the aqueous phase was adjusted to pH 2

7. Experimental

and then extracted twice with 50 ml of diethyl ether. The aqueous phase was separated, the pH was adjusted to 6 by 1 M NaOH, and the solution was diluted to 100 ml. 30 ml of this solution containing 12.9 mmol of 2-(2-bromo-2-methyl-propionylamino)-ethanesulfonic acid sodium salt (see Appendix 2 Figure2A.8 for the $^1\text{H-NMR}$ spectrum this intermediate compound) were added to 0.10 g (6×10^{-4} mol) of KI and 14 mmol of sodium dithobenzoate solution (pH 6). The solution was stirred at 57°C for 18 h under nitrogen atmosphere. The pH of the solution was adjusted to 2 and then extracted twice with 50 ml of diethyl ether. The aqueous phase was separated, and the pH was adjusted to 6 by 1 M NaOH. The solution was diluted with ethanol, and evaporated keeping the temperature below 40°C to minimize the risk of hydrolysis or alcoholysis. The residue was redissolved in the minimum amount of ethanol/ CHCl_3 (25/75 by volume). Insoluble impurities were removed by filtration. The raw product was purified by column chromatography (silicagel, eluent: ethanol/ CHCl_3 25/75 by volume). Yield 0.95 g (20%) of hygroscopic powder. ($\text{C}_{13}\text{H}_{16}\text{NNaO}_4\text{S}_3$, $M_r = 369.46 \text{ g}\cdot\text{mol}^{-1}$): Calc: C 42.26, H 4.37, N 3.79, S 26.04. Found: C 41.05, H 4.32, N 3.50, S 22.54. MS (ESI, negative ions) signal at 345.9 (M-Na^+). $^1\text{H-NMR}$ (Bruker 300 MHz in D_2O): $\delta = 1.64$ (s, 6H, CH_3), 2.96 (t, 2H, $-\text{CH}_2\text{SO}_3$), 3.48 (t, 2H, $-\text{CON-CH}_2-$), 7.37 (m, 2H, (aryl =CH(meta)), 7.55 (m, 1H, (aryl =CH(para)), 7.82 (m, 2H, (aryl =CH(ortho)). $^{13}\text{C NMR}$ (Bruker 75 MHz in D_2O) $\delta = 24.8$ ($-\text{CH}_3$), 36.4 ($-\text{NH-CH}_2-$), 50.1 ($-\text{CH}_2-\text{SO}_3$), 56.5 (S-C-), 127.1 (aryl CH(2)), 129.2 (aryl CH(3)), 133.6 (aryl CH(4)), 145.4 (aryl C(1)), 175.5 ($-\text{CON-}$), 228.7 ($-\text{C}=\text{(S)S-}$). FT-IR (KBr, selected bands) wavenumber in $\text{cm}^{-1} = 3417, 1635, 1538, 1444, 1214, 1049, 871, 761, 686, 647, 619$. UV-Vis (in water): band at $\lambda_{\text{max}} = 483 \text{ nm}$ ($\epsilon = 130 \text{ l}\cdot\text{mol}^{-1}\cdot\text{cm}^{-1}$).

7.4.6. Synthesis of sodium *S*-benzyl-*S'*-2-sulfonatoethyl trithiocarbonate (CTA6)

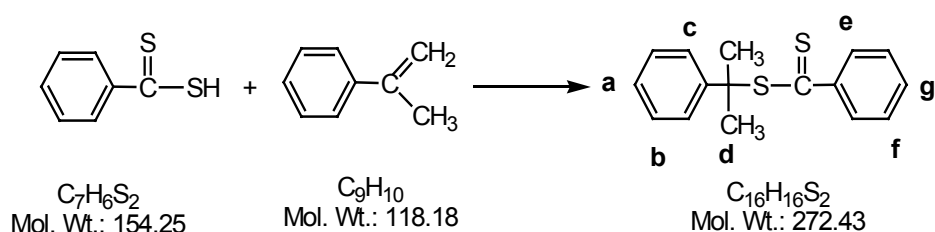


7. Experimental

Reagents: Carbon disulfide (99.9+%, Aldrich), sodium 2-mercaptoethanesulfonate (98+%, Fluka), benzyl chloride (99.5+%, Acros), NaOH pellets (Merck)

Procedure: 1.92 g (11.4mmol) of sodium-2-mercaptoethanesulfonate and 25 ml of deoxygenated 0.5 M NaOH were stirred for 30 min under N₂ atmosphere at ambient temperature, before injecting 3.00 ml (50.5 mmol) of carbon disulfide. The mixture was stirred for 4 h at ambient temperature, before the excess of CS₂ was removed *in vacuo*. Then, 3.85 g (30.4 mmol) of benzylchloride were added to the flask, and the solution was stirred vigorously for 12 h at ambient temperature. Heating the suspension obtained to 70 C° for 20 min gave a clear solution from which yellow crystals precipitated after allowing to cool to ambient temperature. Best results were obtained when stopping precipitation after 1h, as prolonged crystallisation times resulted in co-crystallisation of impurities, which are difficult to separate though increasing the yield. The formed yellow precipitate was filtered off. The filter cake was washed with 50 ml of diethyl ether. The product was dried over P₂O₅ under reduced pressure to yield 1.48g (39%) of yellow crystal sheets. 2 can be re-crystallised from water if further purification is necessary. Decomposition before melting starts at about 300°C. Elemental analysis (C₁₀H₁₁NaO₃S₄), (M_r = 330.45 g·mol⁻¹): Calc: C 36.35, H 3.36, S 38.82; Found: C 36.74, H 3.13, S 38.25. MS (FAB, matrix thioglycerol, negativ ions) signal at 307.0 (M-Na)⁻. ¹H-NMR (Bruker 300 MHz, in DMSO-d₆): δ = 2.73 - 2.79 (m, 2H, -CH₂SO₃), 3.55 - 3.60 (m, 2H, -CH₂-C-SO₃), 4.67 (s, 2H, Φ-CH₂-SC(=S)S-), 7.25 - 7.41 (m, 5H, aromatic =CH-). ¹³C NMR (Bruker 75 MHz in DMSO-d₆) δ = 32.70 (-S-CH₂-CH₂-SO₃), 40.19(Φ-CH₂-SC(=S)S-), 48.86 (CH₂SO₃), 127.52 (aryl CH(4)), 128.49 (aryl CH(2)), 129.08 (aryl CH(3)), 135.05 (aryl C(1)), 223.42(-SC(=S)S-). FT-IR (KBr, selected bands) wavenumber in cm⁻¹ = 3060, 3025, 1229, 1207, 1177, 1118, 1063, 833, 798, 772, 705, 596. UV-Vis (in water): band at λ_{max} = 425 nm (ε = 55 l·mol⁻¹·cm⁻¹).

7.4.7. Synthesis of Cumyldithiobenzoate (CTA7)

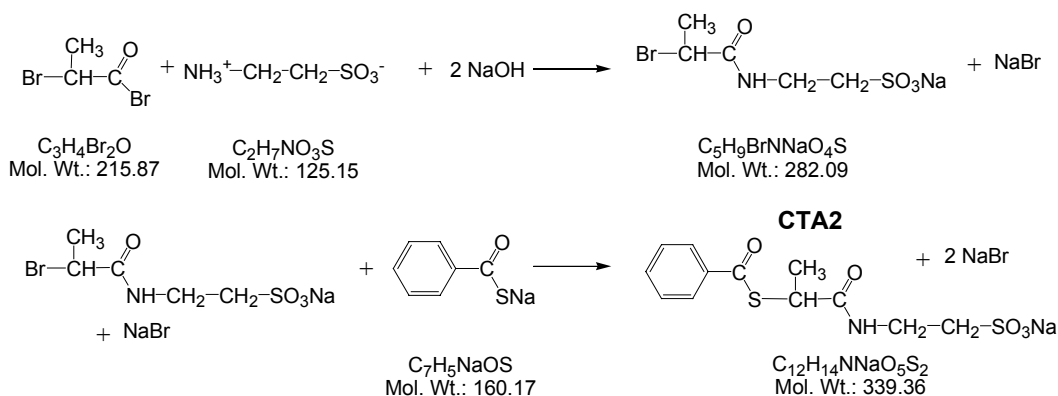


7. Experimental

Reagents: 1.54 g (13.1 mmol) of α -methylstyrene (99+%, Aldrich), 15 mmol of dithiobenzoic acid (prepared via grignard method). CHCl_3 (ACS, Aldrich).

Procedure: Adapted from the procedure defined in US patent [8]. 1.54 g (13.1 mmol) of α -methylstyrene were added to about 15 mmol of dithiobenzoic acid. The mixture was heated to 70 °C for 1 h under N_2 atmosphere. 20 ml of CHCl_3 were injected into the flask through a rubber septum, and the solution was refluxed for 8 h at 70 °C. The solution was extracted with 1 M (aq) NaOH to remove unreacted dithiobenzoic acid. The organic phase was separated, and the solvent was evaporated. The raw product was purified by column chromatography (silica gel, eluent: Hexane/ CHCl_3 85/15 by volume). $^1\text{H-NMR}$ (Bruker 300 MHz in D_2O , labeling of H protons is given in the reaction scheme above): δ in ppm = 2.04 (s, 6H, d), 7.19-7.26 (m, 1H, a), 7.28-7.37 (m, 4H, b and f), 7.44-7.51 (m, 1H, g), 7.54-7.59 (m, 2H, c), 7.84-7.84 (m, 2H, e).

7.4.8. Synthesis of Sodium 2-(2-benzoylsulfanylpropionylimino)ethanesulfonate (thioester analogue of CTA2)



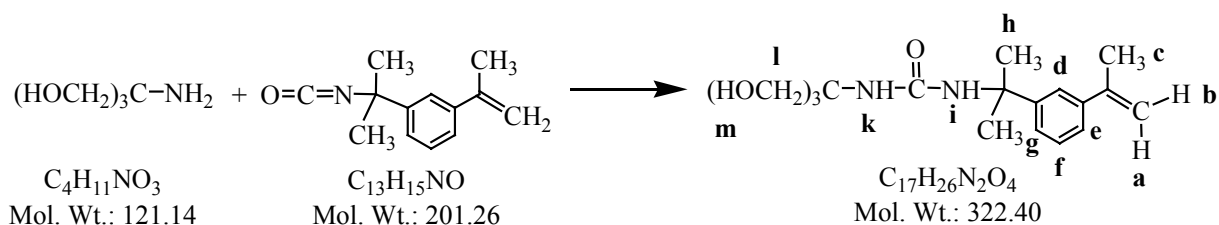
Reagents: KI (99+%, Aldrich), taurine (99+%, Aldrich), 2-bromopropionyl bromide (97+%, Fluka), NaOH pellets (Merck), 1M HCl (Merck), CH_2Cl_2 (technical), thiobenzoic acid (90+%, Acros).

Procedure: An analogous procedure, used for the synthesis of **CTA2**, was employed. Thiobenzoic acid was used instead of dithiobenzoic acid, and HCl was used instead of HBr. The thioester analogue of **CAT2** was obtained as a white solid. Inorganic salt impurities (NaBr and NaCl) were not removed. Yield: 70% (corrected for the amount of 51 wt% of inorganic salt according to elemental analysis). Elemental analysis

7. Experimental

($C_{12}H_{14}NNaO_5S_2$, $M_r = 339.37\text{g}\cdot\text{mol}^{-1}$): Calc: **C** 42.47, **H** 4.16, **N** 4.16, **S** 18.90; C/N = 10.21, C/S = 2.25. Found: **C** 21.68, **H** 1.92, **Br** 25.0, **Cl** 8.8, **N** 2.26, **S** 9.80. C/N = 9.59, C/S = 2.21. $^1\text{H-NMR}$ (Bruker 300 MHz, in D_2O): $\delta = 1.51$ (d, 3H, $-\text{CH}_3$), 3.01 (t, 2H, $-\text{CH}_2\text{SO}_3$), 3.56(t, 2H, $\text{N-CH}_2\text{-C-SO}_3$), 4.27 (q, H, $-\text{CSS-CH-}$), 7.49-7.93 (m, 5H, $=\text{CH-aryl}$). $^{13}\text{C NMR}$ (Bruker 75 MHz in D_2O), $\delta = 16.9$ (S-CH-CH_3 -), 36.0 ($-\text{NH-CH}_2$ -), 43.2 ($-\text{S-CH}(\text{CH}_3)$ -), 50.1 ($-\text{CH}_2\text{-SO}_3\text{Na}$), 127.7 (aryl CH(2)), 129.6 (aryl CH(3)), 135.1 (aryl CH(4)), 136.2 (aryl C(1)), 175.0 ($-\text{C}(=\text{O})\text{H-}$), 194.5 ($-\text{C}(=\text{O})\text{S-}$).

7.4.9. Synthesis of *N*-(tris(hydroxymethyl)methyl)-*N'*-(α,α -dimethyl-3'-isopropenylbenzyl) urea (IMM1)



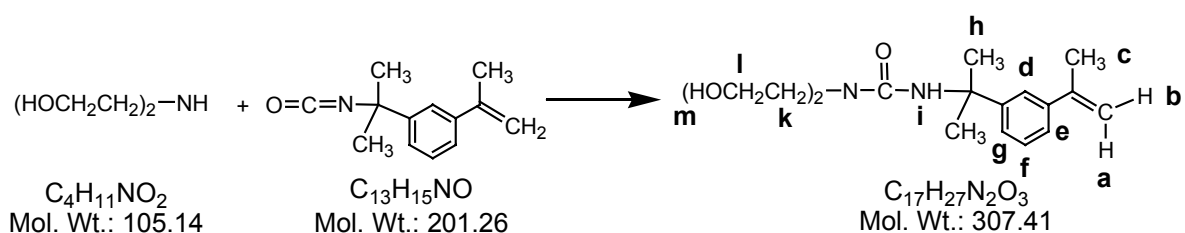
Reagents: 4.99g (41.17 mmol) of α,α,α -tris(hydroxymethyl)methylamine (95+%, Aldrich), 8.28 g (39.08 mmol), α,α -dimethyl-3-isopropenyl-benzyl-isocyanate (99.8+%, Aldrich), methanol (technical grade).

Procedure: 8.28 g (39.08 mmol) of α,α -dimethyl-3-isopropenyl-benzyl-isocyanate were added drop-wise to a solution of 4.99g (41.17 mmol) of α,α,α -tris(hydroxymethyl)methylamine in 30 ml of methanol at ambient temperature. The flask was cooled with a water bath, and the dropping speed was about 1 drop per second. A white paste formed while the addition of isocyanate. The white paste was filtered, and then recrystallized from boiling water. The filter cake was dried in vacuo over phosphorous pentoxide. Yield: 10.2 g (81%) of *N*-(tris (hydroxymethyl) methyl-*N'*)-(α,α -dimethyl-3'-isopropenylbenzyl) urea (**IMM1**). Elemental analysis :($C_{17}H_{26}N_2O_4$, $M_r = 322.40\text{ g}\cdot\text{mol}^{-1}$): Calc: **C** 63.33, **H** 8.13, **N** 8.69. Found: **C** 64.14 , **H** 8.25 , **N** 8.60 MS (APCI, H^+) signal at 323.0. $^1\text{H-NMR}$ (Bruker 300 MHz in DMSO; atom labelling given above in reaction scheme): δ in ppm = 1.50 (s, 6H, h), 2.10 (s, 3H, c), 3.38 (d, 6H, l), 4.99-5.01 (m, 3H, m), 5.08 (s, 1H, a), 5.38 (s, 1H, b), 5.90 (s, 1H, k), 7.00 (s, 1H, i), 7.30-7.24 (m, 3H, g,f,e), 7.42 (s, 1H, d). $^{13}\text{C NMR}$ (Bruker 75 MHz in DMSO) δ in ppm = 158.9, 149.2, 143.4, 140.0, 128.3, 124.6, 123.2,

7. Experimental

122.1, 112.7, 61.8, 61.0, 54.9, 30.6, 20.0. FT-IR (KBr, selected bands) wavenumber cm^{-1} : 3357, 3329, 1625, 1563, 1289, 1050, 1023, 881. Solubility: soluble in hot water, dioxane, methanol (slightly) and THF, and insoluble in CHCl_3 .

7.4.10. Synthesis of *N,N*-bis(2-hydroxyethyl)-*N'*-(α,α -dimethyl-3'-isopropenylbenzyl) urea (**IMM3**)

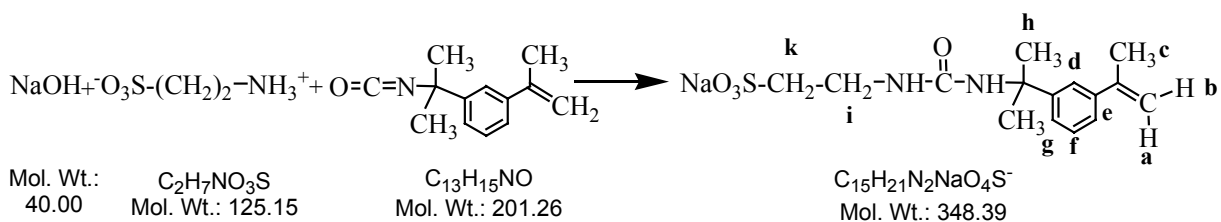


Reagents: 6.48 g (61.33 mmol) of diethanolamine (98+%, Merck), 11.34 g (53.53 mmol) of α,α -dimethyl-3-isopropenyl-benzyl-isocyanate (95+%, Aldrich), methanol (technical grade).

Procedure: 11.34 g (53.53 mmol) of α,α -dimethyl-3-isopropenyl-benzyl-isocyanate were added drop-wise to a solution of 6.48 g (61.33 mmol) of diethanolamine in 11 ml methanol at ambient temperature (dropping speed was about 1 drop per second). Then the mixture was poured in 200 ml water, and a white product precipitated. The white paste was re-dissolved in boiling water, and reprecipitated by cooling. Filtering off and drying in vacuo at 40 °C over phosphorous pentoxide yielded 14.9 g (about 91%) of *N,N*-bis(2-hydroxyethyl)-*N'*-(α,α -dimethyl-3'-isopropenylbenzyl) urea (**IMM3**). Elemental analysis ($\text{C}_{17}\text{H}_{27}\text{N}_2\text{O}_3$, $M_r = 307.41 \text{ g}\cdot\text{mol}^{-1}$): Calc: C 66.64, H 8.55, N 9.26. Found: C 66.79, H 9.21, N 9.26. MS (APCI, H^+) signal at 307.0. $^1\text{H-NMR}$ (Bruker 300 MHz in DMSO; atom labelling given above in reaction scheme): δ in ppm = 1.53 (s, 6H, h), 2.10 (s, 3H, c), 3.27-3.31 (m, 4H, k), 3.48-3.53 (m, 4H, l), 4.99-5.01 (m, 2H, m), 5.07 (s, 1H, b), 5.37 (s, 1H, a), 6.76 (s, 1H, i), 7.30-7.24 (m, 3H, g,f,e), 7.42 (s, 1H, d). $^{13}\text{C NMR}$ (Bruker 75 MHz in DMSO) δ in ppm = 157.6, 149.0, 142.9, 139.7, 127.6, 124.0, 122.4, 121.6, 112.0, 60.5, 54.5, 50.2, 30.0, 21.4. FT-IR (KBr, selected bands) wavenumber in cm^{-1} : 3300, 3088, 2973, 1621, 1560, 1474, 1405, 1273, 1241, 1049, 894, 803, 770). Solubility: soluble in, dioxane, methanol, THF and benzene.

7. Experimental

7.4.11. Synthesis of *N*-(2-sodiumsulonatoethyl)-*N'*-(α,α -dimethyl-3'-isopropenylbenzyl) urea (**IMM15**)

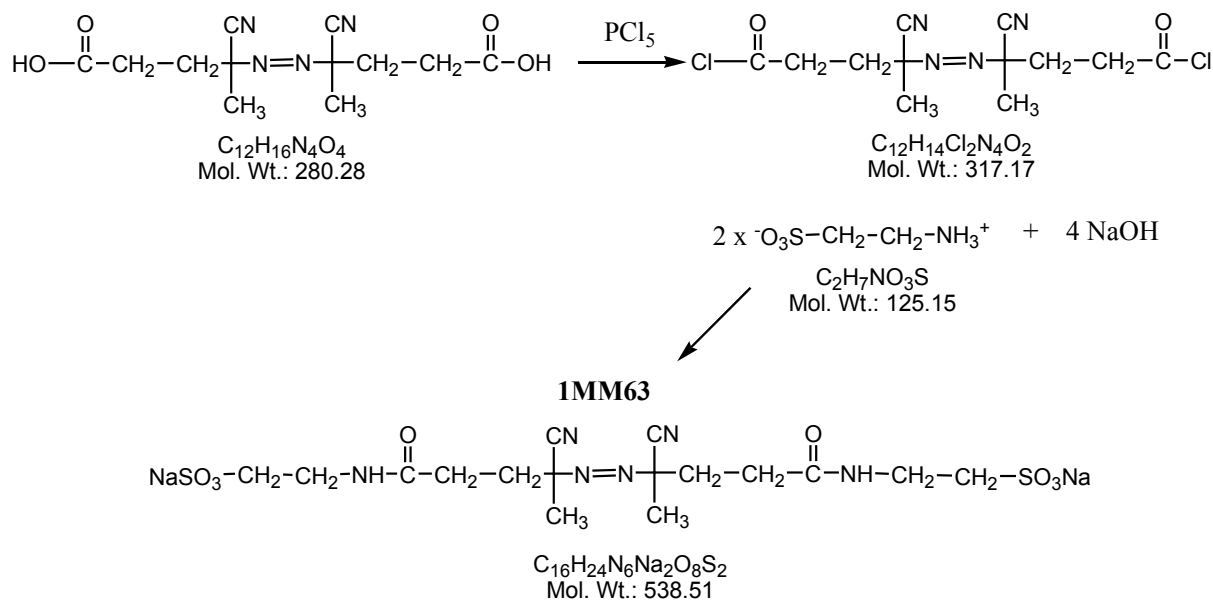


Reagents: 7.55 g (60.4 mmol) of taurine (99+%, Aldrich), 15.00 g (67.1 mmol) α,α -dimethyl-3-isopropenyl-benzyl-isocyanate (95+%, Aldrich), methanol (technical grade), 2.52 g (63.0 mmol), NaOH pellets (Aldrich).

Procedure: 7.55 g (60.4 mmol) of taurine and 2.52 g (63.0 mmol) of NaOH pellets were suspended in 30 ml of methanol and stirred over night. 15.00 g (67.1 mmol) of α,α -dimethyl-3-isopropenyl-benzyl-isocyanate were added to this suspension drop wise at ambient temperature through a dropping funnel (dropping speed was about 1 drop per second). The mixture was cooled with a water bath to remove the heat produced by the reaction. The reaction mixture became homogeneous when the addition was completed. The mixture was precipitated to diethylether. Note that precipitation does not take place immediately. The solution was kept at +4°C for 1 day to increase the yield. The white crystals formed were filtered off, and dried in vacuo. Yield is 14.7 g (~ 70 %). *N*-(2-sodiumsulonatoethyl)-*N'*-(α,α -dimethyl-3'-isopropenylbenzyl) urea (**IMM15**). Elemental analysis : ($C_{15}H_{21}N_2NaO_4S$, $M_r = 348.39 \text{ g}\cdot\text{mol}^{-1}$): Calc: C 51.71, H 6.08, N 8.04, S 9.20. Found: C 50.60, H 6.13, N 7.91, S 8.65. MS (ESI, negative ions) signal at 325.1 ($M-Na^+$). 1H -NMR (Bruker 300 MHz in D_2O ; labelling of H atoms is given in reaction scheme above): δ in ppm = 1.50 (s, 6H, h), 2.06 (s, 3H, c), 2.86 (t, 2H, k), 3.32 (t, 2H, i), 5.07 (s, 1H, a), 5.34 (s, 1H, b), 7.36-7.24 (m, 3H, g,f,e), 7.47 (s, 1H, d). ^{13}C NMR (Bruker 75 MHz in DMSO) δ in ppm = 159.2, 148.6, 144.4, 141.4, 129.0, 124.6, 123.9, 122.1, 112.7, 55.1, 51.2, 35.6, 29.8, 21.3. FT-IR (KBr, selected bands) wavenumber in cm^{-1} = 3455, 3353, 2975, 2937, 1638, 1573, 1202, 1163, 1046, 894, 802. Solubility: soluble in H_2O , dioxane, methanol and $CHCl_3$.

7. Experimental

7.4.12. Synthesis of **1MM63**



Reagents: 4,4'-azobis(4-cyanopentanoic acid) (98+% Fluka), phosphorous pentachloride (99+ % Riedel-deHaën), benzene (99.7 +% Merck), taurine (Aldrich 99%), NaOH pellets (Merck) pentane (99 +% Acros), diethylether (technical grade), dichloromethane (technical grade).

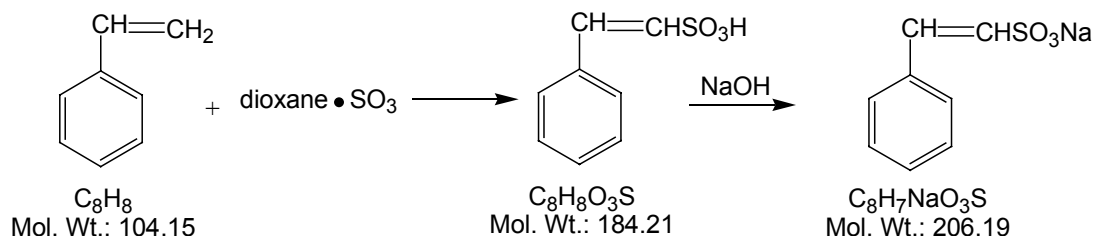
Procedure: In analogy to Smith [9], 1.05 g (3.758 mmol) of 4,4'-azobis (4- cyanopentanoic acid) were dissolved in 20 ml of benzene. 2.05 g (9.5 mmol) of phosphorouspentachloride were added to this solution while cooling with an ice bath. The cooling bath was removed, the mixture was stirred at ambient temperature for 2 h, and benzene was evaporated at 30 °C. The remaining viscous liquid was washed thrice with a mixture of diethylether and pentane (1:3). The remaining solid was dissolved in dichloromethane, and re-precipitated in pentane. A white precipitate (AIBNCOCl) was filtered off and dried in vacuo at ambient temperature.

0.205 g (3.66 mmol) of taurin were dissolved in 3.7 ml of 1 M (aq) NaOH, and then diluted with distilled water to 10 ml. 0.2791 g (0.86 mmol) of initiator (AIBNCOCl) was dissolved in 10 ml of dichloromethane. The two solutions were combined and the two-phase system mixed for 10 h at ambient temperature. Aqueous layer was separated, and the pH of solution was arranged to 6 by addition of HCl. The solution was lyophilized. The final product was a mixture of NaCl, taurin and targeted compound **1MM63** (see for ¹H-

7. Experimental

NMR spectrum Appendix 2 Figure 2A.16). Note: Taurine was used excess to neutralize HCl produced from the acylchloride. Excess taurine may be replaced with same amount of NaOH, so that a taurine free compound could be obtained.

7.4.13. Synthesis of sodium β -styrene sulfonate

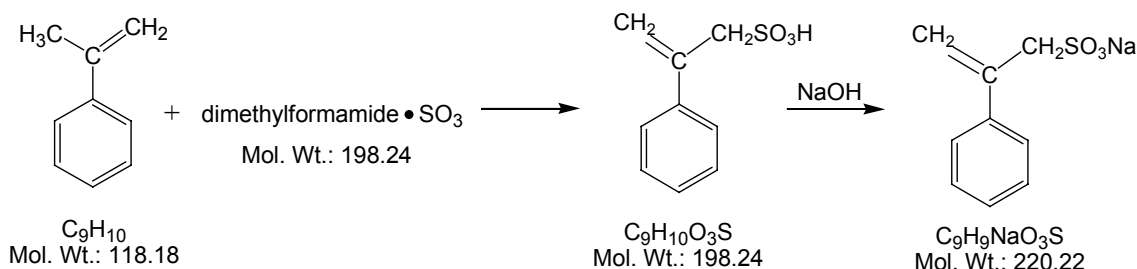


Reagents: Dioxane (dried over Na metal and distilled), 1,2-dichloroethane (99.8 +%, Acros), 1.8 g (17.2 mmol) of styrene (99+%, Aldrich), fuming sulfuric acid (SO_3 20% Riedel-deHaën)

Procedure: Adapted from a procedure in Organic Synthesis [10]. 1.4 g (17.5 mmol) of sulfur trioxide were distilled from fuming sulfuric acid in a flask containing 10 ml of dichloroethane. 1.4 g (17.5 mmol) of dioxane was dissolved in 10 ml of dichloroethane. Dioxane containing solution was added over the sulfur trioxide solution slowly through a dropping funnel while cooling the solution of sulfur trioxide with a dry ice/ethanol bath. The dry ice/ethanol cooling bath was then replaced by an ice bath. 1.8 g (17.2 mmol) of styrene were dissolved in 20 ml of dichloroethane, and this solution was added through a dropping funnel to the solution containing sulfur trioxide-dioxane complex. The suspension of colorless solid changed to a milky tan solution. The ice bath was removed, and solution was heated to reflux for 2 h. Then, the solution was extracted with 17.1 ml of 1M (aq) NaOH to neutralize to organic phase. The aqueous and organic phases were separated. The aqueous phase was extracted thrice with diethylether. The water was evaporated. The monomer is further purified by dissolving in water, and evaporating till the solution becomes milky, and then reprecipitating by cooling. The white precipitate was filtered off and dried in vacuo over phosphorous pentoxide. First crop gave 2.1 g (yield; 62%) of white powder of β -styrene sulfonate (see Appendix 2 Figure 2A.15 for 1H -NMR spectrum). 1H -NMR (Bruker 300 MHz in D_2O) δ in ppm = 6.73 (d, 1H, Ph-CH=C), 7.06 (d, 1H, =CHSO $_3$ Na), 7.16-7.18 (m, 3H, phenyl (meta and para)), 7.27-7.30 (m, 2H, phenyl (ortho)).

7. Experimental

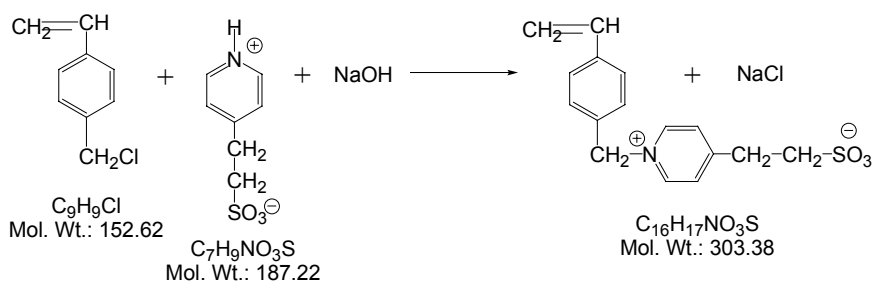
7.4.14. Synthesis of sodium 2-phenyl-prop-2-en sulfonate



Reagents: Sulfurtrioxide dimethylformamide complex (97+%, Fluka), 1,2-dichloroethane (99.8 +%, Acros), α -methylstyrene (99+%, Aldrich).

Procedure: (Adapted from German patent [11]) 15.4 g (0.1 mol) of sulfurtrioxide dimethylformamide complex were suspended in 50 ml of dichloroethane. 12.07 (0.103 mol) of α -methylstyrene were added to the suspension through a dropping funnel while cooling the reaction flask with an ice-bath. This solution was stirred for 8 h at ambient temperature. Then, it was extracted with 100 ml of 1M (aq) NaOH. The aqueous phase was separated and extracted thrice with diethylether. Most of the water was evaporated, and the remaining solution was precipitated in acetone. The precipitate was filtered off, and dried in vacuo. Yield 11.23g (51 %) of white powder of 2-phenyl-prop-2-en sulfonate sodium salt. $^1\text{H-NMR}$ (Bruker 300 MHz in D_2O): 4.08 (s, 2H, $\text{CH}_2\text{SO}_3\text{Na}$), 5.39 (s, 1H, $=\text{CH}_{\text{cis}}\text{H}_{\text{trans}}$), 5.61 (s, 1H, $=\text{CH}_{\text{trans}}\text{H}_{\text{cis}}$), 7.28-7.40 (m, 3H, phenyl (meta and para)), 7.49-7.51 (m, 2H, phenyl (ortho)).

7.4.15. 4-(2-sulfoethyl)-1-(4-vinyl-benzyl) pyridinium betain (M17)



Reagents: 18.72 g (0.1 mole) of 2-(4-pyridine) ethanesulfonic acid (Raschig AG, Ludwigshafen, Germany), 4.0 g (0.1 mole) of NaOH (Merck), formamide (+99 %, Fluka), 15.26 g (0.1 mole) of 4-vinylbenzylchloride (+90 %, Acros), acetone (technical grade).

7. Experimental

Procedure: This compound was a kind gift of M. Vantsian and Dr. J. Storsberg who developed this compound. The synthesis was added to this thesis, as the procedure has not been described in literature yet. 18.72 g (0.1 mole) of 2-(4-pyridine) ethansulfonic acid and 4.0 g (0.1 mole) of NaOH were dissolved in 120 ml of HCONH₂ at ambient temperature. A drop of nitrobenzene and 15.26 g (0.1 mole) of 4-vinylbenzylchloride were added slowly under nitrogen atmosphere, and stirred for 65 h at ambient temperature. The cooled solution was precipitated into acetone, filtered, and the filtrate dried *in vacuo*, to give 29.8 of crude compound containing NaCl. Crystallization from dry ethanol provided the salt free monomer. Elemental analysis (C₁₆H₁₇NO₃S M_r=303.38) Calc: C, 63.34; H, 5.65; N, 4.62; S, 10.57. Found: C, 62.70; H, 5.55; N, 4.71; S, 9.98. MS (FAB, matrix MNBA, negative ions) signal at 301.9 [M-1]⁻. ¹H-NMR (Bruker 300 MHz in D₂O, δ in ppm): 3.18-3.27 (m, 4H, -CH₂-CH₂-SO₃), 5.23 (d, 1H, CH_(cis)H_(trans)=CH-), 5.61 (s, 2H, -CH₂-N⁺), 5.74 (d, 1H, CH_(cis)H_(trans)=CH-), 6.63 (m, 1H, =CH-), 7.30 and 7.40 (d+d, 2H+2H, CH phenylene), 7.84 (d, 2H, CH(3) pyrid) 8.65 (d, 2H, CH(2) pyrid). ¹³C NMR (Bruker 75 MHz in D₂O, δ in ppm) 161.3 (C pyrid), 144.1 (-CH=N⁺), 139.4 (C4 phenylene), 136.3 (=CH), 132.9 (C1 phenylene), 129.9 (C3 phenylene), 128.9 (-=CH-C=N⁺), 127.7 (C2 phenylene), 116.4 (CH₂=), 64.2 (-CH₂-N⁺), 50.2 (-CH₂-SO₃), 31.0 (-CH₂-C-SO₃). FT-IR (KBr, selected bands in cm⁻¹): 3506, 3357, 1683, 1639, 1197, 1054, 692, 617.

References :

- [1] Gottlieb HE, Kotlyar V, Nudelman A. *J. Org. Chem.* **1997**, *62*, 7512.
- [2] Vasilieva YA, Thomas DB, Scales CW, McCormick CL. *Macromolecules* **2004**, *37*, 2728.
- [3] Broos R, Tavernier D, Anteunis M. *J. Chem. Educ.* **1978**, *55*, 813.
- [4] Baussard JF, Habib-Jiwan JL, Laschewsky A, Mertoglu M, Storsberg J. *Polymer* **2004**, *45*, 3615.
- [5] Baussard, J.F; PhD. Thesis, University of Catholique de Louvain (Belgium) **2004**.
- [6] Thang SH, Chong YK, Mayadune RTA, Moad G, Rizzardo E. *Tetrahedron Lett.* **1999**, *40*, 2435.
- [7] Mitsukami Y, Donovan MS, Lowe AB, McCormick CL. *Macromolecules* **2004**, *34*, 2248.

7. Experimental

[8] Le TPT, Moad G, Rizzardo E, Thang S. *Intern. Pat. Appl.* 1998; PCT WO9801478 [CA 1998: 115390].

[9] Smith DA. *Makromol. Chem.* **1967**, *103*, 301.

[10] Rondestvedt CS, Bordwell FG. *Organic Synthesis*, Rabjohn, N. (Editor in Chief), 1967, *collective volume 4*, John Wiley & Sons Inc., New York, 831.

[11] Halcour K, Wagner R. Patent DE 3233762, 1984, [CAN 100:191569 AN 1984: 191569 CAPLUS].

8. GENERAL CONCLUSIONS

The unsuccessful attempts showed that many common synthetic routes, which are efficient for the synthesis of organic soluble RAFT agents, are not convenient for the synthesis of water-soluble RAFT agents. But new water-soluble chain transfer agents, (**CTA2**, **CTA3**, **CTA4** and **CTA6** see Appendix 1 for the structures) for the aqueous RAFT polymerization bearing dithioester and trithiocarbonate moieties could be synthesized via the reaction of dithiocarboxylates or trithiocarbonate salts with proper alkyl halides. The new RAFT agents bear permanent anionic sulfonate moieties, so that they can be used at low pH values when necessary. These are the pH conditions where dithioester groups are most resistant to hydrolysis or which are needed in the polymerization of many acryl amides. These new RAFT agents increased the choice of water-soluble **CTAs** for controlled radical polymerization of different monomers via RAFT method in aqueous solution.

The new RAFT agents are long-term stable in the pH range between 1 and 8 up to 40°C, and show improved resistance to thermal hydrolysis compared to 4-cyano-4-thiobenzoylsulfanylpentanoic acid **CTA1**, which is hitherto the mostly employed RAFT agent for aqueous polymerization systems. The comparative stability tests done with the water-soluble RAFT agent suggest that the stability against hydrolysis of the dithioester moiety is improved by the presence of hydrophobic groups in the close vicinity. However this is not the only parameter affecting the stability in water. The stability tests, which were followed with ¹H-NMR spectroscopy, revealed that the hydrolysis of RAFT agents takes place in several ways. The hydrolysis can happen by the attack of water on thiocarbonyl moiety and/or the alpha carbons of the dithioesters. But, somewhat surprising was the incomplete hydrolysis converting the dithiocarbonyl –C(=S)S– to the thiocarbonyl –C(=O)S– without the cleavage of the thioester at elevated temperatures.

In order to apply the RAFT polymerization in aqueous media successfully, and to maintain good control over polymerization, hydrolysis of the active chain ends must be suppressed. The risk of hydrolysis can be minimized by working at pH below 8 and temperatures below 60°C. If there is a risk of aminolysis because of the unavoidable presence of amines, such as on the polymerization of acrylamides, the pH of

8. General conclusions

polymerization medium shall be kept low (preferentially pH <5) to prevent aminolysis of the active chain ends by protonating the amines.

The various aqueous RAFT polymerizations performed present the typical features of controlled polymerization, such as pseudo first-order kinetics up to high conversions, a linear increase of the number average molar mass with conversion, good agreement between theoretically expected and experimentally determined M_n values, low polydispersities, and efficient synthesis of block copolymers. Importantly, only analysis by several methods provided reliable molar mass data. End group analysis via the dithioester moiety works reasonably well. Moreover, when polymers are synthesized by using **CTA3**, they are labeled by a fluorophore at the initiating end ("R"-group), and both end groups can be quantified independently with simple UV-vis spectroscopic measurements. This allows quantifying the content of activable "dormant" end groups. In water, polymerization of the monomers bearing polymerizable acrylic methacrylic and styrenic moieties yields well-defined polymers at 48°C and 55°C. But the rates of polymerization for methacrylamides were found to be rather slow below 60°C for aqueous RAFT polymerization. Since longer polymerization times are necessary to achieve high conversions, some termination reactions interfere with the polymerization of them. As a result, the control over methacrylamides is low compared to methacrylates, acrylics and styrenics at 55°C or at lower temperatures in water.

Aqueous RAFT process is not only a powerful method to prepare well defined homopolymers, but also to synthesize functional block copolymers with complex structure, i.e. amphiphilic and/or stimuli-sensitive polymers. Several stimuli-responsive polymers were synthesized via RAFT in water. Preliminary studies on the switching of the hydrophilic character of single or of several blocks of these polymers by changing the pH, the temperature or the salt content, demonstrated the variability of the molecular designs suited for stimuli-sensitive polymeric amphiphiles. Furthermore, the structures gave a first idea of the wealth of aggregated structures which can be obtained. In particular, the usefulness of added salt as alternative stimulus was demonstrated for polyzwitterionic blocks, and the opportunities of multiple-sensitive systems were exemplified.

The copolymers bearing polyethyleneglycol based blocks are the focus of great interest, as polyethyleneglycol is known to be biocompatible. Therefore, such copolymers

8. General conclusions

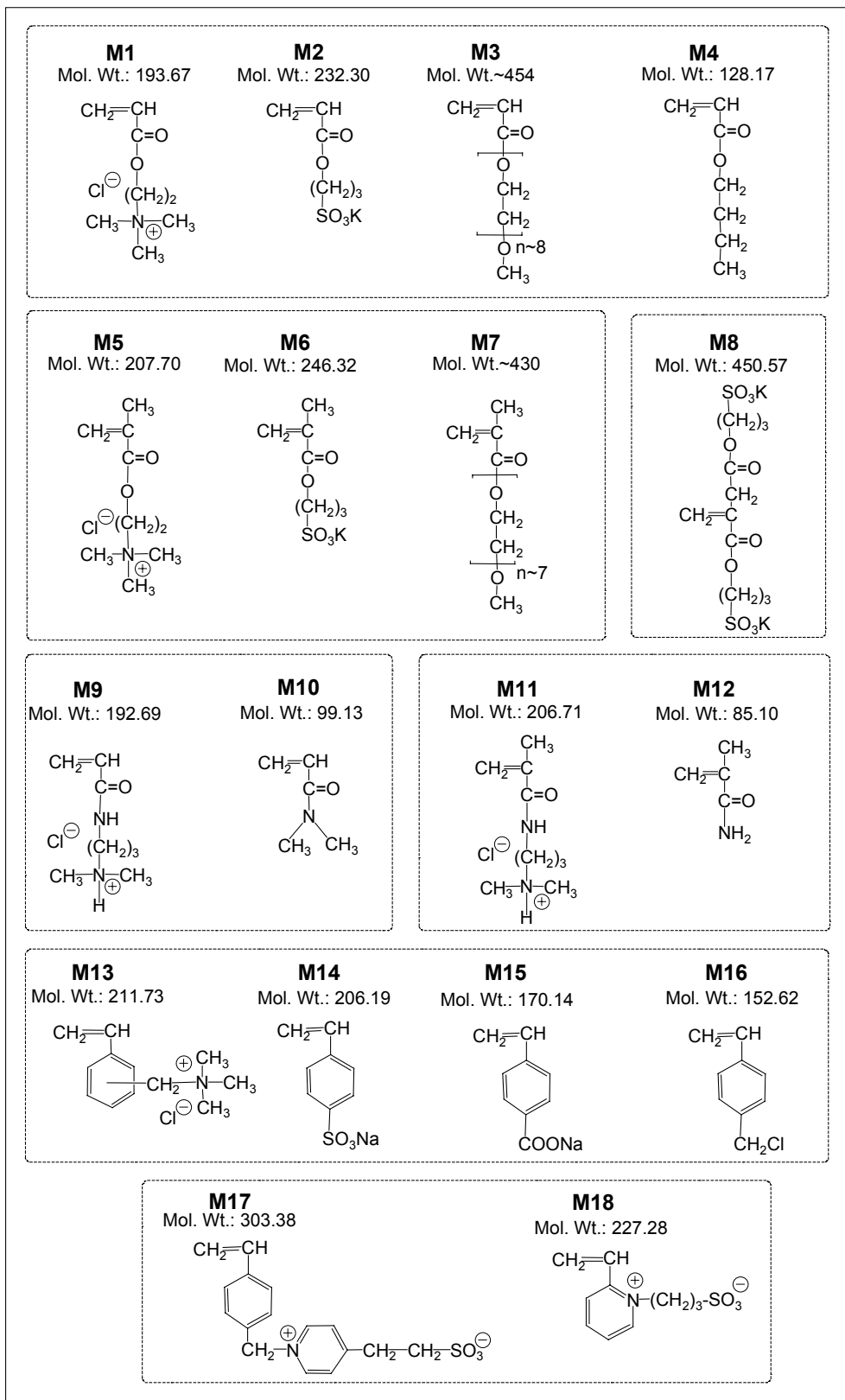
have a great potential to find application in the fields of pharmaceuticals, medical care or biotechnology. (Meth)acrylate based macro monomers bearing polyethyleneglycol side chains were managed to be polymerized via RAFT with good control in water. They can also be used as macro CTAs to prepare block copolymers. One of the copolymers made which bears a second cationic acrylate block, was used to prepare nano-sized particles by complexation with decanoate and perfluorodecanoate in water. The particles prepared with sodium perfluorodecanoate were found to be stable upon dilution. These particles have a polyethyleneglycol based corona, and a perfluorinated hydrophobic core which may be used for the delivery of poorly water-soluble compounds. It was found that these particles do not denature Human Serum Albumin. That is to say that these particles may have chance to be developed further aiming at in vivo uses.

The (co)polymers prepared via the RAFT technique are α,ω -functionalized. One of the chain ends is an initiating radical fragment, and the other end is a thiocarbonylthio group. Thiocarbonylthio end group can be easily converted to thiol group. Such thiol end groups can be readily anchored to surfaces of noble metals like gold, to obtain surface of modified metals or polymer stabilized nano particles of metals. These types of surface modified metals have great potential to find application in various fields e.g. of stimuli mediated transport, catalysis, or electronics.

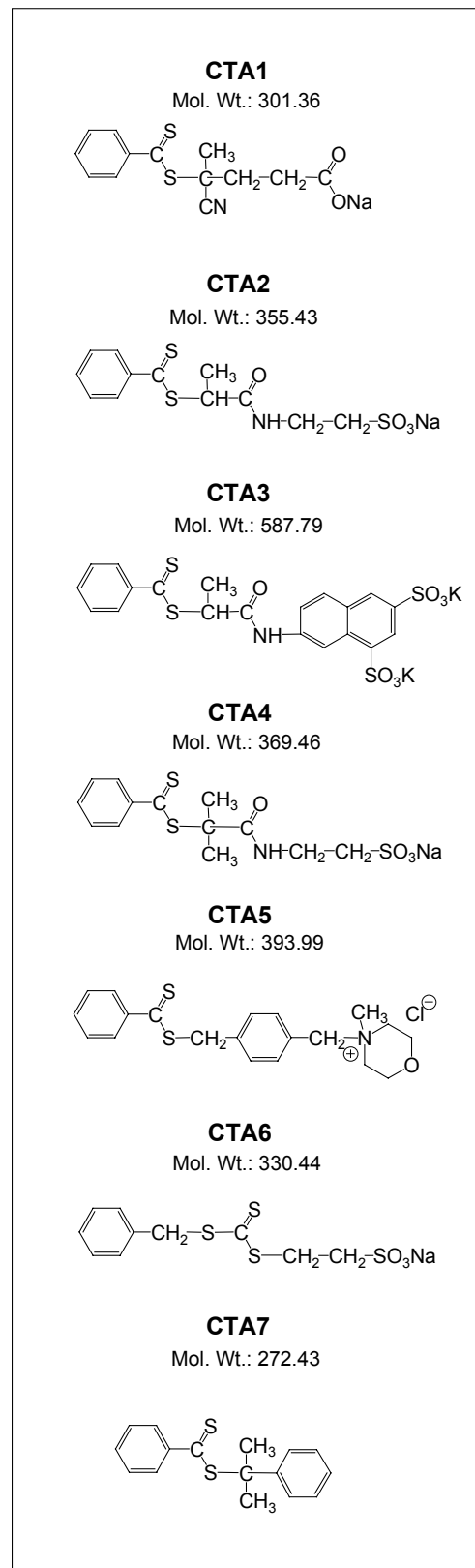
In conclusion, the controlled radical polymerization in aqueous media via RAFT is possible for wide variety of hydrophilic monomers, and the method enables the synthesis of homo- and block (co)polymers in a controlled way to for different purposes.

Appendix 1: The structures of monomers, RAFT agents and initiators used in this study

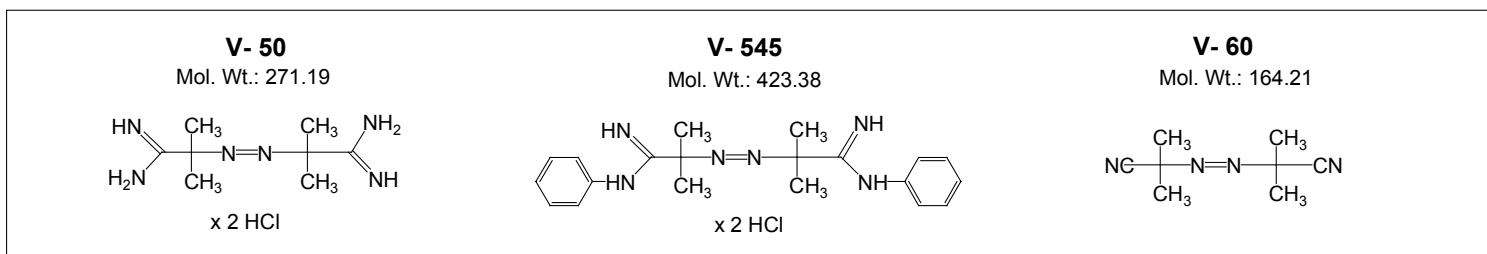
Monomers

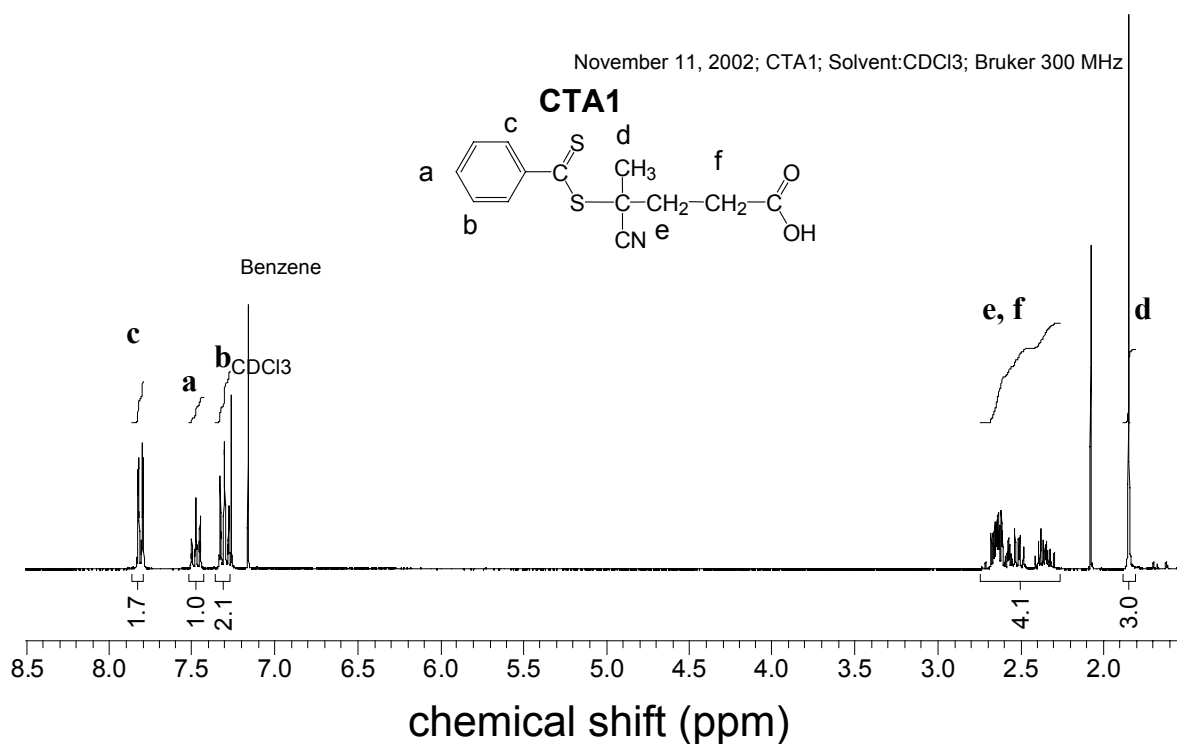
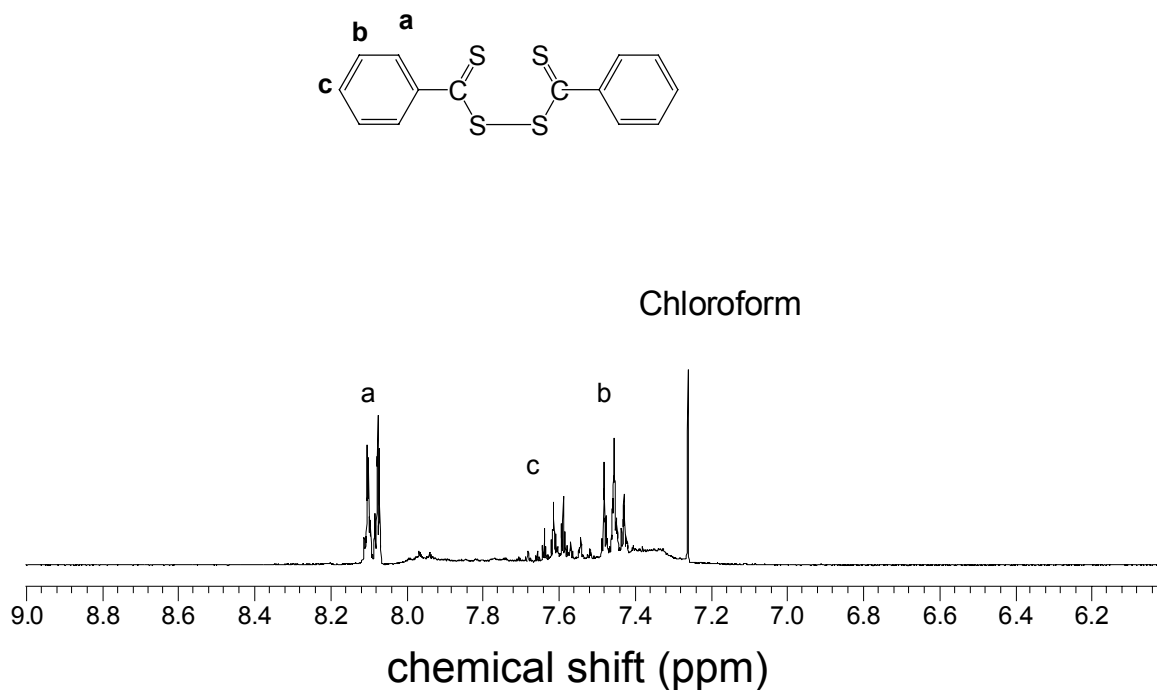


RAFT agents



Initiators



APPENDIX 2: ¹H-NMR FiguresFigure A2.1. ¹H-NMR of CTA1 in CDCl₃August 14, 2003; Solvent: CDCl₃; Bruker 300 MHzFigure A2.2. ¹H-NMR of di(thiobenzoyl) disulfide in CDCl₃

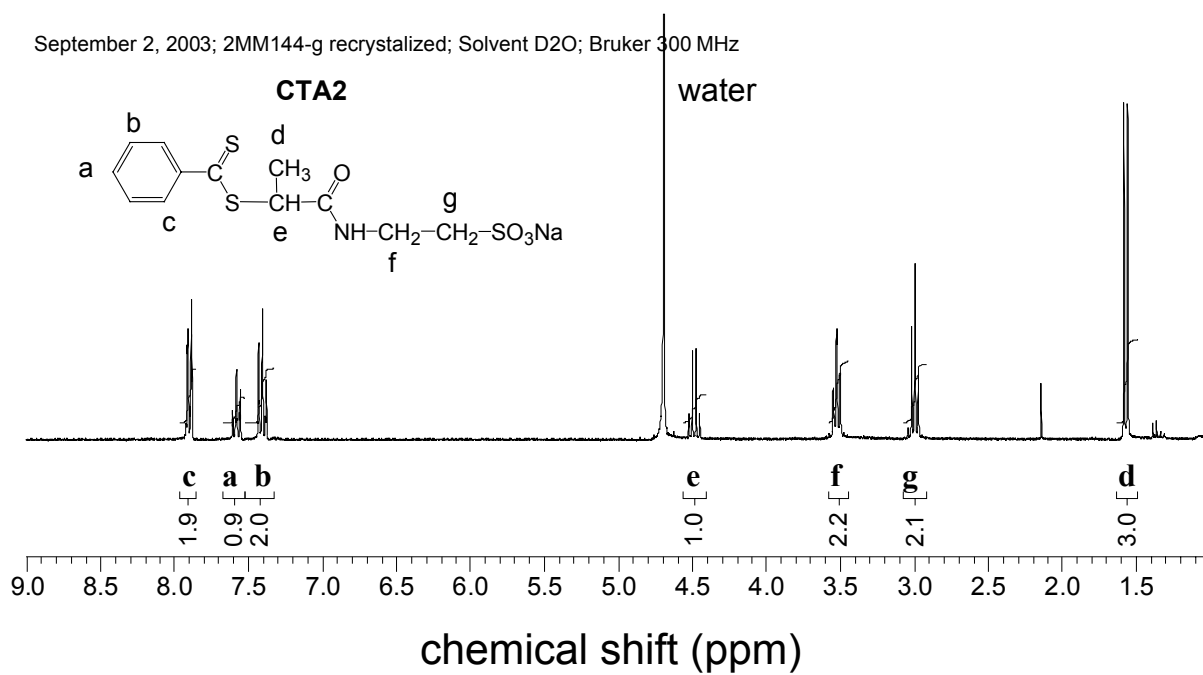


Figure A2.3. $^1\text{H-NMR}$ of CTA3 in D_2O .

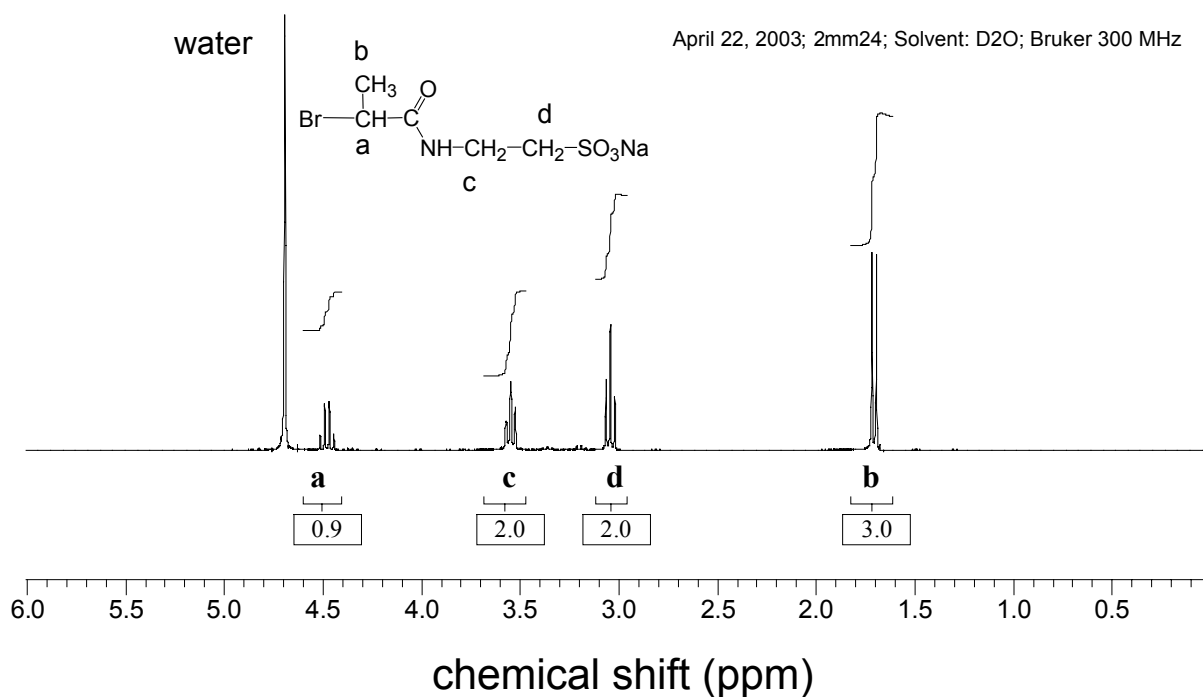
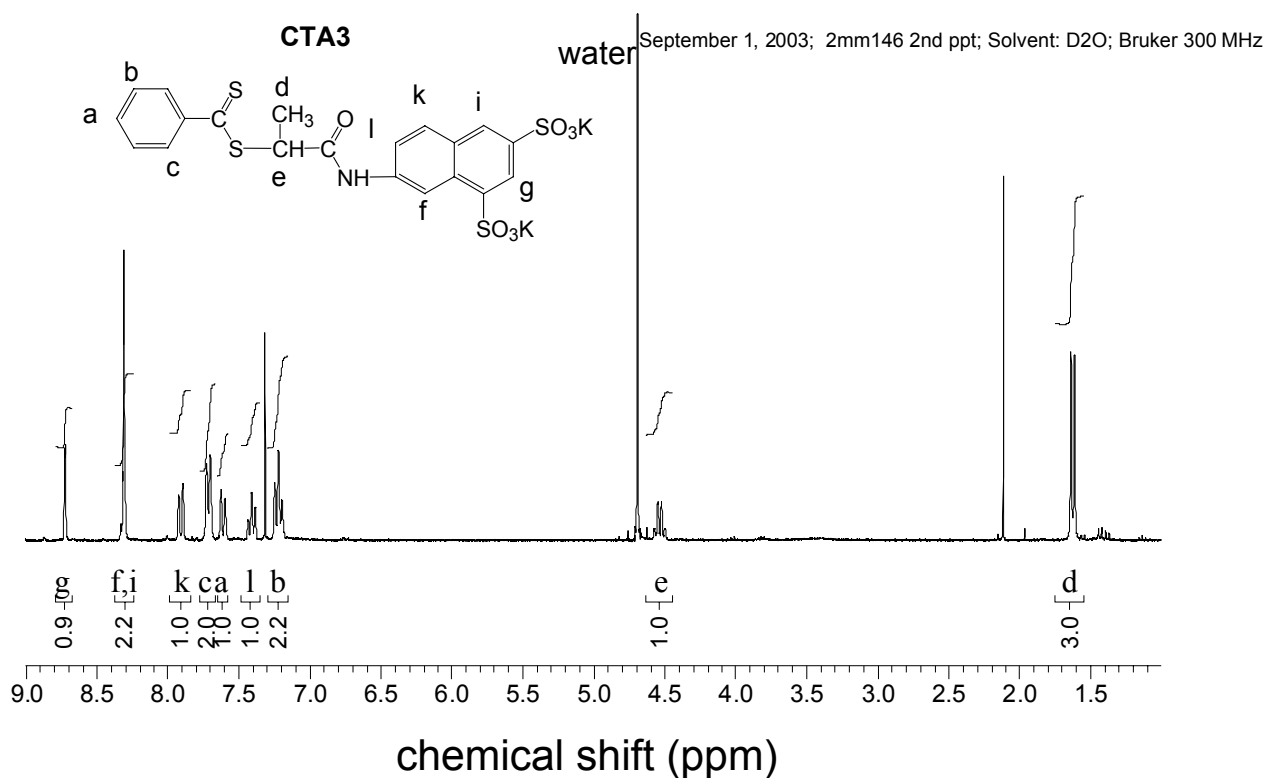
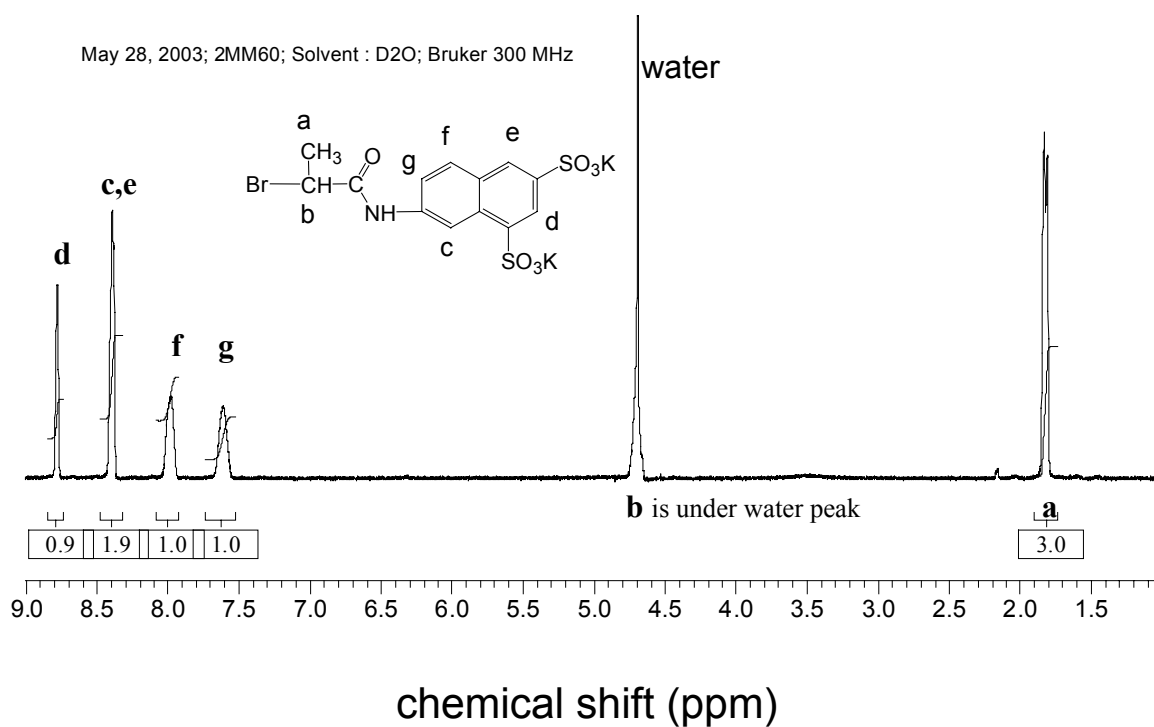


Figure A2.4. $^1\text{H-NMR}$ of sodium 2-(2-bromo propionylamino) ethanesulfonate in D_2O .

Figure A2.5. ¹H-NMR of CTA3 in D₂O.Figure A2.6. ¹H-NMR of 2-(2-bromo-propionylamino)-naphthalene-6,8-disulfonic acid dipotassium salt in D₂O.

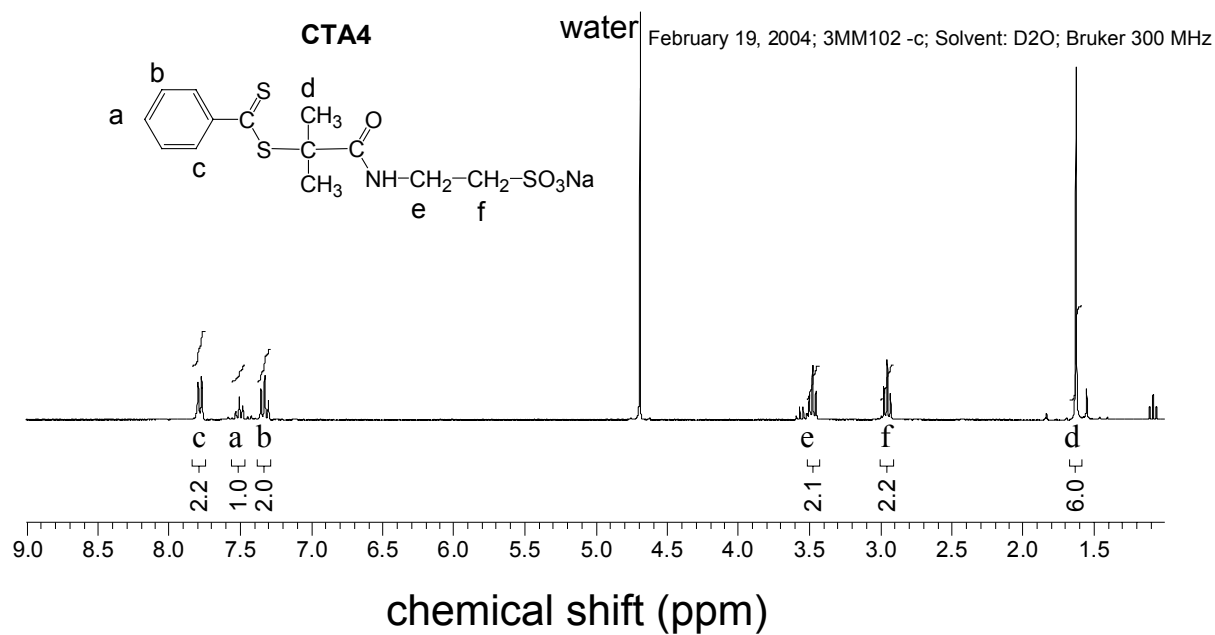


Figure A2.7. $^1\text{H-NMR}$ of CTA4 in D_2O .

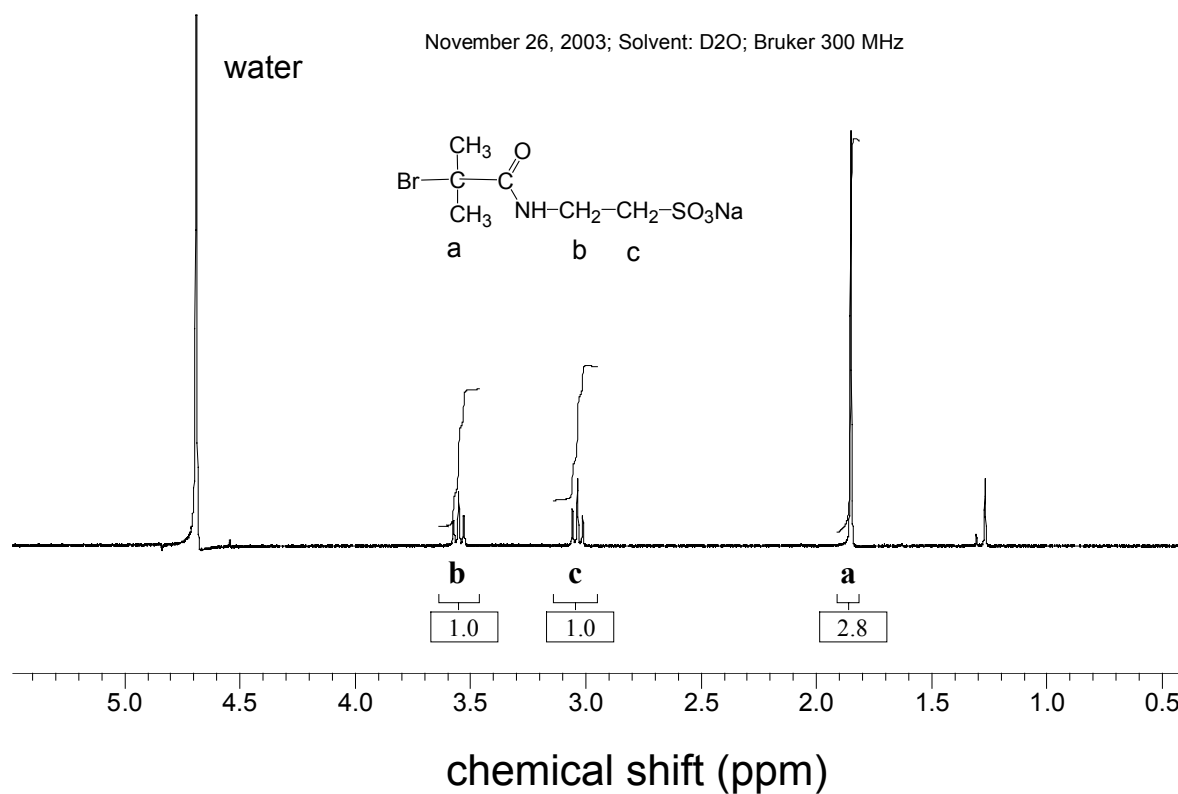


Figure A2.8. $^1\text{H-NMR}$ of sodium 2-(2-bromo 2-methyl propionylamino) ethanesulfonate in D_2O

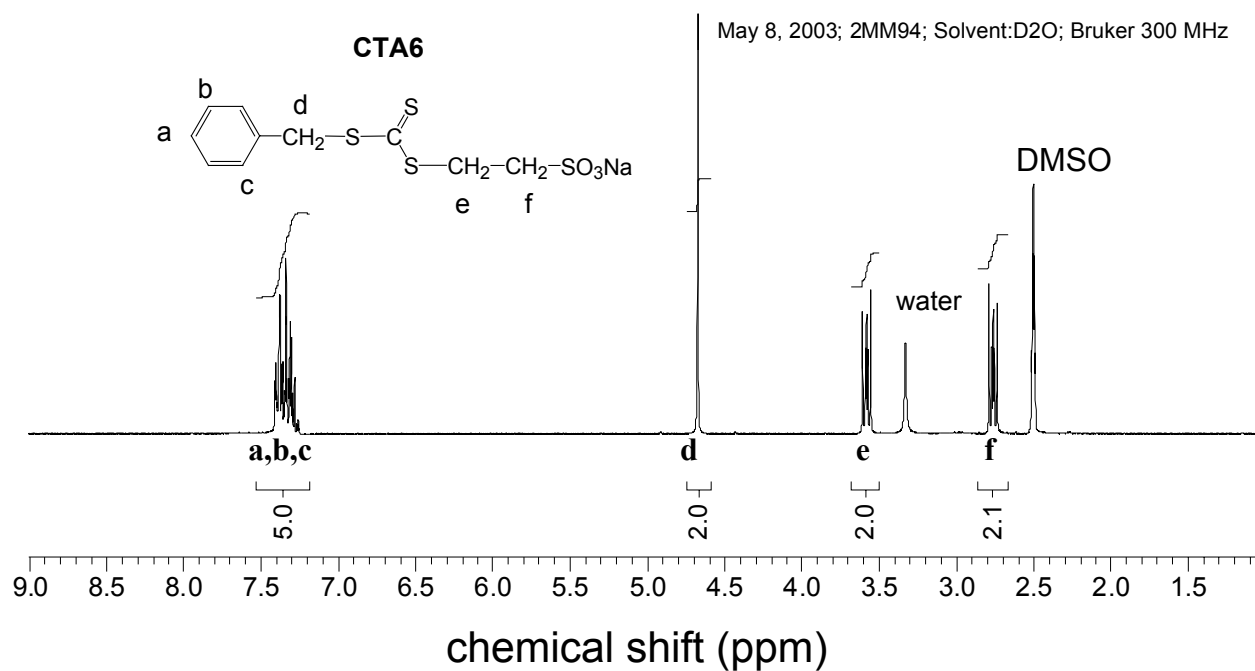


Figure A2.9. $^1\text{H-NMR}$ of CTA6 in DMSO.

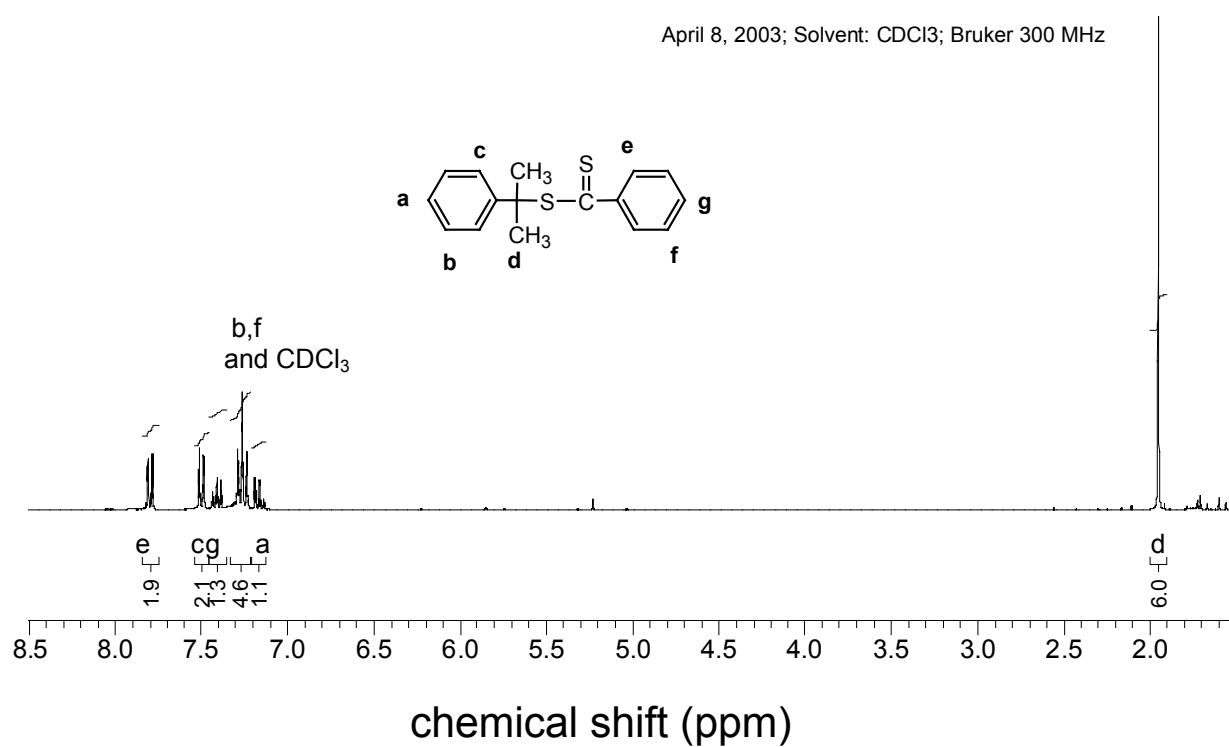
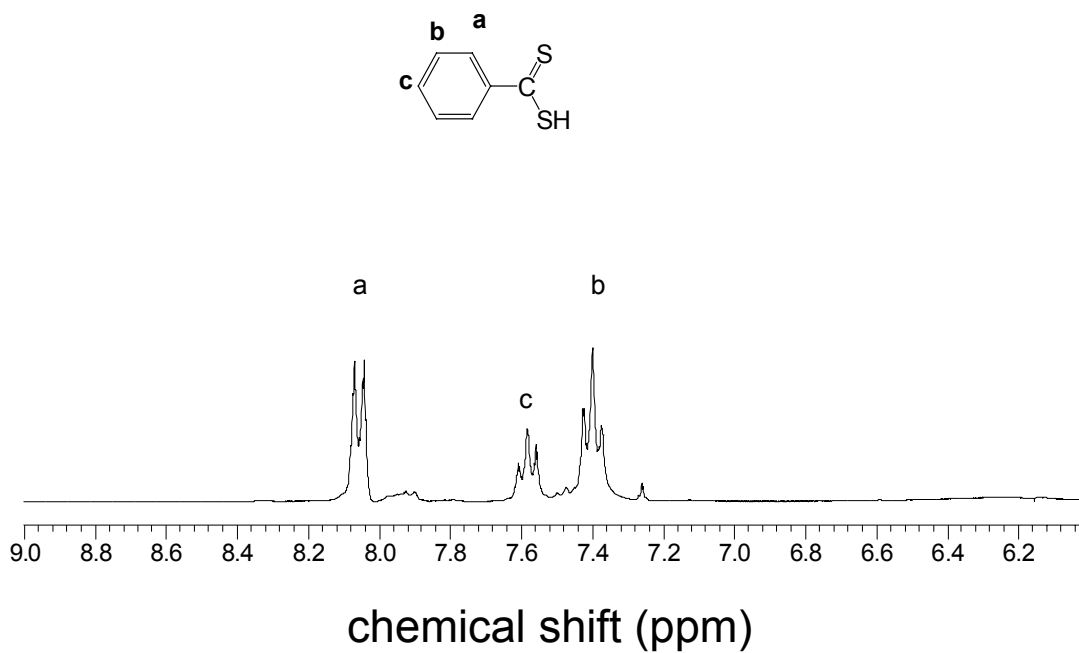
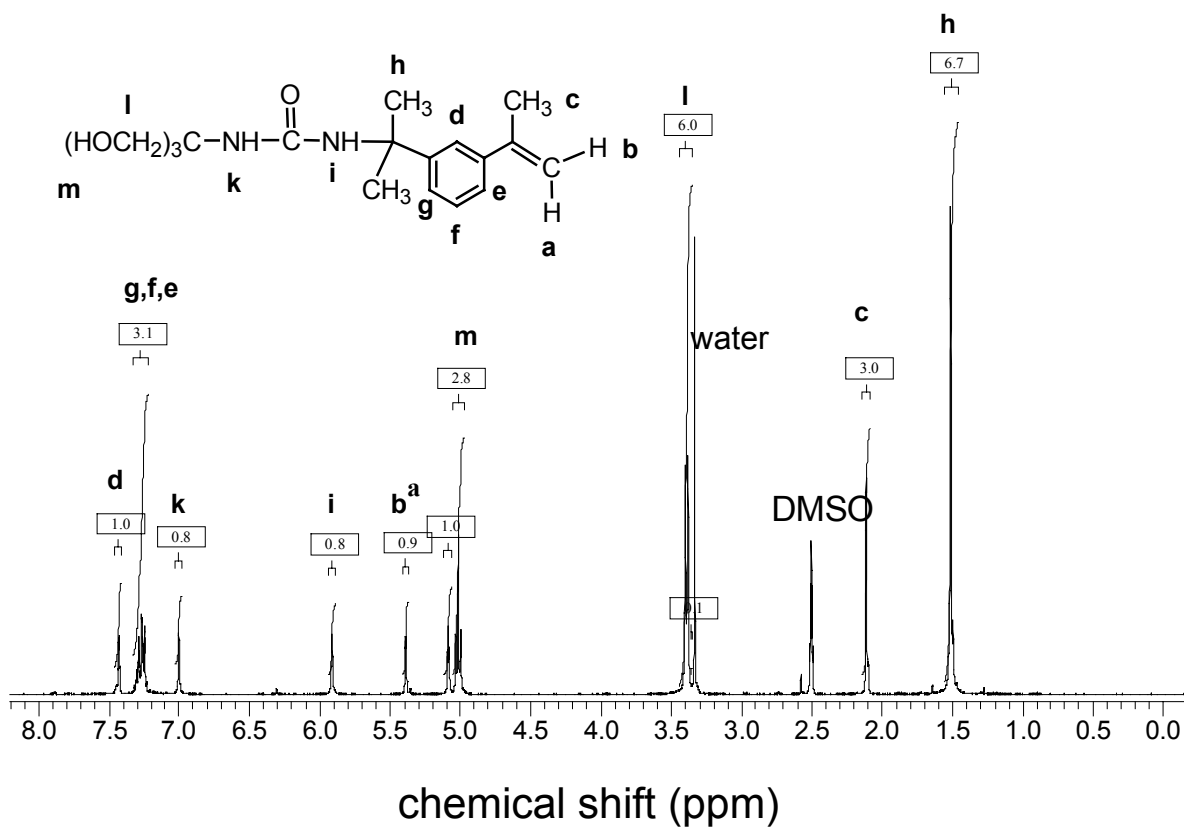


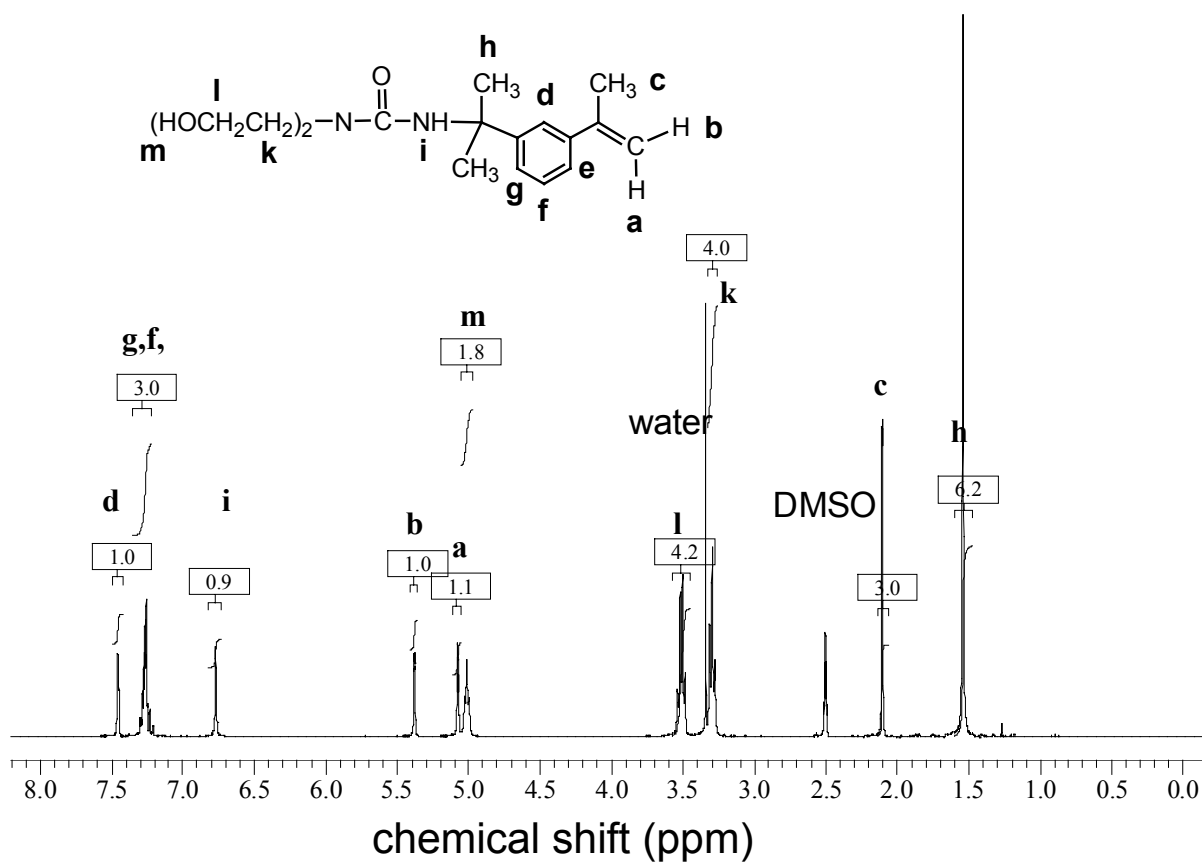
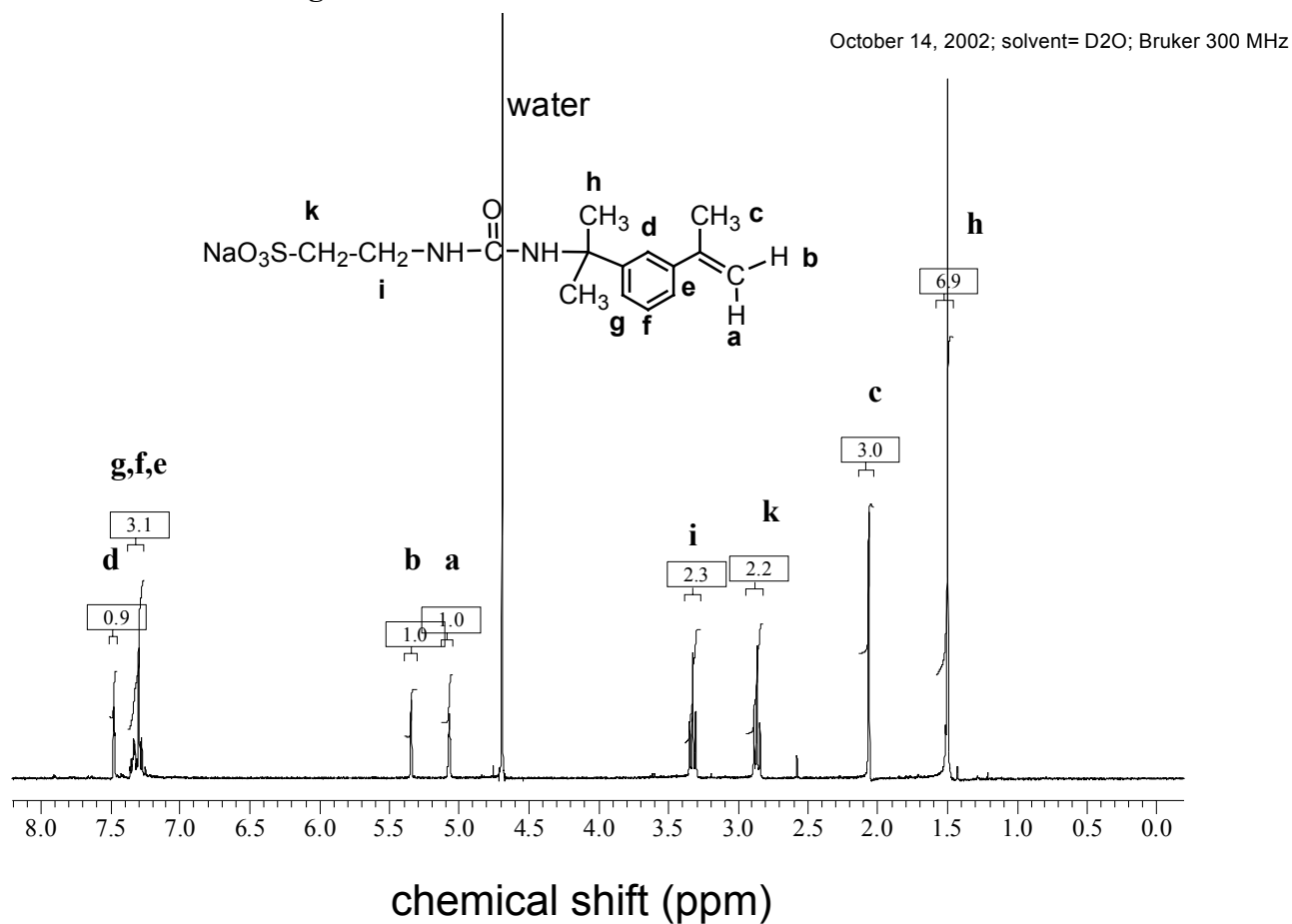
Figure A2.10. $^1\text{H-NMR}$ of CTA7 in CDCl_3 .

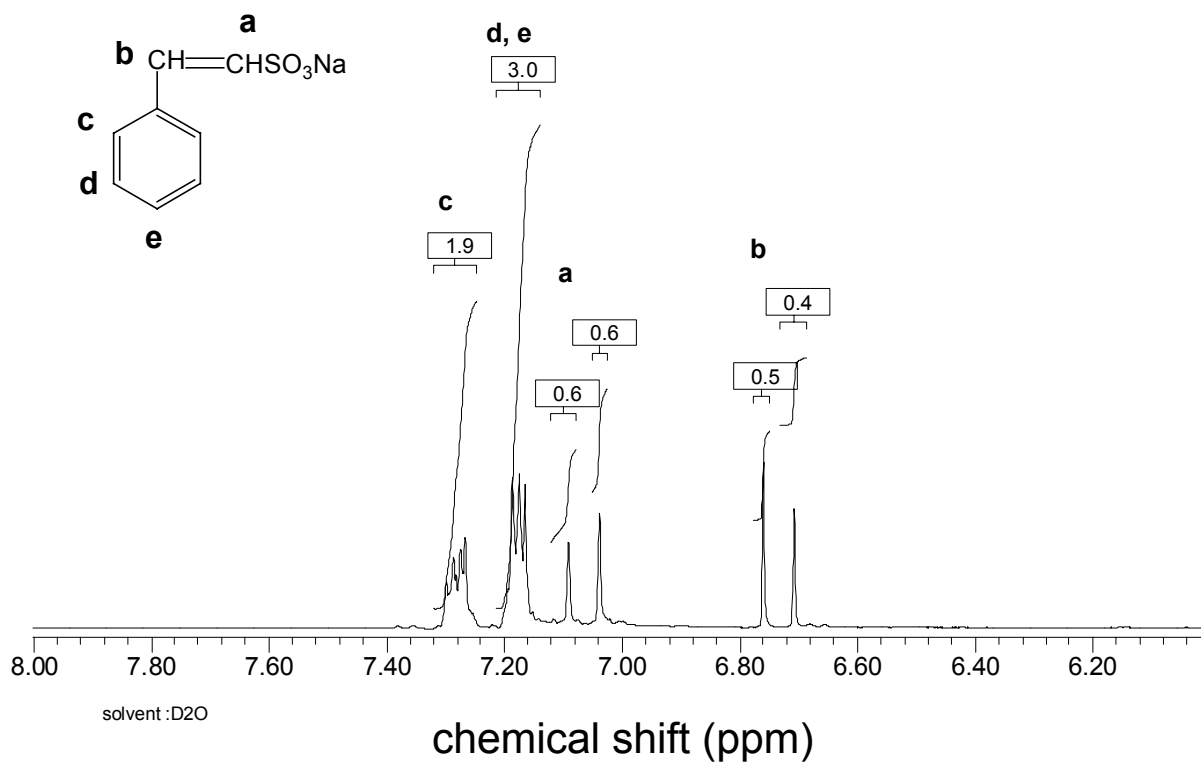
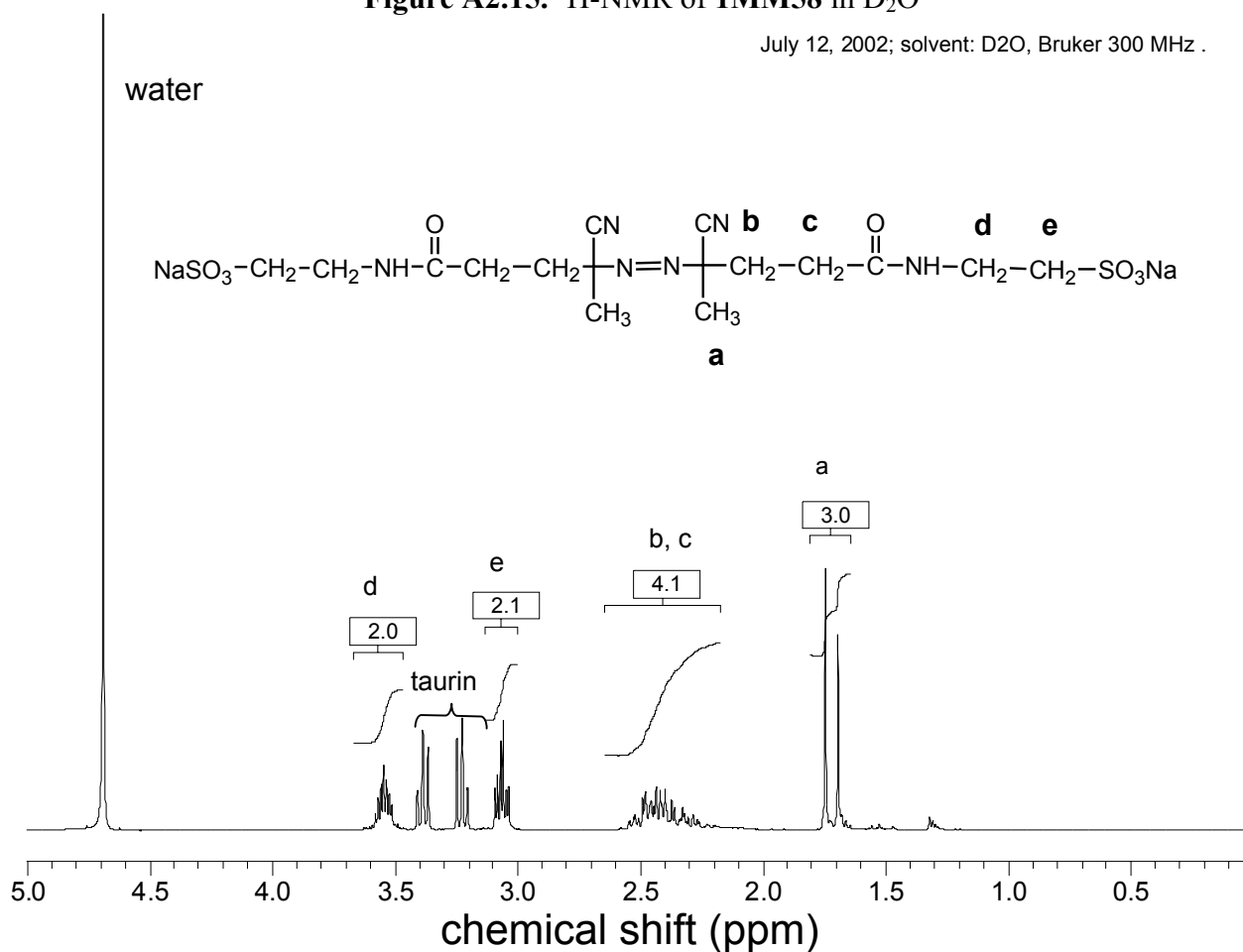
March 4, 2002; Solvent: CDCl₃; Bruker 300 MHzFigure A2.11. ¹H-NMR of dithiobenzoic acid in CDCl₃

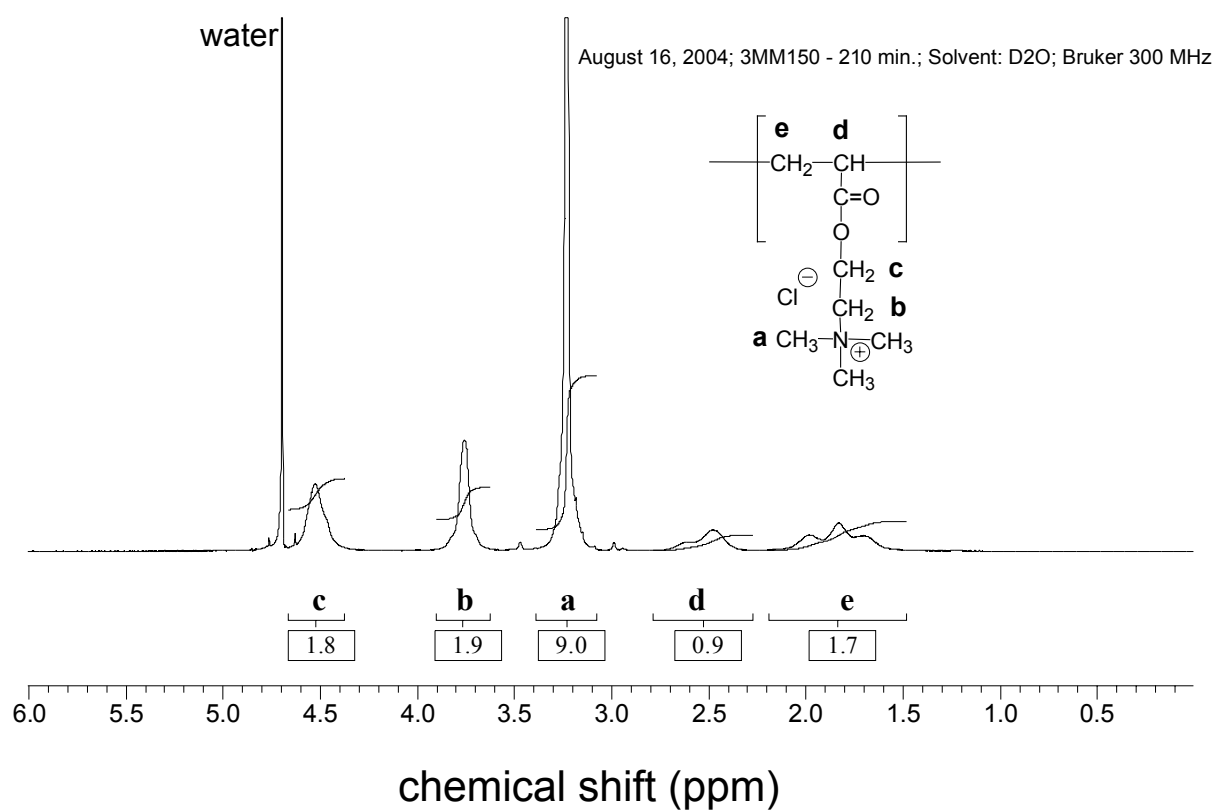
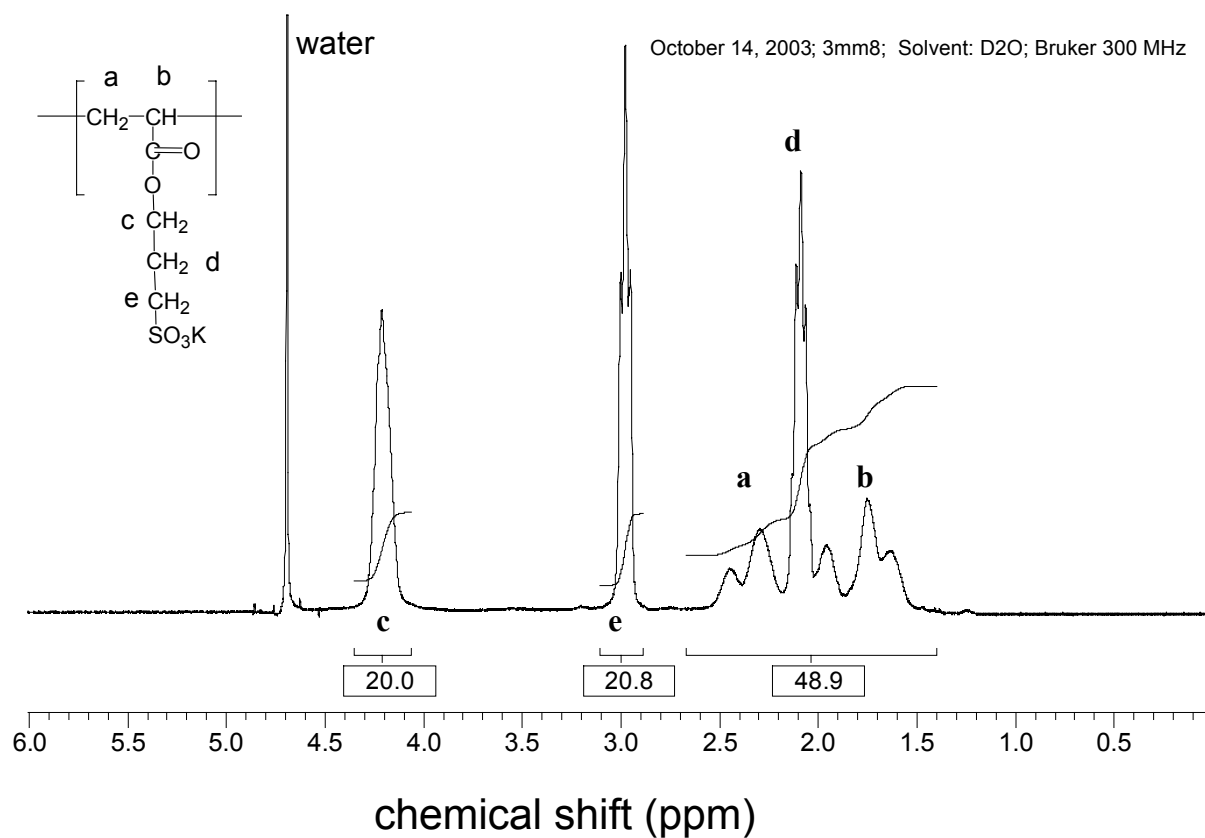
May 6, 2004; solvent = DMSO; Bruker 300 MHz

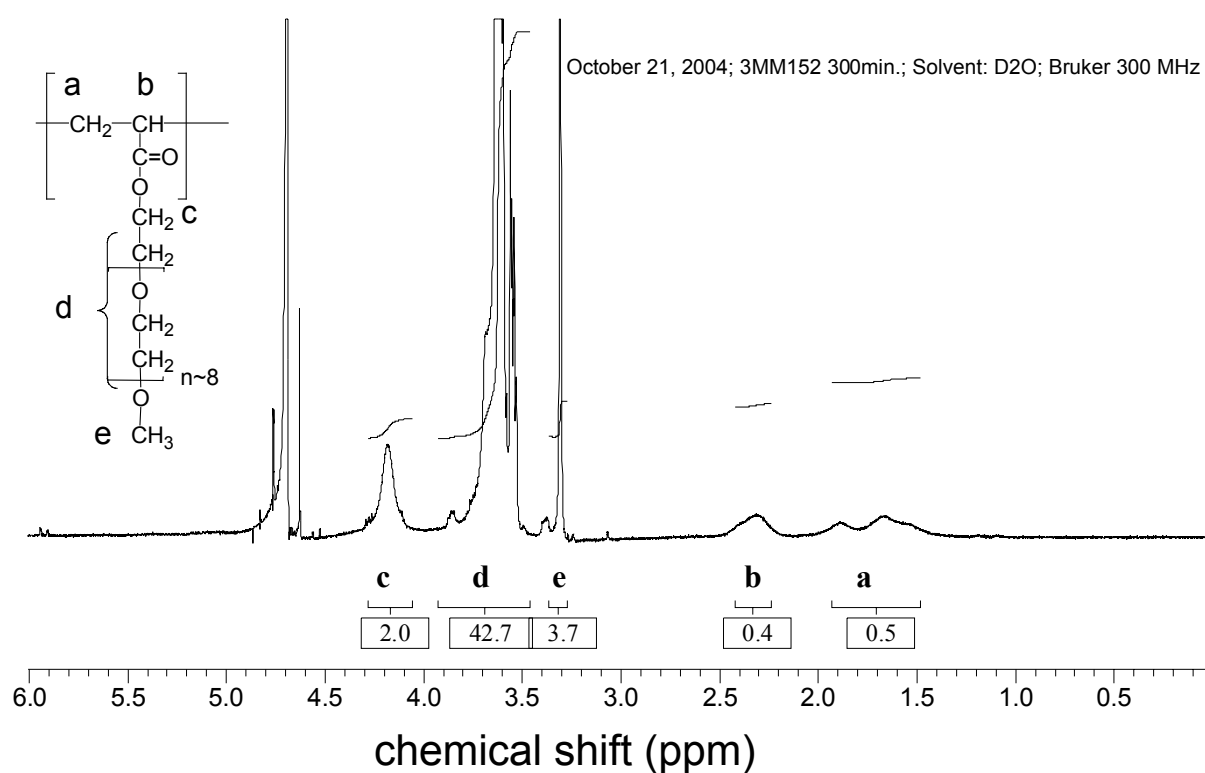
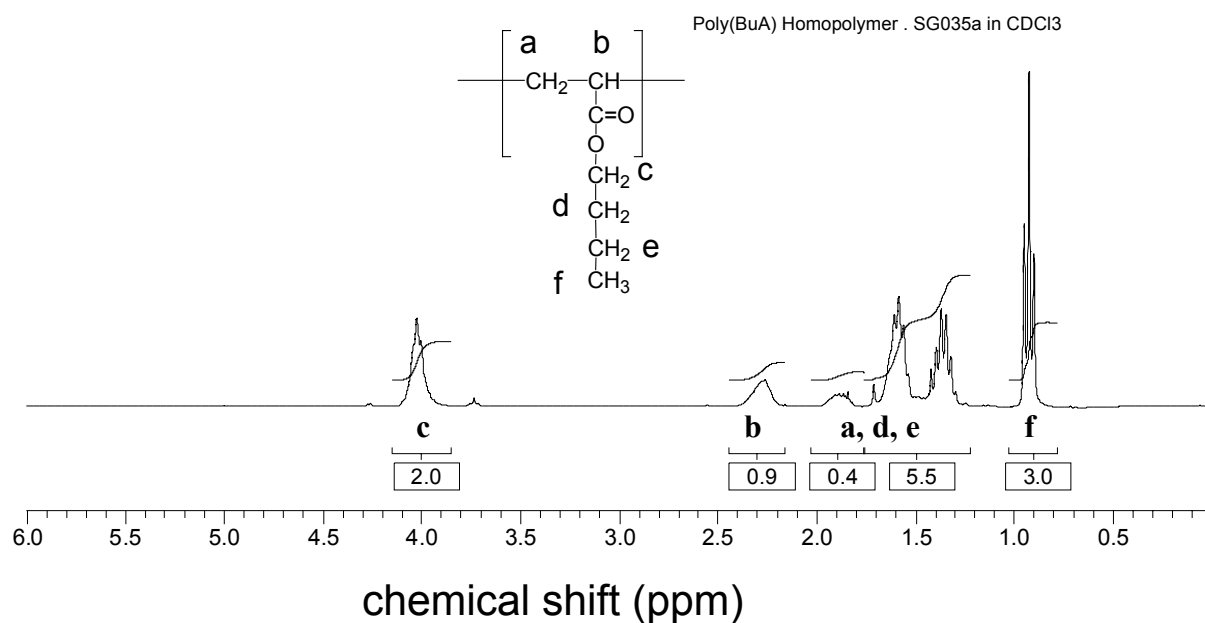
Figure A2.12. ¹H-NMR of 1MM1 in DMSO

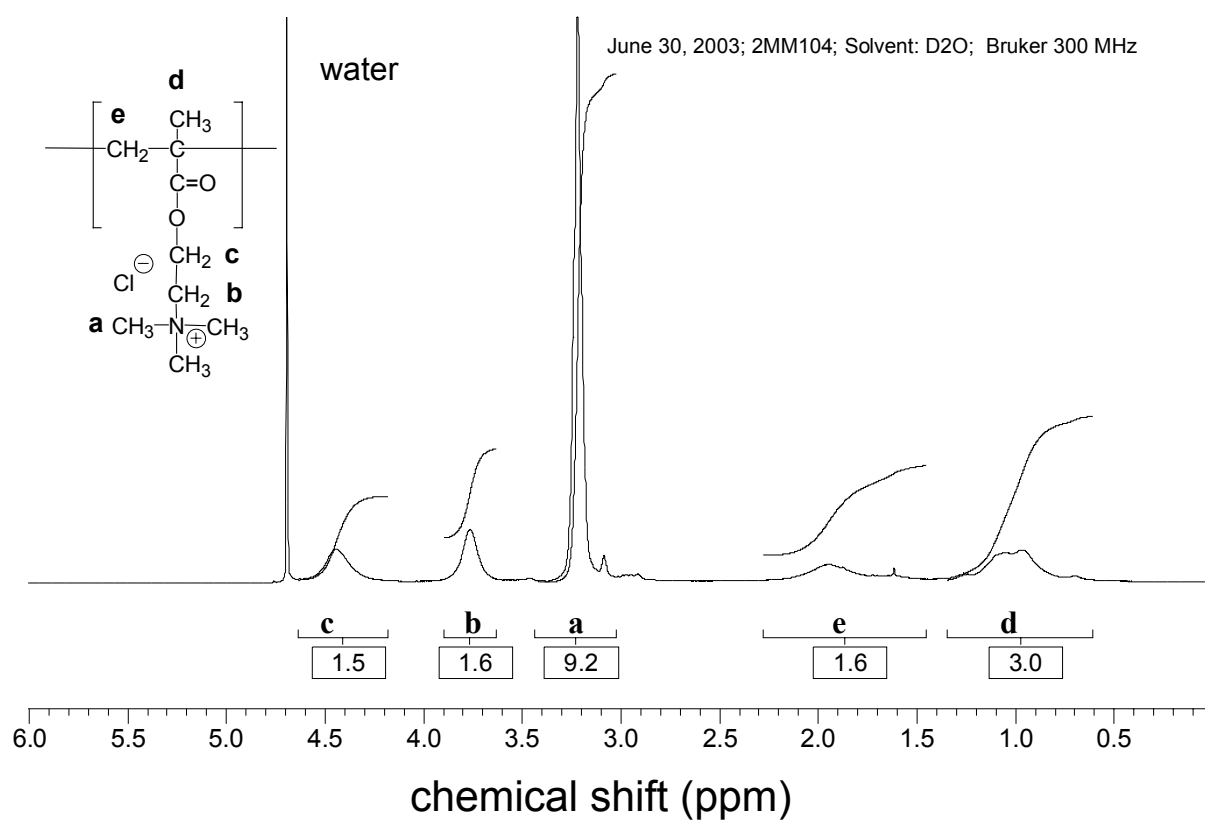
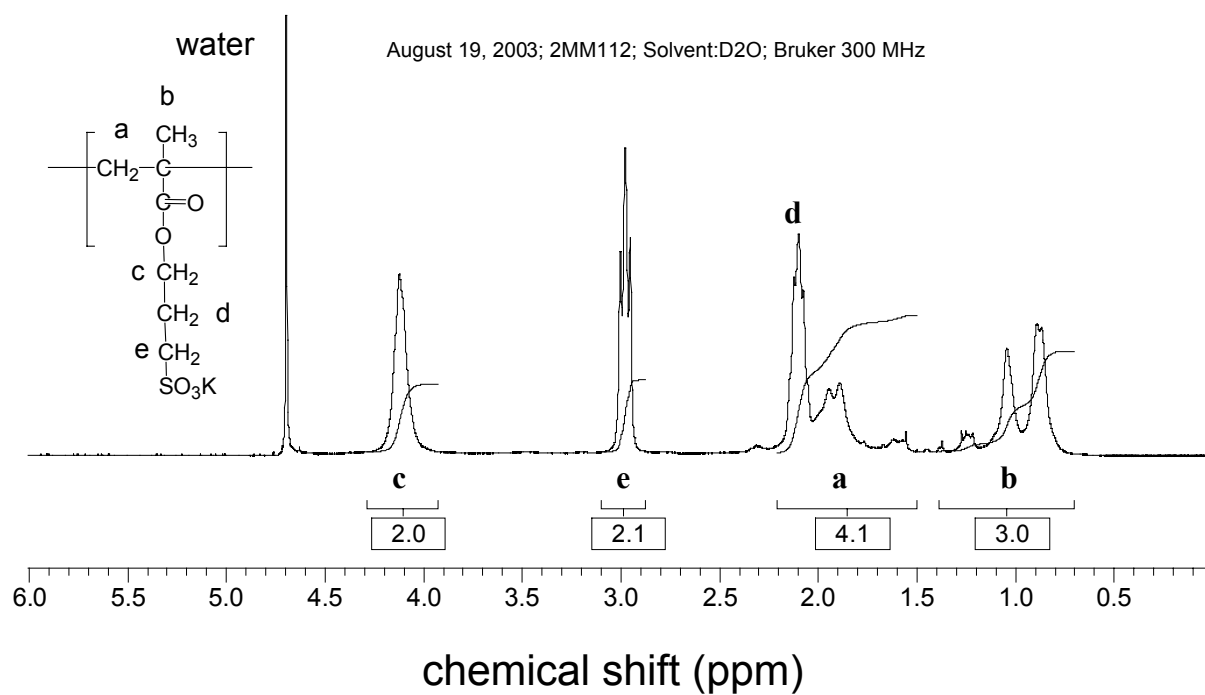
May 6, 2004; solvent: DMSO; Bruker 300 MHz

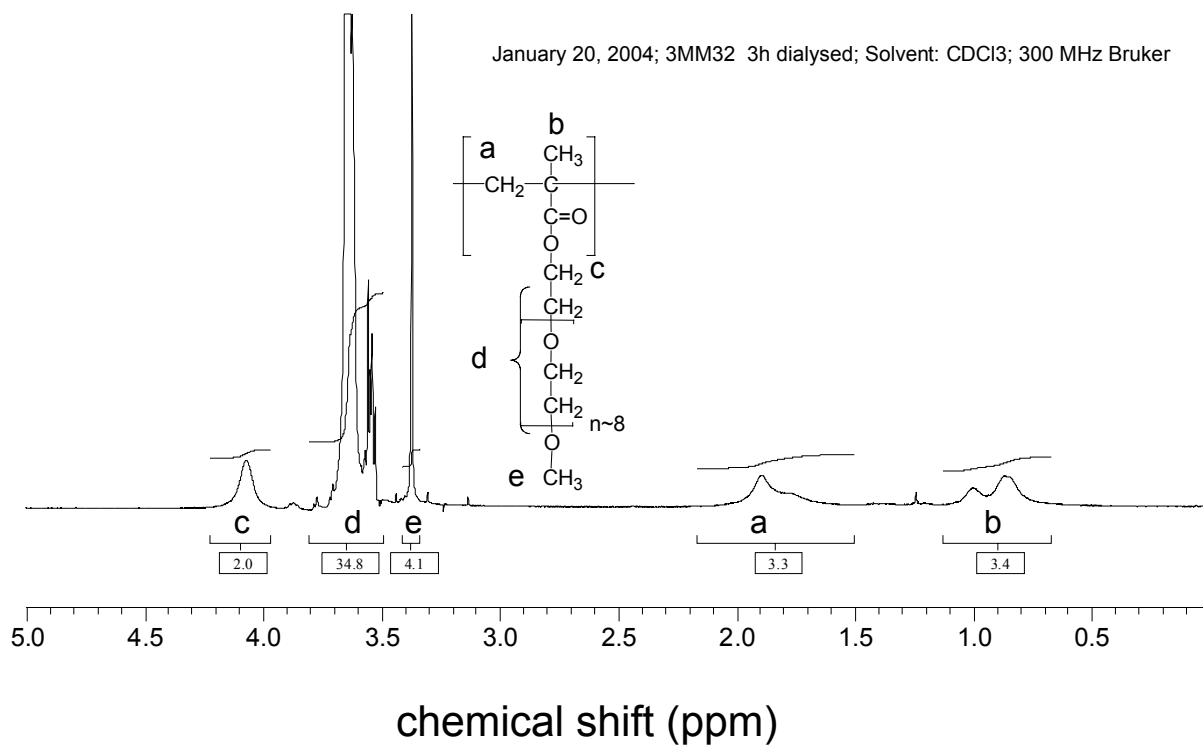
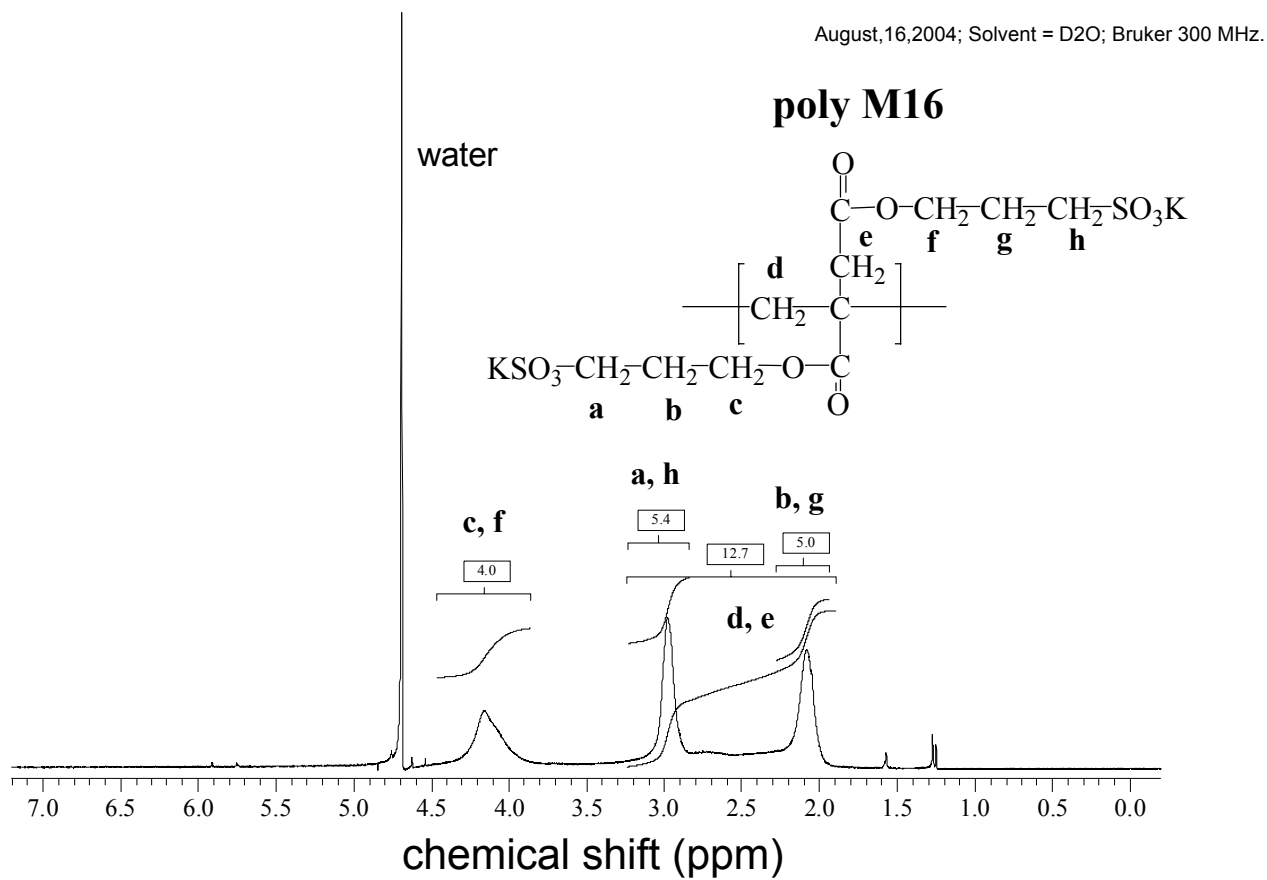
Figure A2.13. $^1\text{H-NMR}$ of 1MM3 in DMSOFigure A2.14. $^1\text{H-NMR}$ of 1MM15 in D_2O

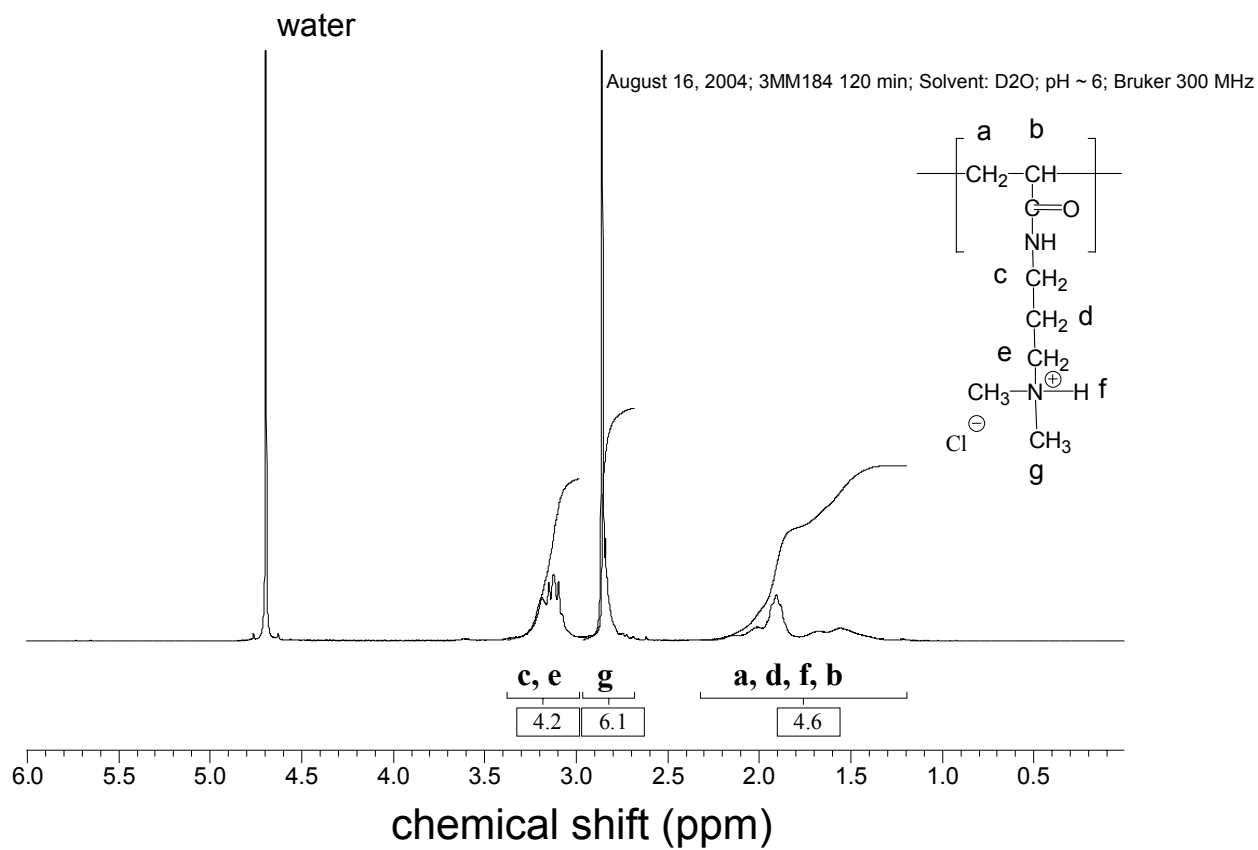
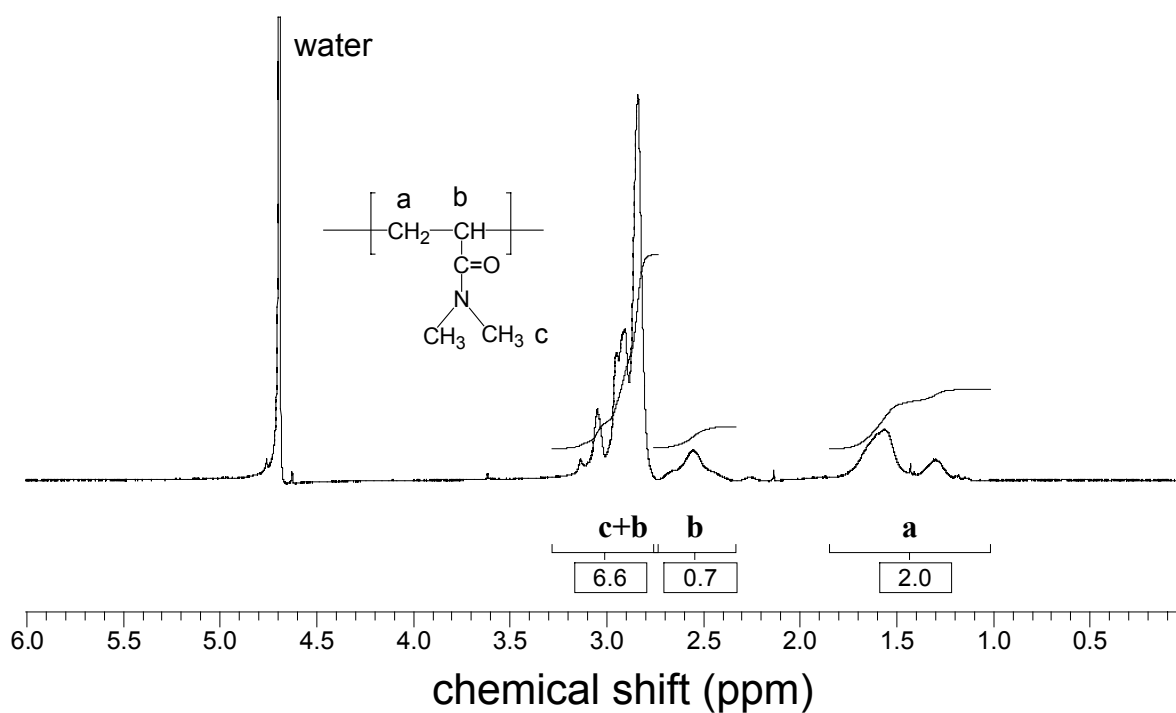
Figure A2.15. ¹H-NMR of 1MM58 in D₂OJuly 12, 2002; solvent: D₂O, Bruker 300 MHz .Figure A2.16. ¹H-NMR of 1MM68 in D₂O

Figure A2.17. ¹H-NMR of polyM1 in D₂OFigure A2.18. ¹H-NMR of polyM2 in D₂O

Figure A2.19. ¹H-NMR of polyM3 in D₂O.Figure A2.20. ¹H-NMR of polyM4 in CDCl₃.

Figure A2.21. ¹H-NMR of polyM5 in D₂O.Figure A2.22. ¹H-NMR of polyM6 in D₂O.

Figure A2.23. ¹H-NMR of polyM7 in D₂O.Figure A2.24. ¹H-NMR of polyM8 in D₂O.

Figure A2.25. ¹H-NMR of polyM9 in D₂O.Figure A2.26. ¹H-NMR of polyM10 in D₂O.

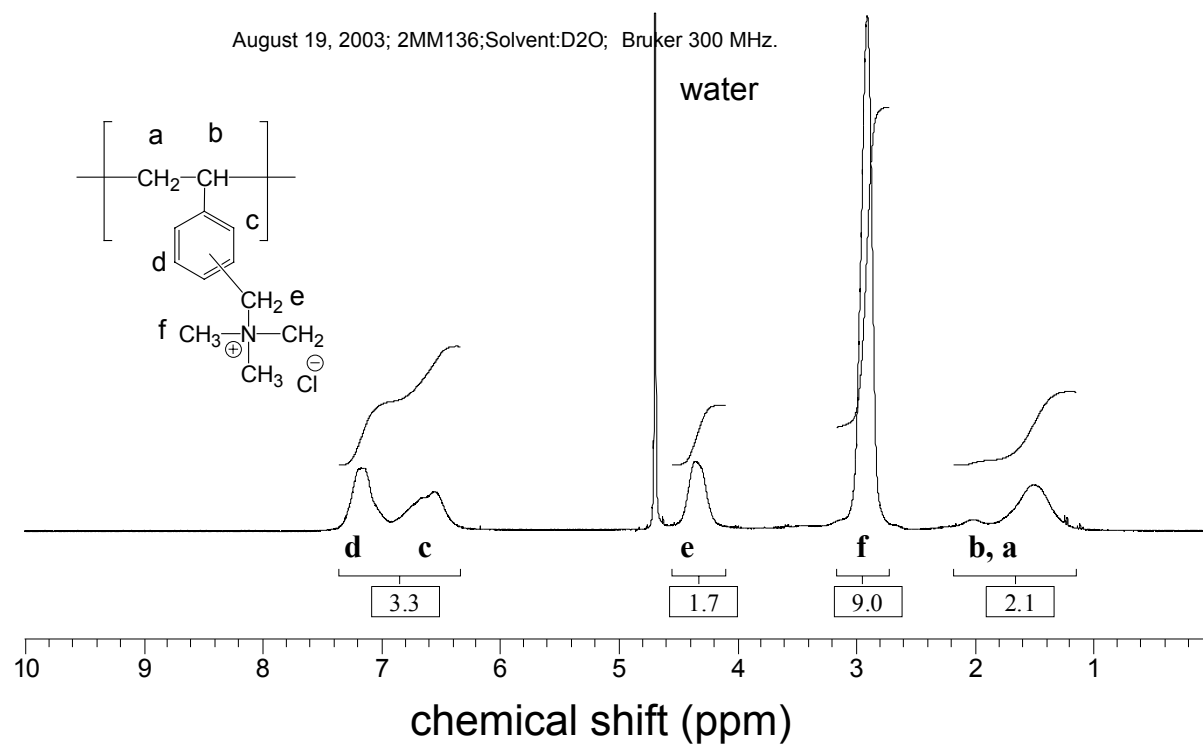


Figure A2.27. ¹H-NMR of polyM13 in D₂O.

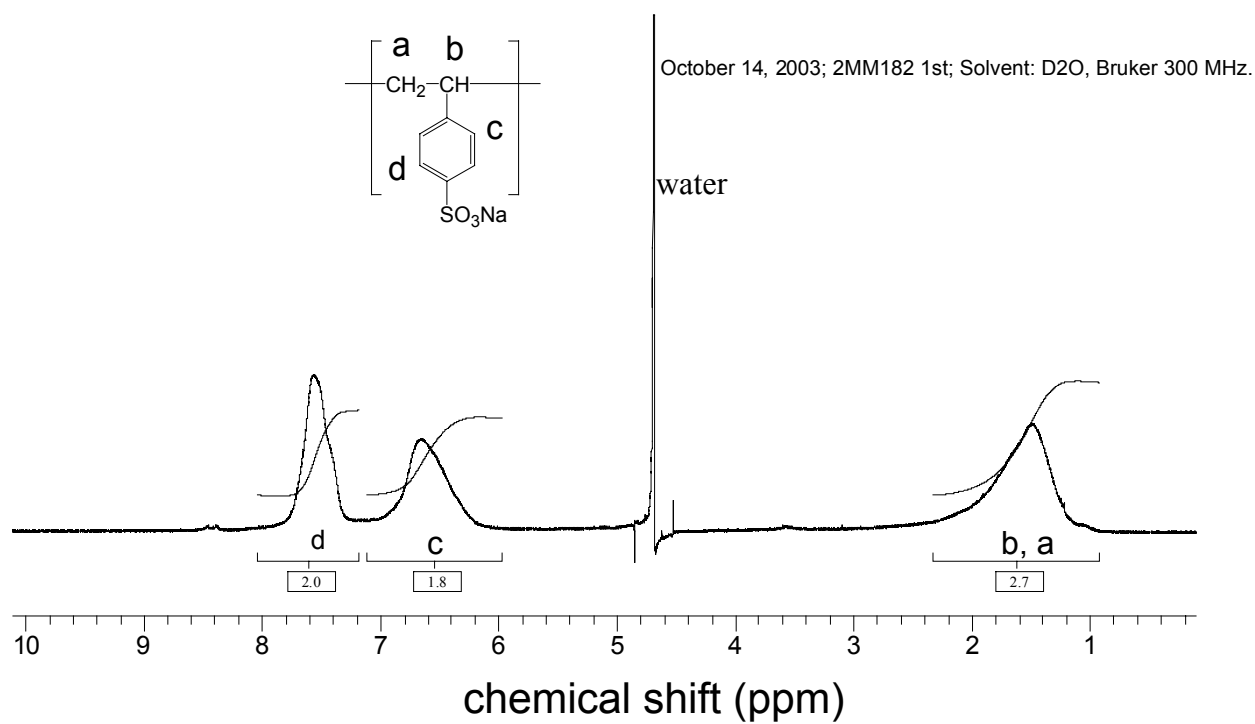


Figure A2.28. ¹H-NMR of polyM14 in D₂O.

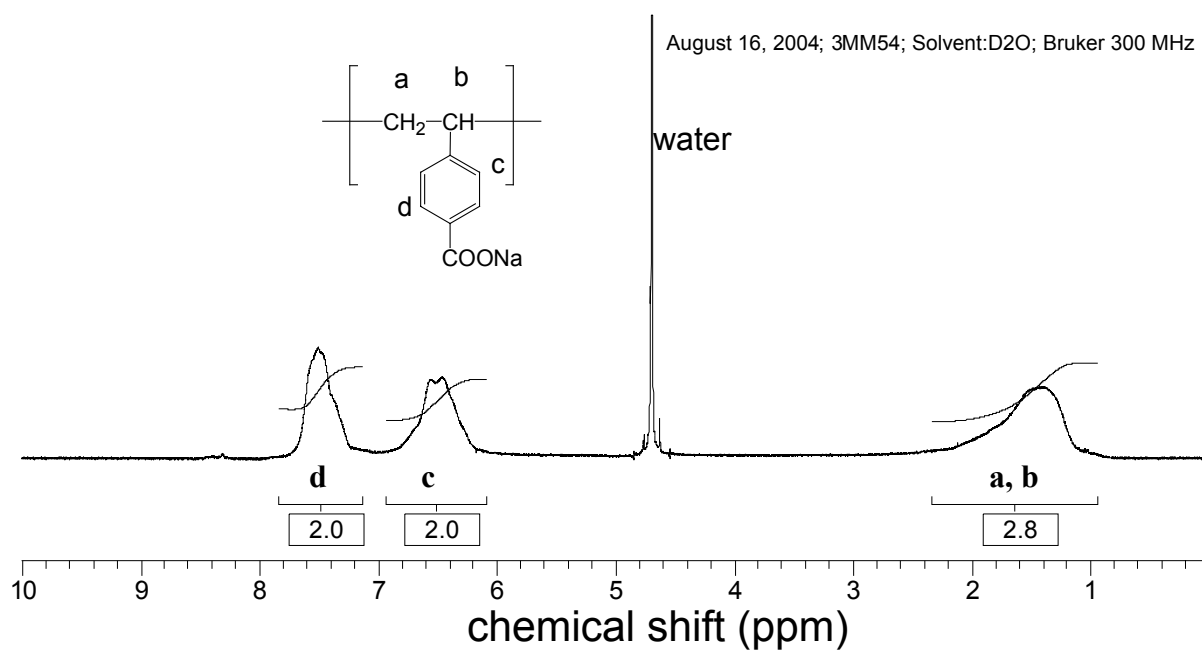


Figure A2.29. ¹H-NMR of polyM15 in D₂O.

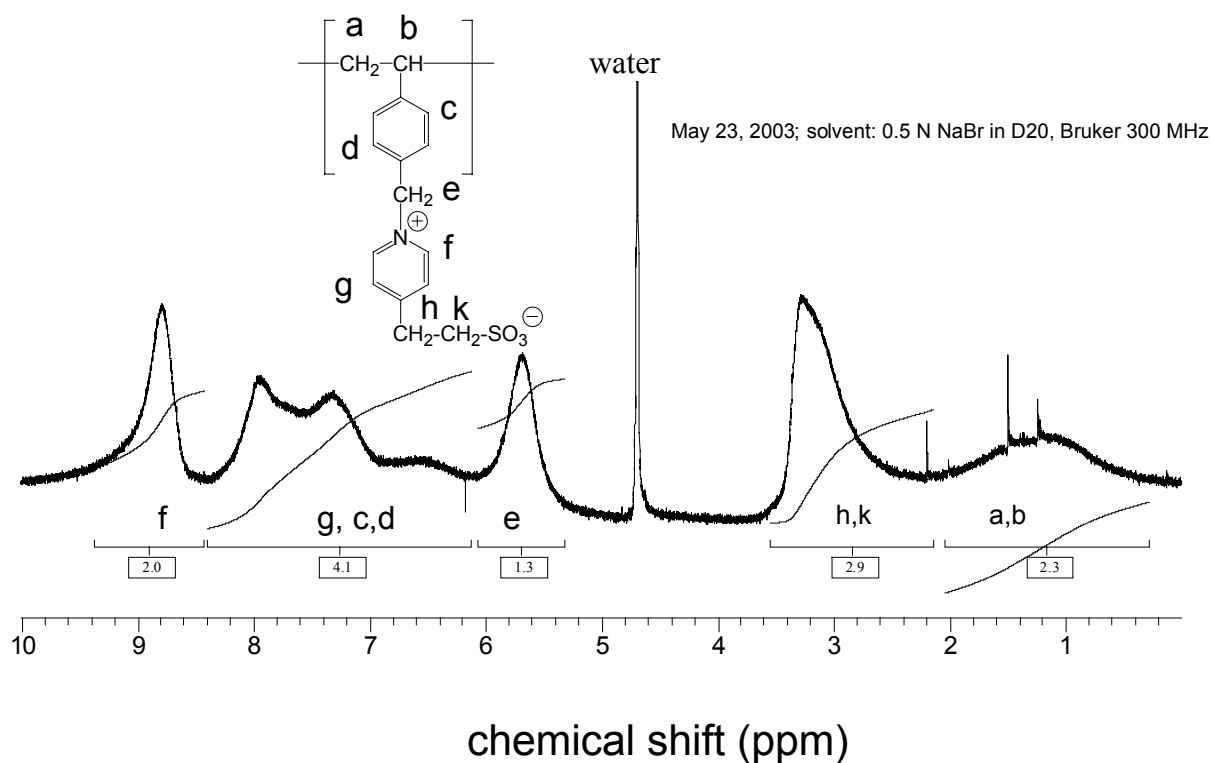
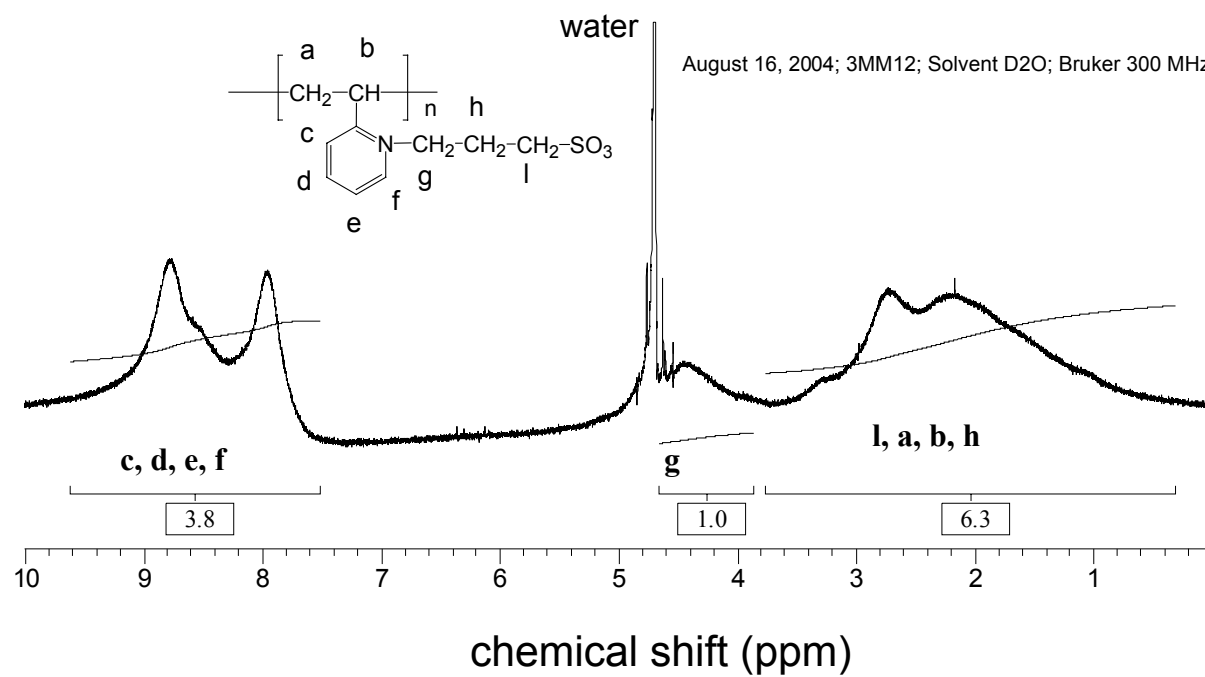


Figure A2.30. ¹H-NMR of polyM17 (M_n~10 K) in 0.5 M NaBr D₂O.



APPENDIX 3: IR Spectra of New Compounds

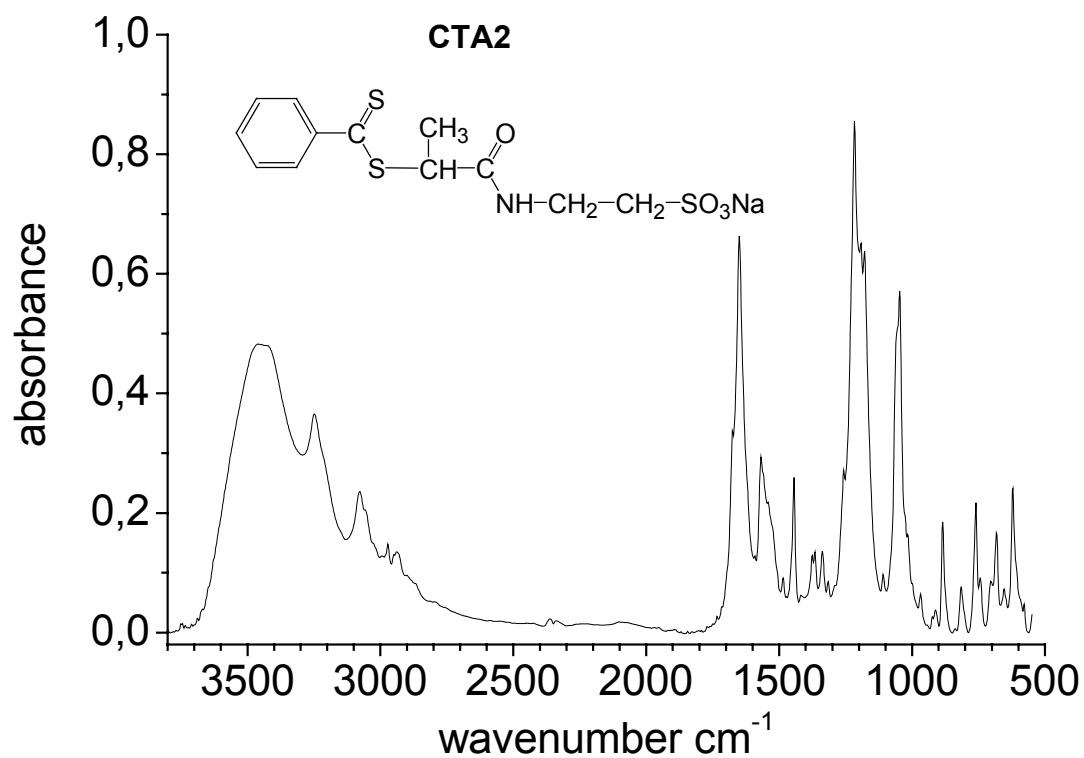


Figure A3.1. FT-IR spectra of CTA2 (KBr, pellet).

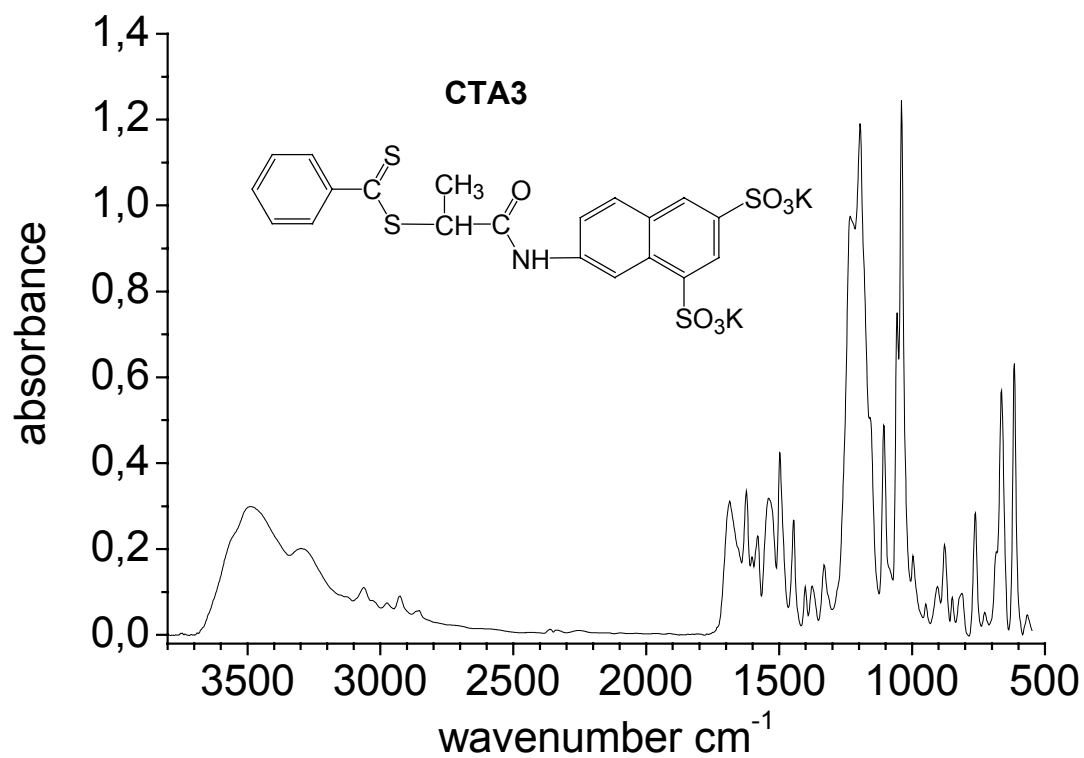


Figure A3.2. FT-IR spectra of CTA3 (KBr, pellet).

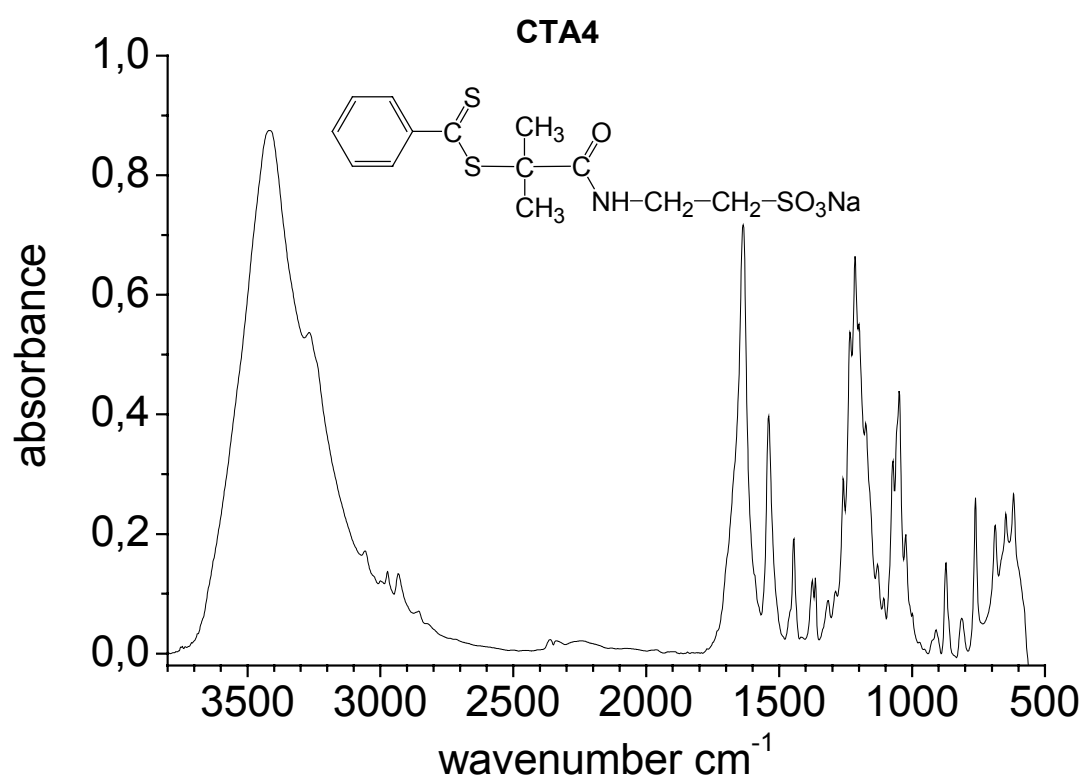


Figure A3.3. FT-IR spectra of CTA4 (KBr, pellet).

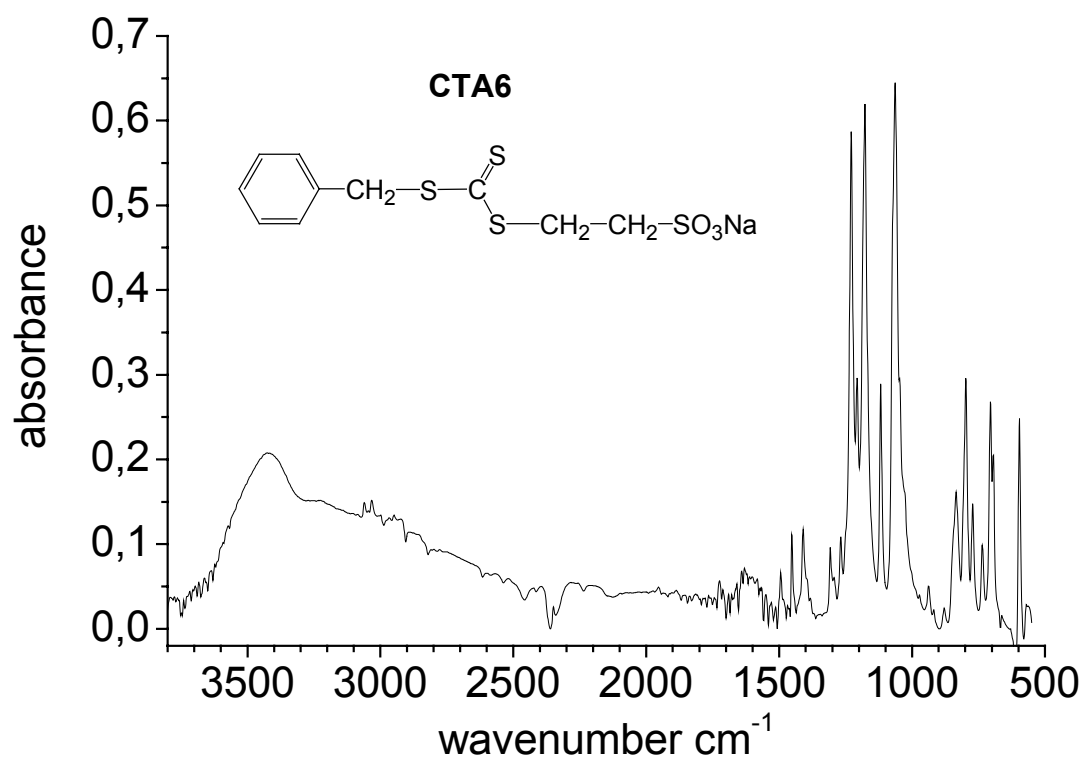


Figure A3.4. FT-IR spectra of CTA6 (KBr, pellet).

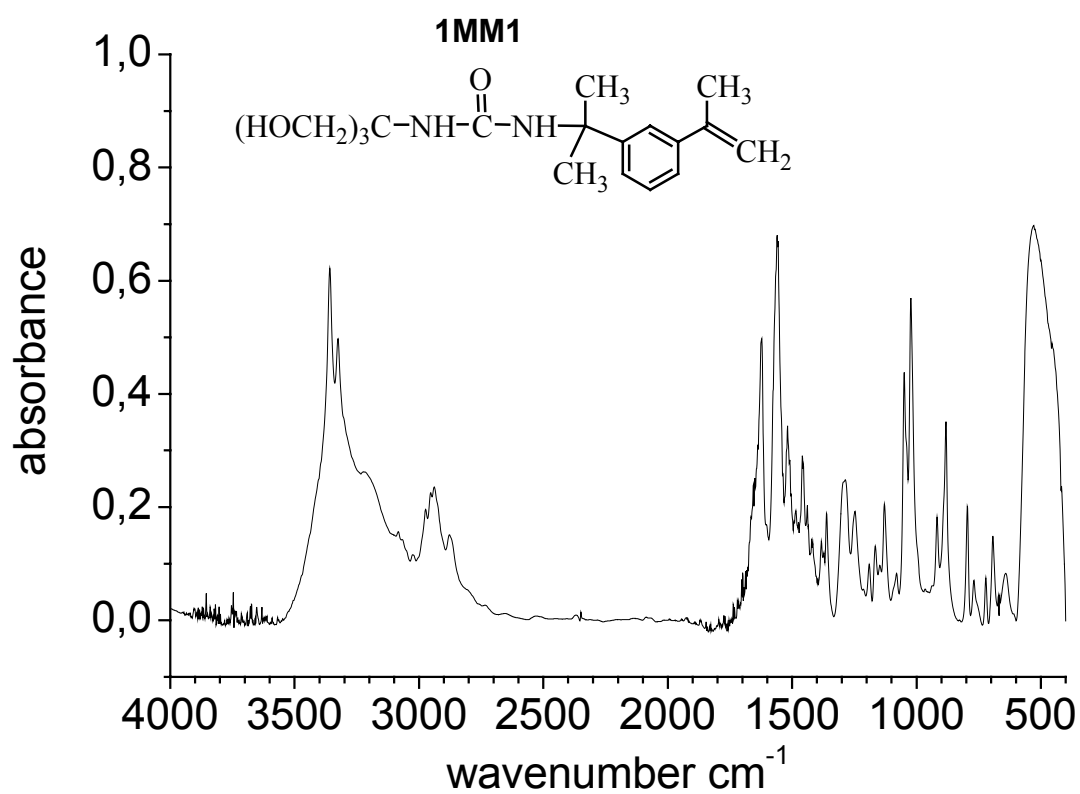


Figure A3.5. FT-IR spectra of **1MM1** (KBr, pellet).

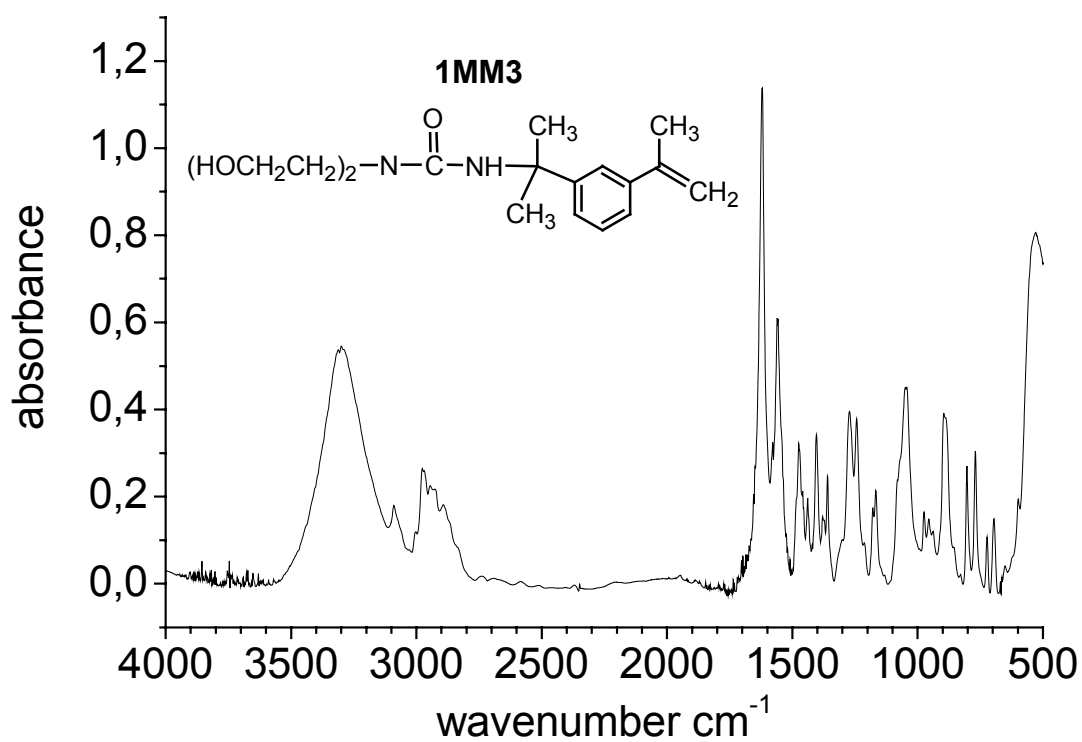


Figure A3.6. FT-IR spectra of **1MM3** (KBr, pellet).

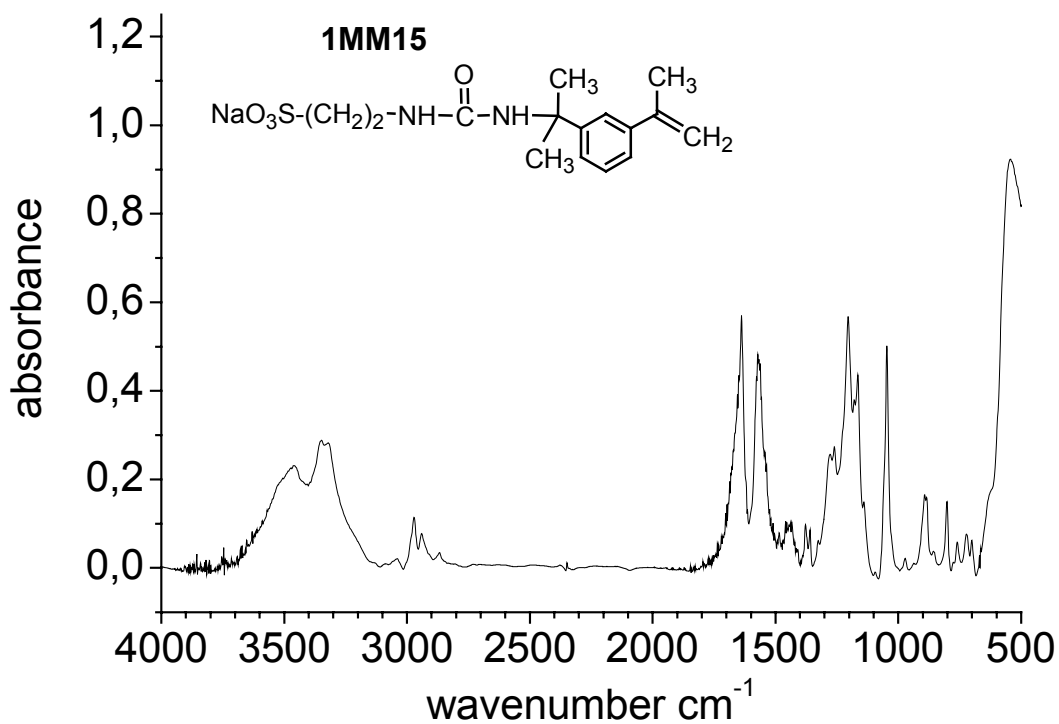


Figure A3.7. FT-IR spectra of 1MM15 (KBr, pellet).

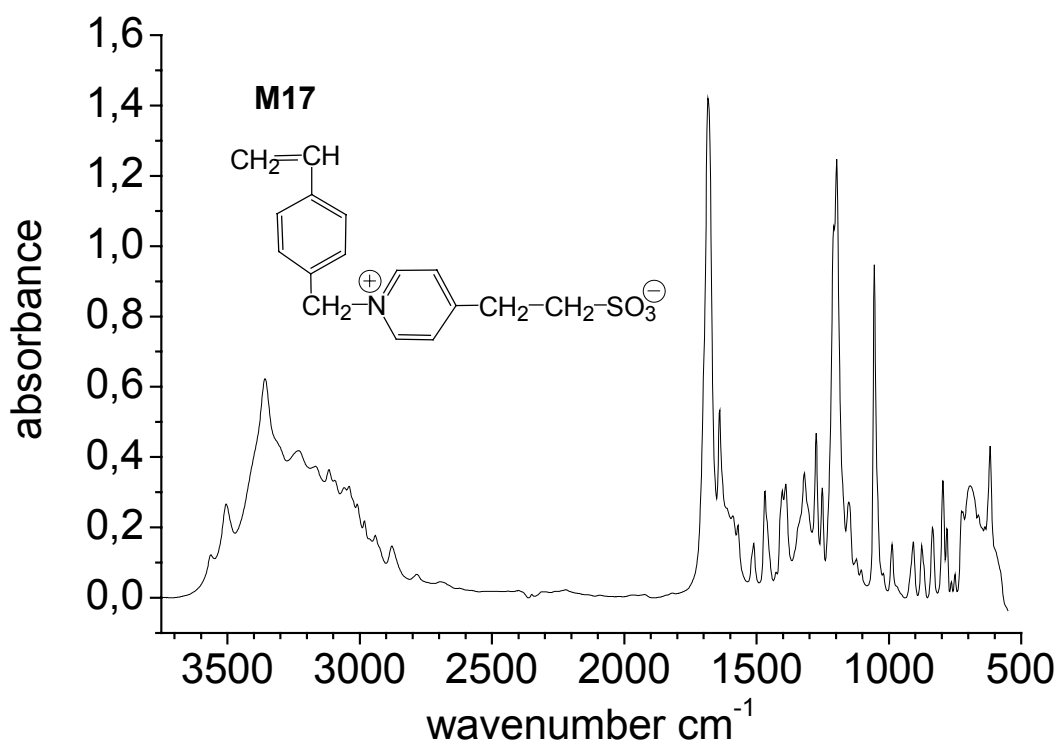


Figure A3.8. FT-IR spectra of M17 (KBr, pellet).